Weak and electromagnetic interactions in the quarkbarton model

Lahanas, A. B.

WEAK AND ELECTROMAGNETIC INTERACTIONS IN THE QUARK PARTON MODEL

A.B.Lahanas

B.Sc. University of Athens

Thesis submitted to the University of Durham for the degree of Doctor of Philosophy

Department of Physics

University of Durham November 1975

To my parents

ABSTRACT

This thesis deals with the naive quark parton model as means of explaining deep inelastic scattering phenomena.

The formalism of the quark model is reviewed as is the parton model and its main results. The Kuti-Weisskopf quark parton model is introduced and used to make predictions for charged and neutral current neutrino experiments.

An attempt is made to improve the Kuti-Weisskopf model predictions and we propose a model in which new hadronic constituents, besides the p,n,λ and charmed p' quarks participate. In this model the new particles are classified in SU(2) triplets of the Weinberg model.

We analyse charged and neutral current neutrino experiments and construct a model which is a modification of a quark model proposed by R.Mc. Elhaney and S.F. Tuan.

In the light of recent work on nonleptonic interactions of the electron we consider both electron positron annihilation and deep inelastic scattering.

Finally, we propose a scheme in which "naive quark parton model' techniques can give $(\log s)^2$ behaviour for the hadronic total cross sections.

HOW TO READ THIS THESIS

The thesis is divided into five chapters and nine appendices. Expressions encountered throughout this thesis are labelled by two numbers, the first of them indicating the corresponding chapter, or appendix, which the expression belongs to. Appendix formulae have the letter A standing in front of these two numbers indicating thus that they belong to an appendix.

For the convenience of the reader all figures and tables are included as parts of the text.

TABLE OF CONTENTS

CHAPTER V.

INTRODUCTION

The internal structure of matter has been the object of speculation of the human mankind for about three thousand years. Democritus† was the first to put forward the problem as to what constituted the smallest part of matter. He argued that matter cannot be subdivided indefinitely but there are fundamental constituents which he called†† "atoms".

The beginning of our century deserves the name of the "Golden Age" of the 'atomic' approach to Physics. In the early nineteen hundreds, almost two and a half thousand years after Democritus, Rutherford proposed his model for the hydrogen atom which consisted of a proton and one electron moving around it in an eliptical orbit. In order to explain the spectra of emission and absorption of the atoms, as well as many other phenomena, physicists were forced to adopt new concepts, such as the quantum. The classical theories of mechanics and electromagnetism seemed to be inadequate in the world of the microcosm and a new theory was developed, that of "Quantum Mechanics". For some time it was thought that the end of the physics would be in the very near future and all problems would be solved. Unfortunately things did not turn out this way. Nowadays, almost fifty years after the development and establishment of the quantum mechanics, things seem to be more complicated than ever.

† Greek philosopher born in 470 B.C.

†† The word atom comes from the Greek word 'ἄτομον' (atomon) and it means something not being able to be cut.

In this interval of fifty years a plethora of other particles besides the proton and the electron have been discovered. The laws governing the interactions of these particles among themselves is not known at least up to the time of writing.

In the meantime the smashing of the atom has become a fact and the word 'atom' has lost its original meaning.

With this large number of particles discovered so far, the problem of Democritus still remains unanswered. Are all these particles elementary, in the sense that they constitute the fundamental blocks of matter, or not?

To bring order to the chaos of many apparently unrelated particles, Gelmann in 1964 proposed the SU(3) symmetry group. The basic representation of this group consists of three fundamental particles, the well known quarks p, n and λ. These quarks carry fractional electric charges and they have baryon number equal to $^1/3$. The known mesons are supposed to consist of a quark-antiquark pair ($q\bar{q}$) and the baryons of three quarks (qqq). Thus the known hadrons are classified in representation of the SU(3) group.

Later this SU(3) group was enlarged to SU(6) so that quark-spin effects were taken into account. However the group SU(6) x O (3) seemed to be more realistic since the motion of quarks was taken into account as well; according to it hadrons behaved as bound states, with orbital excitation, of a quark-antiquark pair (mesons) or of three quarks (baryons).

Various theoretical difficulties lead people to consider other

groups such as $SU(6)_w$ and $SU(6)_w \times O(3)$.

It is evident that larger groups can be found, by assuming the existence of additional quarks carrying new quantum numbers, which accommodate more hadrons. For example the SU(3) group is contained in the bigger SU(4) whose basic representation consists of the three quarks p, n and λ plus another quark the p' which is assumed to carry a new quantum number called charm; the necessity of using SU(4) rather than the SU(3) has experimental support after the discovery of the new particles ψ and ψ' which are supposed to be charm-anticharm bound states.

The way quarks have been treated so far is that suggested by hadron spectroscopy. These quarks are called "constituent quarks" and it is not the only way quarks appear in the context of modern physics. During the last few years much has been said about "current quarks" which is a notion quite different from that of the constituent quark. According to it there is a group, the $[SU(6)_w \times O(3)]_{currents}$, which gives us the currents of the theory (electric, weak etc) in terms of the "current quarks", to be distinguished from the $[SU(6)_w \times O(3)]_{constituent}$ which is the classification group for hadrons. Attempts to connect these two groups by a unitary transformation have been made in the literature. The so called† "Melosh transformation" has exactly this property.

So far quarks have not been observed experimentally. Perhaps this can be achieved in the near or remote future when there are experimental machines of energies higher than those available

† H.J. Melosh: Caltech Ph.D. Thesis (1973)

at present. In the meantime experiments are in progress searching for the fundamental constituent of matter or the "atom" of Democritus if you like.

If hadrons are really composed of more fundamental constituents then by bombarding a hadron by high energetic beam we can go deeply into it and probably break it into its constituents. This is the sort of experiment carried out at SLAC where they study the inclusive process $e^- + p \rightarrow e^- + (\text{Anything})$. Theoretically this process is assumed to occur via the exchange of a spacelike photon which hits the target proton. Having large photon momentum, which in the language of quantum mechanics means small wavelength, we would be able to see details of the proton structure or we could break the proton into its constituents. Free quarks were not detected in this experiment but the data revealed a very important phenomenon that of "Bjorken scaling". In the meantime other experimental groups at NAL and at CERN, using neutrino or antineutrino beams, have studied the reactions $\nu(\bar{\nu}) + N \rightarrow \mu^-(\mu^+) + X$ in which the probe is not a photon but a W-boson. The same scaling phenomenon was also observed in these experiments. Roughly speaking, Bjorken scaling is the statement that the structure functions $F_{1,2,3}(\nu, q^2)$, associated with the processes mentioned before, are not functions of the variables ν and q^2 alone, but they are functions of the ratio ν/q^2 when ν and q^2 are large while ν/q^2 is fixed; the variable q^2 is the momentum squared of the probing particle and ν is the variable $\nu = \frac{s-M^2-q^2}{2M}$, where s denotes the probe and target particle center of mass total energy squared. The kinematical

region ν, q^2 large and ν/q^2 fixed, in which scaling sets in, is called "Bjorken scaling limit".

This phenomenon has been a puzzle to any theoretician and this is the reason why deep inelastic experiments have concentrated many people's interest the last few years.

Among the deep inelastic experiments performed is the experiment measuring the neutral to charged current ratios defined as $\sigma(\nu + N \to \nu + X)/\sigma(\nu + N \to \mu^- + X)$ and $\sigma(\bar{\nu} + N \to \bar{\nu} + X)/\sigma(\bar{\nu} + N \to \mu^+ + X)$. The importance of this experiment must be particularly stressed since in this way it is proved that the neutral currents which enter in some gauge theories do exist!!

In the content of this thesis we deal with the naive quark parton model as means to interpret the data regarding the deep inelastic electroproduction and neutrinoproduction processes. To deal with the existence of the neutral currents Weinberg's renormalizable theory is assumed.

We also consider electron-positron annihilation phenomena; non-leptonic interactions of the electron are considered, in the context of the naive quark parton model, in order to interpret some of the $e^- e^+$ data.

Finally, we make an attempt to explain the rising high energy behaviour of the hadronic cross sections applying quark parton model techniques. Although we deal with scaling and neutral current phenomena, which constitute one of the most exciting parts of elementary particle physics for the last decade, we limit ourselves to the quark parton model approach, in combination with Weinberg's

theory for weak and electromagnetic interactions. Other theoretical approaches used to interpret scaling and neutral current phenomena are not discussed.

Acknowledgements

I am grateful to my supervisor F.D. Gault for his tireless effort in suggesting, criticizing and correcting the manuscripts during the writing of this thesis. I am also grateful to him for guiding me and introducing me to the subject during my stay in the University of Durham. His help and support without which no part of this thesis would have been written is greatly acknowledged.

I also wish to thank Professors B.H. Bransden and E.J. Squires and the staff of the Physics and Mathematics Department of the Durham University for their help and their warm hospitality they offered me.

I want also to express my sincere thanks to F.T. Hadjioannou, Professor of Physics in the University of Athens, who so tirelessly guided my first steps in the science of physics and whose help and support is fully acknowledged.

Thanks are due also to my friend Dr S.D. Vlassopoulos for useful comments and constructive discussions and to my friend Dr G.D. Spathis for so kindly permitting me to include part of a work done with his collaboration.

Finally I thank everyone who contributed in some way so that this thesis could be completed.

CHAPTER I

Introduction

In this chapter we present the basic concepts, physical quantities, and formalism, with which we deal in the following chapters.

We discuss in brief deep inelastic electron-proton scattering and the significance of the structure functions. For the related reactions, $p + p \rightarrow \mu^- \mu^+ + X$ and $e^- + e^+ \rightarrow$ Hadrons, we give the experimentally measured quantities which will be of interest to us in forthcoming chapters.

Neutrino induced reactions, such as $\nu N \rightarrow \mu^- X$ and $\bar{\nu} N \rightarrow \mu^+ X$, are discussed briefly and an introduction to the Weinberg model is given. Bjorken scaling, neutral currents and the existence of charmed particles are also briefly discussed.

We have consciously omitted many other theoretical considerations in the field for two main reasons; first, because of the enormous number of them existing in literature, for which a detailed account would require a great deal of space, and second, because we wish to state only those ones immediately connected with what will be said in the remaining part of this thesis.

II) Electromagnetic Proton, Neutron Form Factors

Before considering the deep inelastic electron-proton scattering, we think it appropriate to say a few words concerning elastic electron-proton scattering, and to discuss the electromagnetic proton

and neutron form factors.

To lowest order of the hyperfine structure constant, $\alpha = \frac{e^2}{4\pi}$, the elastic process $e^- + p \to e^- + p$ is represented pictorially by the following Feynman diagram,

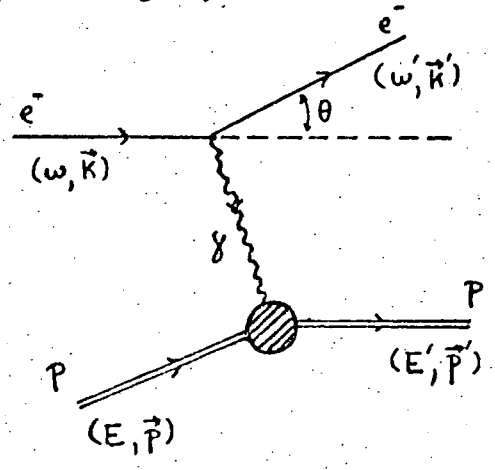

FIGURE 1: Kinematics of elastic electron-proton scattering.

where $(\omega, \vec{K})$ and $(\omega', \vec{K'})$ are the momentum four vectors of the incoming and the outgoing electron respectively, and $(E, \vec{p})$ and $(E', \vec{p'})$ are the corresponding momenta for the incoming and the outgoing proton.

To find the differential cross-section of the above process we need the matrix element $\langle \vec{P}', s' | j^\mu(0) | \vec{P}, s \rangle$, where $j^\mu(x)$ is the electric current and $|\vec{p}, s\rangle$, $|\vec{p}', s'\rangle$ the proton's initial and final states respectively. The indices s and s' denote the spin of the proton.

If the proton was a pointlike object, like the electron say, then its electromagnetic current would be given by $j^\mu(x) = e\bar{\psi}(x)\gamma^\mu\psi(x)$ where $\psi(x)$ is the proton field.

Experiments have shown that the proton has a structure and thus its current should not be of the above form.

Choosing our states normalized covariantly, that is

$$\langle \vec{p}', s' | \vec{p}, s \rangle = (2\pi)^3 (2E) \delta^{(3)}(\vec{p} - \vec{p}') \tag{1.1}$$

we write for the current matrix elements [1,2,3]

$$\langle \vec{p}', s' | j_\mu(0) | \vec{p}, s \rangle = e \bar{u}(p', s') \left[F_1^{(p)}(q^2) \gamma_\mu + i \frac{\mu_p}{2M_p} F_2^{(p)}(q^2) \sigma_{\mu\nu} q^\nu \right] u(p, s) . \tag{1.2}$$

In this formula the spinors are normalized to unity, that is $\bar{u}(p,s) u(p,s') = \delta_{ss'}$; the four vector q^μ is the momentum transfer $q = K - K'$, M_p is the proton mass, μ_p is the proton's anomalous magnetic moment, and e the physical proton charge. The functions $F_1^{(p)}(q^2)$ and $F_2^{(p)}(q^2)$ are called electromagnetic form factors and depend only upon the variable q^2. At zero momentum transfer they have the values

$$F_1^{(p)}(q^2) = F_2^{(p)}(q^2) = 1 . \tag{1.3}$$

In literature [1,2,3,4] one finds the Sachs' form factors defined by

$$G_E^{(p)}(q^2) = F_1^{(p)}(q^2) + \frac{q^2}{4M_p} \mu_p F_2^{(p)}(q^2) \tag{1.4a}$$

$$G_M^{(p)}(q^2) = F_1^{(p)}(q^2) + \mu_p F_2^{(p)}(q^2) . \tag{1.4b}$$

In the coordinate system in which the time like vector p + p' has no space component the two combinations of F_1 and F_2 given in Eqs.(1.4)

correspond to the electric charge distribution and the distribution of the magnetic moment . This is the reason G_E and G_M are often called electric and magnetic form factors respectively.

The differential cross sections $\frac{d^2\sigma}{d\Omega' dE'}$ and $\frac{d\sigma}{d\Omega'}$ in terms of G_E and G_M are given by the expressions [see for example Ref. 1,2]

$$\frac{d^2\sigma}{d\Omega' dE'} = \frac{4\alpha^2}{q^4}\,\delta\left(\frac{q^2}{2M_p}+\frac{P\cdot q}{M_p}\right)\frac{E'^2}{M_p}\left\{M_p\,\frac{\left(G_E^2-\frac{q^2}{4M_p^2}G_M^2\right)}{\left(1-\frac{q^2}{4M_p^2}\right)}\cos^2\frac{\theta}{2} - \frac{q^2}{2M_p^2}G_M^2\sin^2\frac{\theta}{2}\right\} \qquad (1.5a)$$

$$\frac{d\sigma}{d\Omega'} = \frac{\alpha^2}{4E^2}\left(\frac{\cos^2\frac{\theta}{2}}{\sin^4\frac{\theta}{2}}\right)\left(1+\frac{2E}{M_p}\sin^2\frac{\theta}{2}\right)^{-1}\left\{\frac{\left(G_E^2-\frac{q^2}{4M_p^2}G_M^2\right)}{\left(1-\frac{q^2}{4M_p^2}\right)} - \frac{q^2}{2M_p^2}\tan^2\frac{\theta}{2}\right\}. \qquad (1.5b)$$

In the expressions above θ is the laboratory scattering angle and E,E' the energies of the incoming and outgoing electron respectively.

The cross-sections given in Eqs. (1.5) can be measured experimentally and consequently we can have information concerning the behaviour of the form factors. Had the proton been a pointlike particle we would have found $F_1^{(p)}(q^2) = 1$ and $F_2^{(p)}(q^2) = 0$ or the same $G_E^{(p)}(q^2) = 1$ and $G_M^{(p)}(q^2) = 1$ which does not happen.

Experimental data [5] give the following empirical fits for the electric and magnetic form factors of the proton

$$G_E^{(p)}(q^2) = \left(\frac{1}{1+\frac{q^2}{.71}}\right)^2 \qquad (1.6a)$$

$$G_M^{(p)}(q^2) = (1+\mu_p)\,G_E^{(p)}(q^2) \qquad (1.6b)$$

where q^2 is in units of $\left(\frac{GeV}{c}\right)^2$. The form factors $G_E^{(p)}$ and $G_M^{(p)}$ given by Eqs. (1.6) decrease as fast as $1/q^4$ for high momentum transfers.

We give another fit to the data in which $G_E^{(p)}$ and $G_M^{(p)}$ have an exponential fall-off behaviour for high q^2 [6]

$$G_E^{(p)}(q^2) = 27.8\, e^{-|q^2/.04|^{\frac{1}{2}}} \qquad (1.7a)$$

$$G_M^{(p)}(q^2) = (1+\mu_p)\, G_E^{(p)}(q^2) \quad . \qquad (1.7b)$$

Form factors for the neutron can be defined in the same way as for the proton. Because the charge of the neutron is zero $F_1^{(n)}(q^2)$ and $G_E^{(n)}(q^2)$ must vanish while $F_2^{(n)}(q^2)$ approaches 1 in the limit $q^2 \to 0$. Data from electron-deuteron scattering give the following empirical fit for the neutron form factors [5]

$$G_E^{(n)}(q^2) = -\frac{q^2}{4M_n^2}\,\mu_n\, G_E^{(p)}(q^2) \qquad (1.8a)$$

$$G_M^{(n)}(q^2) = \mu_n G_E^{(p)}(q^2) = \frac{\mu_n}{(1+\mu_p)}\, G_M^{(p)}(q^2) \quad . \qquad (1.8b)$$

In Eqs. (1.8) $G_E^{(p)}$ and $G_M^{(p)}$ are given by the Eqs. (1.6). The constants μ_p and μ_n are the anomalous magnetic moments of the proton and neutron respectively and in units of the Bohr magneton they have the values $\mu_p = 1.79$, $\mu_n = -1.91$.

For larger q^2 a better fit is obtained [7] for the neutron electric form factor using the formula

$$G_E^{(n)}(q^2) = -\left(\frac{q^2/4M_n^2}{1+q^2/M_n^2}\right)\mu_n\, G_E^{(p)}(q^2) \quad . \qquad (1.9)$$

I2) Inelastic Electron-Proton Scattering

We proceed now to examine the inelastic reaction $e^- + p \rightarrow e' + X$. The interaction is assumed to be purely electromagnetic and in first order of perturbation theory the process is represented by the following Feynman diagram.

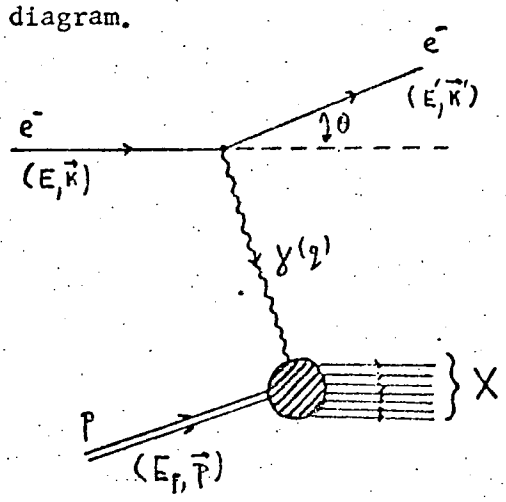

FIGURE 2: Kinematics of inelastic electron-proton scattering.

In the proton's Lab. frame the unpolarised differential cross section $\frac{d^2\sigma}{dE'd\Omega'}$ is given by [see for example Ref. 8 and A.3.9]

$$\frac{d^2\sigma}{dE'd\Omega'} = \frac{4\alpha^2}{Q^4}\frac{E'}{M}\left\{2W_1(\nu,Q^2)\sin^2\frac{\theta}{2} + W_2(\nu,Q^2)\cos^2\frac{\theta}{2}\right\}. \quad (1.10)$$

In this formula the variables Q^2 and ν are defined by

$$Q^2 = -q^2 = -(K-K')^2 \quad (1.11a)$$

$$\nu = \frac{P\cdot q}{M} \quad (1.11b)$$

$K^\mu = (E,\vec{K})$ and $K'^\mu = (E',\vec{K'})$ are the momenta of the incoming and outgoing electron respectively. M is the mass of the proton and p^μ its momentum.

W_1 and W_2 called the structure functions, are real dimensionless and depend on the Q^2 and ν variables.

In terms of the Q^2 and ν the differential cross section $\frac{d^2\sigma}{dQ^2 d\nu}$ is given by the expression

$$\frac{d^2\sigma}{dQ^2 d\nu} = \frac{4\pi\alpha^2}{Q^4}\frac{E'}{ME}\left\{2W_1(\nu, Q^2)\sin^2\frac{\theta}{2} + W_2(\nu, Q^2)\cos^2\frac{\theta}{2}\right\} . \quad (1.12)$$

Note that the variable Q^2 in the physical region of the process $e^- + p \to e^- + X$ is timelike. This is seen from the fact that in proton's Lab. frame $Q^2 = 4EE'\sin^2\frac{\theta}{2} \geq 0$. Comparing (1.10) with (1.5a) we see that for elastic electron-proton scattering the structure functions W_1 and W_2 are

$$W_1^{(el.)}(\nu, Q^2) = \frac{Q^2}{4M}\,\delta\left(\frac{Q^2}{2M} - \nu\right) G_M^{(p)}(-Q^2) \quad (1.13a)$$

$$W_2^{(el.)}(\nu, Q^2) = \frac{M}{\left(1 + \frac{Q^2}{4M^2}\right)}\,\delta\left(\frac{Q^2}{2M} - \nu\right)\left\{G_E^{(p)}(-Q^2) + \frac{Q^2}{4M^2}G_M^{(p)}(-Q^2)\right\} . \quad (1.13b)$$

So far we have dealt with unpolarized phenomena. It would be useful to find expressions for the differential cross sections when the proton target and the electron beam are polarized.

The differential cross section $\frac{d^2\sigma(\uparrow\uparrow)}{dE'd\Omega'}$ when the spins of the beam electron and the target proton are parallel is found to be [see for example Ref. 9 and A.3.15].

$$\frac{d^2\sigma(\uparrow\uparrow)}{dE'd\Omega'} = \frac{\alpha^2}{2Q^4}\frac{E'}{ME}\left\{L^{\mu\nu}(S)W_{\mu\nu}(S) + L^{\mu\nu}(A)W_{\mu\nu}(A)\right\} . \quad (1.14)$$

The corresponding expression when the spins are antiparallel is (see A.3.16)

$$\frac{d^2\sigma(\uparrow\downarrow)}{dE'd\Omega'} = \frac{\alpha^2}{2Q^4}\frac{E'}{ME}\left\{L^{\mu\nu}(S)W_{\mu\nu}(S) - L^{\mu\nu}(A)W_{\mu\nu}(A)\right\} \quad . \quad (1.15)$$

The tensons $L^{\mu\nu}(S)$, $L^{\mu\nu}(A)$, $W^{\mu\nu}(S)$ and $W^{\mu\nu}(A)$ appearing in Eqs. (1.14) and (1.15) are defined in Appendix 3c.

A useful measurable physical quantity is the asymmetry defined by

$$A = \frac{d\sigma(\uparrow\uparrow) - d\sigma(\uparrow\downarrow)}{d\sigma(\uparrow\uparrow) + d\sigma(\uparrow\downarrow)} \quad . \quad (1.16)$$

Using the analytic expressions for $L_{\mu\nu}$ and $W_{\mu\nu}$ the asymmetry A takes on the form

$$A = \frac{(E+E'\cos\theta)d(\nu,Q^2) + (E-E'\cos\theta)g(\nu,Q^2)}{4W_1(\nu,Q^2) + 2W_2(\nu,Q^2)\cot^2\frac{\theta}{2}} \quad (1.17)$$

where the functions $d(\nu,Q^2)$ and $g(\nu,Q^2)$ are scalars depending on ν and Q^2.

The deep inelastic region (DIR) of the process $e^- + p \to e^- + X$ is defined as the region where

$$Q^2 \gg M^2 \ , \ \nu \gg M \ , \ (p+q)^2 \gg M^2, \ 0 \leq x \leq 1 \quad \left(x = \frac{Q^2}{2M\nu}\right).$$

In fact this is the definition of the DIR of any process of the form $\ell + h \to \ell' + X$, where ℓ and ℓ' denote leptons.

I3) The Reaction $p + p \to \mu^- \mu^+ + X$ and Electron-Positron Annihilation Phenomena

Another process of interest is the reaction $p + p \to \mu^- \mu^+ + X$ or in general $h_1 + h_2 \to \ell\bar{\ell} + X$ where h_1 and h_2 denote hadrons and $\ell\bar{\ell}$ a lepton antilepton pair. This was the process used at Brookhaven for the observation of the recently discovered ψ particle; this was first detected [10] at Brookhaven as a resonance with a mass of 3.105 GeV which annihilates into an $e^- e^+$ pair.

If we forget for the time being the problem of the new ψ particle then the above process, in lowest order of $\alpha = \frac{e^2}{4\pi}$, is assumed to take place as is shown in Fig. 3.

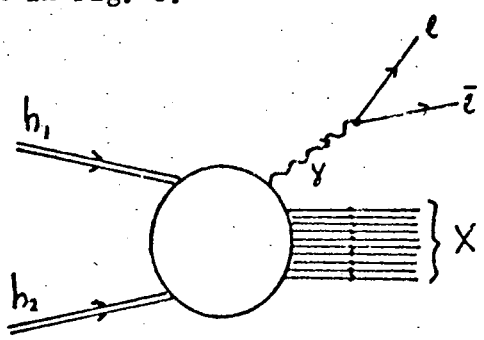

FIGURE 3: The lepton pair production process hadron$_1$-hadron$_2 \to \ell\bar{\ell} + X$

That is the two hadrons h_1 and h_2 collide and the lepton-antilepton pair emerges from the annihilation of one photon.

Experimentally the differential cross section $\frac{d\sigma}{dQ^2}$ is measured, where Q^2 is the mass of the $\ell\bar{\ell}$ pair.

The differential cross section $\frac{d\sigma}{dQ^2}$ is given by [see for example Ref. 11 and 12].

$$\frac{d\sigma}{dQ^2} = \frac{4\pi\alpha^2}{3Q^2}\left(1 + \frac{2m^2}{Q^2}\right)\left(1 - \frac{4m^2}{Q^2}\right)\frac{W(s,Q^2)}{\left\{[s-(M_1+M_2)^2][s-(M_1-M_2)^2]\right\}^{1/2}} \quad (1.18)$$

M_1 and M_2 denote the masses of the hadrons h_1 and h_2 respectively, m is the leptonic mass and Q^2 is the mass of the $\ell\bar{\ell}$ pair. The dimensionless structure function $W(s,Q^2)$ is given by the expression

$$W(s,Q^2) = -\int d^4x \int d^4q\, e^{-iq\cdot x}\, \delta^{(+)}(q^2-Q^2) \langle p_1 p_2(in)|j^\mu(x)\, j_\mu(0)|p_1 p_2(in)\rangle \,. \quad (1.19)$$

p_1 and p_2 are the momenta of h_1 and h_2 and the variable s is given by $s = (p_1+p_2)^2$. In Eq. (1.19) the state $|p_1p_2(in)\rangle$ of the incoming hadrons is normalized covariantly (see . A.1.29) .

Finally a few words concerning the reaction $e^-+e^+ \to$ Hadrons which is of great importance in the current e^-e^+ colliding beam experiments.

Again putting aside problems connected with the ψ particle this process is supposed to occur through the formation of a photon which in turn annihilates to give hadrons. The pictorial representation of the process is shown in Fig. 4.

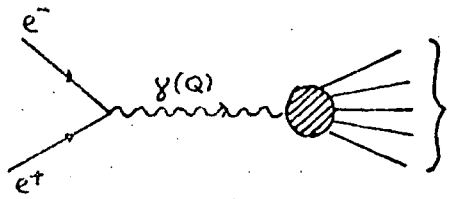

FIGURE 4: Electron-positron annihilation into hadrons via the formation of a timelike photon.

The total cross-sections $\sigma(e^-e^+ \xrightarrow[\gamma]{} \text{Hadrons})$ is given thus by [13]

$$\sigma(e^-e^+ \xrightarrow[\gamma]{} H) = \frac{16\pi\alpha^2}{Q^2}\,\pi(Q^2) \quad (1.20)$$

where $\pi(Q^2)(Q_\mu Q_\nu - Q^2\delta_{\mu\nu}) \equiv$

$$(2\pi)^3 \sum_n \delta^{(4)}(p_n - Q)\langle 0|j_\mu(0)|n\rangle\langle n|j_\nu(0)|0\rangle \,. \quad (1.21)$$

Q^μ is the four vector $(K_1 + K_2)^\mu$ with K_1, K_2 being the four momenta of the electron and positron respectively. In Eq. (1.21) the summation $\sum_n$ is over all final hadronic states.

The total cross-section for the reaction $e^- + e^+ \to \mu^- + \mu^+$ to lowest order of quantum electrodynamics is given by

$$\sigma(e^-e^+ \to \mu^-\mu^+) = \frac{4\pi\alpha^2}{3Q^2} \quad . \tag{1.22}$$

Thus the ratio R defined as

$$R = \frac{\sigma(e^-e^+ \to \text{Hadrons})}{\sigma(e^-e^+ \to \mu^-\mu^+)} \tag{1.23}$$

on account of Eqs. (1.20) and (1.22), is given by the following expression

$$R = 12\pi\, \pi(Q^2) \quad . \tag{1.24}$$

Recent experiments [see, for example, Ref. 14] have measured this ratio for Q^2 up to 25 $(\text{GeV})^2$. This ratio as a function of the variable $\sqrt{Q^2}$ rises and for $\sqrt{Q^2}$ = 5 GeV takes a value between 5 and 6. Data for even higher energies are expected to see the asymptotic behaviour of this ratio for high Q^2.

The reaction $e^- + e^+ \to$ hadron + X is also interesting and will be discussed later on when applying parton model techniques.

Excellent reviews on electron-positron annihilation phenomena can be found in the literature [see for example Ref. 15,16,17].

I4) Bjorken Scaling and Physical Significance of the Structure Functions W_1 and W_2.

a) Bjorken Scaling

In deriving the unpolarized differential cross-section given by Eq. (1.10) use was made of the tensons $L^{\mu\nu}$ and $W^{\mu\nu}$, (see Appendix 3a). In fact the differential cross-section $\frac{d^2\sigma}{d\Omega' dE'}$, is proportional to $L_{\mu\nu} W^{\mu\nu}$ i.e.

$$\frac{d^2\sigma}{d\Omega' dE'} \propto L_{\mu\nu} W^{\mu\nu} \quad . \tag{1.25}$$

The tensor $W^{\mu\nu}$, which is dimensionless, depends on the variables p (proton's momentum) and q(=K-K′). Its general form, obeying current conservation and parity-invariance, is

$$\left.\begin{aligned} W^{\mu\nu}(p,q) = -\left(g^{\mu\nu} - \frac{q^\mu q^\nu}{q^2}\right) W_1(\nu', Q^2) + \\ \frac{1}{M^2}\left(p^\mu - \frac{p\cdot q}{q^2} q^\mu\right)\left(p^\nu - \frac{p\cdot q}{q^2} q^\nu\right) W_2(\nu', Q^2) \, . \end{aligned}\right\} \tag{1.26}$$

The variable ν' which appears in (1.26) is the invariant $\nu' \equiv p.q$ which is related to $\nu = \frac{p.q}{M}$, defined before, by $\nu' = M\nu$. The reason we prefer to work with ν' instead of ν, in this section, is that ν' has the same dimensions as q^2 and thus more convenient in handling dimensional analysis arguments.

Because $W^{\mu\nu}$ is dimensionless it seems reasonable to assume that $W^{\mu\nu}$ scales under the transformation $p \to \lambda p$, $q \to \lambda q$, provided all masses and all dimensional coupling constants are zero. In order for the tensor $W^{\mu\nu}$ to be invariant under the above scale transformation

the functions W_1 and W_2 should undergo the following transformations

$$W_1(\nu', Q^2) \to W_1(\nu', Q^2) \tag{1.27a}$$

$$W_2(\nu', Q^2) \to \lambda^{-2} W_2(\nu', Q^2) \quad . \tag{1.27b}$$

From Eqs. (1.27) it is easy to see that the functions $W_1(\nu', Q^2)$ and $\nu' W_2(\nu', Q^2)/M^2$ scale under the transformation $\nu' \to \lambda\nu'$, $Q^2 \to \lambda Q^2$ i.e.

$$W_1(\nu', Q^2) \to W_1(\nu', Q^2) \tag{1.28a}$$

$$\frac{\nu' W_2(\nu', Q^2)}{M^2} \to \frac{\nu' W_2(\nu', Q^2)}{M^2} \quad . \tag{1.28b}$$

Using the variable ν instead of ν', from (1.28), we have that the functions $W_1(\nu, Q^2)$ and $\frac{\nu W_2(\nu, Q^2)}{M}$ scale under the transformation $\nu \to \lambda\nu$ and $Q^2 \to \lambda Q^2$; thus they are functions of the dimensionless variable $x \equiv \frac{Q^2}{2M\nu}$. So from dimensional analysis arguments we deduce that

$$W_1(\nu, Q^2) = F_1(x) \tag{1.29a}$$

$$\frac{\nu W_2(\nu, Q^2)}{M} = F_2(x) \tag{1.29b}$$

with $F_1(x)$ and $F_2(x)$ dimensionless functions depending only on the variable x.

Bjorken [20] proposed that Eqs.(1.29) might hold in the limit $\nu, Q^2 \to \infty$ and x = fixed in which case all masses and dimensional coupling constants become irrelevant. The limit $\nu, Q^2 \to \infty$ and x = fixed is called "Bjorken limit".

Experimental data seem to support this scaling hypothesis [21]. We look for scaling behaviour in the data by studying the functions $\nu W_2(\nu, Q^2)/M$ and $W_1(\nu, Q^2)$ for fixed value of x and varying Q^2. If these functions tend to limiting values as Q^2 becomes large then we say that we have scaling.

For inelastic electron-proton scattering this phenomenon was observed for values of $Q^2 \geq 1$ GeV^2 and $W \geq 2$ GeV, where W is defined by

$$W^2 \equiv (p+q)^2 = M^2 - Q^2 + 2M\nu \quad . \qquad (1.30)$$

$W \geq 2$ GeV means that we stay away from the region with the prominent neudeon resonances, because W^2 represents the virtual photon - proton energy squared.

This scaling phenomenon is one of the most exciting parts of today's physics. It tells us something about the hadronic structure but what exactly nobody knows.

Physicists have tried to tackle the problem of scaling in various ways. Some people use dilatation invariance techniques [see for example Ref. 18,19], some others prefer to work in the area of the light cone physics [22,23,24] or asymptotic freedom [25,26]. We will not choose any of these ways but we will limit ourselves to the parton model which will be discussed extensively in the next chapter.

b) Physical Significance of $W_1(\nu,Q^2)$ and $W_2(\nu,Q^2)$

The structure functions W_1 and W_2 are the absortive parts of the forward Compton scattering amplitude (spin averaged).

If we denote by σ_T and σ_s the total cross-sections for off-shell ($Q^2 \neq 0$) transverse and scalar photons respectively then we have the following relations [see for example Ref. 8,27,28]

$$W_1(\nu, Q^2) = \frac{K}{4\pi^2\alpha}\,\sigma_T \qquad (1.31)$$

and also,

$$W_2(\nu, Q^2) = \frac{K}{4\pi^2\alpha}\left(\frac{Q^2}{Q^2+\nu^2}\right)(\sigma_T+\sigma_s)\ . \qquad (1.32)$$

The flux factor K becomes equal to ν when $Q^2 = 0$, that is when we have scattering by real photons, while for virtual photons K is arbitrary. Gilman [29] takes this factor to be $K = M(\nu^2 + Q^2)^{1/2}$ while Hand [30] takes it to be $K = M\nu - \frac{Q^2}{2}$.

The function $W_2(\nu,Q^2)$ must have a zero for $Q^2 = 0$ [see for example Ref. 31]; this is obvious from (1.32b) from which it follows that

$$\lim_{Q^2\to 0}\left(\frac{W_2}{Q^2}\right) = \lim_{Q^2\to 0}\frac{K}{4\pi^2\alpha}\,\frac{(\sigma_T+\sigma_s)}{(Q^2+\nu^2)}\ . \qquad (1.33)$$

Since $\lim_{Q^2\to 0}\sigma_T \neq 0$ and $\lim_{Q^2\to 0}\sigma_s = 0$ we get,

from (1.33), $\lim_{Q^2\to 0}\left(\frac{W_2}{Q^2}\right) \neq 0$ and consequently

$$\lim_{Q^2\to 0} W_2(\nu, Q^2) = 0\ . \qquad (1.34)$$

Another important physical quantity is the ratio $R = \frac{\sigma_s}{\sigma_T}$ which is independent of the choice of the flux factor K.

This quantity has been measured and data show that R has a rather small value, in fact $R = .18 \pm .05$ when $0 < \omega = \frac{1}{x} < 10$, and does not depend strongly on ω or Q^2 or ν [32].

In the next chapter we shall see that the smallness of the quantity R means that the majority of the charged constituents inside the proton must carry spin $^1/2$.

I5) Neutrino Induced Reactions.

So far we have dealt only with electromagnetic interactions which are mediated by the exchange of a photon and in which the only leptons participating are the electron the muon and their antiparticles.

In the recent years new techniques have been developed [at CERN and NAL] which allow the production of neutrino and antineutrino beams, and high energy neutrino experiments can be performed.

The inclusive reactions $\nu + N \rightarrow \mu^- + X$ and $\bar{\nu} + N \rightarrow \mu^+ + X$, with N denoting a neucleon and $\mu^-(\mu^+)$ a muon (antimuon), have been studied both at CERN and NAL.

To lowest order, the interactions are assumed to go via the exchange of W - boson as is shown in Fig. 5a and 5b.

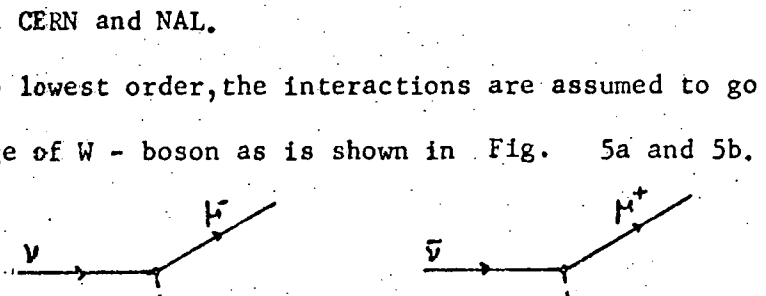

FIGURE 5: W-boson exchange diagrams contributing to the charged current reactions a) $\nu + N \rightarrow \mu^- + X$ and b) $\bar{\nu} + N \rightarrow \mu^+ + X$.

The leptonic vertex has the structure $\sim\{\bar{\mu}\gamma^{\mu}(1-\gamma_5)\nu_{\mu}+(\mu\rightleftarrows e)\}W_{\mu}$ and the coupling constant is g_w. The W^{μ} is the charged vector boson field mediator of the weak processes and analog of the photon in quantum electrodynamics.

The interaction Lagrangian describing the above processes has the form [see for example Ref . 1,2]

$$\mathcal{L} = g_w \left[J_{\mu}^{(-)} W^{\mu +} + J_{\mu}^{(+)} W^{\mu} \right] . \qquad (1.35)$$

The weak current $J_{\mu}^{(-)}$ consists of a leptonic and a hadronic part, the leptonic being

$$J_{\mu}^{(-)\,\text{lep's.}} = \bar{e}\gamma_{\mu}(1-\gamma_5)\nu_e + \bar{\mu}\gamma_{\mu}(1-\gamma_5)\nu_{\mu} . \qquad (1.36)$$

The hadronic part is not known explicity,what we know from experiments is that it contains a strangeness changing ($\Delta S = 1$) and a nonchanging ($\Delta S = 0$) part.

The mass of the vector boson W is assumed to be heavy and from this we have the connection between the current-current theory coupling constant G and the ratio g_w/M_w

$$\frac{G}{\sqrt{2}} = \left(\frac{g_w}{M_w}\right)^2 .$$

It is well known that G has a value which approximately is

$$G \simeq 1.01 \times 10^{-5}/M^2_{\text{proton}} .$$

The differential cross-sections for the reactions $\nu + N \rightarrow \mu^- + X$ and

$\bar{\nu} + N \to \mu^+ + X$ are calculated in exactly the same way as the corresponding expressions in the process $e^- + p \to e^- + X$.

The differential cross sections have the following forms [see for example Ref. 8 and A.3.19]

$$\frac{d^2\sigma^{\nu,\bar{\nu}}}{dE'd\Omega'} = \frac{G^2}{2\pi^2}\frac{E'^2}{M}\left\{2W_1(\nu,Q^2)\sin^2\frac{\theta}{2} + W_2(\nu,Q^2)\cos^2\frac{\theta}{2} \mp \left(\frac{E+E'}{M}\right)W_3(\nu,Q^2)\sin^2\frac{\theta}{2}\right\}. \quad (1.37)$$

The -(+) sign stands for neutrino (antineutrino). In terms of the $Q^2 = -q^2$ and $\nu = p.q/M$ variables we have

$$\frac{d^2\sigma^{\nu,\bar{\nu}}}{dQ^2d\nu} = \frac{G^2}{2\pi^2}\frac{E'}{E}\left\{2W_1(\nu,Q^2)\sin^2\frac{\theta}{2} + W_2(\nu,Q^2)\cos^2\frac{\theta}{2} \mp \left(\frac{E+E'}{M}\right)W_3(\nu,Q^2)\sin^2\frac{\theta}{2}\right\}. \quad (1.38)$$

The structure functions $W_{1,2,3}$ are again dimensionless. Similar arguments to those used in electroproduction to derive the scaling law of the functions $W_1^{(ep)}$ and $\nu W_2^{(ep)}/M$ can be used in the neutrino case. The result is that in the Bjorken limit, $Q^2 \to \infty$ and x = fixed, the functions W_1, $\nu W_{2,3}/M$ scale, that is

$$W_1(\nu,Q^2) \doteq F_1(x) \quad (1.39a)$$

$$\frac{\nu W_{2,3}(\nu,Q^2)}{M} \doteq F_{2,3}(x) \quad (1.39b)$$

Note that a superscript should have been used in the $W_{1,2,3}$ and $F_{1,2,3}$ functions to indicate that we are dealing with neutrino or antineutrino processes and which have been omitted for simplicity reasons.

The scaling behaviour (1.39) can be easily tested as we shall see later.

Using the variables $x = \frac{Q^2}{2M\nu}$ and $y = \frac{\nu}{E}$ and assuming scaling we have

$$\frac{d^2\sigma^{\nu,\bar{\nu}}}{dx\,dy} = \frac{G^2ME}{\pi}\left\{ xy^2 F_1^{(\nu,\bar{\nu})}(x) + \left(1 - y - \frac{Mxy}{2E}\right) F_2^{(\nu,\bar{\nu})}(x) \mp \right.$$
$$\left. \mp xy\left(1 - \frac{y}{2}\right) F_3^{(\nu,\bar{\nu})}(x) \right\} . \qquad (1.40)$$

Using the Callan-Gross [33] relation

$$F_2(x) = 2x F_1(x) \qquad (1.41)$$

Eq. (1.40) takes on the form

$$\frac{d^2\sigma^{\nu,\bar{\nu}}}{dx\,dy} = \frac{G^2ME}{\pi} x\left\{ (1-y)^2\left(F_1 \pm \frac{F_3}{2}\right)^{(\nu,\bar{\nu})} + \left(F_1 \mp \frac{F_3}{2}\right)^{(\nu,\bar{\nu})} \right\} -$$
$$- \frac{G^2M}{\pi} x^2 y F_1^{(\nu,\bar{\nu})}(x) \quad . \qquad (1.42)$$

In (1.42) the sign +(-) stands for neutrino (antineutrino). Eqs. (1.40) and (1.42) hold when the beam energy E satisfies $E \ll \frac{M_W^2}{2M_r}$; in the case we have high beam energies such that $E \sim \frac{M_W^2}{2M}$, then in (1.40) and (1.42) we make the substitution

$$G^2 \to \frac{G^2}{\left(1 - 2xyE\,M/M_W^2\right)} \quad .$$

The total cross-sections $\sigma^{\nu,\bar{\nu}}$ follow directly from either (1.40) or (1.42) by integrating with respect x and y

$$\sigma^{\nu,\bar{\nu}}(E) = A^{\nu,\bar{\nu}} E + B^{\nu,\bar{\nu}} \quad . \qquad (1.43)$$

Thus if scaling holds a linear behaviour of the total cross-sections in the neutrino (antineutrino) energy is expected for energies such that $E \ll \frac{M_W^2}{2M}$. This linear behaviour is supported by data from CERN [34] where we have energies up to $E \simeq 10$ GeV and from NAL [35] where the beam energies reach $E \simeq 200$ GeV.

The structure functions $W_{1,2,3}$ are connected with the absorption cross-sections for longitudinal (σ_s), left-handed (σ_L) and right-handed (σ_R) W-bosons in the following way [see for example Ref. 8,27]

$$\sigma_s = \frac{\pi}{K}\left[\left(\frac{Q^2+\nu^2}{Q^2}\right)W_2 - W_1\right] \qquad (1.44a)$$

$$\sigma_R = \frac{\pi}{K}\left[W_1 + \frac{(Q^2+\nu^2)^{1/2}}{2M}W_3\right] \qquad (1.44b)$$

$$\sigma_L = \frac{\pi}{K}\left[W_1 - \frac{(Q^2+\nu^2)^{1/2}}{2M}W_3\right] \qquad (1.44c)$$

From (1.44b) and (1.44c) we have $\sigma_R - \sigma_L \sim W_3$; in the photon case no W_3 structure function appeared because in electromagnetic interactions parity is conserved and so $\sigma_R = \sigma_L$ which implies $W_3 = 0$.

From the positivity of the σ_L, σ_R, σ_S one obtains the following inequalities

$$\left(1+\frac{\nu^2}{Q^2}\right)W_2 \geqslant W_1 \geqslant \frac{1}{2M}(Q^2+\nu^2)^{1/2}|W_3| \geqslant 0 \qquad (1.45)$$

In this section we discussed the neutrino induced reactions $\nu + N \to \mu^- + X$ and $\bar{\nu} + N \to \mu^+ + X$. The exchanged object mediating these processes is a charged W-boson and for this reason they are called "charged current" reactions.

In the next section we present the Weinberg-Salam model and its neutral current predictions.

I6) The Weinberg-Salam Model and Neutral Currents.

The Weinberg-Salam model [36,37] belongs to a class of gauge theories which have been proved to be renormalizable [38]. In these theories the massless scalar Goldstone bosons, through the Higgs mechanism [39], appear as longitudinal degrees of freedom of the gauge bosons which in this way become massive, while the photon remains massless. The Weinberg-Salam model is a renormalizable theory of weak and electromagnetic interactions, which involves neutral currents as we shall see in this section. There are also gauge theories which do not involve neutral currents; as a representative of such a theory without neutral currents, but involving heavy leptons instead, we mention the Georgi-Glashow model [40].

For a detailed discussion of those gauge theories we refer the reader to a report by E.S. Abers and B.W. Lee [41] and to B. Zumino [42]. We will not go into the details of the model; the only thing we require is the Weinberg-Salam (W-S) model interaction Lagrangian which will be used in forthcoming chapters.

The W-S model interaction Lagrangian is given by the expression [36]

$$\mathcal{L}_{W\text{-}S} = \frac{g}{2\sqrt{2}}\left[2J_\mu^{(-)}W^{\mu\,+} + 2J_\mu^{(+)}W^\mu\right] + \frac{g}{\cos\theta_W}\left[J_\mu^{(3)} - \sin^2\theta_W J_\mu^{(em)}\right]Z^\mu + g\sin\theta_W J_\mu^{(em)}A^\mu \,. \tag{1.46}$$

The constants g and the angle θ_w, the so called Weinberg angle, are the two parameters of the theory; W_μ is the W-boson field, A_μ the electromagnetic field and Z_μ a massive spin-1 field. The currents participating in the theory are defined in the following way; the gauge group of the theory is the SU(2) x U(1) and the leptons and hadrons of the theory are grouped in SU(2) "isospin" multiplets. The current $\vec{J}_\mu = (J_\mu^{(1)}, J_\mu^{(2)}, J_\mu^{(3)})$ is defined as

$$\vec{J}_\mu \overset{def.}{\equiv} \sum_i \bar{\psi}_i \gamma_\mu \vec{T} \psi_i \quad . \tag{1.47}$$

The index i runs over all the left-handed multiplets and $\vec{T} = (T_1, T_2, T_3)$ are the wellknown SU(2) isospin matrices. The current $J_\mu^{(\pm)}$, coupled to the W_μ-boson field, is defined by the following relation

$$J_\mu^{(\pm)} = J_\mu^{(1)} \pm i J_\mu^{(2)} \quad . \tag{1.48}$$

$J_\mu^{(em)}$ is the usual electromagnetic current.

There is another current in the $\mathcal{L}_{w-s}$, which is the so called neutral current, interacting with the Z_μ-vector boson. The neutral current is given by

$$J_\mu^{(neutral)} \overset{def}{\equiv} 2\left(J_\mu^{(3)} - \sin^2\theta_w J_\mu^{(em)}\right) \quad . \tag{1.49}$$

The left and right handed components of the leptons are grouped in SU(2) isospin multiplets as follows

$$L^{(e)} = \left(\frac{1-\gamma_5}{2}\right)\begin{pmatrix} \nu_e \\ e \end{pmatrix} \qquad \text{isospin-}\tfrac{1}{2} \tag{1.50a}$$

$$L^{(\mu)} = \left(\frac{1-\gamma_5}{2}\right)\begin{pmatrix}\nu_\mu\\ \mu\end{pmatrix} \qquad \text{isospin-}\frac{1}{2} \qquad (1.50b)$$

$$R^{(e)} = \left(\frac{1+\gamma_5}{2}\right) e \qquad \text{isospin-0} \qquad (1.50c)$$

$$R^{(\mu)} = \left(\frac{1+\gamma_5}{2}\right) \mu \qquad \text{isospin-0} \qquad . \qquad (1.50d)$$

It is easy to verify that the leptonic part of the current $J_\mu^{(+)}$ is given by

$$J_\mu^{(+)} = \bar{\nu}_e \gamma_\mu \left(\frac{1-\gamma_5}{2}\right) e + \bar{\nu}_\mu \gamma_\mu \left(\frac{1-\gamma_5}{2}\right) \mu \qquad (1.51)$$

and thus From Eq. (1.46) we identify the first term of the Lagrangian $\mathcal{L}_{w-s}$ as the well-known interaction Lagrangian governing the weak processes, provided that $\frac{g}{2\sqrt{2}} = g_w$. The hadrons involved in the theory are assumed to be the three quark fields p, n, and λ, well-known from SU(3) considerations, and another fourth quark denoted by p' introduced by S.L. Glashow, J. Iliopoulos and L. Maiani [43] characterized by a quantum number called "charm."

We wish to say a few words about this new quark. The SU(3) group can be enlarged to a SU(4) group if one introduces as the fourth member the new quark p'. This new particle is assumed to have a new quantum number, called "charm," equal to one. We can group the mesons and baryons in representations of $\{4\}\otimes\{\bar{4}\}$ and $\{4\}\otimes\{4\}\otimes\{4\}$ respectively [44]. It is obvious that new hadrons are predicted in this new SU(4) scheme which had not been observed little time ago; however in November of 1974 a new particle was discovered at NAL [10] having a mass 3.105 GeV. This new particle called ψ (3.105) was also

detected at ADONE[45] and SLAC[46]. The ψ particle annihilates into e^-e^+ as was said previously in this chapter. Little time after the discovery of ψ (3.105) another new particle ψ' having a mass 3.7GeV was reported to have been observed [47]. It is believed that the new particles are new mesons which belong to the $\{15\}$ representation of SU(4) and so "charm" appears to be established by the discovery of ψ and ψ'.

The four hadrons p,n,λ and p' are organized in left and right-handed SU(2) isospin multiplets as follows

$$L^{(p)} = \left(\frac{1-\gamma_5}{2}\right)\begin{pmatrix} p \\ n_c \end{pmatrix} \qquad \text{isospin-}\frac{1}{2} \qquad (1.52a)$$

$$L^{(p')} = \left(\frac{1-\gamma_5}{2}\right)\begin{pmatrix} p' \\ \lambda_c \end{pmatrix} \qquad \text{isospin-}\frac{1}{2} \qquad (1.52b)$$

$$R^{(p)} = \left(\frac{1+\gamma_5}{2}\right)p, \quad R^{(p')} = \left(\frac{1+\gamma_5}{2}\right)p' \qquad \text{isospin-0} \qquad (1.52c)$$

$$R^{(n_c)} = \left(\frac{1+\gamma_5}{2}\right)n_c, \quad R^{(\lambda_c)} = \left(\frac{1+\gamma_5}{2}\right)\lambda_c \qquad \text{isospin-0} \; . \qquad (1.52d)$$

The "Cabibbo-rotated" quarks are defined as

$$n_c = n\cos\theta_c + \lambda\sin\theta_c \qquad (1.53a)$$

$$\lambda_c = -n\sin\theta_c + \lambda\cos\theta_c \; . \qquad (1.53b)$$

θ_c is the well-known Cabibbo angle. It is a straightforward calculation to prove that the hadronic contribution to the current $J_\mu^{(+)}$ is

$$\left.\begin{aligned} J_\mu^{(+)} = {} & \bar{p}\gamma_\mu\left(\frac{1-\gamma_5}{2}\right)n\cos\theta_c + \bar{p}\gamma_\mu\left(\frac{1-\gamma_5}{2}\right)\lambda\sin\theta_c - \\ & \bar{p}'\gamma_\mu\left(\frac{1-\gamma_5}{2}\right)n\sin\theta_c + \bar{p}'\gamma_\mu\left(\frac{1-\gamma_5}{2}\right)\lambda\cos\theta_c \; . \end{aligned}\right\} \qquad (1.54)$$

The first two terms of the current are recognized as the hadronic current of weak interactions containing a $\Delta S = 0$ and a $\Delta S = 1$ part. The last two terms describe the weak decays of the charmed particles consisting of a $\Delta S = 0$, $\Delta C = 1$ and $\Delta S = 1$, $\Delta C = 1$ part, where C denotes the charm quantum number.

As we said earlier two parameters g and θ_w enter the theory. We have already seen that for the first term of $\mathcal{L}_{w-s}$ to describe the weak interactions we must have $\frac{g}{2\sqrt{2}} = g_w$; similarly in order for the last term of $\mathcal{L}_{w-s}$ to describe the electromagnetic interactions we must have $g \sin\theta_w = e$, where e is the electron's charge.

This relation reduces the number of the parameters of the theory from two to one. The masses of the W and Z bosons in terms of the Weinberg angle are given by the following relations

$$M_w = \left(\frac{e^2\sqrt{2}}{8G}\right)^{1/2} \frac{1}{|\sin\theta_w|}, \quad M_z = \frac{M_w}{|\cos\theta_w|} . \qquad (1.55)$$

G is the current-current theory coupling constant ($G \simeq 1.01 \times 10^{-5}/m_p^2$).

Because of the relations (1.47) the masses of the vector bosons have lower bounds given by

$$M_w \geqslant 37\ \text{GeV}, \quad M_z \geqslant 74\ \text{GeV} . \qquad (1.56)$$

After reviewing the W-S model we are ready to talk about the inclusive processes $\nu + N \to \nu + X$ and $\bar{\nu} + N \to \bar{\nu} + X$.

The second term of the $\mathcal{L}_{w-s}$, the neutral current term ($\sim J_\mu^{(\text{neutral})} Z^\mu$), allows, to first order of the coupling constant G, the inclusive processes mentioned before to occur. Diagrammatically

the interaction is given by the following Feynman graph.

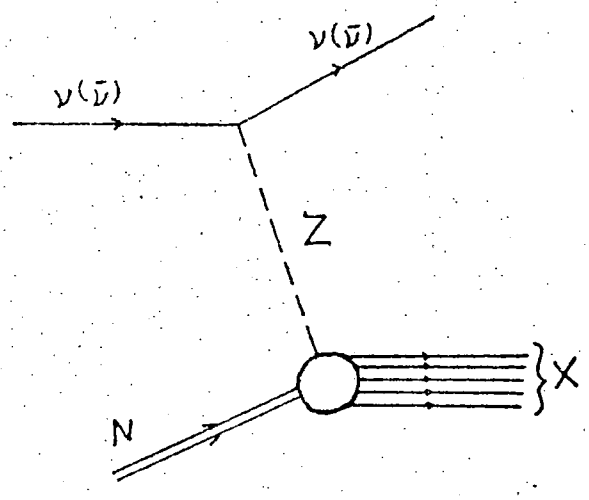

FIGURE 6: Z-boson exchange diagram contributing to the neutral current reactions $\nu(\bar{\nu}) + N \rightarrow \nu(\bar{\nu}) + X$

Experimentally the ratios $\frac{\sigma^{\nu N \rightarrow \nu X}}{\sigma^{\nu N \rightarrow \mu X}}$ and $\frac{\sigma^{\bar{\nu} N \rightarrow \bar{\nu} N}}{\sigma^{\bar{\nu} N \rightarrow \mu^+ X}}$ have been measured both at CERN [48] and NAL[49]. The detection of those ratios is of great importance since it shows that neutral currents exist.

Though the existence of the neutral current does not prove the validity of the Weinberg-Salam theory, it tells us that a good theory of weak and electromagnetic interactions must involve neutral currents. We shall see later, when dealing with parton models, that measurements of the ratios $\frac{\sigma^{\nu N \rightarrow \nu X}}{\sigma^{\nu N \rightarrow \mu^- X}}$ and $\frac{\sigma^{\bar{\nu} N \rightarrow \bar{\nu} X}}{\sigma^{\bar{\nu} N \rightarrow \mu^+ X}}$ might lead us to a determination of the Weinberg angle.

Discussion.

In this chapter we discussed inelastic processes in which leptons and hadrons were participating. The inelastic processes $e^- p \to e^- X$ $\nu N \to \mu^- X$ and $\bar{\nu} N \to \mu^+ X$ in their deep inelastic region are of great importance, since they might lead us to the solution of the problem as to what a hadron is made of. In these processes either a photon or a W-boson can be used as a probe for examining the internal structure of hadronic matter.

The early data from SLAC, on $e^- p \to e^- X$ scattering, revealed a new feature in the area of hadronic physics that of scaling. According to it the deep inelastic electroproduction functions $\frac{\nu W_2(\nu, Q^2)}{M}$ and $W_1(\nu, Q^2)$ are not functions of the two variables ν and Q^2 but they are functions of the ratio $x = \frac{Q^2}{2M\nu}$, when $Q^2 \geq 1$ GeV^2 and $(p + q)^2 \geq 4$ GeV^2. Bjorken had proposed such a scaling law in the kinematical region, $Q^2, \nu \to \infty$ and x = fixed, the so called "Bjorken limit". Data with neutrino and antineutrino beams soon followed and the reactions $\nu N \to \mu^- X$ $\bar{\nu} N \to \mu^+ X$ were studied. Bjorken scaling hypothesis applied to these processes gives total cross-sections which are linear functions of the beam energy. This linear behaviour is indeed confirmed by the experiments. During the last years experimental data on the deep inelastic region of the reactions $e^- p \to e^- X$, $\nu N \to \mu^- X$ and $\bar{\nu} N \to \mu^+ X$ have been accumulated and Bjorken scaling seems to be very well supported. Undoubtedly "scaling" is a striking phenomenon of the hadronic physics and makes the physics of deep inelastic phenomena one of the most exciting fields of research.

The inclusive processes $\nu N \to \nu X$ and $\bar{\nu} N \to \bar{\nu} X$ in their deep inelastic region are also important. In the last few years much progress has been made in the area of gauge theories and many theories for weak and electromagnetic interactions have been proved to be renormalizable. Some of these involve heavy leptons, not detected so far, and some others involve neutral currents. The Weinberg-Salam model for weak and electromagnetic interactions belongs to the last category. If neutral currents exist then events with no muons in the final state should be observed in the reactions $\nu_\mu N \to \nu_\mu X$ and $\bar{\nu}_\mu N \to \bar{\nu}_\mu X$; such muonless events were really observed first at CERN and later at NAL, and the ratios of the number of muonless events to the number of events with one muon in the final state, for both neutrino and antineutrino, were measured. This proves that neutral currents do exist and tells us that a good theory of weak and electromagnetic interactions must involve neutral currents.

Another great discovery, characterized by many as the discovery of the decade, is that of the new particles ψ and ψ'. If one enlarges the SU(3) group to an SU(4) by the introduction of a new quark p', in addition to the well known p,n and λ, which carries an additive quantum number called "charm", then the hadrons are classified in representations of this new group. Little time ago there was not any experimental support for the necessity of SU(4); in November of 1974 the ψ particle was discovered and a little later ψ' which decays into ψ plus two pions.

These new particles can be classified in the representation {15} of SU(4) which is the SU(4) extension of the SU(3) mesonic octet. According to SU(4) classification of hadrons further mesons and baryons,

some of them carrying and charm quantum number, must be observed. It is worth mentioning that the "charmed" quark p' had been proposed long time before the discovery of ψ's and its necessity is met also in the Weinberg-Salam model.

Scaling, neutral currents and the new particles were the basic parts of the first chapter though not discussed extensively.

The scaling behaviour of the structure functions, the detection of the neutral currents and the discovery of the new particles open new paths to the hadronic physics; however much work should be done in this area and this makes this part of hadronic physics more exciting.

CHAPTER II

Introduction

A large variety of theoretical models have been proposed in the last years in order to understand the physics of the deep inelastic phenomena. Among them is the parton model whose basic points are briefly discussed in this chapter.

The parton model idea was first applied in order to understand the physics of the process $e^- p \to e^- X$ in its deep inelastic region and is due originally to Feynman [50]. He assumed that the nucleon is built of fundamental pointlike constituents which he called "partons". If the time of interaction of the photon with the pointlike constituents is short, so that the constituents do not interact while the photon current acts, then the nucleon is viewed by the incoming photon as a bunch of free, static, components. This is the impulse approximation applied to inelastic electron-nucleon scattering, and holds in a frame in which the nucleon has infinite momentum. When viewed from this frame the proper motion of the constituents is slowed down because of time dilatation; on the other hand the nucleon is Lorentz-contracted in such a way as the incoming photon finds one parton with which it interacts while the remaining constituents, because of the time dilatation, are just spectators. Thus the scattering of the virtual photon by the nucleon is seen as scattering by the individual constituents.

This is, in brief, the naive parton model; we shall apply it to deep inelastic processes and make predictions. As we shall

see parton model implies scaling i.e. gives the scaling behaviour for the inelastic electroproduction and neutrino production structure functions. In this chapter the main parton formulae to be used subsequently are given and the Kuti-Weisskopf [51] quark parton model is discussed.

III) The Parton Model

In this section we discuss the parton model in more detail and in the next section we shall see its predictions for the structure functions of deep inelastic electroproduction and neutrino production scattering. There are many articles on the model where its principles and the fundamental formulae can be found [see for example Ref. 8,12,27 28, 52-59], since the model has been well advertized; here we limit ourselves to the most important features of the model.

We turn our attention to the electroproduction process $e^- + p \to e^- + X$; things are not altered substantially for other reactions like $\nu N \to \mu^- X$ or $\bar{\nu} N \to \mu^+ X$, say. The process is assumed to take place through the exchange of a photon as is shown in Fig. 2. Because the parton model is supposed to apply in frames in which the momentum of the proton is infinite, we work in such a frame and denote the proton's momentum by $\vec{P}$. If the proton consists of a number N of partons then the i^{th} parton carries a momentum $\vec{P}_i$ such that,

$$\vec{P}_i = x_i \vec{P} + \vec{K}_i \quad \text{with } o \leq x_i \leq 1 \qquad (2.1)$$

with $\vec{K}_i$ a small transverse momentum. From momentum conservation

we have that

$$\sum_{i=1}^{N} x_i = 1 \quad . \qquad (2.2)$$

The physical picture we want to employ is the following. The probe, a virtual photon, hits the proton and interacts with one of its constituents. During the interaction the remaining constituents are considered as free as we have said before. After the interaction takes place the partons are converted in hadrons [see Fig. 7].

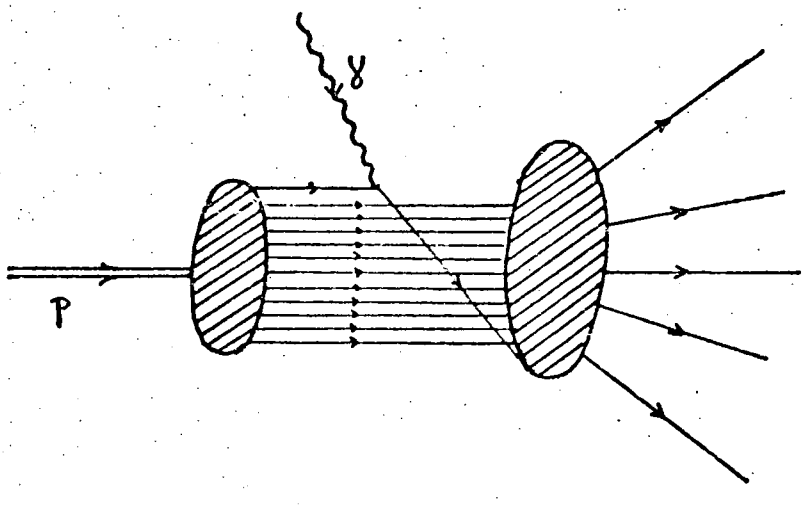

FIGURE 7: Parton-current interaction mechanism contributing to the process $e^- + p \rightarrow e^- + X$.

If the scattering from the individual partons is incoherent we write for the differential cross section $\frac{d\sigma}{dE'd\Omega'}$ of the process $e^- p \rightarrow e^- X$

$$\frac{d^2\sigma}{dE'd\Omega'} = \sum_i \int_0^1 f_i^{(p)}(x_i) \, \frac{d^2\sigma(x_i)}{dE'd\Omega'} \, dx_i \quad . \qquad (2.3)$$

In Eq. (2.3) the index i runs over the kinds of the partons and $f_i^{(p)}(x)$ denotes the average number of partons of i-type carrying fraction x of proton's momentum; $\frac{d^2\sigma(x_i)}{dE'd\Omega'}$ is the differential cross section for elastic scattering by this parton. Thus provided that there is a kinematical region for which incoherent scattering of the constituents occurs we will, perhaps, be able to make a prediction for the differential cross section of the process $e^- p \to e^- X$. The Bjorken region is such a kinematical region. The best frame to see this is the Breit frame of the parton and the photon it interacts with, as is represented in Fig. 8 [8].

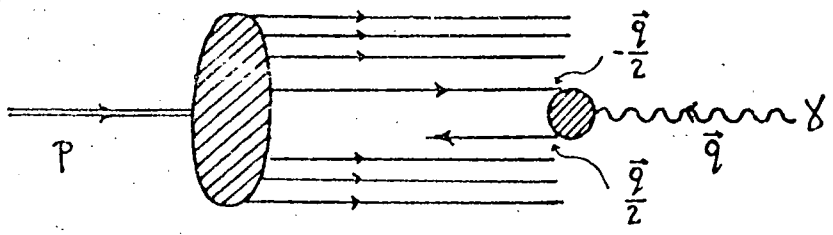

FIGURE 8: Parton-current interaction mechanism as is seen in parton's Breit frame.

The proton is moving along the z axis, say, having momentum $\vec{p}$. Each parton travels almost in the same direction with it (small tranverse momentum). If the photon has momentum $\vec{q}$ then the interacting partons have momenta $-\frac{\vec{q}}{2}$ and $\frac{\vec{q}}{2}$ respectively before and after the collision. Note that in this frame $q^\mu = (0,\vec{q})$ so that the Bjorken variable $x = \frac{Q^2}{2M\nu}$ is $x = \frac{|\vec{q}|}{2|\vec{p}|}$. The Bjorken limit is attained when $|\vec{p}| \to \infty$ keeping x = fixed; thus after the interaction the parton

has a large momentum $x|\vec{P}|$ and travels to the negative $\vec{P}$ direction while the other partons travel to the opposite direction. This scattered parton does not interact with the remaining constituents after its interaction with the photon.

At this point let us say something about the spin of partons. The Breit frame is the proper one for such a discussion. As is seen in Figure 8 the parton absorbs a photon which is virtual and so can be either longitudinal or transverse. If the parton has spin zero it carries no angular momentum along $\vec{q}$ and therefore it cannot absorb a transverse photon, thus $\sigma_T = 0$ and consequently $R = \frac{\sigma_s}{\sigma_T} = \infty$ for spin-0 partons. If the parton has spin-$\frac{1}{2}$ because its helicity is unchanged by the electromagnetic interaction in the limit of large $|\vec{q}|$, it follows that it must absorb one unit of spin from the photon; hence in this case $\sigma_s = 0$ and $R = 0$. Experimentally we know that this ratio R is small, in fact $R = .18 \pm .05$ [32,60] and the majority, if not all, of the partons would appear to carry spin-$\frac{1}{2}$.

The vanishing of σ_s has another consequence. From Eqs.(1.31) and (1.32) or (1.44a) in the Bjorken limit we have

$$2xW_1(\nu,Q^2) = \frac{\nu W_2(\nu,Q^2)}{M} \tag{2.4}$$

or, if scaling holds,

$$2xF_1(x) = F_2(x) \tag{2.5}$$

This is the well-known Callan-Gross relation [33].

Having discussed the general ideas of the parton model we now proceed to the point of calculating the physical quantities of interest.

II2) Parton Model Calculations.

As it is evident from (2.3) the cross sections $\frac{d^2\sigma(x_i)}{dE'd\Omega}$ must be calculated, when Q^2 is large and x=fixed (Bjorken limit), in order to calculate the electroproduction differential cross section.

In the limit of large proton's momenta, i.e. $|\vec{P}| \to \infty$, the momentum of the i-type parton is $P_i^\mu \simeq x_i P^\mu$ where P^μ is the proton's momentum.

From Eq. (1.10) we have

$$\frac{d^2\sigma(x_i)}{dE'd\Omega'} = \frac{4\alpha^2}{Q^4}\frac{E'^2}{M_i}\left\{2W_1^{(i)}(\nu,Q^2)\sin^2\frac{\theta}{2} + W_2^{(i)}(\nu,Q^2)\cos^2\frac{\theta}{2}\right\} \qquad (2.6)$$

with $M_i = x_i M$.

The functions $W_{1,2}^{(i)}$ are given by (1.13a) and (1.13b) with G_E, G_M replaced by the unity, since partons are assumed structureless.

If Q_i is the charge of the i-type quark we find,

$$W_1^{(i)}(\nu,Q^2) = Q_i^2\frac{x}{2}\delta(x-x_i) \qquad (2.7a)$$

$$\frac{\nu W_2^{(i)}(\nu,Q^2)}{M} = Q_i^2 x\,\delta(x-x_i) \qquad (2.7b)$$

with $x = \frac{Q^2}{2M\nu}$.

From Eqs. (2.3), (2.7a) and (2.7b) we derive the parton model electroproduction structure functions

$$W_1^{(ep)}(\nu,Q^2) \overset{Bj}{=} \frac{1}{2}\sum_i Q_i^2 f_i^{(p)}(x) \qquad (2.8a)$$

$$\frac{\nu W_2^{(ep)}(\nu,Q^2)}{M} \overset{Bj}{=} x\sum_i Q_i^2 f_i^{(p)}(x) \qquad (2.8b)$$

The symbol "B_j" above the equality sign indicates that these expressions are valid in the Bjorken limit. Note that $W_1^{(ep)}$ and $\nu W_3^{(ep)}/M$ are functions of the variable x alone, i.e. they scale; from here on we shall denote them by $F_1^{(ep)}(x)$ and $F_2^{(ep)}(x)$ respectively. $F_1^{(ep)}$ and $F_2^{(ep)}$ satisfy the Callan-Gross relation as can be verified from (2.8a) and (2.8b).

We now turn our attention to neutrino reactions and try to derive the corresponding unpolarized cross sections. As we have seen (see 1.46), the Lagrangian interaction has the form $\mathcal{L} = g_w[2J_\mu^{(-)}W^{\mu +} + h.c.]$; the leptonic and hadronic parts of $J_\mu^{(-)}$ are given in (1.51) and (1.54) respectively. To calculate the $\frac{d^2\sigma}{dE'd\Omega'}$ for the process $\nu N \to \mu^- X$ we need again the cross section $\frac{d^2\sigma(x_i)}{dE'd\Omega'}$ of the individual quarks. For the scattering $\nu n \to \mu^- p$ we find

$$\frac{d^2\sigma^{(\nu n)}(x_i)}{dE'd\Omega'} = \delta(x-x_i)\frac{G^2}{2\pi^2}\frac{E'^2}{M}\cos^2\theta_c\left\{\frac{2Mx}{\nu}\cos^2\frac{\theta}{2} + 2\left(1+\frac{Mx}{\nu}\right)\sin^2\frac{\theta}{2} + \left(\frac{E+E'}{M}\right)\frac{2M}{\nu}\sin^2\frac{\theta}{2}\right\}. \qquad (2.9)$$

Comparing (2.9) with (1.37) we have for the structure functions $W_{1,2,3}^{(\nu n)}$, regarding the scattering $\nu n \to \mu^- p$ in the Bjorken limit,

$$W_1^{(\nu n)}(\nu, Q^2) = \delta(x-x_i)\cos^2\theta_c \qquad (2.10a)$$

$$\frac{\nu W_2^{(\nu n)}(\nu, Q^2)}{M} = 2x\,\delta(x-x_i)\cos^2\theta_c \qquad (2.10b)$$

$$\frac{\nu W_3^{(\nu n)}(\nu, Q^2)}{M} = -2\,\delta(x-x_i)\cos^2\theta_c\,. \qquad (2.10c)$$

For the scattering $\nu\bar{p} \to \mu^- \bar{n}$, the structure functions are the same except for a minus sign in the W_3. The remaining structure functions can be derived easily. In general if a term $\frac{1}{2} f \bar{q}' \gamma^\mu (1-\gamma_5) q$ appears in the current $J^{(+)}_\mu$, then the structure functions $W_{1,2,3}$ and $W_{1,2,3}$ for scattering $\nu q \to \mu^- q'$ and $\nu\bar{q}' \to \mu^- \bar{q}$ respectively, are given by the following expressions

$$W_1^{(\nu s)}(\nu, Q^2) = f^2 \delta(x - x_i) \qquad (2.11a)$$

$$\frac{\nu W_2^{(\nu s)}(\nu, Q^2)}{M} = 2f^2 x\, \delta(x - x_i) \qquad (2.11b)$$

$$\frac{\nu W_3^{(\nu s)}(\nu, Q^2)}{M} = -2\epsilon_s f^2 \delta(x - x_i)\,. \qquad (2.11c)$$

In Eqs (2.11) "s" denotes either a q or a $\bar{q}'$ and ϵ_s is +1 for q and -1 for $\bar{q}'$.

The structure functions for the inclusive processes $\nu h \to \mu^- X$ and $\bar{\nu} h \to \mu^+ X$, with "h" denoting either a proton or a neutron, are calculated in the same way as we did for the electro production case. When the current is given by Eq. (1.54) the structure functions are given, above the charm production threshold, by the equations

$$F_1^{(\nu h)}(x) = f_n^{(h)}(x) + f_\lambda^{(h)}(x) + f_{\bar{p}}^{(h)}(x) + f_{\bar{p}'}^{(h)}(x) \qquad (2.12a)$$

$$F_3^{(\nu h)}(x) = -2\left\{ f_n^{(h)}(x) + f_\lambda^{(h)}(x) - f_{\bar{p}}^{(h)}(x) - f_{\bar{p}'}^{(h)}(x) \right\} \qquad (2.12b)$$

and

$$F_3^{(\bar{\nu}h)}(x) = f_p^{(h)}(x) + f_{p'}^{(h)}(x) + f_{\bar{n}}^{(h)}(x) + f_{\bar{\lambda}}^{(h)}(x) \qquad (2.13a)$$

$$F_3^{(\bar{\nu}h)}(x) = -2\left\{ f_p^{(h)}(x) + f_{p'}^{(h)}(x) - f_{\bar{n}}^{(h)}(x) - f_{\bar{\lambda}}^{(h)}(x) \right\} \qquad (2.13b)$$

The $F_2^{(\nu h, \bar{\nu} h)}$ are given by the Callan-Gross relation $F_2^{(\nu h, \bar{\nu} h)} = 2x\, F_1^{(\nu h, \bar{\nu} h)}$.

Before closing this section, for completeness we give the parton model result for the cross section $\frac{d\sigma}{dQ^2}$ of the process $p + p \to \ell\bar{\ell} + X$, where $\sqrt{Q^2}$ is the mass of the $\ell\bar{\ell}$ pair [see for example Ref. 56].

$$\frac{d\sigma}{dQ^2} = \frac{4\pi\alpha^2}{3Q^2}\,\frac{1}{s}\int_0^1 dx\,dy\,\delta(xy-\tau)\sum_i Q_i^2 f_i^{(p)}(x) f_{\bar{i}}^{(p)}(y) \qquad (2.14)$$

In this expression the variable τ is defined by $\tau = Q^2/s$. Note that $Q^4 \frac{d\sigma}{dQ^2}$ scales, that is it is a function of the variable τ only.

Having given the basic parton model formulae we are ready to make predictions provided that the explicit form of the distribution functions $f_i^{(h)}(x)$ is given.

II3) General Results of the Parton Model - Relations Among the Structure Functions.

There are several relations the distribution functions $f_i^{(h)}(x)$ should satisfy, and thus any reasonable quark parton model should respect them.

Since the physical meaning of the distribution functions $f_i^{(h)}(x)$ is the average number of quarks of type i carrying fraction x of hadron's "h" momentum, it follows that for any additive quantum number A

we have

$$\sum_i \int_0^1 A_i f_i^{(h)}(x)\,dx = A_h \quad . \tag{2.15a}$$

A_h is the quantum number of the hadron "h" and A_i the corresponding number for the quark i. Momentum, charge, baryon number, strangeness, third component of isospin and charm are additive quantum numbers and so from (2.15a) several sum rules can be derived. From (2.15a) we have, when A is the momentum,

$$\sum_i \int_0^1 x f_i^{(h)}(x)\,dx = 1 \tag{2.15b}$$

The proton and neutron distribution functions are connected by isospin reflection and one has the following relations

$$f_p^{(p)}(x) = f_n^{(n)}(x) \;,\quad f_n^{(p)}(x) = f_p^{(n)}(x) \;,\quad f_{\lambda,\lambda'}^{(p)}(x) = f_{\lambda,\lambda'}^{(n)}(x) \tag{2.16a}$$

$$f_{\bar{p}}^{(p)}(x) = f_{\bar{n}}^{(n)}(x) \;,\quad f_{\bar{n}}^{(p)}(x) = f_{\bar{p}}^{(n)}(x) \;,\quad f_{\bar{\lambda},\bar{\lambda}'}^{(p)}(x) = f_{\bar{\lambda},\bar{\lambda}'}^{(n)}(x) \quad . \tag{2.16b}$$

There are also several relations connecting the structure functions of the processes $e^-p \to e^-X$, $e^-n \to e^-X$, $\nu p \to \mu^-X$, $\bar{\nu}p \to \mu^+X$, $\nu n \to \mu^-X$ and $\bar{\nu}n \to \mu^+X$. We consider the case in which the Cabbibo angle θ_c is zero (for the case $\theta_c \neq 0$ see [8] and references therein).

The following relation is easily verified using our expression for the structure functions ($\theta_c = 0$)

$$2x\left(F_1^{(ep)} - F_1^{(en)}\right) = F_3^{(\nu p)} - F_3^{(\nu n)} \quad . \tag{2.17}$$

This relation depends on the charge of the constituents. In the Sakata (or Fermi-Yang) model the λ-quark is neutral and we find

$$4(F_1^{(ep)} - F_1^{(en)}) = F_3^{(\nu p)} - F_3^{(\nu n)} \quad . \tag{2.18}$$

Using the fact that $f_\lambda^{(p)}$, $f_{\bar{\lambda}}^{(p)} \geq 0$ the following inequality is derived (below the threshold for production of charmed states)

$$F_1^{(\nu p)} + F_1^{(\nu n)} \leq \frac{18}{5}\left(F_1^{(ep)} + F_1^{(en)}\right) \quad . \tag{2.19}$$

In the Sakata (or Fermi-Yang) model λ and $\bar{\lambda}$ do not contribute to $F_1^{(ep,en)}$ since they are neutral; in this case the inequality sign in (2.19) is replaced by equality sign and $\frac{18}{5}$ is replaced by 2.

The following relation known as Alder sum rule [61] also holds

$$\int_0^1 \frac{dx}{x}\left\{F_2^{(\nu n)} - F_2^{(\nu p)}\right\} = 2 \quad . \tag{2.20}$$

Another sum rule is [62]

$$\int_0^1 \left\{F_3^{(\nu p)} + F_3^{(\nu n)}\right\} dx = -6 \quad . \tag{2.21}$$

In the Sakata (or Fermi-Yang) model $6 \to -2$. Except the above relations and sum rules some useful inequalities can be also derived. One can easily verify that

$$\int_0^1 dx\, F_1^{(ep,en)}(x) \geq (\min Q_q^2) \sum_q \int_0^1 dx\, x f_q^{(p,n)}(x) \tag{2.22}$$

In (2.22) $\sum_q$ runs over all the charged constituents. Assuming that the only consistuents are the p,p',n and λ quarks plus some neutral ones, "gluons", we have min $Q_q^2 = \frac{1}{9}$ and $\sum_q \int_0^1 dx\, f_q^{(p,n)}(x) = 1-\epsilon$ where ϵ is the fraction of the proton's (or neutron's) momentum carried by the gluons.

From (2.22) we have then the inequality

$$\int_0^1 F_2^{(ep,en)}(x)\,dx \geq \frac{(1-\epsilon)}{9}, \quad 0 \leq \epsilon \leq 1 \quad . \tag{2.23}$$

Using the isospin reflection relations (2.16a) and (2.16b) and the fact that max $Q_q^2 = \frac{4}{9}$ we derive the inequality

$$\int_0^1 \left\{ F_2^{(ep)} + F_2^{(en)} \right\} dx \leq \frac{5}{9} \quad . \tag{2.24}$$

Several inequalities have been derived by Nachtmann [63] the most interesting being

$$\frac{1}{4} \leq \frac{F_2^{(en)}(x)}{F_2^{(ep)}(x)} \leq 4 \quad . \tag{2.25}$$

As we shall see later for $x \to 1$ the experimental data show that the $\frac{F_2^{(en)}}{F_2^{(ep)}}$ ratio tends to the lower limit of Nachtmann's inequality.

II4) The Kuti-Weisskopf Quark Parton Model

We have seen that all parton model formulae are expressed in terms of the distribution functions $f_i^{(h)}(x)$; so in order to make predictions and to compare with experiment, one has to know explicitly these distribution functions. In this section the Kuti-Weisskopf quark

parton model [51] is presented; this model based on simple assumptions leads to a determination of proton and neutron distribution functions.

The first assumption is that proton (or neutron) is made of three quarks the so-called "valence quarks", plus a sea of quark-antiquark pairs which is called "core". The valence quarks give proton (or neutron) the quantum numbers while the core carries vacuum quantum numbers. As we shall see later the valence quarks contribute to the nondiffractive scattering of the proton (or neutron) and the core contributes to the diffractive scattering; this will become clear when we have the explicit form of the distribution functions.

Except the quarks and antiquarks it is assumed that there are also additional core constituents, carrying zero charge, which are used to bind the quarks together to form the nucleon. These constituents are called "gluons".

Kuti and Weisskopf assumed that the probability distribution of quarks in the core is proportional to the phase space and is given by

$$dP_c(x) = \frac{8}{6} \frac{dx}{(x^2 + \mu^2/p^2)^{1/2}} \quad . \tag{2.26}$$

P is the proton's momentum and μ the quark mass; x is the fraction of proton's momentum carried by the quark. The factor "6" which appears in the denominator has been put for convenience.

The corresponding distribution for a valence quark is assumed to be

$$dP_v(x) = \frac{x^{1-\alpha(0)}}{(x^2 + \mu^2/p^2)^{1/2}} dx \quad . \tag{2.27}$$

The distribution of gluons is the same as in (2.26) but the factor g is different. The gluon distribution is therefore written as

$$dP_g(x) = g' \frac{dx}{(x^2 + \mu^2/p^2)^{1/2}} \quad . \tag{2.28}$$

With these assumptions the proton's distribution functions are calculated to be (for details see Ref. 51).

$$f_p^{(p)}(x) = 2v(x) + c(x) \quad , \quad f_n^{(p)}(x) = v(x) + c(x) \tag{2.29a}$$

$$f_{\bar{p}}^{(p)}(x) = f_{\bar{n}}^{(p)}(x) = f_{\lambda}^{(p)}(x) = f_{\bar{\lambda}}^{(p)}(x) = c(x) \tag{2.29b}$$

$$f_g^{(p)}(x) = 6 \frac{g'}{g} c(x) \tag{2.29c}$$

where the functions $v(x)$ and $c(x)$, known as valence distribution and core distribution functions, are given by

$$v(x) = B^{-1}(1-\alpha(0),\ \gamma + 2(1-\alpha(0)))\ x^{-\alpha(0)}\ (1-x)^{-1+\gamma+2(1-\alpha(0))} \tag{2.30a}$$

$$c(x) = \frac{g}{6}\ x^{-1}\ (1-x)^{-1+\gamma+3(1-\alpha(0))} \quad . \tag{2.30b}$$

The constant γ is given by $\gamma = g + g'$. In Eqs.(2.29) the superscript denotes a proton and the subscript the kind of the quark; g stands for gluon.

Note that in the limit $x \to 0$ the core contributions are the dominant ones while when $x \to 1$ the valence contribution dominate provided that $\alpha(0) < 1$.

The corresponding distribution functions for the neutrons are found if one uses the isospin reflection relations (2.16a) and (2.16b), and the fact $f_g^{(p)}(x) = f_g^{(n)}(x)$.

Note that in the original Kuti-Weisskopf model no charmed quarks appear the only constituents being the conventional quarks plus the gluons.

The model has three parameters g, g' and $\alpha(0)$. The electroproduction structure function $F_2^{(ep)}(x)$ is found by using (2.8b) and Eqs.(2.29), and has the form

$$F_2^{(ep)}(x) = x\,u(x) + \frac{4}{3}\,x\,c(x) \quad . \tag{2.31}$$

Similarly for the neutron

$$F_2^{(en)}(x) = \frac{2}{3}\,x\,u(x) + \frac{4}{3}\,x\,c(x) \quad . \tag{2.32}$$

Note that the ratio $F_2^{(en)}/F_2^{(ep)}$ has the value $^2/3$ for $x = 1$; this is in disagreement with the data which show that this ratio is close to $^1/4$ for $x \sim .8$ [77] .

The asymptotic behaviour of $F_2^{(ep,en)}$ near $x \approx 1$ is given by

$$F_2^{(ep,en)}(x) \underset{x\to 1}{\sim} (1-x)^{-1+\gamma+2(1-\alpha)} \quad . \tag{2.33}$$

Kuti and Weisskopf using a relation found by Bloom and Gilman [64] find that

$$-1 + \gamma + 2(1-\alpha(0)) = 3 \tag{2.34}$$

and thus the number of parameters is reduced to one.

Applying Regge phenomenology we can have an estimate for the parameter $\alpha(0)$.

The Regge limit for the virtual processes $\gamma(Q^2)+p \to \gamma(Q^2)+p$ and $\gamma(Q^2)+n \to \gamma(Q^2)+n$ is approached when the mass Q^2 of the photon is kept fixed while the energy ν tends to infinity. Thus the Regge limit is obtained for Q^2 = fixed and $x \to 0$. The structure functions $F_2^{(ep)}$ and $F_2^{(en)}$ are the imaginary parts of the amplitudes† for the processes mentioned before . In the limit $x \to 0$ the core part approaches a constant value suggesting it to be the "diffractive" part of the process. The valence parts of $F_2^{(ep)}$ and $F_2^{(en)}$ are different; the difference $F_2^{(ep)}-F_2^{(en)}$ should be mediated by the exchange of an A_2 Regge frajectory which for $t = 0$ has intercept $\alpha_{A_2}(0) = \frac{1}{2}$. So we conclude that $\alpha(0)$ must be taken equal to $1/2$ at least for values of x close to zero.

Taking this value for the parameter $\alpha(0)$ the functions $v(x)$ and $c(x)$ have the forms

$$v(x) = B^{-1}\left(\tfrac{1}{2}, 4\right)\ x^{-1/2}(1-x)^3 \qquad (2.35a)$$

$$c(x) = \frac{g}{6}x^{-1}(1-x)^{7/2} \qquad (2.35b)$$

There is only one parameter left now and this is estimated by fitting the electroproduction data. A good fit is obtained by taking $g = 1$ [51] and consequently $g' = 2$. This tells us that

---

† In the forward direction.

the number of gluons in the core is twice the number of quarks and antiquarks in the core. With the same value for the parameter "g" a good fit to the $p + p \rightarrow \mu^- \mu^+ + X$ data† is obtained.

We do not wish to discuss the model any further, the details of it can be found in the Kuti-Weisskopf paper [51] .

II5) Neutrino Induced Reactions and the Kuti-Weisskopf Parton Model

In the previous section we discussed the Kuti-Weisskopf (K-W) quark parton model. Its successes in fitting the deep inelastic electroproduction data and data regarding the process $p + p \rightarrow \mu^- \mu^+ + X$ are discussed in reference [51].

In this section we would like to see the predictions of the model when one employs the Weinberg-Salam theory of weak and electromagnetic interactions. When one assumes the W-S (Weinberg-Salam) model then the electroproduction scattering predictions are altered. The reason is that in the process $e^- p \rightarrow e^- X$ the Z-exchange term contributes as well, in addition to the one photon term, as is shown in Fig. 9.

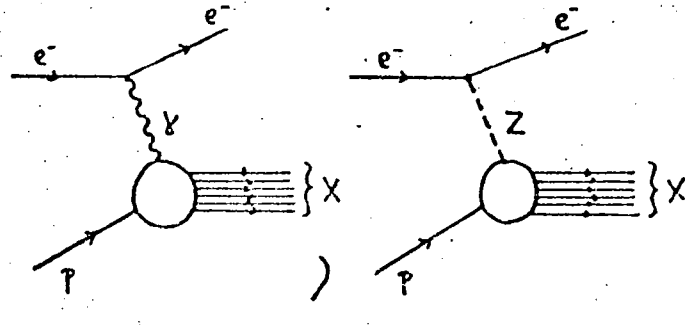

FIGURE 9: Photon and Z-boson exchange diagrams contributing to the process $e^- + p \rightarrow e^- + X$.

† The fit of Ref. [51] is for the quantity $\frac{d\sigma}{dm_{\mu^-\mu^+}}$ where $m_{\mu^-\mu^+}$ is the mass of the $\mu^-\mu^+$ pair .

However the contribution of the second diagram of Fig. 9 does not significantly alter the results since it is a small term .
The relevant structure function has been calculated by others [65] and has the form

$$F_2^{(ep)}(x) = F_{2_\gamma}^{(ep)}(x) + R_{\gamma-Z}(x) \quad . \tag{2.36}$$

$F_2^{(ep)}$ is the one photon-exchange term and the $R_{\gamma-Z}$ term is due to the exchange of a Z-boson which is small in comparison with $F_{2_\gamma}^{(ep)}$. The same happens in the reaction $pp \to \mu^-\mu^+ + X$ as well; that is the Z-term does not significantly alter the results and we can say that in general K-W model predictions, in the context of W-S model, are still valid.

We focus our attention to the "charged current" reactions $\nu N \to \mu^- X$ and $\bar{\nu} N \to \mu^+ X$ * whose total cross sections will be denoted by $\sigma^{CC}(\nu)$ and $\sigma^{CC}(\bar{\nu})$ from now on. After that the total cross section $\sigma^{NC}(\nu)$ and $\sigma^{NC}(\bar{\nu})$, for the "neutral current" processes $\nu N \to \nu X$ and $\bar{\nu} N \to \bar{\nu} X$ respectively, will be considered. The structure functions F_1 and F_3 for the neutrino and antineutrino charged exchanged reactions, are given by Eqs.(2.12) and (2.13).

---

* For convenience the muonic and electronic neutrino ν_μ and ν_e will be denoted by ν and ν' respectively.

Following the K-W model we write for the distribution function $f_i^{(h)}(x)$

$$f_i^{(h)}(x) = N_i^{(h)} v(x) + c(x) \tag{2.37a}$$

where the functions $v(x)$ and $c(x)$ are given by†

$$v(x) = B^{-1}(\tfrac{1}{2};4)\, x^{-1/2}(1-x)^3 \tag{2.37b}$$

$$c(x) = G_g\, x^{-1}(1-x)^{7/2} \quad . \tag{2.37c}$$

$c(x)$ is the core distribution function for the charged quarks (not the gluons) and the value of the constant Gg will be determined by fitting the electroproduction data.

The factors $N_i^{(h)}$ appearing in 2.37a takes the following values

$$\left.\begin{aligned} N_p^{(p)} = N_n^{(n)} = 2\,, \quad N_n^{(p)} = N_p^{(n)} = 1 \\ N_i^{(p)} = N_i^{(n)} = 0 \qquad \text{when } i \neq p \text{ or } n \text{ quark}. \end{aligned}\right\} \tag{2.38}$$

Thus the structure functions for the charged current reactions, when we are above the threshold for charm production, are given by

$$F_1^{(\nu N)}(x) = F_1^{(\bar{\nu} N)}(x) = \frac{3}{2} v(x) + 4c(x) \tag{2.39a}$$

$$F_3^{(\nu N)}(x) = F_3^{(\bar{\nu} N)}(x) = -3v(x) \quad . \tag{2.39b}$$

---

† B(a,b) is the wellknown beta function; see for instance "Table of Integrals, Series and Products" by I.S.Grandshteyn and I.M.Ryzhic, (Academic Press 1965)

The $F_2^{(\nu,\bar{\nu})}$ structure functions are calculated by the Callan-Gross relation $F_2 = 2xF_1$. When we are below the threshold for production of charmed states we have

$$F_1^{(\nu N)}(x) = F_1^{(\bar{\nu} N)}(x) = \frac{3}{2} v(x) + 2c(x) \tag{2.40a}$$

$$F_3^{(\nu N)}(x) = F_3^{(\bar{\nu} N)}(x) = -3v(x) \quad . \tag{2.40b}$$

Eqs. (2.40) hold in the approximation $\theta_c \approx 0$. On account of (1.42) the charge current total cross sections are given by the relations

$$\sigma^{cc}(\nu,\bar{\nu}) = \frac{G^2 ME}{\pi}\left\{\frac{1}{3}\int_0^1 x F_+^{(\nu,\bar{\nu})}(x)\,dx + \int_0^1 x F_-^{(\nu,\bar{\nu})}(x)dx\right\} - \left.\frac{G^2 M}{2\pi}\int_0^1 x^2 F_1^{(\nu,\bar{\nu})}(x)dx \quad .\right] \tag{2.41}$$

The functions $F_\pm$ are defined by

$$F_\pm^{(\nu,\bar{\nu})} \overset{def.}{\equiv} F_1^{(\nu,\bar{\nu})} \pm \frac{F_3^{(\nu,\bar{\nu})}}{2} \quad . \tag{2.42}$$

To make predictions we have to estimate the value of the constant Gg. With the introduction of the charmed quarks the core contribution to the electroproduction structure function is

$$F_c^{(ep,en)}(x) = \frac{20}{9} G_g (1-x)^{7/2} \quad . \tag{2.43}$$

As we saw in the previous section the core contribution was given by

$$F_c^{(ep,en)}(x) = \frac{4}{3} x\, c(x) = \frac{2}{9} g (1-x)^{7/2} \tag{2.44}$$

and a good fit was obtained by taking g = 1; thus comparing with (2.43) we see that a good choice for the paramter Gg is Gg = $\frac{1}{10}$.

Thus the predictions of the K-W model for the charged current reactions above and below the charm production threshold are given below:

(see A.6.24 ,A.6.25)

Below threshold:

$$\sigma^{cc}(\nu) = \frac{G^2 ME}{\pi} .39 \qquad (2.45a)$$

$$\sigma^{cc}(\bar{\nu}) = \frac{G^2 ME}{\pi} .17 \qquad (2.45b)$$

Above threshold:

$$\sigma^{cc}(\nu) = \frac{G^2 ME}{\pi} .45 \qquad (2.46a)$$

$$\sigma^{cc}(\bar{\nu}) = \frac{G^2 ME}{\pi} .23 \qquad (2.46b)$$

The last term of Eq. (2.41) has been omitted because it is small and negligible for high energies. The values of the ratio $\sigma(\bar{\nu})/\sigma(\nu)$ are given below:

Below threshold:

$$\frac{\sigma^{cc}(\bar{\nu})}{\sigma^{cc}(\nu)} = .43 \qquad (2.47a)$$

Above threshold:

$$\frac{\sigma^{cc}(\bar{\nu})}{\sigma^{cc}(\nu)} = .51 \qquad (2.47b)$$

The average values $\langle xy \rangle_{\nu,\bar{\nu}}$ are experimentally measurable quantities and are defined by

$$\langle xy \rangle_{\nu,\bar{\nu}} = \frac{1}{\sigma^{cc}(\nu,\bar{\nu})} \int_0^1 dx\, dy \; \frac{d^2\sigma^{cc}(\nu,\bar{\nu})}{dx\, dy} xy \quad . \qquad (2.48)$$

The K-W model predictions are given below (see A.6.24,A.6.25) for two cases below and above the threshold for production of charmed states :

Below threshold:

$$\langle xy \rangle_{\nu} = .128 \qquad (2.49a)$$

$$\langle xy \rangle_{\bar{\nu}} = .070 \qquad (2.49b)$$

Above threshold:

$$\langle xy \rangle_{\nu} = .120 \qquad (2.50a)$$

$$\langle xy \rangle_{\bar{\nu}} = .074 \qquad (2.50b)$$

In Table I we summarize the predictions of K-W quark parton model for the quantities $\sigma^{cc}(\nu)$, $\sigma^{cc}(\bar{\nu})$, $\sigma^{cc}(\bar{\nu})/\sigma^{cc}(\nu)$ and $\langle xy \rangle_{\nu,\bar{\nu}}$.

TABLE I

	Below threshold	Above threshold
$\sigma^{cc}(\nu)$	$\frac{G^2 ME}{\pi} \cdot 39$	$\frac{G^2 ME}{\pi} \cdot 45$
$\sigma^{cc}(\bar{\nu})$	$\frac{G^2 ME}{\pi} \cdot 17$	$\frac{G^2 ME}{\pi} \cdot 23$
$\frac{\sigma^{cc}(\bar{\nu})}{\sigma^{cc}(\nu)}$	.43	.51
$\langle xy \rangle_{\nu}$	.128	.120
$\langle xy \rangle_{\bar{\nu}}$	.070	.074

TABLE I: The predictions of the Kuti-Weisskopf quark parton model for the two cases of below and above the charm threshold.

We examine now the neutral current reactions $\nu N \to \nu N$, $\bar{\nu} N \to \bar{\nu} N$ whose total cross sections are denoted by $\sigma^{NC}(\nu)$ and $\sigma^{NC}(\bar{\nu})$ respectively. What have been actually measured experimentally, are the ratios $\left(\frac{NC}{CC}\right)_{\nu,\bar{\nu}}$ defined as $\left(\frac{NC}{CC}\right)_{\nu,\bar{\nu}} = \frac{\sigma^{NC}(\nu,\bar{\nu})}{\sigma^{CC}(\nu,\bar{\nu})}$. Data for the neutral to charged current ratios $\left(\frac{NC}{CC}\right)_{\nu,\bar{\nu}}$ are now available [48,49]. However when comparing with the Gargamelle data [48] one must be cautious for the following reason.

In the Gargamelle experiment the hadrons in the final state have an energy which exceeds a minimum value $E_{min} = 1$ Gev. This energy cut-off restricts the values of the variable y to lie in the range $\frac{\nu_{min}}{E} \leq y \leq 1$; the selection criterion for the Gargamelle experiment is $\nu_{min} = 1$. The ratios measured in this experiment, denoted by $\left(\frac{NC}{CC}\right)^{cut}_{\nu,\bar{\nu}}$ from now on, are the ratios of the number of the neutral current events to the number of the charged current events with energy of the final hadrons $E_H > 1$ Gev.

If one writes the differential cross-section $\frac{d\sigma}{dy}^{NC,CC}(\nu,\bar{\nu})$ in the following form

$$\frac{d\sigma^{\alpha}(\nu,\bar{\nu})}{dy} = \frac{G^2 ME}{\pi}\left\{(1-y)^2 a^{\alpha}(\nu,\bar{\nu}) + b^{\alpha}(\nu,\bar{\nu})\right\}, \quad (2.51)$$

where the superscript α denotes either NC or CC, then the $\left(\frac{NC}{CC}\right)^{cut}_{\nu,\bar{\nu}}$ ratios are given by [66]

$$\left(\frac{NC}{CC}\right)^{cut}_{\nu} = \frac{\left(\frac{1}{3} - \Delta\right) a^{NC}(\nu) + b^{NC}(\nu)}{\left(\frac{1}{3} - \Delta\right) a^{CC}(\nu) + b^{CC}(\nu)} \quad (2.52a)$$

$$\left(\frac{NC}{CC}\right)^{cut}_{\bar{\nu}} = \frac{\left(\frac{1}{3} - \bar{\Delta}\right) a^{NC}(\bar{\nu}) + b^{NC}(\bar{\nu})}{\left(\frac{1}{3} - \bar{\Delta}\right) a^{CC}(\bar{\nu}) + b^{CC}(\bar{\nu})} \quad (2.52b)$$

The constants Δ and $\bar{\Delta}$ are estimated from the neutrino and antineutrino spectrum of the Gargamelle experiment and they have the values $\Delta = .185$, $\bar{\Delta} = .200$[see Ref. 66]. Note that in the absence of this cut in the energy of the final hadrons $\Delta = \bar{\Delta} = 0$ and $\left(\frac{NC}{CC}\right)^{cut}_{\nu,\bar{\nu}}$ become the ratios $\left(\frac{NC}{CC}\right)_{\nu,\bar{\nu}}$. So we see that in order to compare the theoretical predictions with the experimental values we must calculate the constants $a^{CC}(\nu,\bar{\nu})$, $a^{NC}(\nu,\bar{\nu})$, $b^{CC}(\nu,\bar{\nu})$, $b^{NC}(\nu,\bar{\nu})$. Note that the $a^{NC}(\nu,\bar{\nu})$ and $b^{NC}(\nu,\bar{\nu})$ are functions of the parameter $\sin^2\theta_w$. For the parameters $a^{CC}(\nu,\bar{\nu})$, $b^{CC}(\nu,\bar{\nu})$ we have

$$a^{cc}(\nu) = b^{cc}(\bar{\nu}) = \int_0^1 x F_+^{(\nu)}(x)dx \qquad (2.53a)$$

$$b^{cc}(\nu) = a^{cc}(\bar{\nu}) = \int_0^1 x F_-^{(\nu)}(x)dx \qquad (2.53b)$$

and a similar definition holds for the $a^{NC}(\nu,\bar{\nu})$, $b^{NC}(\nu,\bar{\nu})$.

Thus we find

Below threshold:

$$a^{cc}(\nu) = b^{cc}(\bar{\nu}) = .044 \qquad (2.54a)$$

$$b^{cc}(\nu) = a^{cc}(\bar{\nu}) = .378 \qquad (2.54b)$$

Above threshold:

$$a^{cc}(\nu) = b^{cc}(\bar{\nu}) = .089 \qquad (2.55a)$$

$$b^{cc}(\nu) = a^{cc}(\bar{\nu}) = .422 \; . \qquad (2.55b)$$

To evaluate $a^{NC}(\nu,\bar{\nu})$ and $b^{NC}(\nu,\bar{\nu})$ one must recall the neutral current term of the Weinberg-Salam Lagrangian given in (1.46)

$$\mathcal{L}^{(neutral)} = \frac{g}{2\cos\theta_w}\left\{2J_\mu^{(3)} - 2\sin^2\theta_w J_\mu^{(em)}\right\}Z^\mu \; . \qquad (2.56)$$

The $J_\mu^{(3)}$ current is given by (1.47)

$$J_\mu^{(3)} = \sum_i \bar{\psi}_i \gamma_\mu T^{(3)} \psi_i \qquad (2.57)$$

where the summation index i runs over the left handed multiplets. The neutral current Lagrangian interaction term given by (2.56) can take the following form

$$\mathcal{L}^{(\text{neutral})} = \frac{g}{2\cos\theta_w} Z^\mu \sum_i \bar{\phi}_i \gamma_\mu \left\{ \left(\frac{n_i}{2} - 2z Q_i \right) - \frac{n_i}{2} \gamma_5 \right\} \phi_i \ . \qquad (2.58)$$

The index "i" now runs over all fields participating in the theory (leptons and hadrons); Q_i is the charge of the ϕ_i and $z \equiv \sin^2\theta_w$; n_i is a constant depending on the SU(2) multiplet $\left(\frac{1-\gamma_5}{2}\right)\phi_i$ belongs to, and on the position of it inside the multiplet. Thus when the only hadronic constituents are the quarks p, n, λ and p' we have

$$n_p = n_{p'} = 1, \quad n_n = n_\lambda = -1 \ . \qquad (2.59a)$$

For the leptons e^-, μ^-, ν_e and ν_μ we have

$$n_e = n_\mu = -1, \quad n_{\nu_e} = n_{\nu_\mu} = 1 \qquad (2.59b)$$

The structure functions $F_1^{(\nu h,\ \bar{\nu} h)}$ and $F_3^{(\nu h,\ \bar{\nu} h)}$ for scattering $\nu h \to \nu X$ and $\bar{\nu} h \to \bar{\nu} X$ are given by the following relations (see A.5.16 - A.5.18)

$$F_1^{(\nu h,\bar{\nu} h)}(x) = \sum_i f_i^{(h)}(x) A^i \qquad (2.60a)$$

$$F_3^{(\nu h,\bar{\nu} h)}(x) = -2 \sum_i f_i^{(h)}(x) \xi_i C^i \,. \qquad (2.60b)$$

When i denotes a quark the constants A^i, B^i, C^i are given by the relations (see A.5.2 - A.5.4).

$$A^i = \frac{1}{2}\left\{\left(\frac{n_i}{2} - 2zQ_i\right)^2 + \frac{n_i^2}{4}\right\} \qquad (2.61a)$$

$$C^i = \frac{n_i}{2}\left(\frac{n_i}{2} - 2zQ_i\right) \qquad (2.61b)$$

$$\xi_i = +1 \,. \qquad (2.61c)$$

For an antiquark $\bar{i}$ we have

$$A^{\bar{i}} = A^i, \quad C^{\bar{i}} = C^i, \quad \xi_{\bar{i}} = -1 \,. \qquad (2.62)$$

From Eqs. (2.60), (2.61) and (2.62) we find the relevant structure functions for the processes $\nu N \to \nu X$ and $\bar{\nu} N \to \bar{\nu} X$:

$$F_1^{(\nu N)}(x) = F_1^{(\bar{\nu} N)}(x) = \left(\frac{20}{9} z^2 - 2z + 1\right)\left(\frac{3}{4} u(x) + 2c(x)\right) \qquad (2.63a)$$

$$F_3^{(\nu N)}(x) = F_3^{(\bar{\nu} N)}(x) = -\frac{3}{2}(-2z+1)\, u(x) \qquad (2.63b)$$

The constants $a^{NC}(\nu,\bar{\nu})$ and $b^{NC}(\nu,\bar{\nu})$ are given by the following relations, if one takes into account the fact that $\int_0^1 x\, u(x)\, dx = \frac{1}{9}$ and $\int_0^1 x\, c(x)\, dx = \frac{1}{45}$ (see A.6.23a, A.6.23b)

$$a^{NC}(\nu) = b^{NC}(\bar{\nu}) = \left(\frac{23}{81} z^2 - \frac{4}{45} z + \frac{2}{45}\right) \qquad (2.64a)$$

$$b^{NC}(\nu) = a^{NC}(\bar{\nu}) = a^{NC}(\nu) + \frac{1}{6}(-2z+1) \,. \qquad (2.64b)$$

TABLE II

Z	R-NEU CUT	R-ANEU CUT	R-NEU	R-ANEU
0.01	0.491	0.493	0.490	0.492
0.02	0.481	0.484	0.480	0.482
0.03	0.471	0.475	0.471	0.473
0.04	0.462	0.466	0.461	0.464
0.05	0.452	0.458	0.452	0.455
0.06	0.443	0.451	0.443	0.447
0.07	0.434	0.443	0.434	0.439
0.08	0.425	0.437	0.425	0.432
0.09	0.416	0.430	0.417	0.425
0.10	0.408	0.425	0.408	0.419
0.11	0.399	0.419	0.400	0.411
0.12	0.391	0.414	0.392	0.405
0.13	0.383	0.410	0.384	0.399
0.14	0.375	0.406	0.376	0.393
0.15	0.367	0.402	0.369	0.388
0.16	0.359	0.399	0.361	0.383
0.17	0.352	0.396	0.354	0.379
0.18	0.345	0.394	0.347	0.374
0.19	0.337	0.392	0.340	0.371
0.20	0.330	0.391	0.333	0.367
0.21	0.323	0.390	0.327	0.364
0.22	0.317	0.390	0.320	0.361
0.23	0.310	0.390	0.314	0.358
0.24	0.303	0.390	0.308	0.356
0.25	0.297	0.391	0.302	0.354
0.26	0.291	0.392	0.297	0.352
0.27	0.285	0.394	0.291	0.351
0.28	0.279	0.396	0.286	0.350
0.29	0.273	0.399	0.280	0.350
0.30	0.268	0.402	0.275	0.349
0.31	0.262	0.405	0.270	0.349
0.32	0.257	0.409	0.266	0.350
0.33	0.252	0.414	0.261	0.350
0.34	0.247	0.419	0.257	0.352
0.35	0.242	0.424	0.253	0.353
0.36	0.237	0.430	0.248	0.355
0.37	0.233	0.436	0.245	0.357
0.38	0.228	0.443	0.241	0.359
0.39	0.224	0.450	0.237	0.362
0.40	0.220	0.457	0.234	0.365
0.41	0.216	0.465	0.231	0.368
0.42	0.212	0.474	0.228	0.372
0.43	0.209	0.483	0.225	0.376
0.44	0.205	0.492	0.222	0.380
0.45	0.202	0.502	0.220	0.385
0.46	0.199	0.512	0.217	0.390
0.47	0.196	0.523	0.215	0.395
0.48	0.193	0.534	0.213	0.401
0.49	0.190	0.546	0.211	0.407
0.50	0.187	0.558	0.209	0.413
0.51	0.185	0.570	0.208	0.420
0.52	0.183	0.583	0.206	0.427
0.53	0.180	0.596	0.205	0.434
0.54	0.178	0.610	0.204	0.442

TABLE II (continued)

y	R-NEU CUT	R-ANEU CUT	R-NEU	R-ANEU
0.55	0.177	0.624	0.203	0.450
0.56	0.175	0.639	0.203	0.459
0.57	0.173	0.654	0.202	0.467
0.58	0.172	0.670	0.202	0.476
0.59	0.171	0.686	0.202	0.485
0.60	0.170	0.702	0.202	0.495
0.61	0.169	0.719	0.202	0.505
0.62	0.168	0.737	0.202	0.515
0.63	0.167	0.755	0.202	0.526
0.64	0.167	0.773	0.203	0.537
0.65	0.166	0.792	0.204	0.548
0.66	0.166	0.811	0.205	0.560
0.67	0.166	0.830	0.206	0.572
0.68	0.166	0.850	0.207	0.584
0.69	0.167	0.871	0.209	0.596
0.70	0.167	0.892	0.210	0.609
0.71	0.168	0.913	0.212	0.623
0.72	0.168	0.935	0.214	0.636
0.73	0.169	0.957	0.216	0.650
0.74	0.170	0.980	0.219	0.665
0.75	0.171	1.003	0.221	0.679
0.76	0.173	1.027	0.224	0.694
0.77	0.174	1.051	0.227	0.709
0.78	0.176	1.075	0.230	0.725
0.79	0.177	1.100	0.233	0.741
0.80	0.179	1.126	0.236	0.757
0.81	0.181	1.152	0.240	0.774
0.82	0.184	1.178	0.243	0.791
0.83	0.186	1.205	0.247	0.809
0.84	0.188	1.232	0.251	0.825
0.85	0.191	1.260	0.255	0.843
0.86	0.194	1.288	0.260	0.862
0.87	0.197	1.316	0.264	0.880
0.88	0.200	1.345	0.269	0.899
0.89	0.203	1.375	0.273	0.918
0.90	0.207	1.404	0.278	0.938
0.91	0.210	1.435	0.284	0.958
0.92	0.214	1.466	0.289	0.978
0.93	0.218	1.497	0.294	0.998
0.94	0.222	1.528	0.300	1.019
0.95	0.226	1.561	0.306	1.041
0.96	0.230	1.593	0.312	1.062
0.97	0.235	1.626	0.318	1.084
0.98	0.239	1.659	0.324	1.106
0.99	0.244	1.693	0.331	1.129
1.00	0.249	1.728	0.338	1.152

TABLE II. The predictions of the Kuti-Weisskopf model for the ratios $(NC/CC)^{cut}_{\nu,\bar{\nu}}$, $(NC/CC)_{\nu,\bar{\nu}}$. The values given correspond to the case of being above the charm threshold. In this table R-NEU CUT, R-ANEU CUT, R-NEU and R-ANEU denote the ratios $(NC/CC)^{cut}_{\nu}$, $(NC/CC)^{cut}_{\bar{\nu}}$, $(NC/CC)_{\nu}$ and $(NC/CC)_{\bar{\nu}}$ respectively.

TABLE III

7	R-NEU CUT	R-ANEU CUT
.01	.556	.756
.02	.545	.742
.03	.534	.728
.04	.523	.715
.05	.513	.703
.06	.502	.691
.07	.492	.680
.08	.482	.670
.09	.472	.660
.10	.462	.651
.11	.452	.643
.12	.443	.636
.13	.434	.629
.14	.425	.623
.15	.416	.617
.16	.407	.612
.17	.399	.608
.18	.390	.605
.19	.382	.602
.20	.374	.600
.21	.366	.598
.22	.359	.598
.23	.351	.598
.24	.344	.598
.25	.336	.600
.26	.329	.602
.27	.322	.604
.28	.316	.608
.29	.309	.612
.30	.303	.617
.31	.297	.622
.32	.291	.628
.33	.285	.635
.34	.280	.642
.35	.274	.651
.36	.269	.660
.37	.264	.669
.38	.259	.679
.39	.254	.690
.40	.249	.702
.41	.245	.714
.42	.240	.727
.43	.236	.741
.44	.232	.755
.45	.229	.770
.46	.225	.786
.47	.222	.802
.48	.218	.819
.49	.215	.837
.50	.212	.855
.51	.209	.875
.52	.207	.894
.53	.204	.915
.54	.202	.936
.55	.200	.958
.56	.198	.981
.57	.196	1.004
.58	.195	1.028
.59	.193	1.052
.60	.192	1.078
.61	.191	1.104
.62	.190	1.130
.63	.189	1.158
.64	.189	1.186
.65	.189	1.214
.66	.188	1.244
.67	.188	1.274
.68	.188	1.305
.69	.189	1.336
.70	.189	1.368
.71	.190	1.401
.72	.191	1.434
.73	.192	1.469
.74	.193	1.504
.75	.194	1.539
.76	.195	1.575
.77	.197	1.612
.78	.199	1.650
.79	.201	1.688
.80	.203	1.727
.81	.205	1.767
.82	.208	1.807
.83	.211	1.848
.84	.213	1.890
.85	.216	1.932
.86	.220	1.975
.87	.223	2.019
.88	.226	2.064
.89	.230	2.109
.90	.234	2.155
.91	.238	2.201
.92	.242	2.248
.93	.247	2.296
.94	.251	2.345
.95	.256	2.394
.96	.261	2.444
.97	.266	2.494
.98	.271	2.546
.99	.276	2.598
1.00	.282	2.650

TABLE III . The predictions of the Kuti-Weisskopf model for the ratios $(NC/CC)_{\nu}^{cut}$ and $(NC/CC)_{\bar{\nu}}^{cut}$. The values given correspond to the case of being below the charm threshold. In this table R-NEU CUT and R-ANEU CUT denote the ratios $(NC/CC)_{\nu}^{cut}$ and $(NC/CC)_{\bar{\nu}}^{cut}$ respectively.

Thus having estimated the $a^{NC}(\nu,\bar{\nu})$ and $b^{NC}(\nu,\bar{\nu})$ we can, by virtue of Eqs. (2.52), find the ratios $\left(^{NC}/_{CC}\right)^{cut}_{\nu,\bar{\nu}}$ for different values of the parameter $Z = \sin^2\theta_w$. The corresponding ratios without the energy cut are given by Eqs. (2.52) but with $\Delta = \bar{\Delta} = 0$. In Table II the ratios $\left(^{NC}/_{CC}\right)^{cut}_{\nu,\bar{\nu}}$ and $\left(^{NC}/_{CC}\right)_{\nu,\bar{\nu}}$ are given for values of the parameter $Z = \sin^2\theta_w$ ranging from .01 to 1.00. Note that we have assumed that we are above the charm production threshold. Data from the CERN-Gargamelle group should be compared also with the case in which we are below the charm production threshold; in Table III the values of the ratios $\left(^{NC}/_{CC}\right)^{cut}_{\nu,\bar{\nu}}$ are given assuming that we are below this threshold. Before any comparison with the experimental data is made we shall review some of the neutrino and antineutrino data.

II6) Data on Deep Inelastic Neutrino and Antineutrino Induced Reactions.

Much data on neutrino and antineutrino induced reactions in the deep inelastic region have been accumulated the last years [see 67,68]. In this section we review some of these regarding the processes $\nu N \to \mu^- X$, $\bar{\nu}N \to \mu^+ X$ and $\nu N \to \nu X$, $\bar{\nu}N \to \bar{\nu}X$ in their deep inelastic region. In Table IV we give data of the CERN Gargamelle group taken from References 34 and 69. The quantities A, B, B' appearing in the table IV are defined as follows:

$$A = \int_0^1 2x F_1(x)dx \Big/ \int_0^1 F_2(x)dx \qquad (2.65a)$$

$$B = -\int_0^1 x F_3(x)dx \Big/ \int_0^1 F_2(x)dx \qquad (2.65b)$$

$$B' = -\int_0^1 x^2 F_3(x)dx \Big/ \int_0^1 x F_2(x)dx \qquad (2.65c)$$

If the Callan-Gross relation $F_2(x) = 2xF_1(x)$ holds then the right hand limits of A and B are valid (Table IV).

Note also that because of the relation $Q^2 = 2MExy$ we have $\langle Q^2 \rangle_{\nu,\bar{\nu}} = 2ME \langle xy \rangle_{\nu,\bar{\nu}}$. In the Table IV the electronic and meconic neutrinos ν_e and ν_μ are denoted by ν and ν' respectively (see footnote of page 47).

Besides these data from the Gargamelle group newer data were reported at higher beam energies, up to $E \sim 20$ geV [70], by the same group. Also the Harvard-Pensylvania-Wisconsin experiment (HPW) and the Caltech experiment provided data for even higher energies [71]. In tables IVa,b,c we give some data of the three groups Gargamelle, HPW, and Caltech reported by D.C. Cundy [72] at the London Conference on High Energy Physics in 1974.

Finally for the parameter $z = \sin^2\theta_w$ an upper bound $z < .3$ is found from a study of the reaction $\bar{\nu}_e + e \to \bar{\nu}_e + e$ [68]. This limit should be taken with some caution because the $\bar{\nu}_e$ flux is not measured but is known by calculations.

Also from $1\pi^o$ analysis the following result is obtained [68]

$$z > .2\text{-}.5$$

The result depends on the correction chosen for the nuclear effects.*

In this section we briefly reviewd some of the neutrino and antineutrino data. For more data and details regarding the experimental set-up we refer the reader to Ref. 67,68 and 73.

---

* The measure of the nuclear effect is done by the observation of the quantity $r = \dfrac{\sigma(\nu + n \to \mu^- + \pi^+ + n) + \sigma(\nu + p \to \mu^- + \pi^+ + p)}{\sigma(\nu + n \to \mu^- + \pi^o + p}$

The experimental value of r from the CERN freon experiment is $r = 2.3 \pm .9$.

TABLE IV

Physical quantity	Experimental value	Reference
$\sigma^{cc}(\nu)$	$(.77\pm.09)E^{\dagger,\#}$ (In units of $10^{-38}cm^2$)	(34)
$\sigma^{cc}(\bar{\nu})$	$(.32\pm.06)E^{\dagger,\#}$ (In units of $10^{-38}cm^2$)	(34)
$\sigma^{cc}(\bar{\nu})/\sigma^{cc}(\nu)$	$.38\pm.02^{\dagger}$	(34)
$\langle Q^2\rangle_{\nu}$	$(.21\pm.02)E^{\dagger,\#}$ (In units of $(Gev/c)^2$)	(34)
$\langle Q^2\rangle_{\bar{\nu}}$	$(.14\pm.03)E^{\dagger,\#}$ (In units of $(Gev/c)^2$)	(34)
$\langle xy\rangle_{\nu}$	$.12\pm.01$	(34)
$\langle xy\rangle_{\bar{\nu}}$	$.07\pm.01$	(34)
$\sigma^{cc}(\nu)$	$(.93\pm.17)E$ (In units of $10^{-38}cm^2$)	(67)
$\sigma^{cc}(\bar{\nu})$	$(.37\pm.09)E$ (In units of $10^{-38}cm^2$)	(67)
$\sigma^{cc}(\bar{\nu}')/\sigma^{cc}(\nu')$ ‡	$.40\pm.12$	(67)
$\sigma^{cc}(\nu')/\sigma^{cc}(\nu)$ ‡	$1.26\pm.23$	(67)
$\sigma^{cc}(\bar{\nu}')/\sigma^{cc}(\bar{\nu})$	$1.32\pm.32$	(67)
$(NC/CC)^{cut}_{\nu,\bar{\nu}}$	$.21\pm.03$	(48)
$(NC/CC)^{cut}_{\nu,\bar{\nu}}$	$.45\pm.09$	(48)
A	$.87\pm.05 \leq A \leq 1$	(34)
B	$.87\pm.05 \leq B \leq .90\pm.04$	(34)
B′	$.87\pm.08$	(34)
$\int_0^1 F_2^{(\nu N)}(x)dx$	$.49\pm.03 \leq \int F_2 \leq .51+.03$	(34)

TABLE IV. Experimental values of various physical quantities of interest. In the last column the corresponding references are given.

---

† This is the fit of reference (34) for E>2 Gev.

The actual fit of reference (34) is of the form aE+b. Here the constant b is omitted.

‡ The electronic and muonic neutrinos are denoted by ν' and ν respectively.

TABLE IVa

Experimental group	$\sigma^{cc}(\nu)$	$\sigma^{cc}(\bar{\nu})$
Gargamelle	$(.76\pm.08)E^{\dagger}$	$(.28\pm.03)E^{\dagger}$
Caltech	$(.83\pm.11)E^{\dagger}$	$(.28\pm.05)E^{\dagger}$
HPW ‡	$(.70\pm.13)E^{\dagger}$	$(.28\pm.09)E^{\dagger}$
Mean value	$(.78\pm.07)E^{\dagger}$	$(.28\pm.025)E^{\dagger}$

TABLE IVa. Data for the charged current total cross sections $\sigma^{cc}(\nu)$ and $\sigma^{cc}(\bar{\nu})$ as measured by three different groups.

---

† In units of 10^{-38} cm^2.

‡ Harvard-Pensylvania-Wisconsin collaboration.

TABLE IVb

Experimental group	Energy region	$\sigma^{cc}(\bar{\nu})/\sigma^{cc}(\nu)$
Gargamelle	1 - 10 Gev	$.38\pm.02$
Caltech	40 Gev 110 Gev	$.40\pm.11$ $.23\pm.11$
HPW ‡	10 - 30 Gev	$.41\pm.11$
A value of R estimated from the slopes is $R = .36+.05$. This gives limits on the values of A and B : $.92(+.1) \leq A \leq 1$, $.92(+.1) \leq B \leq .94$		
The experimental value of the quantity $\int_0^1 F_2^{(\nu N)}(x)dx = .51\pm.05$		$\int_0^1 F_2^{(\nu N)}(x)dx$ is (see Ref.72)

TABLE IVb. Data for the ratio $R = \sigma^{cc}(\nu)/\sigma^{cc}(\nu)$ as measured by three different groups. Bounds for the quantities A and B as well as the experimental value for the quantity $\int_0^1 F_2^{(\nu N)}(x)dx$ are also given.

‡ Harvard-Pensylvania-Wisconsin collaboration.

TABLE IVc

Experimental group	$(NC/CC)_{\nu}$	$(NC/CC)_{\bar{\nu}}$
Gargamelle	$.22 \pm .03$ *	$.43 \pm .12$ *
Caltech	.22 **	.33 **
HPW	$.12 \pm .04$	$.32 \pm .08$

* In these ratios the energy of the outgoing hadrons is greater than 1 Gev.

** These results should be mainly taken as a demonstration of the existence of neutral currents.

TABLE IVc. Data for the neutral to charged current ratios $(NC/CC)_{\nu,\bar{\nu}}$ measured by three different groups.

II7) Kuti-Weisskopf Quark Parton Model Predictions and Comparison with Experimental Data.

We give the predictions of the K-W quark parton model for the neutrino and antineutrino reactions $\nu N \to \mu^- X$, $\bar{\nu} N \to \mu^+ X$, $\nu N \to \nu X$ and $\bar{\nu} X \to \bar{\nu} X$. The predictions of the model for the processes $e^- p \to e^- X$ and $pp \to \mu^- \mu^+ + X$, in their deep inelastic region, can be found in Kuti and Weisskopf's paper [51].

In Table V the predictions of the model are given for the two cases of above and below the threshold for production of charmed states. For the evaluation of B and B' use was made of the relations

$$\int_0^1 x\,v(x)\,dx = \frac{1}{9} \quad , \quad \int_0^1 x^3 v(x)\,dx = \frac{1}{33} \quad , \quad \int_0^1 x\,c(x)\,dx = \frac{1}{45}$$

and $\int_0^1 x^2 c(x)\,dx = \frac{2}{495}$ (see A.6.23a, A.6.23b). The predictions of the model for scattering by electronic neutrinos and antineutrinos (ν', $\bar{\nu}'$) are the same as those for muonic neutrinos and antineutrinos from ν_μ-ν_e universality. The first column of the Table V should be compared only with data from the Gargamelle group, since data from Caltech and HPW groups are for high energies and surely above the charm production threshold. The second column must be compared with data from all groups.

i) Below the Charm Production Threshold.

Comparing with the experimental values of the Table IV we see that the physical quantities $\sigma^{CC}(\bar{\nu})$, $\langle xy \rangle_{\nu,\bar{\nu}}$, A, B, B' are in good

agreement. The cross section $\sigma^{CC}(\nu)$ is smaller than the experimental one given in the Table IV

The quantity $\int_0^1 F_2^{(\nu N)}(x)dx$ is not within the limits given in the same table. The situation is even worse with the quantities $\sigma^{CC}(\bar{\nu})/\sigma^{CC}(\nu)$ and $(^{NC}/_{CC})^{cut}_{\nu,\bar{\nu}}$. The ratio $\sigma^{CC}(\bar{\nu})/\sigma^{CC}(\nu)$ is more than two standard deviations removed from the experimental value $.38 \pm .02$. As far as the ratios $(^{NC}/_{CC})^{cut}_{\nu,\bar{\nu}}$ are concerned, we observe from the table III that in order to have $(^{NC}/_{CC})^{cut}_{\nu} \leq .25$ (see Table IVc) we need $Z > .39$ which gives $(^{NC}/_{CC})^{cut}_{\nu} \geq .69$ a result too far away from the experimental value $(^{NC}/_{CC})^{cut}_{\nu} = .43 \pm .12$ (see Table IVc).

The conclusion is that the K-W model does not fit the data in the case where we are below the charm production threshold. This might be due to the fact that the Gargamelle data are above the charm production threshold; thus a comparison of the K-W model predictions, given in the second column of Table V, with the experimental data should be made.

ii) Above the Charm Production Threshold

$\sigma^{CC}(\nu)$ and $\sigma^{CC}(\bar{\nu})$ are in agreement with the experimental values given in the table IV. However the value of $\sigma^{CC}(\bar{\nu})$ is a little larger than the mean value of $\sigma^{CC}(\bar{\nu})$ given in Table IVa. $\langle xy \rangle_{\nu,\bar{\nu}}$ are in good agreement with the values given in the Table IV.

The quantities A and B satisfy the conditions $B \leq .90 \pm .04$

and $A \leq 1$ and thus they agree with the data given in the Table IV and IVb. B' has a value smaller than that given by experiment and shown in the Table IV. The integral $\int_0^1 F_2(x)dx$ has the value .511 to be compared with the limits given in the Table IV and with the value given in the Table IVb. For the ratios $(^{NC}/_{CC})^{cut}_{\nu,\bar{\nu}}$ we see from the Table II that good fit is obtained with the experimental values measured by the Gargamelle group, and given in the Tables IV and IVa; note that there are values of Z for which, the experimental values of the ratios $(^{NC}/_{CC})^{cut}_{\nu,\bar{\nu}}$ measured by the Gargamelle group, and the value of $(^{NC}/_{CC})_{\bar{\nu}}$ measured by the HPW group, are fitted simultaneously. Unfortunately, for these values of Z we have $(^{NC}/_{CC})_{\nu} \geq .21$. Thus no value of Z fits simultaneously the four ratios.

Finally for the ratio $\sigma^{CC}(\bar{\nu})/\sigma^{CC}(\nu)$ we have to observe that it disagrees badly with the experiment; the values of this ratio given by the Gargamelle group is $.38 \pm .02$ (Table IV) while in the Table IVb a value of this ratio equal to $.36 \pm .05$ is given. The theoretical prediction $\sigma^{CC}(\bar{\nu})/\sigma^{CC}(\nu) = .511$ in no way is compared with these values.

Thus the conclusion is that the Kuti-Weisskopf quark parton model does not fit the neutrino and antineutrino induced reactions data given in the Tables IV - IVc.

TABLE V

	Below charm threshold	Above charm threshold
$\sigma^{cc}(\nu)$ $\sigma^{cc}(\bar{\nu})$	$(.596)E^{\dagger}$ (In units of 10^{-38} cm^2) $(.260)E^{\dagger}$ (In units of 10^{-38} cm^2)	$(.688)E^{\dagger}$ (In units of 10^{-38} cm^2) $(.352)E^{\dagger}$ (In units of 10^{-38} cm^2)
$\sigma^{cc}(\bar{\nu})/\sigma^{cc}(\nu)$	.435	.511
$\langle xy \rangle_{\nu}$ $\langle xy \rangle_{\bar{\nu}}$	.128 .070	.120 .074
$(NC/CC)_{\nu,\bar{\nu}}$	See the tables II and III	
A	1	1
B	.789	.652
B'	.849	.738
$\int_0^1 F_2^{(\nu N)}(x)dx$	.422	.511

TABLE V. Predictions of the Kuti-Weisskopf model for the mainpphysical quantities concerning deep inelastic neutrinoproduction experiments. The predictions in the first and the second column correspond to the two cases of below and above the charm threshold respectively.

---

† $G_M^2/\pi = 1.53\times10^{-38}$ cm^2/Gev^2 for $G_M^2 = 1.01\times10^{-38}$

Discussion.

The basic ideas and the derivation of the most important formulae of the naive quark parton model were given in this chapter. Sum rules and relations among the distribution functions were also considered.

The main characteristics of the Kuti-Weisskopf quark parton model were presented and the model predictions for the charged current reaction $\nu N \to \mu^- X$, $\bar{\nu} N \to \mu^+ X$ and neutral current reactions $\nu N \to \nu$ $\bar{\nu} N \to \bar{\nu} N$ were given. Towards the end of the chapter we reviewed the main experimental data on neutrino and antineutrino induced reactions, and a comparison of the K-W model with these was made.

The conclusion was that K-W quark parton model fails to fit the existing neutrino and antineutrino data. Thus the model must be either abandoned or modified.

In an attempt to fit the data on deep inelastic electron and neutrino scattering, modifications of the original K-W quark parton model will be considered in the third chapter.

CHAPTER III

Introduction

In the second chapter we briefly reviewed the Kuti-Weisskopf quark parton model and the predictions of the model for neutrino and antineutrino induced reactions were considered .

In the first part of this chapter we make an attempt to improve the predictions of the K-W model by changing the form of the currents involved in the theory. This is done by adding new hadronic constituents whose left-handed components are grouped in SU(2) triplets in the Weinberg model.

General comments on the model are discussed at the end of the first part of this chapter.

In the second part an analysis of the quark parton model is made without using any specific parton model.

Based on the results derived from this analysis we build a quark parton model whose predictions for neutrino (antineutrino) induced reactions and deep inelastic electron-proton scattering are discussed.

PART A

III1)$_A$ A Modified Kuti-Weisskopf Model Using Additional Hadronic Constituents.

In the previous section the K-W quark parton model and its predictions for neutrino and antineutrino induced reactions were discussed. In this chapter we make an attempt to improve the predictions of the model by changing the form of the currents involved in the theory.

We begin our discussion with the ratio $\sigma^{CC}(\bar{\nu})/\sigma^{CC}(\nu)$ which was found to be too large in the original K-W model. The charge current total cross sections have the forms $\sigma^{CC}(\bar{\nu}) = \upsilon + c$ and $\sigma^{CC}(\nu) = 3\upsilon + c$, where υ and c are the valence and core contributions respectively. If one wishes to reduce the value of the ratio $\sigma^{CC}(\bar{\nu})/\sigma^{CC}(\nu)$ then a plausible way would be to decrease either the core or the valence contributions; but in this way the cross section $\sigma^{CC}(\nu)$ becomes small and does not agree with the experimental values given in the Tables IV and IVa. Thus we come to the conclusion that another scheme must be invented which enlarges only the value of the total cross section $\sigma^{CC}(\nu)$ and not that of $\sigma^{CC}(\bar{\nu})$. We are able to do this by introducing additional hadronic constituents in the Weinberg-Salam model.

It is well known that the gauge group of the Weinberg theory is the $SU(2) \times U(1)$. According to it particles are classified in left handed multiplets and right handed singlets of SU(2). In the Weinberg-Salam model there are four fundamental quarks p, n, λ and p' as we saw in the first chapter. These quarks are classified in left handed isospin doublets as follows

$$L^{(1)} = \left(\frac{1-\gamma_5}{2}\right)\begin{pmatrix} p \\ n_c \end{pmatrix}, \quad L^{(1)'} = \left(\frac{1-\gamma_5}{2}\right)\begin{pmatrix} p' \\ \lambda_c \end{pmatrix} \qquad (3.1)$$

with $n_c = n\cos\theta_c + \lambda\sin\theta_c$, $\lambda_c = -n\sin\theta_c + \lambda\cos\theta_c$.

We assume now that in addition to the conventional quark fields p, p', n, λ we have another six quark fields $p_1, p_1', n_1, \lambda_1, \phi_1, \phi_2$ [74]. The $p_1, p_1', n_1, \lambda_1, \phi_1, \phi_2$ quarks are classified in left handed isospin triplets as follows:

$$L^{(2)} = \left(\frac{1-\gamma_5}{2}\right)\begin{pmatrix} p_1 \\ n_1^c \\ \phi_1 \end{pmatrix}, \quad L^{(2)'} = \left(\frac{1-\gamma_5}{2}\right)\begin{pmatrix} p_1' \\ \lambda_1^c \\ \phi_2 \end{pmatrix} . \qquad (3.2)$$

The reason we introduce new triplets in the theory will become obvious later. The right-handed parts of the above fields are SU(2) singlets.

The new badronic constituents induce alterations in the weak and neutral currents; in (1.47) we define the current

$\vec{J}_\mu = \sum_i \bar{\psi}_i \gamma_\mu \vec{\tau} \psi_i$ where "i" runs over all the isospin multiplets and $\vec{\tau} = (\tau^{(1)}, \tau^{(2)}, \tau^{(3)})$ are the isospin matrices. The weak and neutral currents are defined by the relations

$$J_\mu^{(+)\,\text{Weak}} = J_\mu^{(1)} + i J_\mu^{(2)} \tag{3.3a}$$

$$J_\mu^{(\text{neutral})} = 2\left(J_\mu^{(3)} - \sin^2\theta_w J_\mu^{(\text{em})}\right) \tag{3.3b}$$

In the representation $\{1\}$ of SU(2) the matrices $\tau^{+} = \tau^{(1)} + i\tau^{(2)}$ and $\tau^{(3)}$ are given by

$$\tau^{(+)} = \sqrt{2}\begin{pmatrix} 0 & 1 & 0 \\ 0 & 0 & 1 \\ 0 & 0 & 0 \end{pmatrix}, \quad \tau^{(3)} = \begin{pmatrix} 1 & 0 & 0 \\ 0 & 0 & 0 \\ 0 & 0 & -1 \end{pmatrix} . \tag{3.4}$$

Thus we have

$$\bar{L}^{(2)} \gamma_\mu \tau^{(+)} L^{(2)} = \sqrt{2}\left\{\bar{P}_1 \gamma_\mu \left(\frac{1-\gamma_5}{2}\right) n_1^c + \bar{n}_1^c \gamma_\mu \left(\frac{1-\gamma_5}{2}\right) \phi_1\right\} \tag{3.5a}$$

$$\bar{L}'^{(2)} \gamma_\mu \tau^{(3)} L'^{(2)} = \sqrt{2}\left\{\bar{P}_1' \gamma_\mu \left(\frac{1-\gamma_5}{2}\right) \lambda_1^c + \bar{\lambda}_1^c \gamma_\mu \left(\frac{1-\gamma_5}{2}\right) \phi_2\right\} . \tag{3.5b}$$

It is evident now that the hadronic part of the weak current takes the form,

$$\left.\begin{aligned} J_\mu^{(+)\,\text{Weak}} &= \bar{P} \gamma_\mu \left(\frac{1-\gamma_5}{2}\right) n_c + \bar{P}' \gamma_\mu \left(\frac{1-\gamma_5}{2}\right) \lambda_c + \\ &+ \sqrt{2}\left\{\bar{P}_1 \gamma_\mu \left(\frac{1-\gamma_5}{2}\right) n_1^c + \bar{P}_1' \gamma_\mu \left(\frac{1-\gamma_5}{2}\right) \lambda_1^c + \right. \\ &\left. + \bar{n}_1^c \gamma_\mu \left(\frac{1-\gamma_5}{2}\right) \phi_1 + \bar{\lambda}_1^c \gamma_\mu \left(\frac{1-\gamma_5}{2}\right) \phi_2\right\} . \end{aligned}\right\} \tag{3.6}$$

The hadronic part of the $J_\mu^{(3)}$ current is given by the expression:

$$2J_\mu^{(3)} = \bar{p}\gamma_\mu\left(\frac{1-\gamma_5}{2}\right)p + \bar{p}'\gamma_\mu\left(\frac{1-\gamma_5}{2}\right)p' - \bar{n}\gamma_\mu\left(\frac{1-\gamma_5}{2}\right)n - \bar{\lambda}\gamma_\mu\left(\frac{1-\gamma_5}{2}\right)\lambda + \\ + \bar{p}_1\gamma_\mu(1-\gamma_5)p_1 + \bar{p}_1'\gamma_\mu(1-\gamma_5)p_1' - \phi_1\gamma_\mu(1-\gamma_5)\phi_1 - \phi_2\gamma_\mu(1-\gamma_5)\phi_2 . \quad (3.7)$$

It is evident that the constants n_i of (2.58) have the following values:

$$n_p = n_{p'} = -n_n = -n_\lambda = 1 \quad (3.7a)$$

$$n_{p_1} = n_{p_1'} = -n_{\phi_1} = -n_{\phi_2} = 2 \quad (3.7b)$$

$$n_{n_1} = n_{\lambda_1} = 0 \quad (3.7c)$$

In the weak current of the expression (3.6) the first term is the well-known Cabbibo current which consists of a $\Delta S = 1$ and a $\Delta S = 0$ part (strangeness changing and nonchanging).

The second term is due to Glashow, Iliopoulos and Maiani [43] who introduced another fourth quark p' which carries a new quantum number called "charm" equal to one. The second term is the $|\Delta C| = 1$ part of the weak hadronic current.

In exactly the same spirit the particles p_1, p_1' are assigned a new quantum denoted by "h" and equal to one.

Similarly the quarks ϕ_1 and ϕ_2 carry another quantum number denoted by "h'" and equal to one. The particles n_1 and λ_1 carry $h = h' = 0$. As far as the other quantum numbers of the quarks p_1, p_1', n_1, λ_1 are concerned they are the same as those of the p, p', n, λ quarks.

In this way, the weak hadronic current contains also $|\Delta h| = |\Delta h'| = 1$ parts.

The reason we introduced these new quantum numbers will be explained in the next section.

III2)$_A$ Predictions of the Modified Kuti- Weisskopf Model for the Charged Current Reactions.

We come now to the point of calculating the charge current reactions total cross sections. The calculation is straightforward because the additional terms in the weak current have a form identical to the usual Cabbibo current.

We are able to fit the data by requiring that the terms $\bar{n}_1^c \gamma_\mu (1-\gamma_5)\phi_1$ and $\bar{\lambda}_1^c \gamma_\mu (1-\gamma_5)\phi_2$ do not give any contribution. This can be justified by saying that at present energies the $|\Delta h'| = 1$ term of the weak current is suppressed, in other words we are below the threshold for the production of states having $h' \neq 0$. Thus the effective weak current is

$$J_\mu^{(+)\,\text{Weak}} = \bar{P}\gamma_\mu\left(\frac{1-\gamma_5}{2}\right)n_c + \bar{P}'\gamma_\mu\left(\frac{1-\gamma_5}{2}\right)\lambda_c + \\ + \sqrt{2}\left\{\bar{P}_1\gamma_\mu\left(\frac{1-\gamma_5}{2}\right)n_1^c + \bar{P}_1'\gamma_\mu\left(\frac{1-\gamma_5}{2}\right)\lambda_1^c\right\} \qquad (3.8)$$

Note that the $|\Delta h| = 1$ part does give its own contribution unlike the $|\Delta h'| = 1$ term; thus the role of the new quantum numbers h and h' introduced in the first section of this chapter now becomes apparent.

Without difficulty we can write down the expressions for the structure functions $F_{1,3}^{(\nu h,\ \bar{\nu} h)}$

† $$F_1^{(\nu h)}(x) = \left\{f_n^{(h)}(x) + f_\lambda^{(h)}(x) + f_{\bar{P}}^{(h)}(x) + f_{\bar{P}'}^{(h)}(x)\right\} + \\ + 2\left\{f_{n_1}^{(h_1)}(x) + f_{\lambda_1}^{(h)}(x) + f_{\bar{P}_1}^{(h)}(x) + f_{\bar{P}_1'}^{(h)}(x)\right\} \qquad (3.9a)$$

† $$F_3^{(\nu h)}(x) = -2\left\{f_n^{(h)}(x) + f_\lambda^{(h)}(x) - f_{\bar{P}}^{(h)}(x) - f_{\bar{P}'}^{(h)}(x)\right\} - \\ - 4\left\{f_{n_1}^{(h)}(x) + f_{\lambda_1}^{(h)}(x) - f_{\bar{P}_1}^{(h)}(x) - f_{\bar{P}_1'}^{(h)}(x)\right\} \qquad (3.9b)$$

---

† See footnote of the following page

$$^{*}F_1^{(\bar{\nu}h)}(x) = \left\{ f_p^{(h)}(x) + f_{p'}^{(h)}(x) + f_{\bar{n}}^{(h)}(x) + f_{\bar{\lambda}}^{(h)}(x) \right\} + 2\left\{ f_{p_1}^{(h)}(x) + f_{p_1'}^{(h)}(x) + f_{\bar{n}_1}^{(h)}(x) + f_{\bar{\lambda}_1}^{(h)}(x) \right\} \quad (3.10a)$$

$$^{*}F_3^{(\bar{\nu}h)}(x) = -2\left\{ f_p^{(h)}(x) + f_{p'}^{(h)}(x) - f_{\bar{n}}^{(h)}(x) - f_{\bar{\lambda}}^{(h)}(x) \right\} - 4\left\{ f_{p_1}^{(h)}(x) + f_{p_1'}^{(h)}(x) - f_{\bar{n}_1}^{(h)}(x) - f_{\bar{\lambda}_1}^{(h)}(x) \right\} . \quad (3.10b)$$

We then assume that the n-type constituent quark of the SU(3) triplet is a mixture of the n and n_1 quarks, which are grouped in SU(2) doublets and triplets, and will be denoted by n'. Its wave function can be written then as

$$|n'\rangle = \cos\omega |n_1\rangle + \sin\omega |n\rangle \quad (3.11)$$

where ω is a mixing angle.

The constituents p_1, p_1', ϕ_1, ϕ_2 can exist only as core constituents since all known hadrons are assumed to carry h = h' = 0. Thus the wave function of the p-type constituent quark of the SU(3) triplet, which is denoted by p', is written as

$$|p'\rangle = \cos\varphi |p\rangle + \sin\varphi |p_1\rangle \quad (3.11a)$$

with the mixing angle φ having the value $\varphi = 0$.

It is obvious now that the proton and neutron wave functions are given by,

$$|\text{proton}\rangle = |p'p'n' + \text{core}\rangle = \cos\omega\, |ppn_1 + \text{core}\rangle + \sin\omega\, |ppn + \text{core}\rangle \quad (3.12a)$$

$$|\text{neutron}\rangle = |p'n'n' + \text{core}\rangle = \cos^2\omega\, |pn_1n_1 + \text{core}\rangle + \sin(2\omega)\, |pnn_1 + \text{core}\rangle + \sin^2\omega\, |pnn + \text{core}\rangle . \quad (3.12b)$$

---

* We assume that we are above the threshold for the production of charmed states.

The distribution functions $f_i^{(h)}(x)$ are written as

$$f_i^{(h)}(x) = N_i^{(h)}\, v(x) + c(x) \tag{3.13}$$

with $v(x)$ and $c(x)$ given by Eqs. (2.37). The factor $N_i^{(h)}$ has the following meaning

$N_i^{(h)}$ = (average number of valence quarks of the i-type in the hadron "h").

Thus for the proton and neutron we have

$$N_{n_1}^{(p)} = \cos^2\omega \quad , \quad N_n^{(p)} = \sin^2\omega \quad , \quad N_p^{(p)} = 2 \qquad \Big\} (3.14a)$$

$$N_{n_1}^{(n)} = (2\cos^4\omega + \sin^2 2\omega)M^2 \quad , \quad N_{n_1}^{(n)} = (2\sin^4\omega + \sin^2 2\omega)M^2 \quad , \quad N_p^{(n)} = 1 \Big\} (3.14b)$$

$$N_i^{(p,n)} = 0 \quad \text{when} \quad i \neq p, n, n_1 \quad \text{quark} \quad . \qquad \Big\} (3.14c)$$

The factor M^2 which appears in the expressions above is given by

$$M^2 = (\cos^4\omega + \sin^4\omega + \sin^2 2\omega)^{-1} \quad . \tag{3.15}$$

From Eqs. (3.9) we have for the neutrino and antineutrino structure functions $F_{1,3}^{(\nu N, \bar{\nu} N)}$.

$$F_1^{(\nu N)}(x) = \left(\frac{3+2\mu}{2}\right) v(x) + 12\, c(x) \tag{3.16a}$$

$$F_3^{(\nu N)}(x) = -(3+2\mu)\, v(x) \tag{3.16b}$$

$$F_1^{(\bar{\nu}N)}(x) = \frac{3}{2}u(x) + 12c(x) \qquad (3.16c)$$

$$F_3^{(\bar{\nu}N)}(x) = -3u(x) \qquad (3.16d)$$

The constant μ is given by

$$\mu = \frac{1}{2}\left(N_{n_1}^{(p)} + N_{n_1}^{(n)}\right) \qquad (3.17)$$

As we said before the valence and core distribution functions are given by the Eqs. (2.37) and their first moments are (see A.6.23a,A.6.23b)

$$\int_0^1 x u(x)\,dx = \frac{1}{9}\,, \quad \int_0^1 x c(x)\,dx = \frac{2}{9}G_g \qquad (3.18)$$

The constant Gg is estimated by fitting the data for the structure function $F_2^{(ep)}(x)$. In the Kuti-Weisskopf's paper [51] a good fit is obtained by taking $(\sum_i Q_i^2)G_g = \frac{2}{9}$ where the index i runs over all quarks and antiquarks with charge Q_i. In our model $(\sum_i Q_i^2) = \frac{104}{9}$ and thus Gg = $\frac{1}{52}$. With this value for the constant Gg and for $\mu = \frac{1}{2}$ we have:

$$\sigma^{cc}(\nu) = \frac{G^2ME}{\pi}\,.513 \simeq .78E^{*} \qquad (3.19a)$$

$$\sigma^{cc}(\bar{\nu}) = \frac{G^2ME}{\pi}\,.180 \simeq .27E^{*} \qquad (3.19b)$$

$$\sigma^{cc}(\bar{\nu})/\sigma^{cc}(\nu) = .35 \qquad (3.19c)$$

---

* In units of 10^{-38} cm^2.

These values are to be compared with the experimental ones given in the Tables IV, IVa, and IVb of the second chapter.

The appearance of the μ-term in Eqs. (3.16) is of vital importance; the enhancement of the value of the charged current cross section $\sigma^{CC}(\nu)$ is due to this term. No μ-term appears in the structure functions $F_{1,3}^{(\bar{\nu}N)}$ and this has a consequence the reduction of the ratio $\sigma^{CC}(\bar{\nu})/\sigma^{CC}(\nu)$.

One could ask whether this scheme is able to fit the data by grouping the new constituents in SU(2) doublets instead of triplets; thus the model would be more economical in the sense that it would require less number of constituents. Unfortunately this is not the case; the structure functions $F_{1,3}^{(\nu N)}$ would be given by the expressions

$$F_1^{(\nu N)}(x) = \frac{1}{2}\left(N_n^{(p)} + N_{n_1}^{(p)} + N_n^{(n)} + N_{n_1}^{(n)}\right)u(x) + 8c(x) \qquad (3.20a)$$

$$F_3^{(\nu N)}(x) = -\left(N_n^{(p)} + N_{n_1}^{(p)} + N_n^{(n)} + N_{n_1}^{(n)}\right)u(x) \qquad (3.20b)$$

and consequently no μ-term appears to enlarge the value of $\sigma^{CC}(\nu)$, because $N_n^{(p)} + N_{n_1}^{(p)} + N_n^{(n)} + N_{n_1}^{(n)} = 3$, and therefore no fit with the data would be obtained. For this reason we abandoned the SU(2) - doublet idea and preferred to work with the triplet scheme.

In the Table VI the predictions of the model for the charged current reactions $\nu(\bar{\nu}) + N \to \mu^-(\mu^+) + X$ are given. They are in agreement with the experimental values of the Tables IV, IVa, IVb of the second chapter.

TABLE VI

$\sigma^{cc}(\nu)$	$\frac{G^2 ME}{\pi} .513 \simeq .78E\ 10^{-38}\ cm^2$
$\sigma^{cc}(\bar{\nu})$	$\frac{G^2 ME}{\pi} .180 \simeq .27E\ 10^{-38}\ cm^2$
$\sigma^{cc}(\bar{\nu})/\sigma^{cc}(\nu)$	.35
$\langle xy \rangle_\nu$	.128
$\langle xy \rangle_{\bar{\nu}}$	.072

TABLE VI: The predictions of the modified Kuti-Weisskopf for the quantities $\sigma^{cc}(\nu,\bar{\nu})$ $\sigma^{cc}(\bar{\nu})/\sigma^{cc}(\nu)$ and $\langle xy \rangle_{\nu,\bar{\nu}}$

III3) A Predictions of the Modified Kuti-Weisskopf Model for the Neutral Current Reactions.

We proceed now to examine the predictions of the model for the neutral to charge current ratios $(^{NC}/_{CC})_{\nu,\bar{\nu}}$.

The structure functions $F_{1,3}^{(\nu N,\bar{\nu}N)}$ are calculated using the expressions given by Eqs. (2.60) and (2.61). Using (3.13) and the fact that $\mu = \frac{1}{2}(N_{n_1}^{(p)} + N_{n_1}^{(n)})$ we get

$$F_1^{(\nu N,\bar{\nu}N)}(x) = \left\{\frac{3}{2}(A^p + A^n) - \mu(A^n - A^{n_1})\right\} v(x) + \left\{\sum_i A^i\right\} c(x) \qquad (3.21a)$$

$$F_3^{(\nu N,\bar{\nu}N)}(x) = -2\left\{\frac{3}{2}(C^p + C^n) - \mu(C^n - C^{n_1})\right\} v(x) \quad . \qquad (3.21b)$$

The parameters A^i, C^i, which are functions of the variable $Z = \sin^2\theta_w$, are given by Eqs. (2.61). By a straightforward calculation we find

$$F_1^{(\nu N,\bar{\nu}N)}(x) = \left\{\frac{15}{9}Z^2 - \left(\frac{3}{2} - \frac{\mu}{3}\right)Z + \left(\frac{3-\mu}{4}\right)\right\} v(x) + 2\left\{\frac{104}{9}Z^2 - 10Z + 5\right\} c(x) \qquad (3.22a)$$

$$F_3^{(\nu N,\bar{\nu}N)}(x) = -2\left\{-\left(\frac{3}{2} - \frac{\mu}{3}\right)Z + \left(\frac{3-\mu}{4}\right)\right\} v(x) \quad . \qquad (3.22b)$$

Thus the constants $a^{NC}(\nu,\bar{\nu})$ and $b^{NC}(\nu,\bar{\nu})$ defined by the relations

$$a^{NC}(\nu) = b^{NC}(\bar{\nu}) = \int_0^1 \left(F_1 + \frac{1}{2}F_3\right) dx \qquad (3.23a)$$

$$b^{NC}(\nu) = a^{NC}(\bar{\nu}) = \int_0^1 \left(F_1 - \frac{1}{2}F_3\right) dx \qquad (3.23b)$$

receive the following forms

$$a^{NC}(\nu) = b^{NC}(\bar{\nu}) = \left\{\frac{15}{9}Z^2\right\}U + 2\left\{\frac{104}{9}Z^2 - 10Z + 5\right\}C \qquad (3.24a)$$

$$b^{NC}(\nu) = a^{NC}(\bar{\nu}) = a^{NC}(\nu) + 2\left\{-\left(\frac{3}{2} - \frac{4}{3}\right)Z + \left(\frac{3-4}{4}\right)U\right\} \qquad (3.24b)$$

In Eqs.(3.24) U and C are the first moments of the functions $u(x)$ and $c(x)$ respectively. Putting $\mu = \frac{1}{2}$, $U = \frac{1}{9}$ and $C = \frac{1}{234}$ we have from Eqs.(3.24)

$$a^{NC}(\nu) = b^{NC}(\bar{\nu}) = .2839Z^2 - .0854Z + .0427 \qquad (3.25a)$$

$$b^{NC}(\nu) = a^{NC}(\bar{\nu}) = a^{NC}(\nu) + (.1389 - .2963Z) \; . \qquad (3.25b)$$

The ratios $\left({}^{NC}/_{CC}\right)^{cut}_{\nu,\bar{\nu}}$ are given by the Eqs.(2.52) with Δ and $\bar{\Delta}$ having the values .185 and .200 respectively. The ratios $\left({}^{NC}/_{CC}\right)_{\nu,\bar{\nu}}$ are given again by Eqs. (2.52) but with $\Delta = \bar{\Delta} = 0$. The $a^{CC}(\nu,\bar{\nu})$, $b^{CC}(\nu,\bar{\nu})$, necessary in calculating these ratios, are given below.

$$\left.\begin{aligned} a^{CC}(\nu) &= b^{CC}(\bar{\nu}) = .0513 \\ b^{CC}(\nu) &= .4957 \; , \; a^{CC}(\bar{\nu}) = .3849 \end{aligned}\right\} \; . \qquad (3.26)$$

In the Table VII the values of $\left({}^{NC}/_{CC}\right)^{cut}_{\nu,\bar{\nu}}$ and $\left({}^{NC}/_{CC}\right)_{\nu,\bar{\nu}}$ are given for values of $Z_{cut} = \sin^2\theta_w$ ranging from .01 to 1.00.

TABLE VII

Z	R-NFU CUT	R-ANFU CUT	R-NFU	R-ANFU
.01	.366	.639	.374	.563
.02	.358	.627	.366	.552
.03	.350	.615	.359	.541
.04	.343	.604	.351	.531
.05	.336	.594	.344	.521
.06	.329	.584	.337	.511
.07	.322	.575	.330	.502
.08	.315	.566	.323	.494
.09	.308	.558	.316	.485
.10	.301	.551	.309	.477
.11	.295	.544	.303	.470
.12	.289	.538	.297	.463
.13	.282	.533	.290	.457
.14	.276	.528	.284	.450
.15	.270	.524	.279	.445
.16	.265	.520	.273	.439
.17	.259	.517	.267	.434
.18	.253	.515	.262	.430
.19	.248	.513	.257	.426
.20	.243	.512	.251	.422
.21	.237	.512	.246	.419
.22	.232	.512	.242	.416
.23	.227	.513	.237	.414
.24	.223	.514	.232	.412
.25	.218	.516	.228	.411
.26	.213	.519	.224	.409
.27	.209	.522	.220	.409
.28	.205	.526	.216	.409
.29	.201	.531	.212	.409
.30	.197	.536	.208	.409
.31	.193	.542	.205	.410
.32	.189	.548	.202	.412
.33	.185	.556	.198	.414
.34	.182	.563	.195	.416
.35	.178	.572	.192	.419
.36	.175	.581	.190	.422
.37	.172	.590	.187	.425
.38	.169	.601	.185	.429
.39	.166	.611	.182	.434
.40	.164	.623	.180	.438
.41	.161	.635	.178	.444
.42	.159	.648	.176	.449
.43	.156	.661	.174	.455
.44	.154	.675	.173	.462
.45	.152	.690	.171	.469
.46	.150	.705	.170	.476
.47	.148	.721	.169	.484
.48	.146	.738	.168	.492
.49	.145	.755	.167	.501
.50	.144	.773	.167	.510
.51	.142	.791	.166	.519
.52	.141	.810	.166	.529
.53	.140	.830	.165	.539
.54	.139	.850	.165	.550

TABLE VII (continued)

z	R-NEU CUT	R-ANEU CUT	R-NEU	R-ANEU
.55	.138	.871	.165	.561
.56	.138	.892	.165	.573
.57	.137	.915	.166	.585
.58	.137	.937	.166	.597
.59	.137	.961	.167	.610
.60	.136	.985	.168	.623
.61	.136	1.010	.169	.637
.62	.137	1.035	.170	.651
.63	.137	1.061	.171	.665
.64	.137	1.087	.172	.680
.65	.138	1.115	.174	.696
.66	.138	1.142	.176	.711
.67	.139	1.171	.177	.728
.68	.140	1.200	.179	.744
.69	.141	1.230	.181	.761
.70	.142	1.260	.184	.779
.71	.144	1.291	.186	.797
.72	.145	1.323	.189	.815
.73	.146	1.355	.191	.834
.74	.148	1.388	.194	.853
.75	.150	1.421	.197	.872
.76	.152	1.455	.200	.892
.77	.154	1.490	.204	.913
.78	.156	1.525	.207	.934
.79	.159	1.561	.211	.955
.80	.161	1.598	.214	.977
.81	.164	1.635	.218	.999
.82	.166	1.673	.222	1.021
.83	.169	1.711	.227	1.044
.84	.172	1.751	.231	1.067
.85	.175	1.790	.235	1.091
.86	.178	1.831	.240	1.115
.87	.182	1.872	.245	1.140
.88	.185	1.913	.250	1.165
.89	.189	1.956	.255	1.191
.90	.193	1.999	.260	1.216
.91	.197	2.042	.265	1.243
.92	.201	2.086	.271	1.269
.93	.205	2.131	.276	1.297
.94	.209	2.176	.282	1.324
.95	.213	2.222	.288	1.352
.96	.218	2.269	.294	1.381
.97	.223	2.316	.301	1.409
.98	.227	2.364	.307	1.439
.99	.232	2.413	.314	1.468
1.00	.237	2.462	.320	1.499

TABLE VII. The predictions of the modified Kuti-Weisskopf model for the ratios $(NC/CC)^{cut}_{\nu,\bar{\nu}}$ and $(NC/CC)^{cut}_{\nu,\bar{\nu}}$. The values given correspond to the case of being above the charm threshold. In this table R-NEU CUT, R-ANEU CUT, R-NEU and R-ANEU denote the ratios $(NC/CC)^{cut}_{\nu}$, $(NC/CC)^{cut}_{\bar{\nu}}$, $(NC/CC)_{\nu}$ and $(NC/CC)_{\bar{\nu}}$ respectively.

The ratios $(NC/CC)^{cut}_{\nu,\nu}$ for $.17 \leq z \leq .32$ agree with the experimental values $(^{NC}/_{CC})^{cut}_{\nu} = .22 \pm .03$, $(^{NC}/_{CC})^{cut}_{\bar{\nu}} = .43 \pm .12$ of the Gargamelle group given in the Table IVc. For the value $Z \simeq .28$ we have $(^{NC}/_{CC})^{cut}_{\nu} \simeq .20$ $(^{NC}/_{CC})^{cut}_{\bar{\nu}} \simeq .52$ and $(^{NC}/_{CC})_{\bar{\nu}} \simeq .40$; thus for this value of the parameter Z the ratios $(^{NC}/_{CC})^{cut}_{\nu,\bar{\nu}}$ and $(^{NC}/_{CC})_{\bar{\nu}}$ are fitted simultaneously. Note that this value of Z is less than .3, the upper bound of Z estimated from the study of the reaction $\bar{\nu}_e + e \to \bar{\nu}_e + e$ as discussed in the second chapter. Unfortunately for $Z \simeq .28$ we have $(^{NC}/_{CC})_{\nu} \simeq .21$ while experiment requires $(^{NC}/_{CC})_{\nu} \leq .16$.

For no value of Z the four ratios $(^{NC}/_{CC})^{cut}_{\nu,\bar{\nu}}$, $(^{NC}/_{CC})_{\nu,\bar{\nu}}$ are fitted simultaneously as were not in the original K-W model either.

III4)$_A$ General Comments on the Model.

(i) By introducing new hadronic constituents the form of the hadronic part of the weak current is altered. In fact additional terms appeared in the wellknown form (see 1.54), which were interpreted as the $|\Delta h| = 1$ and $|\Delta h'| = 1$ parts of the current, after the introduction of the new quantum numbers h and h'. All known hadrons are assigned $h = h' = 0$ and so the new terms does not participate in their decays.

(ii) The Adler sum rule $\int_0^1 \{F_2^{(\nu n)} - F_2^{(\nu p)}\} dx = 1$ (see 2.20) is replaced by another sum rule in which the right hand side of the equation above is a function of the angle ω (see 3.11). For the value of $\mu = \frac{1}{2}$, which corresponds to $\cos\omega \approx .45$ ($\omega \approx 63^\circ$), we find

$$\int_0^1 \{F_2^{(\nu n)} - F_2^{(\nu p)}\} \approx 1.6$$

(iii) For the value $\mu = \frac{1}{2}$ we find from equation (3.14)

$$N_{n_1}^{(p)} = .203 \quad , \quad N_{n}^{(p)} = .797 \qquad (3.27a)$$

$$N_{n_1}^{(n)} = .796 \quad , \quad N_{n}^{(n)} = 1.204 \quad . \qquad (3.27b)$$

If the new quarks are assumed to be heavier than the conventional ones p,p', n, λ then because there are almost four times as many n_1 "valence" quarks in the neutron as there are in the proton we might naively expect the neutron to be heavier than the proton.

(iv) The introduction of the new constituents introduces Jackiw-Adler type anomalies [75] and if one wishes to eliminate them he must introduce an equal number of other hadronic constituents or new leptons. Remember that in models based on SU(2) x U(1) symmetry the condition that there be no anomolies is $\sum_i (I_3^i)^2 Q_i = 0$ [see for example Ref. 76]

(v) For the ratio $R = \frac{\sigma(e^-e^+ \to \text{Hadrons})}{\sigma(e^-e^+ \to \mu^-\mu^+)}$ (see 1.23) the model predicts a value which is $R = \frac{52}{9} \approx 5.8$ to be compared with the experimental value which lies between 5 and 6 for an incoming energy $\sqrt{s} = 5$ GeV ($s = (p_{e^-} + p_{e^+})^2$).

The three quark model (noncolored) predicts $R = \frac{2}{3}$ and the colored three quark model R = 2. Also the Han-Nambu † model gives R = 4 [see for example Ref. 56].

---

† M.Y. Han and Y. Nambu: Phys. Rev. 139, B1006 (1965).

In the next section we try to make an analysis of the quark parton model based on the available so far neutrino and antineutrino data. No additional constituents will be assumed except the conventional four quarks p, n, λ and p'.

PART B

III1)$_B$ The Quark Parton Model and Neutrino Reactions.

Based on some of the neutrino and antineutrino data, we make an analysis of the quark parton model without recourse to any specific model. The only assumption is that the momentum distribution functions split into a valence and a core part. No additional quarks except the p, p', n, λ are introduced in the theory.

We write once again the distribution functions $f_i^{(h)}(x)$ in the following form (see 2.37a)

$$f_i^{(h)}(x) = N_i^{(h)} v(x) + c(x) \qquad (3.28)$$

with $N_i^{(h)}$ having the values (see 2.38)

$$\left.\begin{aligned} N_p^{(p)} = N_n^{(n)} = 2, \quad N_n^{(p)} = N_p^{(n)} = 1 \\ N_i^{(p)} = N_i^{(n)} = 0 \quad \text{when} \quad i \neq p, n \text{ quark} \end{aligned}\right\} \qquad (3.29)$$

The differential cross sections $\frac{d\sigma}{dy}^{CC,NC}$ are written in the form (see 2.51)

$$\frac{d\sigma^{\nu,\bar{\nu}}}{dy} = \frac{G^2 ME}{\pi} \left\{ (1-y)^2 a^{\nu,\bar{\nu}} + b^{\nu,\bar{\nu}} \right\} \qquad (3.30)$$

where the superscript "α" denotes either CC or NC. For the definition of $a^{\alpha}(\nu,\bar{\nu})$ and $b^{\alpha}(\nu,\bar{\nu})$ see Eqs. (2.53) of the second chapter. The structure functions $F_{1,3}$ for the charge current reactions $\nu(\bar{\nu}) + N \to \mu^{-}(\mu^{+}) + X$ are given by the expressions † (see Eqs. 2.39)

$$F_1^{(\nu N,\bar{\nu}N)}(x) = \frac{1}{2}\left(3u(x) + 8c(x)\right) \tag{3.31a}$$

$$F_3^{(\nu N,\bar{\nu}N)}(x) = -3u(x) \quad . \tag{3.31b}$$

In some parton models the distribution functions $f_i^{(h)}(x)$ have the forms

$$\left.\begin{aligned} f_p^{(p)}(x) &= f_n^{(n)}(x) = 2u_1(x) + c(x) \\ f_n^{(p)}(x) &= f_p^{(n)}(x) = u_2(x) + c(x) \\ f_i^{(p,n)}(x) &= c(x) \quad \text{when } i \neq p,n \text{ quark} \end{aligned}\right\} \tag{3.32}$$

In this case the forms of $F_{1,3}$ given by Eqs. (3.31) do not change; we simply replace $3u(x)$ by $(2u_1(x) + u_2(x))$. So whenever in an expression we see a $u(x)$ it is either $u(x)$ or $(2u_1(x) + u_2(x))/3$. From the Eqs. (3.31) we have for the constants $a^{cc}(\nu,\bar{\nu})$ and $b^{cc}(\nu,\bar{\nu})$

$$a^{cc}(\nu) = b^{cc}(\bar{\nu}) = 4c \tag{3.33a}$$

$$b^{cc}(\nu) = a^{cc}(\bar{\nu}) = 3u + 4c \quad . \tag{3.33b}$$

---

† We assume that we are above the charm production threshold.

In the expressions above u and c denote the first moments of $u(x)$ and $c(x)$ respectively, that is $u = \int_0^1 x u(x) dx$, $c = \int_0^1 x c(x) dx$. The cross sections $\sigma^{CC}(\nu,\bar{\nu})$ and the ratio $R = \sigma^{CC}(\bar{\nu})/\sigma^{CC}(\nu)$ are given by the following relations

$$\sigma^{CC}(\nu) = \frac{G^2 ME}{\pi} u\left(3 + \frac{16}{3}\rho\right) \equiv \alpha(\nu) E \qquad (3.34a)$$

$$\sigma^{CC}(\bar{\nu}) = \frac{G^2 ME}{\pi} u\left(1 + \frac{16}{3}\rho\right) \equiv \alpha(\bar{\nu}) E \qquad (3.34b)$$

$$R = \sigma^{CC}(\bar{\nu})/\sigma^{CC}(\nu) = \frac{3+16\rho}{9+16\rho} \quad . \qquad (3.34c)$$

The constant ρ in Eqs. (3.34) is defined by,

$$\rho = c/u \quad . \qquad (3.35)$$

To calculate the ratios $(^{NC}/_{CC})^{cut}_{\nu,\bar{\nu}}$ and $(^{NC}/_{CC})_{\nu,\bar{\nu}}$ we need the constants $a^{NC}(\nu,\bar{\nu})$ and $b^{NC}(\nu,\bar{\nu})$.

The neutral current reactions structure functions $F_{1,3}^{(\nu N,\bar{\nu}N)}$ are given by the expression (see Eqs. 2.63)

$$F_1^{(\nu N,\bar{\nu}N)}(x) = \frac{1}{2}\left(\frac{20}{9}Z^2 - 2Z + 1\right)\left(\frac{3}{2}u(x) + 4c(x)\right) \qquad (3.35a)$$

$$F_3^{(\nu N,\bar{\nu}N)}(x) = \frac{3}{2}(2Z-1)\,u(x) \qquad (3.35b)$$

and thus we have

$$a^{NC}(\nu) = b^{NC}(\bar{\nu}) = \left\{\frac{15}{9}Z^2 + 2\left(\frac{20}{9}Z^2 - 2Z + 1\right)\rho\right\}u \qquad (3.35c)$$

$$b^{NC}(\nu) = a^{NC}(\bar{\nu}) = \left\{\left(\frac{15}{9}Z^2 - 3Z + \frac{3}{2}\right) + 2\left(\frac{20}{9}Z^2 - 2Z + 1\right)\rho\right\}u \quad . \qquad (3.35d)$$

Remember that by Z we denote the variable $\sin^2\theta_w$.

The ratios $(^{NC}/_{CC})_{\nu,\bar{\nu}}$ and $(^{NC}/_{CC})^{cut}_{\nu,\bar{\nu}}$ are given by the following expressions

$$\left(\frac{NC}{CC}\right)_{\nu} = \frac{20}{9}\left(\frac{3+8\rho}{9+16\rho}\right)Z^2 - Z + \frac{1}{2} \tag{3.36a}$$

$$\left(\frac{NC}{CC}\right)_{\bar{\nu}} = \frac{20}{9}\left(\frac{3+8\rho}{3+16\rho}\right)Z^2 - Z + \frac{1}{2} \tag{3.36b}$$

$$\left(\frac{NC}{CC}\right)^{cut}_{\nu} = \left(\frac{1.91+5.10\rho}{3.00+4.59\rho}\right)Z^2 - Z + \frac{1}{2} \tag{3.36c}$$

$$\left(\frac{NC}{CC}\right)^{cut}_{\bar{\nu}} = \left(\frac{1.88+5.04\rho}{.40+4.53\rho}\right)Z^2 - Z + \frac{1}{2} \tag{3.36d}$$

Note that for a value of the ratio $\sigma^{CC}(\bar{\nu})/\sigma^{CC}(\nu)$ equal to $\frac{1}{3}$ and consequently for $\rho = 0$ we have

$$\left(\frac{NC}{CC}\right)_{\nu} = \frac{20}{27}Z^2 - Z + \frac{1}{2} \tag{3.37a}$$

$$\left(\frac{NC}{CC}\right)_{\bar{\nu}} = \frac{20}{9}Z^2 - Z + \frac{1}{2} \tag{3.37b}$$

Eqs. (3.37) are the same with the ratios found in Ref. 56 and 66. In the Tables VIII, VIIIa,b,c,d the values of the $(^{NC}/_{CC})^{cut}_{\nu,\bar{\nu}}$ and $(^{NC}/_{CC})_{\nu,\bar{\nu}}$ are given for values of $Z = \sin^2\theta_w$ ranging for .01 to 1.00 and for $R = \sigma^{CC}(\bar{\nu})/\sigma^{CC}(\nu)$ equal to .36, .37, .38, .39 and .40.

TABLE VIII

R = 0.36

Z	R-NEU CUT	R-ANEU CUT	R-NEU	R-ANEU
0.01	0.490	0.490	0.490	0.490
0.02	0.480	0.482	0.480	0.481
0.03	0.471	0.474	0.471	0.472
0.04	0.461	0.466	0.461	0.463
0.05	0.452	0.460	0.452	0.455
0.06	0.442	0.454	0.443	0.448
0.07	0.433	0.449	0.434	0.440
0.08	0.424	0.445	0.425	0.433
0.09	0.415	0.442	0.416	0.427
0.10	0.407	0.439	0.408	0.421
0.11	0.398	0.438	0.399	0.415
0.12	0.389	0.437	0.391	0.410
0.13	0.381	0.437	0.383	0.405
0.14	0.373	0.437	0.375	0.401
0.15	0.365	0.439	0.367	0.397
0.16	0.357	0.441	0.359	0.394
0.17	0.349	0.444	0.352	0.391
0.18	0.341	0.448	0.344	0.388
0.19	0.334	0.453	0.337	0.386
0.20	0.325	0.458	0.330	0.384
0.21	0.319	0.464	0.323	0.383
0.22	0.312	0.471	0.317	0.382
0.23	0.305	0.479	0.310	0.381
0.24	0.298	0.487	0.304	0.381
0.25	0.291	0.497	0.297	0.381
0.26	0.284	0.507	0.291	0.382
0.27	0.278	0.518	0.285	0.383
0.28	0.271	0.529	0.279	0.385
0.29	0.265	0.542	0.274	0.387
0.30	0.259	0.555	0.268	0.389
0.31	0.253	0.569	0.263	0.392
0.32	0.247	0.584	0.257	0.395
0.33	0.241	0.600	0.252	0.399
0.34	0.235	0.616	0.247	0.403
0.35	0.230	0.634	0.243	0.407
0.36	0.225	0.652	0.238	0.412
0.37	0.219	0.670	0.233	0.417
0.38	0.214	0.690	0.229	0.423
0.39	0.209	0.710	0.225	0.429
0.40	0.204	0.732	0.221	0.436
0.41	0.200	0.754	0.217	0.443
0.42	0.195	0.776	0.213	0.450
0.43	0.191	0.800	0.210	0.458
0.44	0.186	0.824	0.206	0.466
0.45	0.182	0.849	0.203	0.475
0.46	0.178	0.875	0.200	0.484
0.47	0.174	0.902	0.197	0.494

TABLE VIII (continued)

Y	R-NEU CUT	R-ANEU CUT	R-NEU	R-ANEU
0.48	0.170	0.930	0.194	0.504
0.49	0.167	0.958	0.191	0.514
0.50	0.163	0.987	0.189	0.525
0.51	0.160	1.017	0.187	0.536
0.52	0.157	1.047	0.184	0.548
0.53	0.153	1.079	0.182	0.560
0.54	0.150	1.111	0.180	0.572
0.55	0.148	1.144	0.179	0.585
0.56	0.145	1.178	0.177	0.598
0.57	0.142	1.213	0.175	0.612
0.58	0.140	1.248	0.174	0.626
0.59	0.137	1.284	0.173	0.641
0.60	0.135	1.321	0.172	0.656
0.61	0.133	1.359	0.171	0.671
0.62	0.131	1.397	0.170	0.687
0.63	0.129	1.437	0.170	0.703
0.64	0.128	1.477	0.169	0.720
0.65	0.126	1.518	0.169	0.737
0.66	0.124	1.560	0.169	0.754
0.67	0.123	1.602	0.169	0.772
0.68	0.122	1.645	0.169	0.790
0.69	0.121	1.689	0.170	0.809
0.70	0.120	1.734	0.170	0.828
0.71	0.119	1.780	0.171	0.848
0.72	0.119	1.826	0.172	0.868
0.73	0.118	1.874	0.173	0.888
0.74	0.118	1.922	0.174	0.909
0.75	0.117	1.970	0.175	0.931
0.76	0.117	2.020	0.176	0.952
0.77	0.117	2.070	0.178	0.974
0.78	0.117	2.122	0.180	0.997
0.79	0.118	2.174	0.182	1.020
0.80	0.118	2.226	0.184	1.043
0.81	0.118	2.280	0.186	1.067
0.82	0.119	2.334	0.188	1.091
0.83	0.120	2.389	0.191	1.116
0.84	0.121	2.445	0.193	1.141
0.85	0.122	2.502	0.196	1.166
0.86	0.123	2.560	0.199	1.192
0.87	0.124	2.618	0.202	1.219
0.88	0.126	2.677	0.205	1.245
0.89	0.127	2.737	0.208	1.272
0.90	0.129	2.797	0.212	1.300
0.91	0.131	2.859	0.216	1.328
0.92	0.133	2.921	0.220	1.356
0.93	0.135	2.984	0.223	1.385
0.94	0.137	3.048	0.228	1.414
0.95	0.139	3.113	0.232	1.444
0.96	0.142	3.178	0.236	1.474
0.97	0.144	3.244	0.241	1.505
0.98	0.147	3.311	0.246	1.536
0.99	0.150	3.379	0.251	1.567
1.00	0.153	3.448	0.256	1.599

TABLE VIII. The quark parton model predictions of the Weinberg model for the ratios $(NC/CC)^{cut}_{\nu,\bar{\nu}}$ and $(NC/CC)_{\nu,\bar{\nu}}$. The value of the ratio $R = q^{cc}(\bar{\nu})/q^{cc}(\nu)$ is equal to .36. In this table R-NEU CUT, R-ANEU CUT, R-NEU and R-ANEU denote the ratios $(NC/CC)^{cut}_{\nu}$, $(NC/CC)^{cut}_{\bar{\nu}}$, $(NC/CC)_{\nu}$ and $(NC/CC)_{\bar{\nu}}$ respectively.

TABLE VIIIa

****
*   *
* R=0.37 *
*   *
****

Z	R-NEU CUT	P-ANEU CUT	R-NEU	R-ANEU
0.01	0.490	0.490	0.490	0.490
0.02	0.480	0.481	0.480	0.481
0.03	0.471	0.473	0.471	0.472
0.04	0.461	0.466	0.461	0.463
0.05	0.452	0.459	0.452	0.455
0.06	0.442	0.453	0.443	0.447
0.07	0.433	0.448	0.434	0.440
0.08	0.424	0.444	0.425	0.433
0.09	0.415	0.440	0.416	0.427
0.10	0.407	0.437	0.408	0.421
0.11	0.398	0.435	0.399	0.415
0.12	0.389	0.434	0.391	0.410
0.13	0.381	0.433	0.383	0.405
0.14	0.373	0.433	0.375	0.400
0.15	0.365	0.434	0.367	0.396
0.16	0.357	0.435	0.359	0.393
0.17	0.349	0.438	0.352	0.389
0.18	0.341	0.441	0.345	0.387
0.19	0.334	0.445	0.337	0.384
0.20	0.326	0.449	0.330	0.382
0.21	0.319	0.454	0.324	0.381
0.22	0.312	0.461	0.317	0.380
0.23	0.305	0.467	0.310	0.379
0.24	0.298	0.475	0.304	0.378
0.25	0.291	0.483	0.298	0.379
0.26	0.285	0.492	0.291	0.379
0.27	0.278	0.502	0.285	0.380
0.28	0.272	0.512	0.280	0.381
0.29	0.265	0.524	0.274	0.383
0.30	0.259	0.536	0.268	0.385
0.31	0.253	0.548	0.263	0.388
0.32	0.248	0.562	0.258	0.391
0.33	0.242	0.576	0.253	0.394
0.34	0.236	0.591	0.248	0.398
0.35	0.231	0.607	0.243	0.402
0.36	0.225	0.623	0.239	0.407
0.37	0.220	0.641	0.234	0.412
0.38	0.215	0.659	0.230	0.417
0.39	0.210	0.677	0.226	0.423
0.40	0.205	0.697	0.222	0.429
0.41	0.201	0.717	0.218	0.436
0.42	0.196	0.738	0.214	0.443
0.43	0.192	0.760	0.211	0.450
0.44	0.188	0.782	0.207	0.458
0.45	0.184	0.805	0.204	0.467
0.46	0.180	0.829	0.201	0.475
0.47	0.176	0.854	0.198	0.484

TABLE VIIIa (continued)

y	R-NEU CUT	R-ANEU CUT	R-NEU	R-ANEU
0.48	0.172	0.879	0.195	0.494
0.49	0.168	0.905	0.193	0.504
0.50	0.165	0.932	0.192	0.514
0.51	0.161	0.960	0.188	0.525
0.52	0.158	0.989	0.186	0.536
0.53	0.155	1.018	0.184	0.548
0.54	0.152	1.048	0.182	0.560
0.55	0.149	1.078	0.180	0.572
0.56	0.147	1.110	0.179	0.585
0.57	0.144	1.142	0.177	0.598
0.58	0.142	1.175	0.176	0.612
0.59	0.140	1.208	0.175	0.626
0.60	0.137	1.243	0.174	0.641
0.61	0.135	1.278	0.173	0.655
0.62	0.133	1.314	0.173	0.671
0.63	0.132	1.350	0.172	0.686
0.64	0.130	1.388	0.172	0.703
0.65	0.129	1.426	0.172	0.719
0.66	0.127	1.465	0.172	0.736
0.67	0.126	1.504	0.172	0.753
0.68	0.125	1.545	0.172	0.771
0.69	0.124	1.586	0.172	0.789
0.70	0.123	1.628	0.173	0.809
0.71	0.122	1.670	0.174	0.827
0.72	0.122	1.713	0.175	0.845
0.73	0.121	1.758	0.176	0.865
0.74	0.121	1.802	0.177	0.886
0.75	0.121	1.848	0.178	0.907
0.76	0.121	1.894	0.180	0.928
0.77	0.121	1.941	0.181	0.950
0.78	0.121	1.989	0.183	0.972
0.79	0.121	2.038	0.185	0.994
0.80	0.122	2.087	0.187	1.017
0.81	0.123	2.137	0.189	1.042
0.82	0.123	2.188	0.192	1.063
0.83	0.124	2.239	0.194	1.087
0.84	0.125	2.292	0.197	1.111
0.85	0.126	2.345	0.200	1.136
0.86	0.128	2.398	0.203	1.161
0.87	0.129	2.453	0.206	1.187
0.88	0.131	2.508	0.209	1.213
0.89	0.132	2.564	0.213	1.239
0.90	0.134	2.621	0.216	1.266
0.91	0.136	2.679	0.220	1.293
0.92	0.138	2.737	0.224	1.321
0.93	0.140	2.796	0.228	1.349
0.94	0.143	2.856	0.233	1.378
0.95	0.145	2.916	0.237	1.408
0.96	0.148	2.977	0.241	1.438
0.97	0.150	3.039	0.246	1.469
0.98	0.153	3.102	0.251	1.501
0.99	0.156	3.165	0.255	1.533
1.00	0.159	3.230	0.261	1.567

TABLE VIIIa. The quark parton model predictions of the Weinberg model for the ratios $(NC/CC)^{cut}_{\nu,\bar{\nu}}$ and $(NC/CC)_{\nu,\bar{\nu}}$. The value of the ratio $R = \sigma^{CC}(\bar{\nu})/\sigma^{CC}(\nu)$ is equal to .37. In this table R-NEU CUT, R-ANEU CUT, R-NEU and R-ANEU denote the ratios $(NC/CC)^{cut}_{\nu}$, $(NC/CC)^{cut}_{\bar{\nu}}$, $(NC/CC)_{\nu}$ and $(NC/CC)_{\bar{\nu}}$ respectively.

TABLE VIIIb

R=0.38

Z	R-NEU CUT	R-ANEU CUT	R-NEU	R-ANEU
0.01	0.490	0.490	0.490	0.490
0.02	0.480	0.481	0.480	0.481
0.03	0.471	0.473	0.471	0.472
0.04	0.461	0.466	0.461	0.463
0.05	0.452	0.459	0.452	0.455
0.06	0.442	0.453	0.443	0.447
0.07	0.433	0.447	0.434	0.443
0.08	0.424	0.443	0.425	0.433
0.09	0.415	0.439	0.416	0.426
0.10	0.407	0.435	0.408	0.420
0.11	0.398	0.433	0.399	0.414
0.12	0.390	0.431	0.391	0.409
0.13	0.381	0.430	0.383	0.404
0.14	0.373	0.429	0.375	0.400
0.15	0.365	0.430	0.367	0.395
0.16	0.357	0.431	0.360	0.392
0.17	0.349	0.432	0.352	0.388
0.18	0.342	0.435	0.345	0.385
0.19	0.334	0.438	0.338	0.383
0.20	0.327	0.441	0.331	0.381
0.21	0.319	0.446	0.324	0.379
0.22	0.312	0.451	0.317	0.378
0.23	0.305	0.457	0.311	0.377
0.24	0.298	0.464	0.304	0.376
0.25	0.292	0.471	0.298	0.376
0.26	0.285	0.479	0.292	0.376
0.27	0.279	0.488	0.286	0.377
0.28	0.272	0.497	0.280	0.378
0.29	0.266	0.507	0.274	0.380
0.30	0.260	0.518	0.269	0.382
0.31	0.254	0.530	0.264	0.384
0.32	0.248	0.542	0.259	0.387
0.33	0.242	0.555	0.253	0.390
0.34	0.237	0.569	0.249	0.393
0.35	0.232	0.583	0.244	0.397
0.36	0.226	0.598	0.239	0.401
0.37	0.221	0.614	0.235	0.406
0.38	0.216	0.631	0.231	0.411
0.39	0.211	0.648	0.227	0.417
0.40	0.206	0.666	0.223	0.423
0.41	0.202	0.685	0.219	0.429
0.42	0.197	0.704	0.215	0.436
0.43	0.193	0.724	0.212	0.443
0.44	0.189	0.745	0.208	0.451
0.45	0.185	0.766	0.205	0.459
0.46	0.181	0.789	0.202	0.467
0.47	0.177	0.811	0.199	0.476

TABLE VIIIb (continued)

z	R-NEU CUT	R-ANEU CUT	R-NEU	R-ANEU
0.48	0.173	0.835	0.197	0.465
0.49	0.170	0.859	0.194	0.494
0.50	0.166	0.884	0.192	0.504
0.51	0.163	0.910	0.189	0.515
0.52	0.160	0.937	0.187	0.526
0.53	0.157	0.964	0.185	0.537
0.54	0.154	0.991	0.184	0.548
0.55	0.151	1.020	0.182	0.560
0.56	0.149	1.049	0.180	0.573
0.57	0.146	1.079	0.179	0.585
0.58	0.144	1.110	0.178	0.599
0.59	0.142	1.141	0.177	0.612
0.60	0.140	1.173	0.176	0.626
0.61	0.138	1.206	0.175	0.641
0.62	0.136	1.240	0.175	0.656
0.63	0.134	1.274	0.174	0.671
0.64	0.133	1.309	0.174	0.686
0.65	0.131	1.345	0.174	0.702
0.66	0.130	1.381	0.174	0.719
0.67	0.129	1.418	0.174	0.736
0.68	0.128	1.456	0.175	0.753
0.69	0.127	1.494	0.175	0.771
0.70	0.126	1.533	0.176	0.789
0.71	0.125	1.573	0.176	0.807
0.72	0.125	1.614	0.177	0.826
0.73	0.125	1.655	0.179	0.845
0.74	0.124	1.697	0.180	0.865
0.75	0.124	1.740	0.181	0.885
0.76	0.124	1.783	0.183	0.905
0.77	0.125	1.827	0.185	0.926
0.78	0.125	1.872	0.186	0.947
0.79	0.125	1.918	0.188	0.969
0.80	0.126	1.964	0.191	0.991
0.81	0.127	2.011	0.193	1.014
0.82	0.128	2.059	0.196	1.037
0.83	0.128	2.107	0.198	1.060
0.84	0.130	2.156	0.201	1.084
0.85	0.131	2.206	0.204	1.108
0.86	0.132	2.256	0.207	1.132
0.87	0.134	2.307	0.210	1.157
0.88	0.135	2.359	0.214	1.182
0.89	0.137	2.412	0.217	1.208
0.90	0.139	2.465	0.221	1.234
0.91	0.141	2.519	0.225	1.261
0.92	0.143	2.574	0.229	1.288
0.93	0.146	2.629	0.233	1.315
0.94	0.148	2.686	0.237	1.343
0.95	0.151	2.742	0.242	1.371
0.96	0.153	2.800	0.247	1.399
0.97	0.156	2.858	0.251	1.428
0.98	0.159	2.917	0.256	1.456
0.99	0.162	2.977	0.261	1.487
1.00	0.166	3.037	0.267	1.518

TABLE VIIIb. The quark parton model predictions of the Weinberg model for the ratios $(NC/CC)^{cut}_{\nu,\bar{\nu}}$ and $(NC/CC)_{\nu,\bar{\nu}}$. The value of the ratio $R = \sigma^{cc}(\bar{\nu})/\sigma^{cc}(\nu)$ is equal to .38 .In this table R-NEU CUT,R-ANEU CUT,R-NEU and R-ANEU denote the ratios $(NC/CC)^{cut}_{\nu}$, $(NC/CC)^{cut}_{\bar{\nu}}$, $(NC/CC)_{\nu}$ and $(NC/CC)_{\bar{\nu}}$ respectively.

TABLE VIIIc

R=0.39

Z	R-NEU CUT	R-ANEU CUT	R-NEU	R-ANEU
0.01	0.490	0.490	0.490	0.490
0.02	0.480	0.481	0.480	0.481
0.03	0.471	0.473	0.471	0.472
0.04	0.461	0.465	0.461	0.463
0.05	0.452	0.458	0.452	0.455
0.06	0.442	0.452	0.443	0.447
0.07	0.433	0.446	0.434	0.440
0.08	0.424	0.442	0.425	0.433
0.09	0.415	0.437	0.416	0.426
0.10	0.407	0.434	0.408	0.420
0.11	0.398	0.431	0.399	0.414
0.12	0.390	0.428	0.391	0.409
0.13	0.381	0.427	0.383	0.403
0.14	0.373	0.426	0.375	0.399
0.15	0.365	0.426	0.367	0.395
0.16	0.357	0.426	0.360	0.391
0.17	0.349	0.427	0.352	0.387
0.18	0.342	0.429	0.345	0.384
0.19	0.334	0.432	0.338	0.381
0.20	0.327	0.435	0.331	0.379
0.21	0.320	0.438	0.324	0.377
0.22	0.313	0.443	0.317	0.376
0.23	0.306	0.448	0.311	0.375
0.24	0.299	0.454	0.304	0.374
0.25	0.292	0.460	0.298	0.374
0.26	0.285	0.468	0.292	0.374
0.27	0.279	0.475	0.286	0.374
0.28	0.273	0.484	0.281	0.375
0.29	0.266	0.493	0.275	0.377
0.30	0.260	0.503	0.270	0.378
0.31	0.255	0.514	0.264	0.380
0.32	0.249	0.525	0.259	0.383
0.33	0.243	0.537	0.254	0.386
0.34	0.238	0.549	0.249	0.389
0.35	0.232	0.562	0.245	0.393
0.36	0.227	0.576	0.240	0.397
0.37	0.222	0.591	0.236	0.401
0.38	0.217	0.606	0.232	0.406
0.39	0.212	0.622	0.227	0.411
0.40	0.207	0.639	0.224	0.417
0.41	0.203	0.656	0.220	0.423
0.42	0.199	0.674	0.216	0.429
0.43	0.194	0.692	0.213	0.436
0.44	0.190	0.712	0.210	0.443
0.45	0.186	0.732	0.206	0.451
0.46	0.182	0.752	0.203	0.459
0.47	0.178	0.774	0.201	0.467

TABLE VIIIc (continued)

z	R-NEU CUT	R-ANEU CUT	R-NEU	R-ANEU
0.48	0.175	0.796	0.198	0.476
0.49	0.171	0.818	0.195	0.485
0.50	0.168	0.842	0.193	0.496
0.51	0.165	0.866	0.191	0.505
0.52	0.162	0.890	0.189	0.515
0.53	0.159	0.916	0.187	0.526
0.54	0.156	0.942	0.185	0.537
0.55	0.153	0.968	0.184	0.549
0.56	0.151	0.996	0.182	0.561
0.57	0.148	1.024	0.181	0.573
0.58	0.146	1.052	0.180	0.586
0.59	0.144	1.082	0.179	0.599
0.60	0.142	1.112	0.178	0.613
0.61	0.140	1.143	0.177	0.627
0.62	0.138	1.174	0.177	0.641
0.63	0.137	1.206	0.176	0.656
0.64	0.135	1.239	0.176	0.671
0.65	0.134	1.272	0.176	0.687
0.66	0.133	1.306	0.176	0.703
0.67	0.132	1.341	0.177	0.719
0.68	0.131	1.377	0.177	0.736
0.69	0.130	1.413	0.178	0.753
0.70	0.129	1.449	0.178	0.770
0.71	0.129	1.487	0.179	0.788
0.72	0.128	1.525	0.180	0.806
0.73	0.128	1.564	0.182	0.825
0.74	0.128	1.603	0.183	0.844
0.75	0.128	1.644	0.184	0.864
0.76	0.128	1.684	0.186	0.884
0.77	0.128	1.726	0.188	0.904
0.78	0.129	1.768	0.190	0.925
0.79	0.129	1.811	0.192	0.946
0.80	0.130	1.854	0.194	0.967
0.81	0.131	1.899	0.197	0.989
0.82	0.132	1.943	0.199	1.011
0.83	0.133	1.989	0.202	1.034
0.84	0.134	2.035	0.205	1.057
0.85	0.135	2.082	0.208	1.081
0.86	0.137	2.130	0.211	1.104
0.87	0.138	2.178	0.214	1.129
0.88	0.140	2.227	0.218	1.153
0.89	0.142	2.276	0.222	1.178
0.90	0.144	2.327	0.225	1.204
0.91	0.146	2.378	0.229	1.230
0.92	0.149	2.429	0.234	1.256
0.93	0.151	2.482	0.238	1.283
0.94	0.154	2.534	0.242	1.310
0.95	0.156	2.588	0.247	1.337
0.96	0.159	2.642	0.252	1.365
0.97	0.162	2.697	0.257	1.393
0.98	0.165	2.753	0.262	1.422
0.99	0.168	2.809	0.267	1.451
1.00	0.172	2.866	0.272	1.480

TABLE VIIIc. The quark parton model predictions of the Weinberg model for the ratios $(NC/CC)^{cut}_{\nu,\bar{\nu}}$ and $(NC/CC)_{\nu,\bar{\nu}}$. The value of the ratio $R = \sigma^{cc}(\bar{\nu})/\sigma^{cc}(\nu)$ is equal to .39. In this table R-NEU CUT, R-ANEU CUT, R-NEU and R-ANEU denote the ratios $(NC/CC)^{cut}_{\nu}$, $(NC/CC)^{cut}_{\bar{\nu}}$, $(NC/CC)_{\nu}$ and $(NC/CC)_{\bar{\nu}}$ respectively.

TABLE VIIId

R=0.40

Z	R-NEU CUT	R-ANTI CUT	R-NEU	R-ANTI
0.01	0.490	0.490	0.490	0.490
0.02	0.480	0.481	0.480	0.481
0.03	0.471	0.473	0.471	0.472
0.04	0.461	0.465	0.461	0.463
0.05	0.452	0.458	0.452	0.455
0.06	0.442	0.452	0.443	0.447
0.07	0.433	0.446	0.434	0.440
0.08	0.424	0.441	0.425	0.432
0.09	0.415	0.436	0.416	0.426
0.10	0.407	0.432	0.408	0.419
0.11	0.398	0.429	0.399	0.414
0.12	0.390	0.426	0.391	0.408
0.13	0.381	0.424	0.383	0.403
0.14	0.373	0.423	0.375	0.398
0.15	0.365	0.422	0.368	0.394
0.16	0.357	0.422	0.360	0.390
0.17	0.350	0.423	0.352	0.386
0.18	0.342	0.424	0.345	0.383
0.19	0.334	0.425	0.338	0.380
0.20	0.327	0.429	0.331	0.378
0.21	0.320	0.432	0.324	0.376
0.22	0.313	0.436	0.318	0.374
0.23	0.306	0.440	0.311	0.373
0.24	0.299	0.445	0.305	0.372
0.25	0.292	0.451	0.299	0.372
0.26	0.286	0.457	0.293	0.371
0.27	0.279	0.464	0.287	0.372
0.28	0.273	0.472	0.281	0.372
0.29	0.267	0.480	0.275	0.374
0.30	0.261	0.489	0.270	0.375
0.31	0.255	0.499	0.265	0.377
0.32	0.249	0.509	0.260	0.379
0.33	0.244	0.520	0.255	0.382
0.34	0.238	0.531	0.250	0.385
0.35	0.233	0.544	0.245	0.388
0.36	0.228	0.556	0.241	0.392
0.37	0.223	0.570	0.236	0.396
0.38	0.218	0.584	0.232	0.401
0.39	0.213	0.599	0.228	0.406
0.40	0.208	0.614	0.224	0.411
0.41	0.204	0.630	0.221	0.417
0.42	0.200	0.647	0.217	0.423
0.43	0.195	0.664	0.214	0.430
0.44	0.191	0.682	0.211	0.436
0.45	0.187	0.701	0.207	0.444
0.46	0.183	0.720	0.205	0.451
0.47	0.180	0.740	0.202	0.460

TABLE VIIId (continued)

Z	R-NEU CUT	R-ANEU CUT	R-NEU	R-ANEU
0.48	0.176	0.760	0.199	0.468
0.49	0.173	0.781	0.197	0.477
0.50	0.170	0.803	0.194	0.486
0.51	0.166	0.826	0.192	0.496
0.52	0.163	0.849	0.190	0.506
0.53	0.160	0.873	0.189	0.516
0.54	0.158	0.897	0.187	0.527
0.55	0.155	0.922	0.185	0.538
0.56	0.153	0.948	0.184	0.550
0.57	0.150	0.974	0.183	0.562
0.58	0.148	1.001	0.182	0.574
0.59	0.146	1.029	0.181	0.587
0.60	0.144	1.057	0.180	0.600
0.61	0.142	1.086	0.179	0.614
0.62	0.141	1.115	0.179	0.627
0.63	0.139	1.145	0.179	0.642
0.64	0.138	1.176	0.179	0.656
0.65	0.136	1.208	0.179	0.672
0.66	0.135	1.240	0.179	0.687
0.67	0.134	1.272	0.179	0.703
0.68	0.134	1.306	0.180	0.719
0.69	0.133	1.340	0.180	0.736
0.70	0.132	1.374	0.181	0.753
0.71	0.132	1.410	0.182	0.770
0.72	0.132	1.446	0.183	0.788
0.73	0.131	1.482	0.184	0.806
0.74	0.131	1.520	0.186	0.825
0.75	0.131	1.557	0.187	0.844
0.76	0.132	1.596	0.189	0.863
0.77	0.132	1.635	0.191	0.883
0.78	0.133	1.675	0.193	0.903
0.79	0.133	1.715	0.195	0.924
0.80	0.134	1.756	0.198	0.944
0.81	0.135	1.798	0.200	0.966
0.82	0.136	1.841	0.203	0.987
0.83	0.137	1.884	0.206	1.010
0.84	0.138	1.927	0.209	1.032
0.85	0.140	1.972	0.212	1.055
0.86	0.142	2.016	0.215	1.078
0.87	0.143	2.062	0.219	1.102
0.88	0.145	2.108	0.222	1.126
0.89	0.147	2.155	0.226	1.150
0.90	0.149	2.203	0.230	1.175
0.91	0.152	2.251	0.234	1.200
0.92	0.154	2.300	0.238	1.226
0.93	0.156	2.349	0.243	1.252
0.94	0.159	2.399	0.247	1.278
0.95	0.162	2.450	0.252	1.305
0.96	0.165	2.501	0.257	1.332
0.97	0.168	2.553	0.262	1.360
0.98	0.171	2.606	0.267	1.387
0.99	0.175	2.659	0.272	1.416
1.00	0.178	2.713	0.278	1.444

TABLE VIIId. The quark parton model predictions of the Weinberg model for the ratios $(NC/CC)^{cut}_{\nu,\bar{\nu}}$ and $(NC/CC)_{\nu,\bar{\nu}}$. The value of The ratio $R = \sigma^{cc}(\bar{\nu})/\sigma^{cc}(\nu)$ is equal to .40. In this table R-NEU CUT, R-ANEU CUT, R-NEU and R-ANEU denote the ratios $(NC/CC)^{cut}_{\nu}$, $(NC/CC)^{cut}_{\bar{\nu}}$, $(NC/CC)_{\nu}$ and $(NC/CC)_{\bar{\nu}}$ respectively.

TABLE IX

	R = .36		R = .38		R = .40	
z	$(NC/CC)_{\nu}^{cut}$	$(NC/CC)_{\bar{\nu}}^{cut}$	$(NC/CC)_{\nu}^{cut}$	$(NC/CC)_{\bar{\nu}}^{cut}$	$(NC/CC)_{\nu}^{cut}$	$(NC/CC)_{\bar{\nu}}^{cut}$
.20	.338	.530	.347	.553	.357	.571
.22	.323	.541	.332	.560	.342	.574
.24	.308	.556	.318	.569	.327	.580
.26	.295	.574	.304	.582	.313	.588
.28	.281	.595	.290	.597	.300	.600
.30	.269	.619	.278	.616	.287	.614
.32	.257	.647	.266	.638	.275	.632
.34	.245	.678	.254	.664	.263	.652
.36	.234	.713	.243	.692	.252	.675
.38	.224	.751	.233	.723	.242	.701
.40	.214	.792	.223	.758	.232	.731

TABLE IX. The quark parton model predictions of the Weinberg model for the ratios $(NC/CC)_{\nu,\bar{\nu}}^{cut}$ for the below the charm production thresnold. The values shown correspond to values of the ratio $R = \sigma^{cc}(\bar{\nu})/\sigma^{cc}(\nu)$ equal to .36,.38 and .40 respectively.

The best fit to the experimental data for the ratios $(^{NC}/_{CC})^{cut}_{\nu,\bar{\nu}}$ is for R = .40 and for values of Z such that $.30 \lesssim Z \lesssim .35$. For these values of Z we have $(^{NC}/_{CC})_{\nu} \approx .24$ and $(^{NC}/_{CC})_{\bar{\nu}} \approx .38$; the last ratio is within the experimental limits (see Table IVc); unfortunately the ratio $(^{NC}/_{CC})_{\nu}$ is in disagreement with the experimental value $.12 \pm .04$ (see Table IVc). Thus for no value of z the four ratios $(^{NC}/_{CC})^{cut}_{\nu,\bar{\nu}}$, $(^{NC}/_{CC})_{\nu,\bar{\nu}}$ are fitted simultaneously.

Note that the value $Z \approx .30$ is consistent with the upper bound $Z < .3$ [see Ref. 68].

So far, in this section, we have assumed that we are above the threshold for the production of charmed states. The Gargamelle data should be compared with the below the charm production case as well. In this case the ratios $\sigma^{CC}(\bar{\nu})/\sigma^{CC}(\nu)$ and $(^{NC}/_{CC})^{cut}_{\nu,\bar{\nu}}$ are given by the following relations

$$R = \sigma^{CC}(\bar{\nu})/\sigma^{CC}(\nu) = \frac{3+8\rho}{9+8\rho} \qquad (3.38a)$$

$$\left(\frac{NC}{CC}\right)^{cut}_{\nu} = \left(\frac{17.22+45.92\rho}{27.00+20.66\rho}\right)Z^2 + \left(\frac{3.00+4.59\rho}{3.00+2.29\rho}\right)\left(-Z+\frac{1}{2}\right) \qquad (3.38b)$$

$$\left(\frac{NC}{CC}\right)^{cut}_{\bar{\nu}} = \left(\frac{127.5+340.0\rho}{27.0+153.0\rho}\right)Z^2 + \left(\frac{3.0+34.0\rho}{3.0+17.0\rho}\right)\left(-Z+\frac{1}{2}\right) . \qquad (3.38c)$$

It is easy to verify that if we replace ρ by 2ρ in the denominators of the expressions (3.38b) and (3.38c), we get the corresponding ratios for above the charm production threshold. In the Table IX the values of $(^{NC}/_{CC})^{cut}_{\nu,\bar{\nu}}$ are given (below the charm production threshold) for Z varying from .2 to .4 and for the values of $R = \sigma^{CC}(\bar{\nu})/\sigma^{CC}(\nu)$ .36, .38 and .40 respectively. We observe that there is no value of Z for which the ratios $(^{NC}/_{CC})^{cut}_{\nu,\bar{\nu}}$ are consistent with the Gargamelle group data.

Choosing the value $\sigma^{cc}(\bar{\nu})/\sigma^{cc}(\nu) = .40$, for which the best fit to the neutral current data is obtained, we have for the charge current reactions total cross sections $\sigma^{cc}(\nu)$ and $\sigma^{cc}(\bar{\nu})$

$$\sigma^{cc}(\nu) = \frac{G^2ME}{\pi}\,\frac{10}{3}\upsilon \equiv \alpha(\nu)\,E \qquad (3.39a)$$

$$\sigma^{cc}(\bar{\nu}) = \frac{G^2ME}{\pi}\,\frac{4}{3}\upsilon \equiv \alpha(\bar{\nu})\,E \quad . \qquad (3.39b)$$

From the Table IVa of the second chapter we see that $\alpha(\nu) = .78 \pm .07$ and $\alpha(\bar{\nu}) = .28 \pm .025$; thus $.71 \leq \alpha(\nu) \leq .85$ and $.255 \leq \alpha(\bar{\nu}) \leq .305$ from which it follows that "υ" must lie within the range†

$$.139 \lesssim \upsilon \lesssim .150 \quad . \qquad (3.40)$$

The Kuti-Weisskopf parton model gives $\upsilon = \frac{1}{9} \simeq .111$ which is outside the limits given by (3.40).

We end this section by concluding that good agreement with the charge current and neutral current reaction data is obtained when $c/\upsilon = \frac{1}{16}$ (this corresponds to taking $R = .40$) and $.139 \leq \upsilon \leq .15$.

In the next section we try to build a quark parton model which fulfills these requirements.

III2)$_B$ A Modification of the R.Mc.Elhaney-S.F.Tuan Parton Model.

Guided by the results of the previous section we try to fit the data by considering modifications of the original K-W quark parton model. Unlike the modified K-W model, which was discussed in the first

† $\frac{G^2M}{\pi} = 1.53 \times 10^{-38}$ cm^2/GeV

part of this chapter, we do not introduce any additional hadronic constituents except the four quarks p,p', n,λ. In the first chapter we briefly discussed the K-W parton model. The details of the model and its prediction for the deep inelastic electro-production scattering can be found in the Kuti and Weisskopf's paper [51]. The model prediction for the ratio $F_2^{(en)}(x)/F_2^{(ep)}(x)$, with $F_2^{(ep)}$ and $F_2^{(en)}$ being the deep inelastic proton and neutron structure functions respectively, gives a value equal to $^2/3$ when x approaches 1. Experimentally [77] this ratio seems to tend to the lower limit of Nachtmann's inequality as $x \to 1$, that is

$$\frac{F_2^{(en)}(x)}{F_2^{(ep)}(x)}_{x\to 1} \to \frac{1}{4} \quad .$$

R.Mc.Elhaney and S.F. Tuan [78] modified the original K-W model. They assumed that the n-type quark valence probability distribution is not given by Eq. (2.27) but by the relation

$$dP_u(x) = \frac{(1-x)x^{1-\alpha(0)}}{(x^2+\mu^2/p^2)^{\frac{1}{2}}} \quad . \qquad (3.41)$$

The p-type quark valence probability distribution is again given by (2.27). The distribution functions $f_i^{(p)}(x)$ and $f_i^{(n)}(x)$ are found to be

$$f_p^{(p)}(x) = f_n^{(n)}(x) = 2u(x) + c(x) \qquad (3.42a)$$

$$f_n^{(p)}(x) = f_p^{(n)}(x) = d(x) + c(x) \qquad (3.42b)$$

$$f_i^{(p,n)}(x) = c(x) \quad \text{when} \quad i \neq p, n \quad \text{quark} \qquad (3.42c)$$

where $v(x)$, $d(x)$ and $c(x)$ are given by the following expressions

$$v(x) = \vec{B}(1-\alpha, 1+\gamma+2(1-\alpha))\, x^{-\alpha}(1-x)^{-1+\gamma+2(1-\alpha)} \times \left\{1 - \frac{(1-\alpha)}{\gamma+2(1-\alpha)}(1-x)\right\} \quad (3.43a)$$

$$d(x) = \vec{B}(1-\alpha, 1+\gamma+2(1-\alpha))\, x^{-\alpha}(1-x)^{\gamma+2(1-\alpha)} \quad (3.43b)$$

$$c(x) = G_g\, x^{-1}(1-x)^{-1+\gamma+3(1-\alpha)} \quad . \quad (3.43c)$$

The constant α is equal to $^1/2$ as in the original K-W model. Also from the behaviour $F_2^{(ep)}(x) \sim (1-x)^3$ of the structure function $F_2^{(ep)}(x)$ near zero, we have $-1 + \gamma + 2(1-\alpha) = 3$ and because $\alpha = \frac{1}{2}$ this implies $\gamma = 3$. For these values of the constants γ and α, the first moment of the function $(2v(x) + d(x))/3$ has the value .106 which is too small to be within the limits given by (3.40). Thus the model does not fit the neutrino and antineutrino data. As far as the electroproduction data are concerned we see that because $\frac{d(x)}{v(x)} \underset{x\to 1}{\to} 0$ it follows that $\frac{F_2^{(en)}(x)}{F_2^{(ep)}(x)} \underset{x\to 1}{\to} \frac{1}{4}$ agreeing thus with experiment [77]. The model fit to the electroproduction structure function $F_2^{(ep)}(x)$ can be found in R.Mc.Elhaney and S.F. Tuan's paper [78]. There we see that the model does not fit the data very well.

We modify the model by assuming that the valence and core distribution function $v(x)$, $d(x)$ and $c(x)$ given by Eqs. (3.43) have the following forms

$$v(x) = \cos^2\omega\, v_1(x) + \sin^2\omega\, v_2(x) \quad (3.44a)$$

$$d(x) = \cos^2\omega\, d_1(x) + \sin^2\omega\, d_2(x) \quad (3.44b)$$

$$c(x) = \cos^2\omega\, c_1(x) + \sin^2\omega\, c_2(x) \quad . \quad (3.44c)$$

$u_1(x)$, $d_1(x)$ and $c_1(x)$ are given by the expressions (3.43a), (3.43b) and (3.43c) respectively for $\gamma = 3$ and $\alpha = \frac{1}{2}$. The functions $u_2(x)$, $d_2(x)$ and $c_2(x)$ correspond to different values of the parameters α and γ. We obtained good agreement with data by taking $\alpha = 0$ and $\gamma = 2$, having thus

$$u_2(x) = 5(1-x)^3\left\{1 - \frac{1}{4}(1-x)\right\} \qquad (3.45a)$$

$$d_2(x) = 5(1-x)^4 \qquad (3.45b)$$

$$c_2(x) = G_g\, x^{-1}(1-x)^4 \qquad (3.45c)$$

The decomposition of the valence and core distribution functions into two parts, as written in Eqs. (3.44), can be justified by saying that the proton's and neutron's wave functions are written in the form

$$|proton\rangle = \cos\omega\,|ppn+core\rangle_1 + \sin\omega\,|ppn+core\rangle_2 \qquad (3.46a)$$

$$|neutron\rangle = \cos\omega\,|pnn+core\rangle_1 + \sin\omega\,|pnn+core\rangle_2 \qquad (3.46b)$$

The states $|\,\rangle_1$ and $|\,\rangle_2$ are assumed to be orthogonal to each other and they only differ in the way the constituents are bound to form a hadron. Thus for the state $|\,\rangle_1$ the probability to find a valence p-type quark is $u_1(x)$ while for the state $|\,\rangle_2$ is $u_2(x)$, in general different from $u_1(x)$. The same happens for the other quarks. It is evident now that the probability to find a p-quark as a valence constituent is given by (3.44a).

Similarly the n-quark valence distribution function is given by (3.44b).

Note that in order to have the minimum number of parameters we take the core function $c_1(x)$ and $c_2(x)$ to have the same constants, that is $G_1=G_2=G_8$

The choice $\alpha = 0$,for the functions u_2, d_2 and c_2,can not correspond to either a Regge trajectory passing through $\alpha = 0$ or to a fixed pole at $J= 0$.† At any rate,in this model,the choice $\alpha = 0$ is a parametrization which fits,as we shall see, the deep inelastic neutrino and electron data and need not be related to Regge dynamics.

With this choice for the functions $U(x)$, $d(x)$ and $c(x)$ the asymptotic behaviour of the functions $F_2^{(ep)}(x)$ and $F_2^{(en)}(x)$ at $x \approx 0$ and $x \approx 1$ is not altered. Also the ratio $F_2^{(en)}(x)/F_2^{(ep)}(x)$ tends to $\frac{1}{4}$ as $x \to 1$.

The determination of the angle ω is done by requiring that the first moment of the function $V(x) = (2u(x) + d(x))/3$ lies within the limits given by (3.40). Also the constant G_8 of the core distribution function is determined from the value of the ratio $\rho\ (\equiv {}^{c}/_{u})$. We take ρ to be equal to $\rho = \frac{1}{16}$, the value of ρ for which the best fit to the ratios $({}^{NC}/_{CC})^{cut}_{\nu,\nu}$, $({}^{NC}/_{CC})_{\nu,\bar{\nu}}$ is obtained. In the Table X the predictions of the model for the neutrino and antinuetrino reactions are given for three different values of the parameter $\lambda \equiv \cos^2\omega$; the values of λ are .624, .559, and .500 ,which correspond to taking $\int_0^1 xV(x)dx$ equal to .139, .145, and .150 respectively. The value .139 is the low limit of (3.40) and .150 is the upper limit.

---

† This is a consequence of the fact that the forward amplitude $T(\nu, Q^2)$ for the virtual process $\gamma(Q^2)+p \to \gamma(Q^2)+p$ is crossing symmetric.

TABLE X

	$\lambda = .624$	$\lambda = .559$	$\lambda = .500$
$\sigma^{cc}(\nu)$	$(.710)E^{\dagger}$	$(.739)E^{\dagger}$	$(.765)E^{\dagger}$
$\sigma^{cc}(\bar{\nu})$	$(.285)E^{\dagger}$	$(.296)E^{\dagger}$	$(.306)E^{\dagger}$
$\sigma^{cc}(\bar{\nu})/\sigma^{cc}(\nu)$	.40	.40	.40
$\langle xy \rangle_{\nu}$	.141	.145	.145
$\langle xy \rangle_{\bar{\nu}}$	.075	.079	.076
A	1	1	1
B	.857	.857	.857
B'	.910	.896	.913
$\int_0^1 F_2^{(\nu N)}(x)dx$	.487	.507	.525
$\int_0^1 F_2^{(\nu p)}(x)dx$	.308	.321	.332
$\int_0^1 F_2^{(\nu n)}(x)dx \Big/ \int_0^1 F_2^{(\nu p)}(x)dx$	2.161	2.161	2.159

* For the ratios $(NC/CC)^{cut}_{\nu,\bar{\nu}}$ and $(NC/CC)_{\nu,\bar{\nu}}$ see the table VIIId

TABLE X. The predictions of the modified R.Mc.Elhaney-S.F.Tuan model, discussed in the second part of chapter III, for the main physical quantities concerning deep inelastic neutrino and antineutrino experiments. The three columns correspond to the three values of the parameter $\lambda = \cos^2\omega$ .624, .559 and .500 respectively.

---

† In units of 10^{-38} cm^2.
$G^2M/\pi = 1.53\times10^{-36}$ cm^2/Gev for $GM^2 = 1.01\times10^{-5}$

In terms of the first and second moments of the functions V(x) and c(x) the quantities B and B' are given by

$$B = \frac{3V}{3V+8C} = \frac{3}{3+8\rho} \qquad (3.47a)$$

$$B' = \frac{3V'}{3V'+8C'} \quad . \qquad (3.47b)$$

V, V', C and C' are defined as $\begin{Bmatrix} V \\ C \end{Bmatrix} = \int_0^1 x \begin{Bmatrix} V(x) \\ c(x) \end{Bmatrix} dx$ and $\begin{Bmatrix} V' \\ C' \end{Bmatrix} = \int_0^1 x^2 \begin{Bmatrix} V(x) \\ c(x) \end{Bmatrix} dx$ †.

The quantity A is equal to A = 1 because of the Callan-Gross relation $F_2(x) = 2xF_1(x)$ [33]. The quantities $\int_0^1 F_2^{(\nu N)}(x)dx$, B and B' agree with the data given in the Tables IV, IVa.

For the quantity $<xy>_\nu$ we observe that is a little larger than the experimental value .12 ± .01 (see Table IV of the second chapter). We will see later that the best fit to the electroproduction data occurs for λ = .624; for this value of λ we have $<xy>_\nu$ = .141. The corresponding values for λ = .559 and λ=500 are even larger than this one as one can see from the Table X.

The value of $<xy>_\nu$ = .141 gives‡ for the quantity $<Q^2>_\nu$ $<Q^2>_\nu$ = .265E. This value is also a little larger than the

---

† The values of the V,V',C,C' in terms of the parameter λ are given in Appendix 6b.

‡ $<Q2>_\nu$ = 2ME $<xy>_\nu$ and M = .940 GeV.

experimental value measured by the Harvard-Pensylvania-Wisconsin collaboration group [see for instance Ref. 79].

For completeness we also give the values of the integral $\int_0^1 F_2^{(\nu p)}(x)dx$ and of the ratio $\int_0^1 F_2^{(\nu n)}(x)dx / \int_0^1 F_2^{(\nu p)}(x)dx$.

Before closing the neutrino experiments we should say something about the y-distributions, defined as $\frac{1}{\sigma}\frac{d\sigma}{dy}$. From Eq. (2.51) we have

$$\frac{1}{\sigma^{cc}(\nu)}\frac{d\sigma^{cc}(\nu)}{dy} = 3\,\frac{(1-y)^2 a^{cc}(\nu) + b^{cc}(\nu)}{a^{cc}(\nu) + 3b^{cc}(\nu)} \qquad (3.48a)$$

$$\frac{1}{\sigma^{cc}(\bar{\nu})}\frac{d\sigma^{cc}(\bar{\nu})}{dy} = 3\,\frac{(1-y)^2 b^{cc}(\nu) + a^{cc}(\nu)}{b^{cc}(\nu) + 3a^{cc}(\nu)} \qquad (3.48b)$$

or because the core moment $\int_0^1 xV(x)dx$ is small compared to the valence one $\int_0^1 xc(x)dx$, we have

$$\frac{1}{\sigma^{cc}(\nu)}\frac{d\sigma^{cc}(\nu)}{dy} \simeq 1 \qquad (3.48c)$$

$$\frac{1}{\sigma^{cc}(\bar{\nu})}\frac{d\sigma^{cc}(\bar{\nu})}{dy} \simeq 3(1-y)^2 \,. \qquad (3.48d)$$

Data exhibit this behaviour as it can be seen in figure 13 of Ref. [72].

After having examined the neutrino and antineutrino induced reactions $\nu(\bar{\nu}) + N \to \mu(\mu^+) + X$ and $\nu(\bar{\nu}) + N \to \nu(\bar{\nu}) + X$ we go over to the electroproduction region and see the predictions of the model.

The relative structure functions $F_2^{(ep)}(x)$ and $F_2^{(en)}(x)$, regarding the processes $e^- p \to e^- X$ and $e^- n \to e^- X$, are given by the following relations

$$F_2^{(ep)}(x) = \frac{8}{9}\,x u(x) + \frac{1}{9}\,x d(x) + \frac{20}{9}\,x c(x) \qquad (3.49a)$$

$$F_2^{(en)}(x) = \frac{2}{9}\,x u(x) + \frac{4}{9}\,x d(x) + \frac{20}{9}\,x c(x) \,. \qquad (3.49b)$$

The functions $xu(x)$, $xd(x)$ and $xc(x)$ for the three cases $\lambda = .624, .559$ and $.500$ are given below. We remind the reader that the constant G_3 of the core distribution function is estimated from the relation $\frac{C}{V} = \frac{1}{16}$, or the same $\int_0^1 xc(x)dx = .0625\left\{\int_0^1 xV(x)dx\right\}$.

$$\lambda=.624\begin{cases} xu(x) = \frac{9}{8}(1-x)^3\{.0853(7+x)\sqrt{x}+.4178(3+x)x\} & (3.50a)\\ xd(x) = 9(1-x)^4\{.0853\sqrt{x}+.2089x\} & (3.50b)\\ xc(x) = \frac{9}{20}(1-x)^{7/2}\{.0564+.0340(1-x)^{1/2}\} & (3.50c)\end{cases}$$

$$\lambda=.559\begin{cases} xu(x) = \frac{9}{8}(1-x)^3\{.0764(7+x)\sqrt{x}+.4900(3+x)x\} & (3.51a)\\ xd(x) = 9(1-x)^4\{.0764\sqrt{x}+.2450x\} & (3.51b)\\ xc(x) = \frac{9}{20}(1-x)^{7/2}\{.0530+.0418(1-x)^{1/2}\} & (3.51c)\end{cases}$$

$$\lambda=.500\begin{cases} xu(x) = \frac{9}{8}(1-x)^3\{.0683(7+x)\sqrt{x}+.5555(3+x)x\} & (3.52a)\\ xd(x) = 9(1-x)^4\{.0683\sqrt{x}+.2777x\} & (3.52b)\\ xc(x) = \frac{9}{20}(1-x)^{7/2}\{.0493+.0493(1-x)^{1/2}\} & (3.52c)\end{cases}$$

In the Table XI the values of the function $F_2^{(ep)}(x)$ are given for the different values of x. In the Tables XIa and XIb the values of the ratio $F_2^{(en)}(x)/F_2^{(ep)}(x)$ and the values of the difference $F_2^{(ep)}(x) - F_2^{(en)}(x)$ are also given. In the Fig. 10 the function $F_2^{(ep)}(x)$ corresponding to $\lambda = .624$ is plotted against x. The $F_2^{(ep)}(x)$ for $\lambda = .624$ is closer to the experimental data [80] and for this reason the plots of the $\lambda = .559$ and $\lambda=500$ cases are not shown.

In the Figs. 11 and 12 the plots of the ratio $F_2^{(en)}(x)/F_2^{(ep)}(x)$ and the difference $F_2^{(ep)}(x) - F_2^{(en)}(x)$, for the $\lambda = .624$ case, are also shown.

TABLE XI

x	$F_2^{(ep)}(x)$		
	$\lambda = .624$	$\lambda = .559$	$\lambda = .500$
.00	.0904	.0948	.0986
.05	.2687	.2695	.2700
.10	.3267	.3318	.3361
.15	.3495	.3585	.3665
.20	.3500	.3619	.3726
.25	.3350	.3488	.3612
.30	.3094	.3241	.3372
.35	.2770	.2916	.3047
.40	.2406	.2544	.2668
.45	.2027	.2152	.2265
.50	.1653	.1761	.1859
.55	.1300	.1389	.1470
.60	.0979	.1050	.1114
.65	.0700	.0753	.0801
.70	.0469	.0506	.0539
.75	.0287	.0311	.0332
.80	.0155	.0168	.0180
.85	.0069	.0075	.0080
.90	.0021	.0023	.0025
1.00	.0000	.0000	.0000

TABLE XI. The predictions of the modified R.Mc.Elhaney-S.F.Tuan model, discussed in the second part of chapter III, for the deep inelastic electroproduction structure function $F_2^{(ep)}(x)$. The three columns correspond to the three values of the parameter $\lambda = \cos^2\omega$, .624,.559 and .500 respectively.

TABLE XIa

x	$F_2^{(en)}(x)/F_2^{(ep)}(x)$		
	$\lambda = .624$	$\lambda = .559$	$\lambda = .500$
.00	1.0000	1.0000	1.0000
.05	.7942	.8003	.8057
.10	.7511	.7556	.7595
.15	.7170	.7205	.7235
.20	.6859	.6886	.6909
.25	.6562	.6583	.6599
.30	.6272	.6288	.6300
.35	.5988	.6000	.6008
.40	.5708	.5716	.5721
.45	.5432	.5436	.5438
.50	.5158	.5159	.5159
.55	.4886	.4885	.4883
.60	.4617	.4614	.4611
.65	.4350	.4346	.4341
.70	.4085	.4080	.4074
.75	.3822	.3816	.3810
.80	.3561	.3554	.3548
.85	.3301	.3294	.3289
.90	.3042	.3036	.3031
.95	.2781	.2776	.2772
1.00	.2500	.2500	.2500

TABLE XIa. The predictions of the modified R.Mc.Elhaney-S.F.Tuan model, discussed in the second part of chapter III, for the ratio $F_2^{(en)}(x)/F_2^{(ep)}(x)$. The three columns correspond to the three values of the parameter $\lambda = \cos^2\omega$, .624, .559 and .500 respectively

TABLE XIb

x	$F_2^{(ep)}(x) - F_2^{(en)}(x)$		
	$\lambda = .624$	$\lambda = .559$	$\lambda = .500$
.00	.0000	.0000	.0000
.05	.0553	.0538	.0524
.10	.0813	.0810	.0808
.15	.0989	.1002	.1013
.20	.1099	.1127	.1151
.25	.1151	.1191	.1228
.30	.1153	.1203	.1247
.35	.1111	.1166	.1216
.40	.1032	.1090	.1141
.45	.0926	.0982	.1033
.50	.0800	.0853	.0900
.55	.0664	.0711	.0752
.60	.0527	.0565	.0600
.65	.0396	.0426	.0453
.70	.0277	.0299	.0319
.75	.0177	.0192	.0205
.80	.0100	.0108	.0116
.85	.0046	.0050	.0054
.90	.0015	.0016	.0017
.95	.0002	.0002	.0002
1.00	.0000	.0000	.0000

TABLE XIb. The predictions of the modified R.Mc.Elhaney-S.F.Tuan model, discussed in the second part of chapter III, for the difference $F_2^{(ep)}(x) - F_2^{(en)}(x)$. The three columns correspond to the three values of the parameter $\lambda = \cos^2\omega$, .624, .559 and .500 respectively.

TABLE XII

	$\lambda = .624$	$\lambda = .559$	$\lambda = .500$	Exp.value	Reference
† I^{ep}	.165	.172	.178	.17+.01	(21,80,81)
† I^{en}	.105	.110	.114	.07+.02	(21,80,81)
† $I^{eN}/I^{\nu N}$	.278	.278	.278	.28	(71,79)
$2\int_0^1 \{F_1^{(ep)} - F_1^{(en)}\}dx$	1/3	1/3	1/3	.27	(82)

TABLE XII. The predictions of the modified R.Mc.Elhaney-S.F.Tuan model, discussed in the second part of chapter III, for the quantities $I^{ep,en}$, $I^{eN}/I^{\nu N}$ and $2\int_0^1 \{F_1^{(ep)} - F_1^{(en)}\}dx$, and for the three values of the parameter $\lambda = \cos^2\omega$, .624, .559 and .500. In the last two columns we give the corresponding experimental value standing against the reference(s) is taken from.

---

† The symbol I^{mh} denotes the integral $\int_0^1 F^{(mh)}(x)dx$

TABLE XIII

$\sigma^{cc}(\nu)$ $\sigma^{cc}(\bar{\nu})$	$G^2ME/\pi\ (.464) = (.710)E\ 10^{-38}cm^2$ $G^2ME/\pi\ (.186) = (.285)E\ 10^{-38}cm^2$
$\sigma^{cc}(\bar{\nu})/\sigma^{cc}(\nu)$	.40
$\langle xy\rangle_\nu$ $\langle xy\rangle_{\bar{\nu}}$ $\langle Q^2\rangle_\nu$ $\langle Q^2\rangle_{\bar{\nu}}$	.141 .075 (.265)E (In units of $(Gev/c)^2$) (.141)E (In units of $(Gev/c)^2$)
A B B' † $I^{\nu N}$ † $I^{\nu p}$ † $I^{\nu n}/I^{\nu p}$ † I^{ep} † I^{en} † $I^{eN}/I^{\nu N}$ $2\int_0^1 \{F_1^{(ep)} - F_1^{(en)}\}dx$	1 .857 .910 .487 .308 2.161 .165 .105 .278 ($\simeq$ 5/18) 1/3
* ω_o	$\simeq$ 150
$(NC/CC)_{\nu,\bar{\nu}}$	see the table VIIId

TABLE XIII. The predictions of the modified R.Mc.Elhaney- S.F.Tuan model, discussed in the second part of chapter III, for the main physical quantities regarding deep inelastic electroproduction and neutrinoproduction experiments. The values shown correspond to a value of the parameter $\lambda = \cos^2\omega$ equal to .624.

† The symbol I^{mh} denotes the integral $\int_0^1 F_2^{(mh)}(x)dx$

* This is the value of ω_o for 90^o/o saturation of Adler sum rule.

FIGURE 10

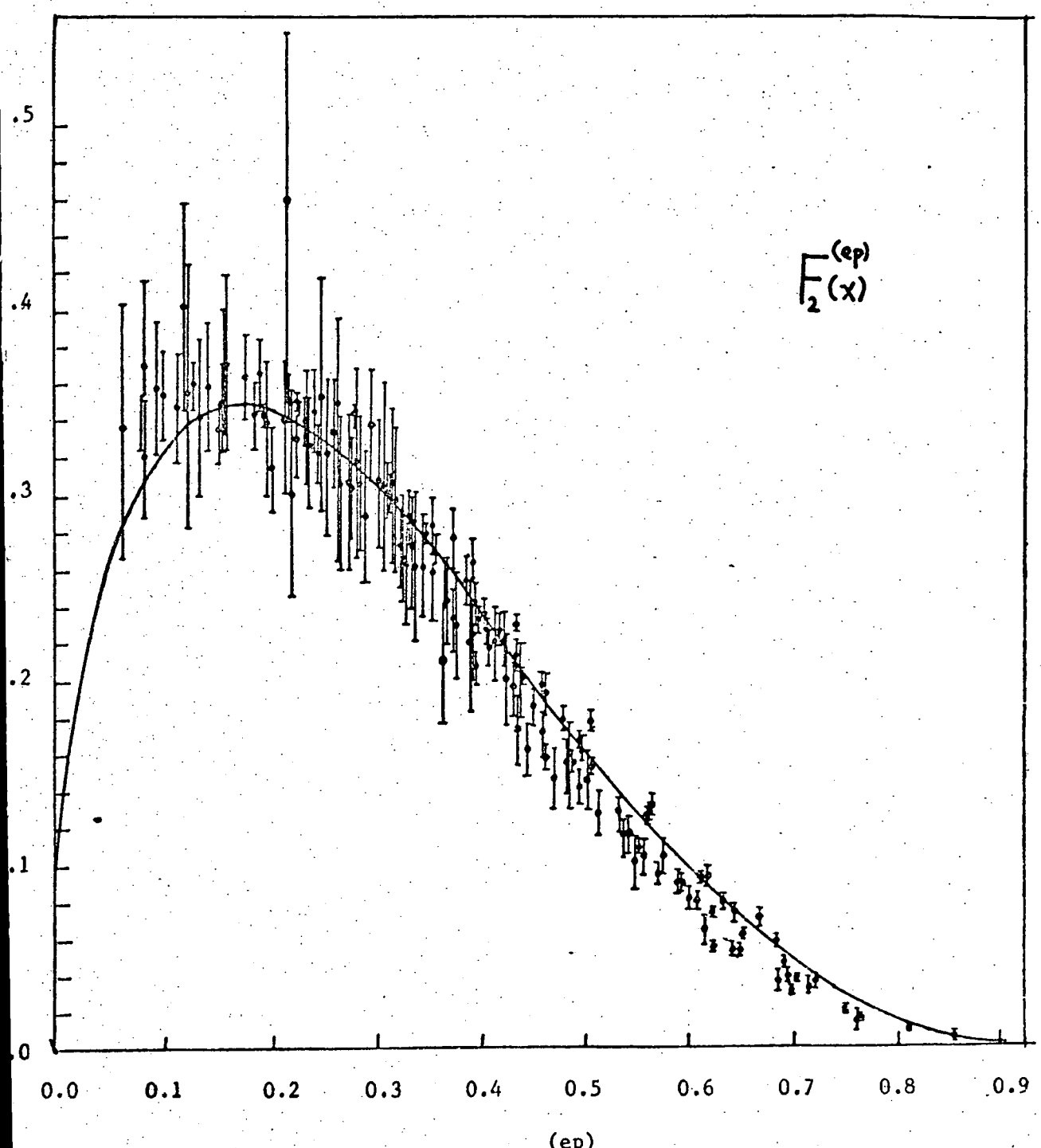

FIGURE 10. The structure function $F_2^{(ep)}(x)$ as plotted versus x. The curve shown is the fit of the modified R.Mc.Elhaney-S.F.Tuan model, discussed in the second part of chapter III, for a value of the parameter $\lambda = \cos^2\omega$ equal to .624 . The data points have been taken from references [21] and [80] .

FIGURE 11

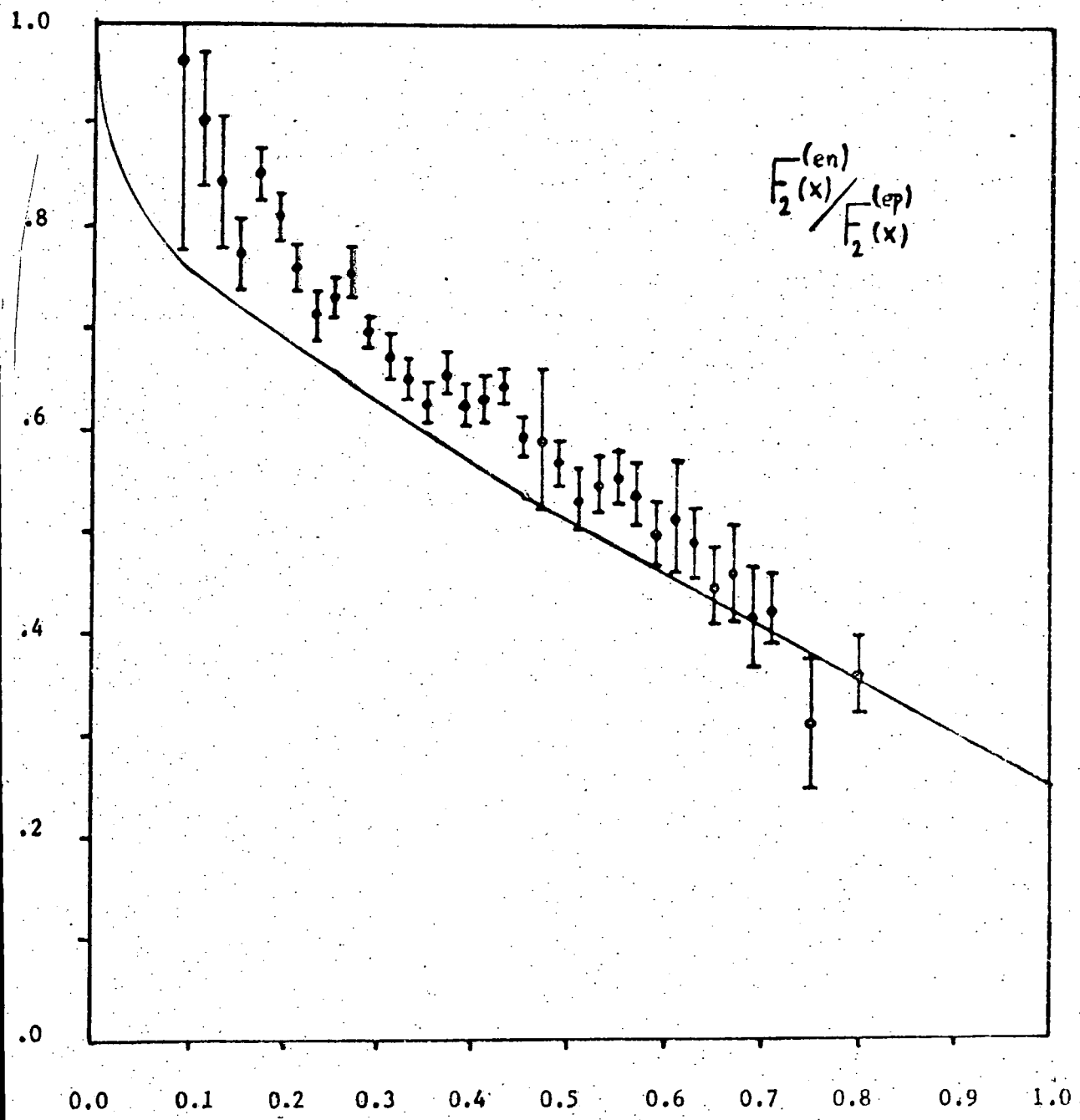

FIGURE 11. The ratio $F_2^{(en)}(x)/F_2^{(ep)}(x)$ as plotted versus x . The curve shown is the fit of the modified R.Mc.Elhaney-S.F.Tuan model, discussed in the second part of chapter III, for a value of the parameter $\lambda = \cos^2\omega$ equal to .624 . The data points have been taken from reference [80] .

FIGURE 12

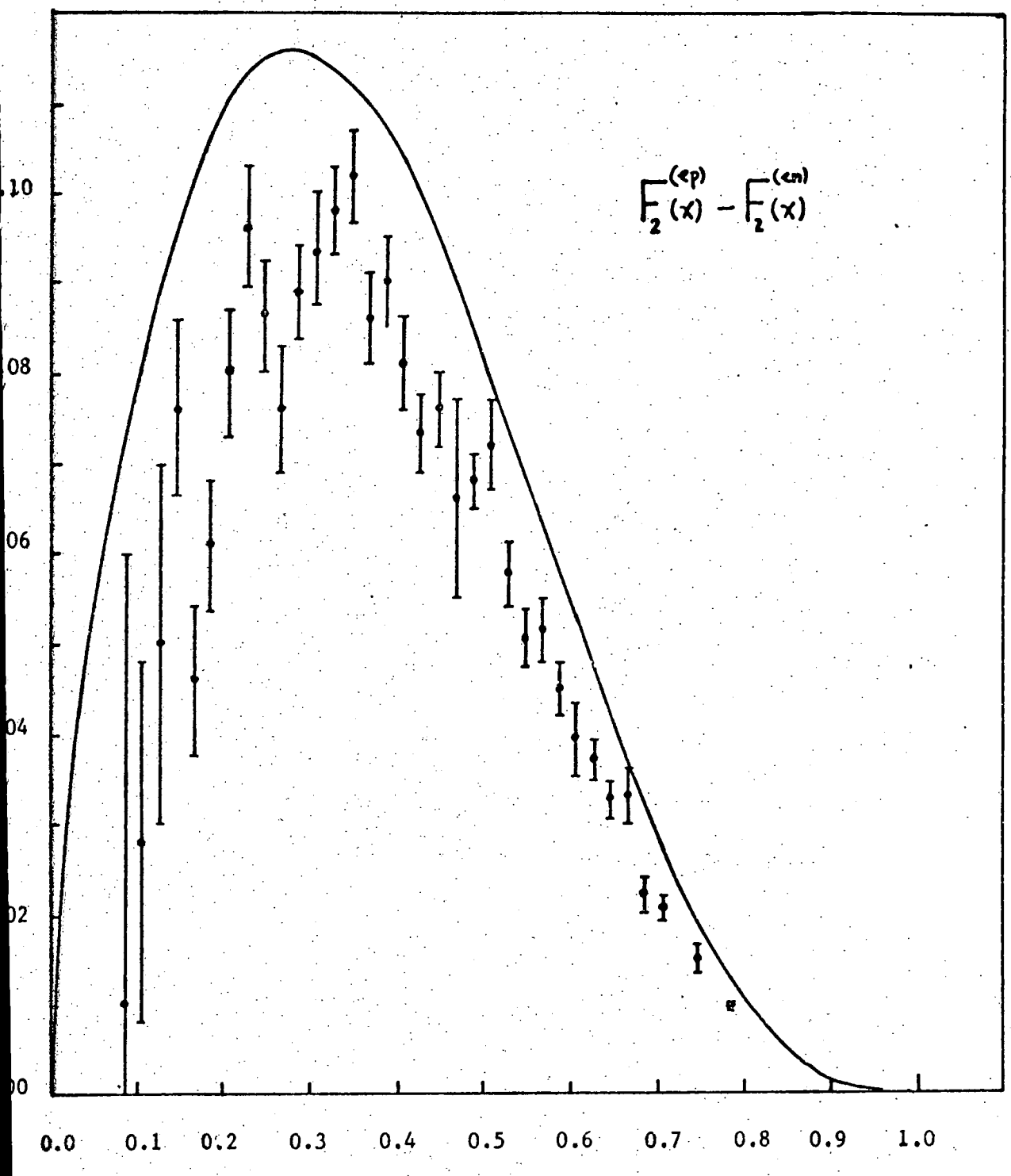

FIGURE 12. The difference $F_2^{(ep)}(x) - F_2^{(en)}(x)$ as plotted versus x. The curve shown is the fit of the modified R.Mc.Elhaney-S.F.Tuan model, discussed in the second part of chapter III, for a value of the parameter $\lambda = \cos^2\omega$ equal to .624 . The data points have been taken from reference [80] .

Our values for the function $F_2^{(ep)}(x)$ are to be compared with the experimental ones [80].†

The shape of the theoretical curve follows smoothly the experimental one, having a maximum at $x \simeq .2$. As far as the ratio $F_2^{(en)}(x)/F_2^{(ep)}(x)$ is concerned we see that for values of $x \geq .2$ it is almost a straight line passing through the point $\frac{1}{4}$ at $x = 1$. The $F_2^{(en)}/F_2^{(ep)}$ curve is in agreement with the experiment data [79,80].

For the difference $F_2^{(ep)}(x) - F_2^{(en)}(x)$ a discrepancy from the experimental points[80] is observed which is higher for smaller values of x.

In the Table XII we give the model predictions, for the various physical quantities, for the three different cases $\lambda = .624$, .559 and .500 respectively. In the last column of the table the experimental value is given with the corresponding reference it has been taken from.

The quantities $\int_0^1 F_2^{(ep)}(x)dx$, $\int_0^1 F_2^{(en)}(x)dx$ are in agreement with the experimental values [21,80,81].

The ratio $\int_0^1 F_2^{(eN)}(x)dx / \int_0^1 F_2^{(\nu N)}(x)dx$, as is seen from (2.19), is greater or equal than $\frac{5}{18}$ when we are below the threshold for the production of charmed states and $\sin\theta_c \approx 0$. Above the charm threshold this ratio is equal to $\frac{5}{18}$. In both cases the equality sign holds neglecting effects from λ, $\bar{\lambda}$, p' and $\bar{p}'$ quarks. Experiment [B.C. Parish et al [71], see also Ref. 79] gives this ratio a value very close to $\frac{5}{18}$ and thus we are in agreement with the data.

---

† For $\lambda < .624$ better fits to the data is obtained but in this case we are not inside the wanted limits given by (3.40).

The difference $\int_0^1 \frac{dx}{x}(F_2^{(ep)}(x) - F_2^{(en)}(x))\{ = 2 \int_0^1 dx(F_1^{(ep)}(x) - F_1^{(en)}(x))\}$ is equal to $\frac{1}{3} \approx .33$ to be compared with the new experimental value for this quantity which is $\simeq .27$ [82]

In the Table XIII the predictions of the model, for the case $\lambda = .624$, are summarized. The value ω_o of ω † for which 90% saturation of Adler sum rule is obtained, that is $\int_0^1 dx[F_1^{(\nu n)}(x) - F_1^{(\nu p)}(x)] = .9$, is also given. The value of ω_o is close to 150, much better than the corresponding value found in R.McElhaney and S.F. Tuan's paper [78] which is $\omega_o \simeq 416$. However our value is still larger than that suggested by Sakurai et al [83] and which must be ≤ 50. In a quark parton model proposed by R.P. Bajpai and S. Mukherjee [84] a value of $\omega_o = 124$ is reported which is close to ours.

So far we have treated the functions $u(x)$, $d(x)$ and $c(x)$ as consisting of two parts; one corresponding to an A_2 Regge trajectory ($\alpha(o) \simeq 1/2$) and another one corresponding to $\alpha(o) \simeq 0$ (see Eqs. 3.44 and 3.45). Instead of choosing $\alpha(o) \simeq 0$ we could have taken a Regge daughter trajectory passing through $\alpha(o) = -1/2$ which, perhaps, is a more plausible scheme. We tried this alternative but the fit to the electroproduction data for the function $F_2^{(ep)}(x)$ was not very good. In fact the value for $F_2^{(ep)}(x)$ at $x = .5$ was found to be $\geq .2$ which is away from the experimental value which is about $\simeq .15$ [see Ref.80] .

Before closing this part we give the predictions of the model for the quantities $Q^4 \frac{d\sigma}{dQ^2}$ and $\frac{d\sigma}{dQ^2}$, regarging the process $p + p \to \mu^- \mu^+ + X$, where Q^2 is the mass squared of the $\mu^- \mu^+$ pair. These quantities are calculated for the case $\lambda = .624$; the cases $\lambda = .559$ and $\lambda = .500$ do not differ substantially.

---

† $\omega = 1/x$

Using the formula (2.14) we find that

$$Q^4 \frac{d\sigma}{dQ^2} = \frac{4\pi\alpha^2}{3} \tau \int_0^1 \int dx\, dy\, \delta(xy - \tau) F(x) c(y) \qquad (3.53a)$$

with F(x) given, in an obvious notation, by the expression

$$F(x) = \frac{1}{9}\left\{ 8u(x) + d(x) + 10\, c(x) \right\} . \qquad (3.53b)$$

Using the explicit forms of the functions $u(x)$, $d(x)$ and $c(x)$ and performing the integrations in (3.53a) we find (see A.7.12)

$$Q^4 \frac{d\sigma}{dQ^2} = \frac{4\pi\alpha^2}{3} \sum_{i=1}^{10} A_i\, G(a_i; b_i; c_i; \tau) . \qquad (3.54)$$

A_i, a_i, b_i, c_i are constants (see A.7.12) and τ is the variable $\tau \equiv Q^2/s$. The function $G(a; b; c; \tau)$ is defined as

$$G(a; b; c; \tau) \equiv (1-\tau)^{b+c+1} F(a, b+1, b+c+2; (1-\tau)) \qquad (3.55)$$

where $F(\nu, \mu, \lambda; z)$ is the well known hypergeometric function. In the Table XIV the values†† of the quantity $Q^4 \frac{d\sigma}{dQ^2}$ are given for τ's ranging from .05 to 1.00; in the same table the predictions of the R.McElhaney and S.F. Tuan's model [78]‡ are also given as well as those of the Kuti-Weisskopf [51] model.

---

‡ The constant "g" of reference 78 is taken equal to 1/2 .

†† The data were obtained by taking a cut of the events leading to a given lepton pair of mass $\sqrt{Q^2}$ [see Ref. 85 and 51] . If we take into account this cut then we find smaller values .

TABLE XIV

τ	$Q^4 \frac{d\sigma}{dQ^2}$		
	A	B	C
.05	6.61×10^{-7}	5.33×10^{-7}	11.16×10^{-7}
.10	3.78×10^{-7}	3.04×10^{-7}	6.37×10^{-7}
.15	2.11×10^{-7}	1.70×10^{-7}	3.55×10^{-7}
.20	1.15×10^{-7}	0.92×10^{-7}	1.92×10^{-7}
.25	6.08×10^{-8}	4.88×10^{-8}	10.15×10^{-8}
.30	3.11×10^{-8}	2.49×10^{-8}	5.18×10^{-8}
.35	1.53×10^{-8}	1.22×10^{-8}	2.54×10^{-8}
.40	7.27×10^{-9}	5.80×10^{-9}	11.99×10^{-8}
.45	3.27×10^{-9}	2.60×10^{-9}	5.37×10^{-9}
.50	1.38×10^{-9}	1.10×10^{-9}	2.27×10^{-9}
.55	5.47×10^{-10}	4.35×10^{-10}	8.95×10^{-10}
.60	1.97×10^{-10}	1.57×10^{-10}	3.22×10^{-10}
.65	6.36×10^{-11}	5.06×10^{-11}	10.37×10^{-11}
.70	1.76×10^{-11}	1.40×10^{-11}	2.87×10^{-11}
.75	3.96×10^{-12}	3.17×10^{-12}	6.47×10^{-12}
.80	6.57×10^{-13}	5.30×10^{-13}	10.79×10^{-13}
.85	6.73×10^{-14}	5.49×10^{-14}	11.13×10^{-14}
.90	2.85×10^{-15}	2.35×10^{-15}	4.77×10^{-15}
.95	1.38×10^{-17}	1.17×10^{-17}	2.36×10^{-17}
1.00	.00	.00	.00

TABLE XIV. The values of the quantity $Q^4 \frac{d\sigma}{dQ^2}$, regarding the lepton pair production process proton + proton $\rightarrow \ell\bar{\ell}$ + anything, for values of the variable τ ranging from .05 to 1.00 .

The column A corresponds to the modified R.Mc.Elhaney-S.F.Tuan model of the third chapter. The columns B and C correspond to the original R.Mc.Elhaney-S.F.Tuan model, and to the original Kuti-Weisskopf model respectively.

TABLE XV

$\sqrt{Q^2}$ (Gev/c)	† $\log_{10} \frac{d\sigma}{d\sqrt{Q^2}}$		
	A	B	C
1.	-33.11	-33.21	-32.89
2.	-34.25	-34.35	-34.03
3.	-35.20	-35.29	-34.97
4.	-36.21	-36.30	-35.99
5.	-37.44	-37.54	-37.22
6.	-39.13	-39.23	-38.92
7.	-42.11	-42.20	-41.89

TABLE XV. The values of the quantity $\log_{10} \frac{d\sigma}{d\sqrt{Q^2}}$, regarding the lepton pair production process proton + proton → $\ell\bar{\ell}$ + anything, for values of the variable $\sqrt{Q^2}$ ranging from 1. Gev/c 7. Gev/c . The columns A,B and C are as in the table XIV.

---

† The differential cross section $\frac{d\sigma}{d\sqrt{Q^2}}$ is in units of $cm^2/(Gev/c)$

Note that the three models give almost the same results, at least as far as the order of magnitude is concerned. The three predictions† disagree badly with the experimental data [85,79] ; in fact data give much higher values for the quantity $Q^4 \frac{d\sigma}{dQ^2}$. This is not due to the specific quark parton models mentioned before but it is a general behaviour of any quark parton model [see Ref, 75 and references therein] which indicates that the Drell-Yan mechanism [see for example Ref. 52] does not have much to say for the process $p + p \rightarrow \mu^- \mu^+ + X$.

The predictions† of the model for the quantity $\frac{d\sigma}{dQ^2}$ are given in the Table XV; the predictions of the two models mentioned before are also given in the same table. The values given in the Table XV correspond to an incident C.M. squared energy $s = 60\ (GeV/c)^2$.

We observe again that the predictions of the three models are close to each other.

---

† See footnote †† of page 90

Discussion

This chapter was divided into two main parts.

In the first part an attempt was made to improve the predictions of the Kuti-Weisskopf model which was discussed in the second chapter. New hadronic constituents were added whose left-handed components were classified in isospin triplets in the Weinberg-Salam model. Two new quantum numbers h and h′ were introduced and their necessity was also discussed. Because of the new constituents additional terms appeared in the hadronic part of the weak current identified as $|\Delta h| = 1$ and $|\Delta h'| = 1$ parts. The predictions of the model for the neutrino and antineutrino induced reactions were given and general features of the model were discussed in the end of the first part.

In the second part we made an analysis of the naive quark parton model based on the available neutrino and antineutrino data.No additional hadronic constituents were assumed , we only assumed Weinberg's renormalizable theory of weak and electromagnetic interactions. From the results of this analysis we built a model a variation of the R.Mc.Elhaney-S.F.Tuan quark parton model. The predictions of the model for deep inelastic neutrino (antineutrino) and electron processes were discussed

CHAPTER IV.

Introduction.

So far parton model techniques were employed in order to interpret the observed scaling phenomena in the deep inelastic region of the reactions $e^- + p \rightarrow e^- + X$ and $\nu(\bar{\nu}) + N \rightarrow \mu^-(\mu^+) + X$.

The neutral current reactions $\nu(\bar{\nu}) + N \rightarrow \nu(\bar{\nu}) + X$ are of great importance and were examined also in the context of the quark parton model.

In the last few years we were able to have high energy electron beams and the reactions $e^- + e^+ \rightarrow$ Hadrons and $e^- + e^+ \rightarrow$ (Hadron) + X have been studied.

In this chapter we first review some of the electron-positron annihilation data and then we give the predictions of the naive quark parton model for the electron-positron reactions mentioned above; we see that the naive quark parton model fails to reproduce the experimental data and one has either to abandon the parton model, at least as far as e^-e^+ phenomena are concerned, or to adopt new theoretical ideas and apply them in the quark parton model picture. Choosing the second alternative and motivated by recent works in the field [86-88] we try to interpret the data assuming nonelectromagnetic interactions of the electron. The consequences of such an assumption are discussed and some predictions are made.

Excellent reviews on e^-e^+ annihilation phenomena are available in the literature [15-17]. In this chapter we limit ourselves to examining the e^-e^+ phenomena in the context of the naive quark parton model.

IV1) Review of Some Data on e^-e^+ Phenomena.

Before any theoretical consideration we think it appropriate to review some of the e^-e^+ data.

(i) The ratio $R = \frac{\sigma(e^-e^+ \to \text{Hadrons})}{\sigma(e^-e^+ \to \mu^-\mu^+)}$ (see 1.23) is very important; it has been measured for energies up to $\sqrt{s}$ = 5 GeV [14,89]. A rise of this ratio is observed as the energy $\sqrt{s}$ increases. For $\sqrt{s}$ = 5 GeV this ratio has a value lying between 5 and 6. As we shall see in the next section the naive quark parton model predicts a constant high energy behaviour for this ratio. Further data is being awaited in order to see the behaviour of this ratio for even higher energies, and whether it approaches a constant or not. However the prediction is made assuming that the annihilation of the e^-,e^+ pair into hadrons takes place via the formation of a photon which in turn annihilates to give hadrons.

(ii) The total multiplicity of the produced hadrons seems to be rising rapidly, while the charged multiplicity and average momentum are rising slowly with the energy [89].

(iii) The majority of the produced hadrons are pions. The average numbers of the produced π's, K's and p's follow approximately the relation $\pi/K/p \sim 100/10/1$ [89].

(iv) The inclusive reaction $e^-+e^+ \to (\text{Hadron}) + X$ has been studied as well. If we denote by z the variable $z = \frac{2p}{\sqrt{s}}$, where p is the magnitude

of the momentum of the outgoing hadron, then the quantity $s\frac{d\sigma}{dz}$ is a function of the variables z and s, that is $s\frac{d\sigma}{dz} = f(z,s)$. We shall see later in this chapter that the naive quark parton model predicts for the quantity $s\frac{d\sigma}{dz}$ to be only a function of z, that is the quantity $s\frac{d\sigma}{dz}$ scales.

Experimentally this scaling behaviour is observed only for $z \geq .5$; for $z \leq .5$ we have a strong s dependence [89].

(v) The cross-section $\frac{d\sigma}{d\cos\theta}$ of the process $e^- + e^+ \rightarrow (\text{Hadron}) + X$ is also of interest. Note that if this process takes place through the formation of a photon, then $\frac{d\sigma}{d\cos\theta}$ is proportional to $\sim(1 + \cos^2\theta)$. The experiment for finding the angular distribution has been performed for $\cos\theta$ varying between -.6 and .6; no such $\sim(1 + \cos^2\theta)$ behaviour was found. In fact the angular distribution is isotropic [89]. Newer data are awaited for smaller values of θ perhaps up to $\theta \simeq 9^\circ$ so that we can finally decide whether the angular distribution is isotropic for all angles.

(vi) Finally the quantity $E\frac{d\sigma}{dp^3}(e^-e^+ \rightarrow h + X)$ scales in a manner resembling hadronic physics [89].

These, in brief, were the main experimental data concerning electron-positron annihilation phenomena. However new experiments are already in progress and newer data are awaited.

IV2) $e^- + e^+ \rightarrow$ Hadrons and the Parton Model.

In this section we shall see how the parton model could be used in order to find the quantity $R = \frac{\sigma(e^-e^+ \rightarrow \text{Hadrons})}{\sigma(e^-e^+ \rightarrow \mu^-\mu^+)}$. We do not

insist on proving formulae since all of them can be found in the literature [see for example Ref. 57, 58].

If we assume that the interaction is of electromagnetic nature then the dissintegration of the e^-e^+ pair into hadrons is done through the formation of a timelike photon as is shown in Fig. 13.

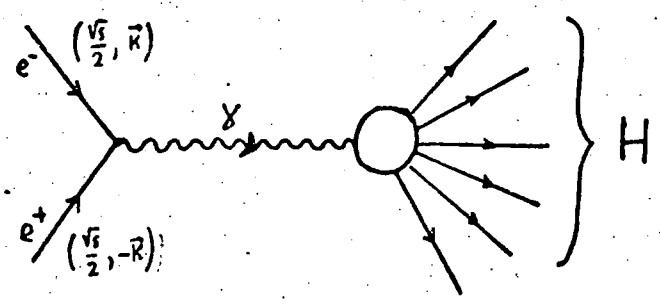

FIGURE 13. e^-e^+ annihilation into hadrons through the formation of a timelike photon in the e^-e^+ center of mass frame.

The hadron-photon vertex is the unknown part of this diagram. It is at this point where someone employs the parton picture. What is assumed is that the photon is coupled to a quark-antiquark pair, which are hadronic constituents, and this pair is converted into hadrons (see Fig. 14).

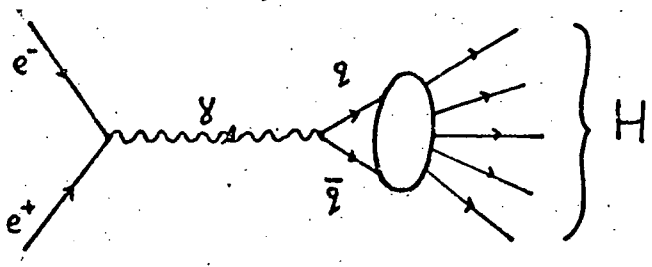

FIGURE 14. Parton mechanism for the process $e^-e^+ \rightarrow$ Hadrons.

The quarks metamorphose into hadrons in the same way as in the electroproduction scattering.

It is not difficult to see that in this way the quantity R is given by the following relation [see for example Ref. 13].

$$R = \frac{1}{2}\sum_{\substack{\text{spin } 1/2 \\ \text{partons}}} Q_i^2 + \frac{1}{8}\sum_{\substack{\text{spin } 0 \\ \text{partons}}} Q_i^2 \quad . \qquad (4.1)$$

The summation is over all partons and their antiparticles; Q_i is the charge (in electron units) of the "i" parton.

From (4.1) one sees that the quantity R has a constant value depending on the charge of the constituents. In the previous section we saw that the experimental situation is quite different; a rise of the quantity R is observed for energies up to $\sqrt{s}$ = 5 GeV [14,89]. One can say that the high energy limit has not been reached yet and that this constant behaviour is attained for higher values of the energy $\sqrt{s}$; thus we must await further data before any final decision is taken.

IV3) $e^- + e^+ \rightarrow$ (Hadron) + X and the Parton Model.

We examine now the inclusive reaction $e^- e^+ \rightarrow h + X$ where h stands for a hadron.

In terms of the parton language the process is described as follows. The $e^- e^+$ pair annihilates into a time-like photon which is coupled to a quark antiquark pair (see Fig. 15).

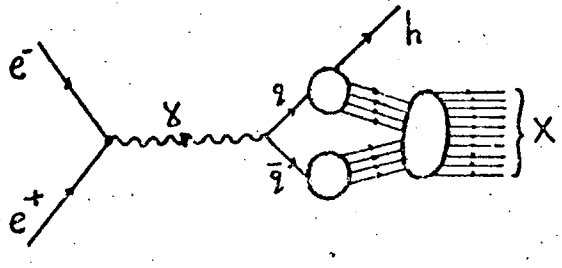

FIGURE 15. Parton mechanism for the process $e^- e^+ \rightarrow$ (Hadron)+ Anything

If we denote by $D_i^{(h)}(x)$‡ the average number of hadrons "h" produced from a parent parton "i" and carrying fraction x of the parton's momentum, then we find‡‡ [57,58]

$$S\,\frac{d\sigma(e^-e^+\to h+X)}{dz\,d\cos\theta} = \frac{\pi\alpha^2}{2}(1+\cos^2\theta)\sum_i Q_i^2 D_i^{(h)}(z)\,. \qquad (4.2)$$

In the expression above the angle θ represents the hadron's "h" scattering angle, in the e^-, e^+ center of mass system, and z is the variable $z = \frac{2p}{\sqrt{s}}$ defined in the first section of this chapter; $\sqrt{s}$ is the center of mass total energy. The summation index "i" in (4.2) runs over all partons and their antiparticles.

The first thing to notice in the expression (4.2) is that the quantity $\frac{d\sigma}{dz d\cos\theta} \sim (1 + \cos^2\theta)$, and thus the angular distribution has a behaviour proportional to $(1 + \cos^2\theta)$. As it was discussed previously the angular distribution is constant for $\cos\theta$ varying between -.6 and .6 [89]. However the situation may change when measurements are performed for values of $|\cos\theta|$ approaching unity.

The second thing is that from (4.2), by integrating with respect $\cos\theta$, we get an expression which is a function of the variable z only.

$$S\,\frac{d\sigma(e^-e^+\to h+X)}{dz} = \frac{4\pi\alpha^2}{3}\sum_i Q_i^2 D_i^{(h)}(z) \qquad (4.3)$$

---

‡ In terms of $D_i^{(h)}(z)$, the multiplicity $\langle n\rangle_h$ of the produced hadrons "h" is given by [58] $\langle n\rangle_h = \sum_i \int_{\frac{2m}{\sqrt{s}}}^{1} D_i^{(h)}(z)dz$ where m is the mass of the hadron "h".

‡‡ From now on we assume that all charged constituents carry spin 1/2 .

Thus the quantity $s\frac{d\sigma}{dz}$ scales, that is it depends on z and not on the variable s. Experimental data exhibit this scaling behaviour only for $z \geq .5$; for $z \leq .5$ we have a strong s-dependence for energies up to $\sqrt{s} = 4.8$ GeV [89]. The conclusion is that the prediction of the quark parton model do not agree with the existing data. Of course we can say that the high energy limit has not been attained yet‡ and that the naive quark parton model predictions hold for even higher energies.

Another alternative would be to assume that there are interactions of the electron which are not of electromagnetic nature. Motivated by works of Pati and Salam [86] we assume coupling of the electron to hadronic constituents. With this coupling scheme all the predictions of the quark parton model on the e^-e^+ annihilation phenomena will be altered. In the rest of this chapter we will see the consequences of such an assumption to the reactions $e^-e^+ \to$ Hadrons, $e^-e^+ \to hX$ and $e^-p \to e^-X$.

IV4) Nonelectromagnetic Interactions of the Electron

In this section we assume that the electron is coupled directly to hadronic constituents so that there are vertices involving electrons,

---

‡ In this case we have to explain why scaling sets in very quickly for spacelike $Q^2 > 1$ GeV^2 but not for timelike Q^2's which reach values up to 25 GeV^2.

quarks, and the mediator of the nonelectromagnetic interactions. Thus, omitting γ-matrices, the nonelectromagnetic Lagrangian interaction has the general form $\mathcal{L} = \sum_q f_q(e^- q X_q)$, where q is a quark (or gluonic) field and X_q is a new field coupled to "e" and "q" fields.

The simplest thing is to assume that the electron is coupled directly to a gluon ϕ, which is assumed to be chargless and carrying spin = $^1/_2$, through a field X having spin 0 or spin 1.

a) First case: Nonelectromagnetic Coupling Through the Interaction with a Spinless Field X.

The simplest Lagrangian interaction in this case has the form

$$\mathcal{L}^{(an.)} = f(\bar{e}\phi X + h.c.) \qquad (4.4)$$

where f is the coupling constant. The superscript (an.) stands for "anomalous" just to indicate that this Lagrangian interaction is the anomalous or otherwise nonelectromagnetic part of the total Lagrangian interaction of the electron. It is obvious that this term gives its own contribution, via the process $e^- e^+ \to \phi\,\bar{\phi}$, to the reactions $e^- + e^+ \to$ Hadrons and $e^- + e^+ \to h + X$. The reaction $e^- e^+ \to \phi\,\bar{\phi}$ is represented pictorially in Fig 16 .

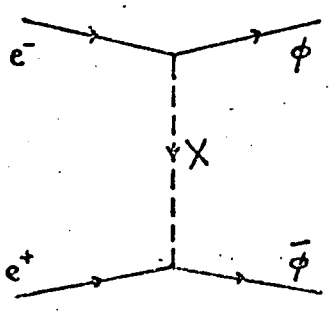

FIGURE 16. The process $e^- e^+ \to$ gluon + antigluon mediated by the exchange of the object X .

For large values of the incoming energy $\sqrt{s}$ we find (see A.8.6) , for the process $e^-e^+ \to \phi\bar{\phi}$,

$$p' \frac{d^2\sigma}{dp'd\cos\theta} = f^4 \frac{(2\pi)^{-1}}{32\sqrt{s}} \delta\left(\frac{\sqrt{s}}{2} - p'\right) \left(\frac{t}{t - M_x^2}\right)^2 . \quad (4.5)$$

The notation is as follows; p' is the magnitude of the momentum of the outgoing gluon and θ its scattering angle in the center of mass frame of the e^- and e^+; 't' is the momentum transfer variable defined by $t \equiv (p_\phi - p_{e^-})^2$. If the mass Mx of the exchanged particle X is large compared with the energies available in the laboratory then (4.5) takes on the form

$$p' \frac{d^2\sigma}{dp'd\cos\theta} = g^2 \frac{(2\pi)^{-1}}{32\sqrt{s}} \delta\left(\frac{\sqrt{s}}{2} - p'\right) \frac{s^2}{4}(1-\cos\theta)^2 \quad (4.6)$$

where g is given by

$$g \equiv \left(\frac{f}{Mx}\right)^2 . \quad (4.7)$$

In the expression (4.6) the t variable has been replaced by $-\frac{s}{2}(1-\cos\theta)$.

From (4.6) we can now, using parton model formulae, calculate the cross section $\frac{d\sigma}{dz d\cos\theta}$ for the inclusive reaction $e^-+e^+ \to h + X$, and also find the expression for the ratio $R = \frac{\sigma(e^-e^+ \to \text{Hadrons})}{\sigma(e^-e^+ \to \mu^-\mu^+)}$.

We start by calculating the cross section $\frac{d^2\sigma}{dz d\cos\theta}$ associated with the process $e^-+e^+ \to h + X$. It is known that [57,58]

$$p \frac{d^2\sigma(e\bar{e}^+ \to h+X)}{dp\, d\cos\theta} = \sum_i \int_0^1 dx_i P_i \frac{d\sigma(x_i)}{dp_i\, d\cos\theta} D_i^{(h)}(x_i) . \quad (4.8)$$

As was explained earlier $D_i^{(h)}(x_i)$ represents the average number of hadrons "h" emerging from a parent parton "i", and carrying fraction x_i of parton's momentum; thus $p = x_i p_i$.

Combining (4.7) and (4.8) we easily get‡

$$s\frac{d^2\sigma(e\bar{e}^+\to h+X)}{dz\,d\cos\theta} = \frac{\pi\alpha^2}{2}(1+\cos^2\theta)\sum_i Q_i^2 D_i^{(h)}(z) + \left.\right\} \quad (4.9)$$
$$+\frac{\pi}{2}\left(\frac{g}{4\pi}\right)^2 \frac{s}{4}(1-\cos\theta)^2\left(D_\phi^{(h)}(z)+D_{\bar{\phi}}^{(h)}(z)\right) \quad .$$

We observe that $s\frac{d^2\sigma}{dzd\cos\theta}$ consists of two parts; the first part is s-independent and is due to the electromagnetic interactions while the second comes from the anomalous interaction term of the Lagrangian (see 4.4) and has an s^2 behaviour.

The cross-section $\frac{d^2\sigma}{dzd\cos\theta}$ still remains $\cos^2\theta$-dependent.

In order to calculate the ratio "R" we need the total cross section for scattering $e^-e^+ \to \phi\bar{\phi}$ From (4.6) we easily find (see A.8.8)

$$\sigma(e\bar{e}^+\to\phi\bar{\phi}) = \frac{g^2}{48\pi}s \quad (4.10)$$

and thus

$$R = \frac{1}{2}\sum_i Q_i^2 + \frac{1}{4}\left(\frac{g}{e^2}\right)^2 s^2 \quad . \quad (4.11)$$

---

‡ From now on we assume that all charged constituents carry spin 1/2.

We see that the ratio R behaves as $\sim s^2$ for large values of the energy s but still small compared with the mass Mx of the heavy object X. For energies $s \gg M_x^2$ by integrating (4.5) with respect p' and $\cos\theta$ we find

$$R = \frac{1}{2}\sum_i Q_i^2 + \frac{3}{4}\left(\frac{f^2}{e^2}\right)^2 \quad . \qquad (4.12)$$

Thus we see that for very high energies such that $s \gg M_x^2$, R is a constant whose value is given by (4.12). Before proceeding any further to examine how this "anomalous" interaction of the electron affects the electroproduction process $e^- p \to e^- X$ we will discuss another possible coupling scheme in which the mediating particle X carries spin 1.

b) Second case: Nonelectromagnetic Coupling Through the Interaction with a Spin-1 Field X.

The simplest Lagrangian interaction has now the form

$$\mathcal{L}^{(an.)} = f\left(\bar{e}\gamma^\mu \phi X_\mu + h.c.\right) \qquad (4.13)$$

The field X_μ now carries spin-1.

We follow the steps of the first case (spin 0 for the field X) and find‡ (see A.8.14)

$$s\,\frac{d^2\sigma(e^-e^+ \to h+X)}{dz\,d\cos\theta} = \frac{\pi\alpha^2}{2}(1+\cos^2\theta)\sum_i Q_i^2 D_i^{(h)}(z) + \left.\right\} (4.14)$$
$$+\frac{\pi}{2}\left(\frac{8}{4\pi}\right)^2\frac{s^2}{2}(5+2\cos\theta+\cos^2\theta)\left(D_\phi^{(h)}(z)+D_{\bar{\phi}}^{(h)}(z)\right)\Bigg]$$

‡ See footnote of page 102 .

For large values of s but such that $s \ll M_x^2$ we have‡ (see A.8.16)

$$R = \frac{1}{2}\sum_i Q_i^2 + 2\left(\frac{g}{e^2}\right)^2 s^2 \quad . \qquad (4.15)$$

For values of s such that $s \gg M_x^2$ we have (see A.8.18)

$$R = \frac{1}{2}\sum_i Q_i^2 + 3\left(\frac{f^2}{e^2}\right)^2 \left(\frac{s}{M_x^2}\right) \quad . \qquad (4.16)$$

Note that unlike the first case the quantity R rises linearly with s for $s \gg M_x^2$.

These anomalous couplings of the electron to gluonic matter do not leave the electroproduction process $e^- p \to e^- X$ unaffected; our task is to investigate the consequences of these new coupling schemes to the process $e^- p \to e^- X$ in its deep inelastic region.

IV5) Deep Inelastic Electroproduction Scattering and Anomalous Interactions of the Electron.

In this section we examine the consequences of the anomalous interactions of the electron, discussed in the previous sections, in the deep inelastic electroproduction region.

Our objective is to find the form of the structure functions $\nu W_2^{(ep)}(\nu, Q^2)/M$ and $W_1^{(ep)}(\nu, Q^2)$ applying quark parton model techniques.

---

‡ See footnote of page 102

The structure functions will be calculated for the two cases discussed in the previous sections and which will be denoted by $(S)^{\ddagger}$ and $(V)^{\ddagger}$ hereforth.

In Figs. 17a and 17b the Feynman graphs (Born terms) of the processes $e^- \phi \to e^- \phi$ and $e^- \bar{\phi} \to e^- \bar{\phi}$ are shown, and whose contribution to the structure functions $\nu W_2^{(ep)}/M$ and $W_1^{(ep)}$ is wanted.

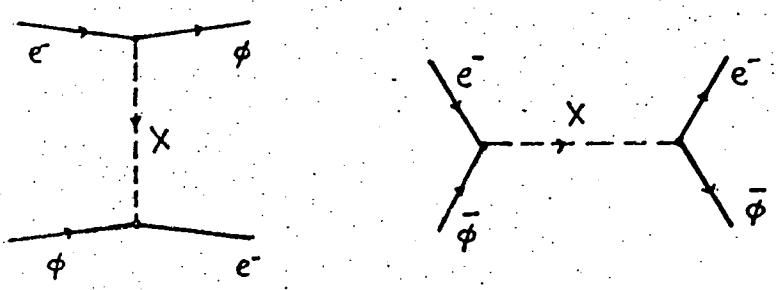

FIGURE 17. a) The process $e^- + \text{gluon} \to e^- + \text{gluon}$ mediated by the exchange of the object X.
b) The process $e^- + \text{antigluon} \to e^- + \text{antigluon}$ via the formation of the object X.

If E' and $\underline{O}'$ is the energy and the scattering angle (in the Lab. frame) of the outgoing electron in the process $e^- p \to e^- X$, then the differential cross sections $\frac{d^2\sigma(x_1)}{dE' d\underline{O}'}$ for the scattering of a gluon (or antigluon) carrying fraction x_1 of the proton's momentum, are given by the following expression (see A.8.28)

---

‡ (S) denotes the coupling $f(\bar{e}\phi X + h.c)$
(V) denotes the coupling $f(\bar{e}\gamma^{\mu}\phi X_{\mu} + h.c)$

$$\left.\begin{aligned}\frac{d^2\sigma^{e\psi\to e\psi}(x_i)}{dE'd\Omega'} &= \frac{4\alpha^2}{Q^4}\frac{E'}{M}\delta(x-x_i)\times \\ &\times\left\{2A^{\psi}\sin^2\frac{\theta}{2}+B^{\psi}\cos^2\frac{\theta}{2}\right\}.\end{aligned}\right\} \quad (4.17)$$

In the expression above the superscript ψ stands for either ϕ or $\bar{\phi}$ and A^{ψ}, B^{ψ} are given by the following formulae (see A.8.29-A.8.34)

$$(S):\quad A^{\phi}=\frac{Q^2}{2}\left(\frac{g^2}{e^4}\right)\left(\frac{x^2M^2}{2}-xME+\frac{Q^2}{2}\right) \quad (4.18a)$$

$$(V):\quad A^{\phi}=Q^2\left(\frac{g^2}{e^4}\right)\left(\frac{3x^2M^2}{2}+xME+\frac{Q^2}{2}\right) \quad (4.18b)$$

$$(S):\quad A^{\bar{\phi}}=\frac{Q^2}{2}\left(\frac{g^2}{e^4}\right)\left(\frac{x^2M^2}{2}+xME\right) \quad (4.18c)$$

$$(V):\quad A^{\bar{\phi}}=Q^2\left(\frac{g^2}{e^4}\right)\left(\frac{3x^2M^2}{2}-xME+Q^2\right) \quad (4.18d)$$

$$(S):\quad B^{\phi}=B^{\bar{\phi}}=\left(\frac{g^2}{e^4}\right)\left(\frac{Q^4x}{4}\right)\frac{M}{\nu} \quad (4.18e)$$

$$(V):\quad B^{\phi}=B^{\bar{\phi}}=\left(\frac{g^2}{e^4}\right)\left(\frac{Q^4x}{2}\right)\frac{M}{\nu} \quad . \quad . \quad (4.18f)$$

The cross section $\frac{d^2\sigma^{e^-\psi\to e^-\psi}}{dE'd\Omega'}(x_i)$ has been written in such a form as to remind us the differential cross section $\frac{d\sigma^2}{d\Omega'dE'}(e^-p\to e^-X)$, (see Eq. 1.10). It is easy now to calculate the electroproduction structure functions; assuming that the gluon distribution functions $f_{\phi}^{(p)}(x)$, $f_{\bar{\phi}}^{(p)}(x)$ are equal to each other, and equal to $c'(x)$, we have

$$(S):\quad \begin{cases} F_2^{(ep)}(x,Q^2)=x\sum_i Q_i^2 f_i^{(p)}(x)+\left(\frac{g^2}{e^4}\right)\frac{Q^4}{2}\,x\,c'(x) & (4.19a)\\ F_1^{(ep)}(x,Q^2)=\frac{1}{2}\sum_i Q_i^2 f_i^{(p)}(x)+\left(\frac{g^2}{e^4}\right)\frac{Q^2}{2}\left(\frac{Q^2}{2}+x^2M^2\right)c'(x) & (4.19b)\end{cases}$$

$$(V):\quad \begin{cases} F_2^{(ep)}(x,Q^2)=x\sum_i Q_i^2 f_i^{(p)}(x)+\left(\frac{g^2}{e^4}\right)Q^4\,x\,c'(x) & (4.20a)\\ F_1^{(ep)}(x,Q^2)=\frac{1}{2}\sum_i Q_i^2 f_i^{(p)}(x)+\left(\frac{g^2}{e^4}\right)Q^2\left(\frac{3Q^2}{2}+3x^2M^2\right)c'(x) & (4.20b)\end{cases}$$

The nonscaling part, due to the anomalous interaction term of the Lagrangian, has been separated out in Eqs. (4.19) and (4.20).

The value of $\left(\frac{g}{e^2}\right)^2$ is estimated from (4.11) and (4.15), for the two cases (S) and(V) respectively:

$$(S): \qquad \left(\frac{g}{e^2}\right) = \frac{2}{s}\left(R - \frac{1}{2}\sum_i Q_i^2\right)^{1/2} \tag{4.21a}$$

$$(V): \qquad \left(\frac{g}{e^2}\right) = \frac{1}{\sqrt{2}s}\left(R - \frac{1}{2}\sum_i Q_i^2\right)^{1/2} \tag{4.21b}$$

Giving R a value ~ 5 for $\sqrt{s} = 5$ GeV and assuming that p,n,λ and p' are the only charged constituents we get

$$(S): \qquad \left(\frac{g}{e^2}\right) \simeq .16\ \text{GeV}^{-2} \tag{4.22a}$$

$$(V): \qquad \left(\frac{g}{e^2}\right) \simeq .06\ \text{GeV}^{-2} \tag{4.22b}$$

Writing the distribution functions $f_i^{(ep)}(x)$ in the wellknown form $f_i^{(p)}(x) = v_i(x) + c_i(x)$, with $c_i(x)$ given by the expressions ‡

$$c_i(x) = \frac{g_i}{n}\, c(x) \quad , \; i = \text{quark or antiquark} \tag{4.23a}$$

$$c_i(x) = \frac{g_i'}{2}\, c(x) \quad , \; i = \phi \text{ or } \bar{\phi} \quad , \tag{4.23b}$$

---

‡ "n" is the total number of quarks plus their antiparticles.— In the Kuti-Weisskopf model $c(x) = x^{-1}(1-x)^{7/2}$.

we get from (4.19a) and (4.20a)

$$(S):\quad F_2^{(ep)}(x,Q^2) = x\sum_i Q_i^2 v_i(x) + \left\{\left(\frac{g^2}{e^4}\right)\frac{Q^4}{4}g_1' + \frac{g_1}{n}\sum_i Q_i^2\right\}xc(x) \qquad (4.24a)$$

$$(V):\quad F_2^{(ep)}(x,Q^2) = x\sum_i Q_i^2 v_i(x) + \left\{\left(\frac{g^2}{e^4}\right)\frac{Q^2}{2}g_1' + \frac{g_1}{n}\sum_i Q_i^2\right\}xc(x)\,. \qquad (4.24b)$$

The values of Q^2 for which at most 10%, say, violation of scaling is observed, are given by the relations

$$(S):\quad Q^2 \lesssim \frac{2}{\sqrt{\lambda}}\left(\frac{g}{e^2}\right)^{-1}\left(\frac{\sum_i Q_i^2}{10n}\right)^{1/2} \qquad (4.25a)$$

$$(V):\quad Q^2 \lesssim \frac{\sqrt{2}}{\sqrt{\lambda}}\left(\frac{g}{e^2}\right)^{-1}\left(\frac{\sum_i Q_i^2}{10n}\right)^{1/2}\,, \qquad (4.25b)$$

where λ is given by $\lambda \equiv {}^{g'}1/g_1$.

The right hand side of the (4.25a) and (4.25b) can be a large number if one assumes that in addition to the gluon ϕ to which the electron is coupled to, there are gluons ϕ' whose distribution function is given by

$$c_{\phi'}(x) = \frac{g_1''}{2}c(x)\,. \qquad (4.26)$$

In such a case the number λ can be as small as we wish and thus the right-hand sides of (4.25a) and (4.25b) as large as we like. To see this note that the sum $\gamma \equiv g_1 + g_1' + g_1''$ is a positive number‡

---

‡ In the Kuti-Weisskopf model $\gamma = 3$.

For the Kuti-Weisskopf model or for the R.McElhaney and S.F. Tuan model discussed in the chapter III, γ is given by $\gamma = 4-2(1-\alpha(o))$ where $\alpha(o) \simeq \frac{1}{2}$.

and the constant g_1 is fixed by fitting electroproduction data; thus taking g_1'' to be very close to $(\gamma - g_1)$, the constant g_1' becomes very small and consequently $\lambda = (g_1'/g_1)$ very close to zero. In the absence of the ϕ'-gluons when g_1 is given g_1' is fixed, because $g_1 + g_1' = \gamma$; so the ratio λ does not become necessarily small. In the Kuti-Weisskopf model for example $\lambda = 2$.

Thus though we expect a "Q^4" violation of scaling, due to the anomalous interaction of the electron, nevertheless assuming the existence of some neutral gluons (ϕ') inside the proton, we can arrange things so that the scaling breaking effects are very small even for very high values of Q^2.

IV6) The Reaction $p + p \to \mu^- \mu^+ + X$ and Anomalous Interactions of the Electron.

The consequences of the anomalous interactions of the electron in the pair leptonic production process $p + p \to \mu^- \mu^+ + X$ are discussed.

We assume that the muon is coupled to the gluonic field ϕ in the same way as the electron ($\mu - e^-$ universality); thus we examine the two cases (S) and (V)‡ discussed in the previous sections.

---

‡ (S) denotes the coupling $f(\mu \phi X + h.c)$
(V) " " $f(\mu \gamma^\tau \phi X_\tau + h.c)$

It is evident that the leptonic pair $\mu^-\mu^+$ can be produced from a ϕ and a $\bar{\phi}$ as is shown in Fig. 18.

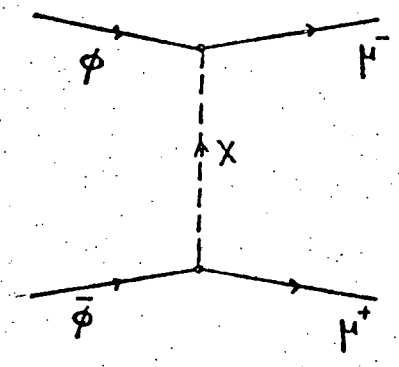

FIGURE 18. Contribution of the X-exchange diagram to the process gluon + antigluon $\rightarrow \mu^-\mu^+$.

The differential cross sections‡ $\frac{d\sigma}{dQ^2}$ for the process $\phi\bar{\phi} \rightarrow \mu^-\mu^+$ are given by the following expressions (see A.8.42, A.8.43).

$$(S): \quad \frac{d\sigma}{dQ^2}(x_1,x_2) = \frac{4\pi \underset{\sim}{g}^2}{3Q^4}\left(\frac{Q^4\tau}{4}\right)\delta(x_1x_2-\tau) \qquad (4.27a)$$

$$(V): \quad \frac{d\sigma}{dQ^2}(x_1,x_2) = \frac{4\pi \underset{\sim}{g}^2}{3Q^4}\left(2Q^4\tau\right)\delta(x_1x_2-\tau) \quad . \qquad (4.27b)$$

x_1 and x_2 are the fraction of the proton's momentum carried by the gluon and antigluon respectively, and $\underset{\sim}{g}$ is defined as $\underset{\sim}{g} \equiv \frac{g}{4\pi}$.

Compare the expressions above with the analogous expression in which the pair $\mu^-\mu^+$ is created from a quark-antiquark pair which annihilates into a photon (see Fig. 19 in page 111)

---

‡ Q^2 denotes the (mass)^2 of the $\mu^-\mu^+$ pair.

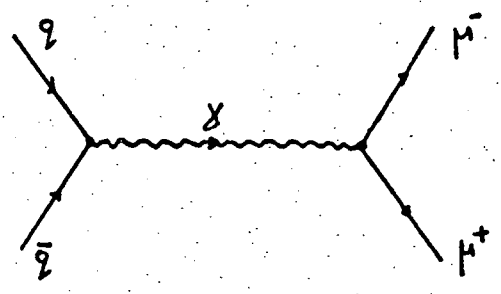

FIGURE 19. Quark- antiquarq annihilation into a $\mu^-\mu^+$ pair via the formation of a timelike photon.

$$\frac{d\sigma}{dQ^2}(q\bar{q} \xrightarrow{\gamma} \mu^-\mu^+) = \frac{4\pi\alpha^2}{3Q^4}\,\tau\,\delta(x_1x_2-\tau) \quad . \tag{4.28}$$

It is obvious now that the quark parton expression for $\frac{d\sigma}{dQ^2}(pp \to \mu^-\mu^+ + X)$ is given by‡

$$(S):\quad \frac{d\sigma}{dQ^2} = \frac{4\pi\alpha^2}{3Q^4}\,\tau\sum_i\int_0^1 dx_1dx_2 f_i^{(p)}(x_1) f_{\bar{i}}^{(p)}(x_2)\,Q_i^2\,\delta(x_1x_2-\tau) + \left.\right]$$
$$+\ \frac{4\pi\alpha^2}{3Q^4}\left(\frac{Q^4}{4}\right)\tau\int_0^1 dx_1dx_2\, f_q^{(p)}(x_1) f_{\bar{q}}^{(p)}(x_2)\,\delta(x_1x_2-\tau)\,. \left.\right] \tag{4.29}$$

For the (V) case we replace $(\frac{Q^4}{4})$ by $(2Q^4)$.

From (4.23a) and (4.23b) we have

$$c_{\phi,\bar{\phi}}(x) = \frac{g_1'}{2}\,c(x) = \frac{n\lambda}{2}\,c_{q,\bar{q}}(x) \tag{4.30}$$

where $\lambda = g_1'/g_1$.

---

‡ In formula (4.29) the summation index i runs over the partons only (not antipartons).

It is easy to see that if (4.30) is taken into account then (4.29) can be written in the following form‡

$$\left.\begin{aligned}\frac{d\sigma}{dQ^2} = \frac{4\pi\alpha^2}{3Q^4}\,\tau\sum_i\int_0^1 dx_1\,dx_2\,Q_i^2\,U_i(x_1)C_i(x_2)\,\delta(x_1x_2-\tau)+\\ \frac{4\pi\alpha^2}{3Q^4}\,\tau\left(\frac{g_i}{n}\right)^2\left\{\sum_i Q_i^2+\left(\frac{g}{e^2}\right)^2\frac{n^2\lambda^2Q^4}{16}\right\}\int_0^1 dx_1\,dx_2\,C(x_1)C(x_2)\,\delta(x_1x_2-\tau).\end{aligned}\right\} \quad (4.31)$$

For the (V) case the $(\frac{Q^4}{4})$ inside the brackets is replaced by $(2Q^4)$.

If $(g/e^2) \sim 10^{-1}$ GeV^{-2} and $\lambda \sim 10^{-2}$ then

$$\left\{\sum_i Q_i^2+\left(\frac{g}{e^2}\right)^2\frac{n^2\lambda^2Q^4}{16}\right\}\sim 1+(10^{-6}Q^4)\,\text{GeV}^{-4}\ ; \quad (4.32)$$

so roughly speaking the anomalous interaction term does not significantly alter the results of $pp \to \mu^-\mu^+ + X$ scattering, provided that $Q^2 \le 10^3$ GeV^2 $(Q^2 = M^2_{\mu^-\mu^+})$.

For example in the (S) case if the right hand side of (4.25a) has a value $\simeq 20$ GeV^2, and the only charged constituents are the known quarks p, n, λ and p', then we find for λ a value $\lambda \simeq 10^{-2}$ provided that we take $\frac{g}{e^2} \simeq .16$ GeV^{-2} (see 4.22a). In this case we find

$$\left\{\sum_i Q_i^2+\left(\frac{g}{e^2}\right)^2\frac{n^2\lambda^2Q^4}{16}\right\}\simeq 1+(10^{-5}Q^4)\,\text{GeV}^{-4} \quad (4.33)$$

---

‡ In formula (4.31) the summation index i runs over the partons only (not antipartons).

Thus we conclude that the scaling breaking effects of the anomalous interaction term to the $pp \to \mu^-\mu^+ + X$ scattering can be negligible, even for high values of $Q^2 = M^2_{\mu^-\mu^+}$, under the same circumstances met in the deep inelastic electron-proton scattering.

IV7) Direct Coupling of the Electron to the Quark Fields

So far we have dealt with nonleptonic interactions of the electron in which the electron was coupled directly to gluonic matter. Couplings of the electron to the constituent quarks can be also assumed. Anomalous interactions of the form $\mathcal{L}^{(an.)} = \sum_q f_q \bar{e} O_\mu q X^\mu + h.c.$ are possible and one expects that the results are qualitatively the same as in the cases discussed in the previous chapters. However the arguments which lead us to the conclusion that the anomalous interaction effects can be negligible in the $e^-p \to e^-X$ and $pp \to \mu^-\mu^+ + X$ scattering do not hold, in general, in this case. The reason is that the factor $1/\sqrt{\lambda}$, which appears in (4.25), is something like $\sim\sqrt{g_1}$, in this case, and this is estimated by fitting the electroproduction data on $F_2^{(ep)}$. Thus the factor $1/\sqrt{\lambda}$ is fixed from electroproduction data and its smallness, which was very important for the arguments stated in the previous sections, is not guaranteed.

Effective Lagrangians of the form $\mathcal{L} \sim (\bar{e} O_\mu e)(\bar{q} O'^\mu q)$ have been studied by Ikaros I.Y. Bigi and J.D. Bjorken [90]. A.Soni [91] also has studied the consequences of some anomalous Lagrangian interactions to the decays $\pi^0 \to e^-e^+$ and $\eta \to \mu^-\mu^+$.

In this section we briefly discuss the anomalous interaction given by the following expression

$$\mathcal{L}^{(an)} = -\sum_q f_q \bar{e} q X_q + h.c. \quad . \qquad (4.34)$$

In the expressions above the index q runs over the quark fields p, n and λ.

As it was said previously the results are expected to be qualitatively the same as in the two cases in which the electron was coupled to a gluonic field. Here we only wish to see how the anomalous interaction (4.34) will affect the decays of π^o and η into e^-e^+ and $\mu^-\mu^+$ respectively.

The quantity $R = \dfrac{\sigma(e^-e^+ \to \text{Hadrons})}{\sigma(e^-e^+ \to \mu^-\mu^+)}$ is needed for this purpose and is given by the following expression‡ (see A.8.46) .

$$R = \sum_q \left\{ Q_q^2 + Q_q \bar{f}_q \frac{s}{2} + \bar{f}_q^2 \frac{s^2}{4} \right\} \quad . \qquad (4.35)$$

The constants $\bar{f}_q$ are defined as $\bar{f}_q = \left(\dfrac{f_q}{eM_q}\right)^2$ where M_q is the mass of the X_q particle which is assumed to be heavy.

The decay of π^o and η mesons into an e^-e^+ or $\mu^-\mu^+$ pair, goes through the mechanism depicted in Fig. 20 (see page 115).

---

‡ The index q runs over the quarks only and not their antiparticles.

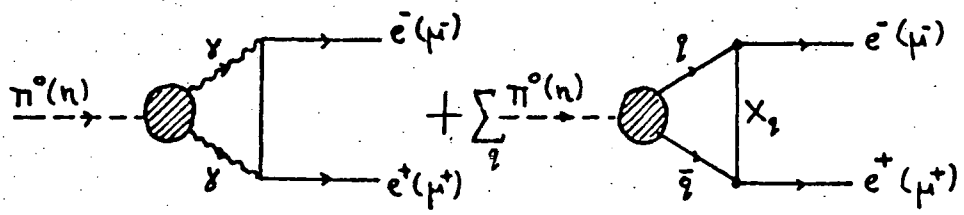

FIGURE 20. Electromagnetic and Anomalous contribution to the decays $\pi \to e^- e^+$ and $\eta \to \mu^- \mu^+$.

The first diagram of the Fig. 20 represents the electromagnetic decay and the second is due to the anomalous interaction of the electron (or muon). The decay width of the anomalous interaction term of the Lagrangian (4.34) is given by (see A.9.14)

$$\Gamma_{(an.)}(m \to \ell\bar{\ell}) = |f(M,o)|^2 \frac{\pi\alpha^2}{2} M^2 \left(1 + \frac{2m_\ell}{M}\right)^2 \left(1 - \frac{4m_\ell^2}{M^2}\right)^{1/2} \left(\sum_q \alpha_q f_q\right)^2 . \quad (4.36)$$

In the expression above M is the mass of the decaying meson and m_ℓ that of the lepton ℓ (either e^- or μ^-). The constants α_q are SU(3) Glebsch-Gordan coefficients.

The $|f(M,o)|^2$ has a value which is approximately [92]

$$|f(M,o)|^2 \simeq \frac{M m_\pi^2}{2} \quad (4.37)$$

with m_π the mass of the π^o meson.

The values of the constants f_q are determined from (4.35). The simplest choice is to assume that all of the f_q's are the same. In such a case we find $\Gamma_{(an.)}(\pi^o \to e^- e^+) = 0$ because $\alpha_p = -\alpha_n = 1/\sqrt{2}$ and

---

See A.9.15 - A.9.18 .

$\alpha_\lambda = 0$ for the π^o meson; that is only the first of the two diagrams in Fig. 20 contributes. For the decay of the η meson taking a value (from 4.35) for the coupling constant $\bar{f} \equiv \bar{f}_q$ equal to[‡] $\bar{f} \simeq 1. \times 10^{-1}$ GeV^{-2}, we find[‡‡] $\Gamma_{(an)}(\eta \to \mu^-\mu^+) \simeq .25$ eV; this width is too large compared with the experimental value $\Gamma(\eta \to \mu^-\mu^+) \simeq .057$ eV [93]. Thus provided that the electromagnetic interference term does not alter significantly this result, the Lagrangian interaction (4.34) with $f_p = f_n = f_\lambda$ is ruled out. However if we use coupling constants such that[‡‡‡] $f_p = f_n = 10^{-1}$GeV^{-2} and $f_\lambda = 1.25 \times 10^{-1}$GeV^{-2} then we find $\Gamma_{(an)}(\eta \to \mu^-\mu^+) \simeq .06$ eV which is very close to the experimental value [93]. For $\pi^o \to e^-e^+$ we find again $\Gamma_{(an)}(\pi^o \to e^-e^+) = 0$.

So we see that by adjusting properly the quark-electron coupling constants we can be in agreement with the experiment and so this new anomalous coupling scheme might be a reasonable physical picture.

---

‡ For this value of $\bar{f}$ we have $R \simeq 5.5$

‡‡ By using A.9.18 .

‡‡‡ This choice of the coupling constant corresponds to taking $R \simeq 6.3$ at $\sqrt{s} = 5$ GeV.

Discussion.

Nonelectromagnetic interactions of the electron were considered in this chapter in order to interpret the recent data on e^+e^- annihilation into hadrons. We coupled the electron directly to a gluonic field ϕ, and a field X, the mediator of this anomalous interaction, so that the anomalous part of the Lagrangian had the general form $\mathcal{L}^{(an)} \sim f\,\bar{e}\phi X$ or $\sim f\bar{e}\gamma^{\mu}\phi X_{\mu}$. The consequences of these coupling schemes were examined in the context of the quark parton model.

The ratio $R = \frac{\sigma(e^-e^+ \to \text{Hadrons})}{\sigma(e^-e^+ \to \mu^-\mu^+)}$ was found to behave as $R \sim a + bs^2$ for high s (but $s \ll M_x^2$).

The cross-section $s\frac{d\sigma(e^-e^+ \to h + X)}{dz}$ had the form $\sim \alpha(z) + s^2\beta(z)$ exhibiting thus a strong s^2 dependence; remember that a strong "s" dependence especially for $z < .5$ is exhibited by the data [89].

The cross section $s\,\frac{d\sigma(e^-e^+ \to hX)}{dz\,d\cos\theta}$ was found to depend on $\cos^2\theta$ while as we saw data [89] require this to be $\cos\theta$ independent at least for $\cos\theta$ varying from -.6 to .6.

The deep inelastic process $e^- + p \to e^- + X$ and the reaction $p + p \to \mu^-\mu^+ + X$ are affected by the anomalous electron coupling.

It was found that the structure function $F_2^{(ep)}$ did not scale but it had the form $F_2^{(ep)}(x,Q^2) \sim f(x) + Q^4 g(x)$. By introducing some other gluons ϕ', as core constituents of the hadron, we could arrange things so that the non-scaling part of $F_2^{(ep)}(x,Q^2)$ gave very small contribution even for very high Q^2. This is an explanation as to why this strong Q^4 non-scaling behaviour has not been seen.

The same arguments applied to the $pp \to \mu^-\mu^+ + X$ reaction as well in which the quantity $Q^4 \frac{d\sigma}{dQ^2}$ ($Q^2 = m^2_{\mu^-\mu^+}$) was found not to scale, that is not to be a function of the variable $\tau = Q^2/s$, but had a Q^4 dependence. Under the same assumptions as in the electroproduction case, we can say that the effects of the anomalous interaction of the electron are negligible and in this case as well even for high values of Q^2 ($= m^2_{\mu^-\mu^+}$).

Finally we considered the anomalous coupling given by a Lagrangian $\mathcal{L} \sim \sum f_q(\bar{e}q)X_q$ and we examined their consequences to he mesonic decays $\pi^o \to e^-e^+$ and $\eta \to \mu^-\mu^+$.

CHAPTER V.

Introduction

In the previous chapters the quark parton model was applied to electromagnetic and weak processes; also in the fourth chapter anomalous interactions of the electron were considered. The question is whether the naive quark parton model can be applied to strong interactions as well.

In this chapter, which occupies a small portion of this thesis, we adopt a strong interaction scheme involving quarks in order to explain the rising of the total cross sections in the hadron-hadron collisions.

V1) Hadron-Hadron Collisions in the Quark Parton Model and Rising Total Cross Sections.

We are interested in finding the total cross sections $\sigma^{h_1 h_2}(s)$ of the process $h_1 h_2 \rightarrow$ Anything, where h_1 and h_2 denote hadrons, applying quark parton model techniques.

Any reasonable model should give a total cross section which is an increasing function for high values of the energy s consistent, at least qualitatively, with the data [see for example Ref. 94] . Consider a Lagrangian interaction having the following form [95].

$$\mathcal{L}_{int} = f \sum_{q} (\bar{q} \gamma^{\mu} \psi_q) \phi_r + h.c. \quad . \qquad (5.1)$$

The index "q" runs over the quark fields; the ψ_q's are fields having masses larger than those of the q's, for reasons which will become clear later, and the same quantum numbers as q.

The field ϕ_μ is the mediator of this kind of interaction and carries zero quantum numbers but has spin-1. The coupling constant f has a value which is much larger than the electromagnetic or weak coupling constants.

The total cross-section for the scattering of two hadrons h_1 and h_2 is given by the following expression

$$\sigma_{tot}^{h_1 h_2}(s) = \frac{1}{2} \sum_{i,j} \int_0^1 dx\,dy\, \sigma^{ij}(x,y) \left\{ f_i^{(h_1)}(x) f_j^{(h_2)}(y) + f_i^{(h_2)}(x) f_j^{(h_1)}(y) \right\} . \quad (5.2)$$

The process takes place through the mechanism shown in Fig. 21†. In (5.2) the indices i and j denote quarks or antiquarks and $\sigma^{ij}(x,y)$ is the total cross-section for scattering of the quarks i and j; the variables x and y denote the fraction of the momentum of the hadrons h_1 or h_2 carried by the quarks i and j respectively. The functions $f_i^{(h)}(x)$ are the wellknown parton momentum distribution functions.

In order to calculate the total cross-section $\sigma_{tot}^{h_1 h_2}(s)$ we need the contribution of the processes $qq' \to \psi_q \psi_{q'}$, $q\bar{\psi}_q \to q'\psi_{q'}$, etc; weak and electromagnetic effects are omitted because "f" is several orders of magnitude larger than the electromagnetic coupling constant $e^2/4\pi$ ($\simeq 1/137$) or the weak coupling constant $G(\simeq 10^{-5}/m_p^2)$. Consider first the process $qq' \to \psi_q \psi_{q'}$, with $q \neq q'$, and consequently $\psi_q \neq \psi_{q'}$, and whose the Born term is shown in Fig. 22†.

---

† See in the next page

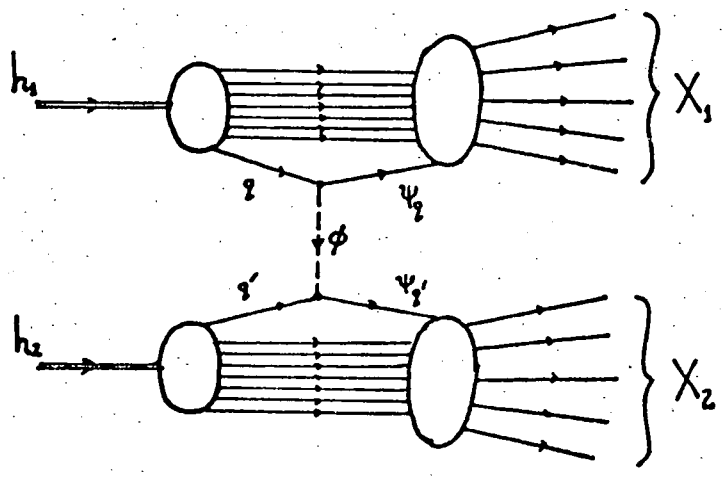

FIGURE 21. Mechanism contributing to the process , $(\text{hadron})_1+(\text{hadron})_2 \rightarrow$ Anything.

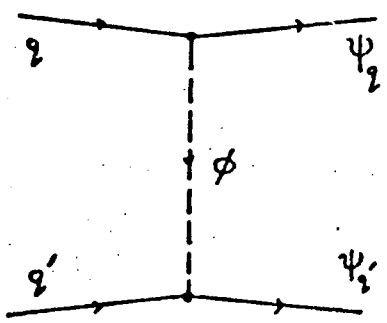

FIGURE 22. The process $q\ q' \rightarrow \psi_q\ \psi_{q'}$ mediated by the exchange of the spin-1 field ϕ_μ.

The cross-section for the process $qq' \to \psi_q \psi_{q'}, (q \neq q')$ has a constant behaviour for large values of the incoming energy; in fact we find‡ $\sigma(s) \propto f^4/M^2$ where M is the mass of the particle ϕ. This behaviour holds as long as $s \gg M^2$, and provided that $q \neq q'$.

In the case of $q = q'$ the amplitude is the sum of the two diagrams of Fig. 23

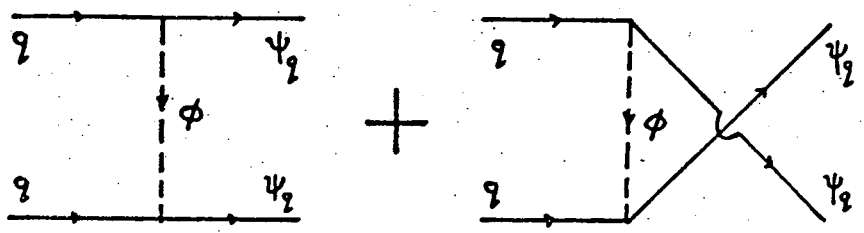

FIGURE 23. The process $qq \to \psi_q \psi_q$ in lowest order of perturbation theory.

In the high energy momentum limit, in which the masses of q and ψ_q are put equal to zero, the cross-section for the process $qq \to \psi_q \psi_q$ is identical to that of the $e^- e^- \to e^- e^-$ process provided that the coupling constant "e" is replaced by "f" and the photon has a mass M equal to that of the ϕ-particle. The differential cross section for the process $e^- e^- \to e^- e^-$ is given by‡‡

$$\frac{d\sigma}{d\Omega} = \frac{\alpha^2}{8E^2}\left\{ \frac{1+\cos^4\theta/2}{\sin^4\theta/2} + \frac{1+\sin^4\theta/2}{\cos^4\theta/2} + \frac{2}{\sin^2\theta/2 \cos^2\theta/2} \right\}. \qquad (5.3)$$

---

‡ See A.8.17 with e^- replaced by q and ϕ by ψ_q.

‡‡ See formula (7.84) of the book "Relativistic Quantum mechanics" J.D. Bjorken and S.D. Drell, McGraw-Hill, New York, (1964).

In our case α should be replaced by $\frac{f^2}{4\pi}$ and $\sin^2\frac{\theta}{2}$, $\cos^2\frac{\theta}{2}$ by $\sin^2\frac{\theta}{2}+\epsilon$, $\cos^2\frac{\theta}{2}+\epsilon$, where ϵ is proportional to M^2/s, that is $\epsilon \propto M^2/s$. It is evident that the expression in the brackets of Eq. (5.3), after the above replacements, has a behaviour $\sim s/M^2$ when integrated with respect θ; this behaviour comes from the first term of (5.3). Thus the total cross-section in the case $qq \to \psi_q \psi_q$ has a behaviour $\sigma(s) \sim f^4/M^2$ also .

No need to examine the asymptotic high energy behaviour of other‡ quark diagrams because we have everything we need for the argument we want to put forward. From (5.2) we have

$$\sigma_{tot}^{h_1 h_2}(s) = \frac{1}{2}\sum_{q,q'}\int_0^1 dx\,dy\,\hat{\sigma}^{qq'\to\psi_q\psi_{q'}}(x,y)\left\{f_q^{(h_1)}(x)f_{q'}^{(h_2)}(y)+f_q^{(h_2)}(x)f_{q'}^{(h_1)}(y)\right\}+(O.T.)\,. \quad (5.4)$$

In the expression above by (O.T) we mean "other terms" which come from other quark processes or from weak and electromagnetic interactions of quarks. The distribution functions $f_i^{(h)}(x)$ can be written in the form,

$$f_i^{(h)}(x) = v_i^{(h)}(x) + c_i^{(h)}(x) \quad (5.5)$$

where $v_i^{(h)}(x)$ and $c_i^{(h)}(x)$ denote the "valence" and "core" contribution respectively. When x tends to zero $v_i^{(h)}(x)$ and $c_i^{(h)}(x)$ behave as

---

‡ In fact only the $qq' \to \psi_q \psi_{q'}$ process would be enough as we shall see later .

$u_i^{(h)}(x) \sim x^{-\alpha(0)}$ and $c_i^{(h)}(x) \sim x^{-1}$; $\alpha(0)$ is the intercept of the leading non Pomeron Regge trajectory [51].

The total cross-section $\sigma^{qq' \to \psi_q \psi_{q'}}_{(x,y)}$ is given by the following expression

$$\sigma^{qq' \to \psi_q \psi_{q'}}(x,y) = g^2 \theta(xys - \mu^2) \quad . \qquad (5.6)$$

g^2 is constant having dimensions of inverse mass square ($g \propto f^2/M$), and s is the variable $s = (p_{h_1} + p_{h_2})^2$; p_{h_1} and p_{h_2} are the momenta of the two hadrons h_1 and h_2 respectively and x,y the fractions of the hadronic momenta carried by the quarks as explained earlier in this chapter.

The theta function appearing in (5.6) has been put in order to have zero cross-section when we are below the threshold for the production of ψ_q and $\psi_{q'}$ particles. In fact a theta function $\theta(s' - 4m_\psi^2)$ must appear where s' is the total centre of mass energy of the q,q' pair. For high s the variable s' is given by $s' \simeq xys + \Sigma\,(\text{quark mass})^2$. Taking into account the fact that the ψ_q's are heavier than the conventional quarks the cross-section $\sigma^{qq' \to \psi_q \psi_{q'}}$ receives the form given by Eq. (5.6) with $\mu^2 > 0$. From Eq. (5.4) we get, on account of Eqs. (5.5) and (5.6), the following expression for the total cross-section $\sigma_{tot}^{h_1 h_2}(s)$

$$\sigma_{tot}^{h_1,h_2}(s) = \frac{1}{2} \sum_{i,j} \int_0^1 dx\,dy\, g^2 \theta(xys - \mu^2) \Big\{ u_i^{(h_1)}(x)\, u_j^{(h_2)}(y) + u_i^{(h_1)}(x)\, c_{j'}^{(h_2)}(y) + c_i^{(h_1)}(x)\, c_{j'}^{(h_2)}(y) \Big\} + (\text{O.T.}) \quad . \qquad (5.7)$$

It is easy to see that $\iint_0^1 dx\,dy\, f(x)\phi(y)\,\theta(sxy - \mu^2)$ is equal to $\int_{\mu^2/s}^1 dx \int_{\mu^2/s}^1 dy\, f(x)\phi(y)$. As $s \to \infty$ this integral is dominated by the behaviour of the functions $f(x)$ and $\phi(y)$ near $x \approx 0$ and $y \approx 0$

respectively. Thus we have

$$\int_{\mu^2/s}^{1} dx \int_{\mu^2/sx}^{1} dy\, f(x)\phi(y) \underset{s\to\infty}{\approx} \int_{\mu^2/s}^{1} dx \int_{\mu^2/sx}^{1} dy\, f^{(as)}(x)\phi^{(as)}(y) + (L.O.T) . \quad (5.8)$$

By $f^{(as)}(x)$ and $\phi^{(as)}(y)$ we denote the asymptotic behaviour of $f(x)$ and $\phi(y)$; (L.O.T) is the contribution of the "lower order terms". When $f(x) = c_q^{(h_1)}(x)$ and $\phi(y) = c_q^{(h_2)}(y)$ then $f^{(as)}(x) \approx 1/x$ and $\phi^{(as)}(y) \approx 1/y$. It is obvious that in this case, from Eq. (5.8), we have

$$\int_{\mu^2/s}^{1} dx \int_{\mu^2/sx}^{1} dy\, c_q^{(h_1)}(x)\, c_{q'}^{(h_2)}(y) \underset{s\to\infty}{\propto} \left(\ln \frac{s}{\mu^2}\right)^2 + (L.O.T.) . \quad (5.9)$$

Similarly

$$\int_{\mu^2/s}^{1} dx \int_{\mu^2/sx}^{1} dy\, U_q^{(h_1)}(x)\, C_{q'}^{(h_2)}(y) \underset{s\to\infty}{\propto} \left(\ln \frac{s}{\mu^2}\right) + (L.O.T.) . \quad (5.10)$$

When $f(x) = U_q^{(h_1)}$ and $\phi(y) = U_q^{(h_2)}(y)$ the integral of the left hand side of Eq. (5.8) has a constant value because $U(x)^{(h_1,h_2)} \underset{x\to 0}{\sim} x^{-\alpha(0)}$ and $\alpha(0) < 1$; thus we have

$$\int_{\mu^2/s}^{1} dx \int_{\mu^2/sx}^{1} dy\, U_q^{(h_1)}(x)\, U_{q'}^{(h_2)}(y) \underset{s\to\infty}{\propto} (\text{constant}) . \quad (5.11)$$

It is evident now that the cross-section $\sigma_{tot}^{h_1h_2}(s)$, for large values of the variable "s", has the behaviour

$$\sigma_{tot}^{h_1h_2}(s) \underset{s\to\infty}{\approx} a\left(\ln \frac{s}{\mu^2}\right)^2 + b\left(\ln \frac{s}{\mu^2}\right) + c . \quad 5.12)$$

Thus a $(\log s)^2$ behaviour for the total cross-section was derived. This high energy behaviour gives a rising total cross section and it is consistent with the Froissart bound [96].

Phenomenological fits to the data for the total cross-section $\sigma_{tot}^{h_1h_2}(s)$ having this $(\log s)^2$ behaviour can be found in the literature [see for example Ref. 97] .

V2) General Comments on the Model.

In order to derive this $(\log s)^2$ behaviour of the total cross-section $\sigma_{tot}^{h_1h_2}(s)$ we needed basically three things: First of all a strong interaction scheme dictated by the Lagrangian (5.1), second the quark parton formula (5.2) and third that the masses of ψ_q's are larger than those of q's .

One might worry because only the Born terms were taken into account or to say that we have violation of unitarity, because ‡ $\sigma^{qq'\to\psi\psi'}(s) \sim$ const., and so on. This is not really a problem. For our calculation the only thing we needed was a mechanism giving constant total cross sections for the processes $qq' \to \psi_q\psi_{q'}$, which is zero when the total incoming energy is less than a certain positive number. Thus any Lagrangian interaction giving $\sigma(s)^{qq'\to \text{anything}} \sim g^2\theta(s-\mu^2)$ would do for our calculation and problems associated with the specific form of the Lagrangian we have chosen should not worry us.

---

‡ As long as a finite number of partial waves contributs to a process we have form unilarity $\sigma_{tot}(s) \leq \frac{\text{constant}}{s}$. See for example "Elementary Particle Theory" by A.D. Martin and T.D. Spearman, North Holland, Amsterdam, 1970.

Note that the $(\log s)^2$ behaviour of the total cross-section is a consequence of the $1/x$ behaviour of the core function $c(x)$ near $x \approx 0$. In other words this $(\log s)^2$ behaviour is due to the statistical distribution of the core quarks inside the hadron and not to dynamics. The only thing we require from dynamics is to give some (quark) + (quark)' → (Anything) cross-sections behaving as $\sigma^{qq' \to \text{anything}}(s) \approx g^2\theta(s-\mu^2)$ for high values of s.

Discussion.

In an attempt to interpret the rising of the total hadronic cross-sections $\sigma_{tot}^{h_1h_2}(s)$ an interaction scheme was assumed in which the constituent quarks were interacting strongly with some other heavier quark fields through a spin-1 field carrying vacuum quantum numbers.

A $(\log s)^2$ behaviour was found for the total cross section $\sigma^{h_1h_2}(s)$, which is consistent with the observed rising [94] and does not violate the Froissart bound [96].

This $(\log s)^2$ behaviour is not a dynamical effect but is due to the statistical distribution of the core quarks inside the hadron.

APPENDIX 1

a) Units

Natural units are used throughout this thesis with $\hbar = c = 1$. One natural unit of length $= \frac{\hbar c}{1\ \text{GeV}} = 1.973 \times 10^{-14}$ cm and $1\ \text{mb} = 10^{-27}\ \text{cm}^2 = .3893$ natural units.

b) Notation

The notation is that of Ref [1]. Hence our metric tensor is $g^{\mu\nu} = g_{\mu\nu} = (1, -1, -1, -1)$ and the contravariant four vector A^μ is defined as $A^\mu = (A^o, \vec{A})$. The corresponding covariant four vector is $A_\mu = (A_o, -\vec{A})$. The momentum operator is $p^\mu = i\partial^\mu = (\frac{i\partial}{\partial x^o}, -i\vec{\nabla})$. The Dirac matrices γ^μ satisfy the anticommutation relations

$$\{\gamma^\mu, \gamma^\nu\}_+ = 2g^{\mu\nu} \qquad \text{(A.1.1)}$$

and are given by the following expressions

$$\gamma^o = \begin{pmatrix} 1 & 0 \\ 0 & -1 \end{pmatrix} \quad , \vec{\gamma} = \begin{pmatrix} 0 & \vec{\sigma} \\ -\vec{\sigma} & 0 \end{pmatrix} \quad . \qquad \text{(A.1.2)}$$

$\vec{\sigma}$ stands for the vector $\vec{\sigma} = (\sigma^1, \sigma^2, \sigma^3)$ where the Pauli matrices $\sigma^1, \sigma^2, \sigma^3$ are given by the following expressions.

$$\sigma^1 = \begin{pmatrix} 0 & 1 \\ 1 & 0 \end{pmatrix}, \sigma^2 = \begin{pmatrix} 0 & i \\ -i & 0 \end{pmatrix}, \sigma^3 = \begin{pmatrix} 1 & 0 \\ 0 & -1 \end{pmatrix} \quad . \qquad \text{(A.1.3)}$$

The antisymmetric tensor $\sigma^{\mu\nu}$ is defined as $\sigma^{\mu\nu} = \frac{i}{2}[\gamma^\mu, \gamma^\nu]$ and the γ^5 matrix as $\gamma^5 = i\gamma^0\gamma^1\gamma^2\gamma^3 = \gamma_5$. Explicit calculation gives

for the γ^5

$$\gamma^5 = \gamma_5 = \begin{pmatrix} 0 & 1 \\ 1 & 0 \end{pmatrix} \quad . \qquad (A.1.4)$$

The scalar product of two vectors A^μ and B^μ is defined as

$$A \cdot B \equiv A^\mu B_\mu = g_{\mu\nu} A^\mu B^\nu = A^0 B^0 - \vec{A} \cdot \vec{B} \quad . \qquad (A.1.5)$$

The slash $\not{A}$ of a vector A^μ is defined as $\not{A} = \gamma^\mu A_\mu$. The Klein-Gordon equation in its covariant form is given by the following expression

$$(\Box + m^2)\phi(x) = 0 \qquad (A.1.6)$$

where $-\Box = -\partial_\mu \partial^\mu = -\frac{\partial^2}{\partial x o^2} + \nabla^2$.

The Dirac equation is given by

$$(i\not{\partial} - m)\psi(x) = 0 \quad . \qquad (A.1.7)$$

The Dirac spinors $u(p,s)$, $v(p,s)$ used throughout are those found in Ref. [1] multiplied by a factor $(2m)^{1/2}$. They satisfy the equations

$$(\not{p} - m)u(p,s) = 0, \quad (\not{p} - m)v(p,s) = 0 \quad . \qquad (A.1.8)$$

In terms of the adjoint spinors $\bar{u} = u^+\gamma^0$, $\bar{v} = v^+\gamma^0$ we have

$$\bar{u}(p,s)(\not{p} - m) = 0, \quad \bar{v}(p,s)(\not{p} - m) = 0 \qquad (A.1.9)$$

The projection operators are

$$u(p,s)\bar{u}(p,s) = (\not{p}+m)\left(\frac{1+\gamma_5 \not{s}}{2}\right) \tag{A.1.10}$$

$$v(p,s)\bar{v}(p,s) = (\not{p}-m)\left(\frac{1+\gamma_5 \not{s}}{2}\right) \tag{A.1.11}$$

where the vector s^μ represents the direction of spin of the physical particle in its rest frame and has the properties $s^2 = -1$, $s.p = 0$.

The following identities hold,

$$\sum_{\pm s} u(p,s)\bar{u}(p,s) = (\not{p}+m) \tag{A.1.12}$$

$$\sum_{\pm s} v(p,s)\bar{v}(p,s) = (\not{p}-m) \tag{A.1.13}$$

$$\bar{u}(p')\gamma^\mu u(p) = \bar{u}(p')\left\{\frac{(p+p')^\mu}{2m} + i\frac{\sigma^{\mu\nu}}{2m}(p'-p)_\nu\right\}u(p) \tag{A.1.14}$$

$$\not{a}\not{b} = a\cdot b - i\sigma_{\mu\nu}a^\mu b^\nu \tag{A.1.15}$$

$$Tr(\not{a}_1\not{a}_2\ldots\not{a}_n) = 0 \quad , \quad n=\text{odd} \tag{A.1.16}$$

$$Tr(\not{a}\not{b}) = Tr(\not{b}\not{a}) = 4\,a\cdot b \tag{A.1.17}$$

$$Tr(\not{a}_1\not{a}_2\not{a}_3\not{a}_4) = 4(a_1\cdot a_3\, a_2\cdot a_4 - a_1\cdot a_4\, a_2\cdot a_3 + a_1\cdot a_2\, a_3\cdot a_3) \tag{A.1.18}$$

$$Tr(\gamma_5\not{a}\not{b}) = 0 \tag{A.1.19}$$

$$Tr(\gamma_5\not{a}\not{b}\not{c}\not{d}) = 4i\,\varepsilon_{\alpha\beta\gamma\delta}a^\alpha b^\beta c^\gamma d^\delta \tag{A.1.20}$$

$$Tr(\not{a}_1\not{a}_2\ldots\not{a}_n\gamma_5) = 0 \quad , \quad n=\text{odd} \tag{A.1.21}$$

$$\gamma^\mu\gamma_\mu = 4 \tag{A.1.22}$$

$$\gamma^\mu\not{a}\gamma_\mu = -2\not{a} \tag{A.1.23}$$

$$\gamma^\mu\not{a}\not{b}\gamma_\mu = 4\,a\cdot b \tag{A.1.24}$$

$$\gamma^\mu\not{a}\not{b}\not{c}\gamma_\mu = -2\not{c}\not{b}\not{a} \tag{A.1.25}$$

$$\gamma^\mu\not{a}\not{b}\not{c}\not{d}\gamma_\mu = 2\{\not{d}\not{a}\not{b}\not{c} + \not{c}\not{b}\not{a}\not{d}\} \tag{A.1.26}$$

$$Tr(\not{a}_1\not{a}_2\ldots\not{a}_{2n}) = Tr(\not{a}_{2n}\ldots\not{a}_2\not{a}_1) \tag{A.1.27}$$

Other useful formulae and identities can be found in Ref. [1].

c) Cross-sections

The differential cross-section for a process $1 + 2 \to 3 + 4 + .. + n$ has the form

$$d\sigma = (2\pi)^4 \frac{\delta^{(4)}(P_i - P_f)}{|\vec{v}_1 - \vec{v}_2|} \frac{1}{(2E_1)} \frac{1}{(2E_2)} \prod_{i=3}^{n} \frac{d^3\vec{P}_i}{(2\pi)^3 (2E_i)} |M|^2 . \quad \text{(A.1.28)}$$

The notation is as follows:

P_i^μ and P_f^μ are the total four momenta of the initial and final states respectively. $\vec{v}_1$ and $\vec{v}_2$ are the velocities of the particles 1 and 2 respectively.

The normalization of our states is the covariant one, that is

$$\langle \vec{P}, s | \vec{P}', s' \rangle = (2\pi)^3 (2E) \delta^{(3)}(\vec{P} - \vec{P}') . \quad \text{(A.1.29)}$$

The spinors $u(p,s)$ and $v(p,s)$ are normalized to $2m$ so that we have

$$\bar{u}(p,s) u(p,s) = 2m , \quad \bar{v}(p,s) v(p,s) = -2m . \quad \text{(A.1.30)}$$

In calculating Feynman diagrams we must be careful as far as the external lines are concerned which are not multiplied by the factors $\frac{(2\pi)^{-3/2}}{\sqrt{2\omega}}$ (for a boson) or $(2\pi)^{-3/2} \left(\frac{m}{E}\right)$ (for a fermion). In calculating the amplitude M in (A.1.28) we apply the Feynman rules by putting 1 (unity) for a spin-0 particle , the corresponding u, $\bar{u}$, v, or $\bar{v}$ spinor for a spin - $\frac{1}{2}$ particle (normalized as in A.1.30), and ϵ^μ for a photon.

The statistical factor "S" is obtained by including a factor $1/m!$. if there are m identical particles in the final state.

APPENDIX 2

The following identities hold

$$L^{\mu\nu}(K,K') \equiv \sum_{s,s'} \bar{u}(K',s')\gamma^{\mu}u(K,s)\,\bar{u}(K,s)\gamma^{\nu}u(K',s') = 4\{K^{\mu}K'^{\nu} + K^{\nu}K'^{\mu} - g^{\mu\nu}K\cdot K' + m^2 g^{\mu\nu}\} \quad \text{(A.2.1)}$$

$$S^{\mu\nu}(K,K') \equiv \sum_{s,s'} \bar{u}(K',s')\gamma^{\mu}(1-\gamma_5)u(K,s)\,\bar{u}(K,s)\gamma^{\nu}(1-\gamma_5)u(K',s') = 8\{K^{\mu}K'^{\nu} + K^{\nu}K'^{\mu} - g^{\mu\nu}K\cdot K' + i\varepsilon^{\mu\nu\alpha\beta}K_{\alpha}K'_{\beta}\} \quad \text{(A.2.2)}$$

$$M^{\mu\nu}(K,K') \equiv \sum_{s,s'} \bar{u}(K',s')\gamma^{\mu}(1-\gamma^5)u(K,s)\,\bar{u}(K,s)\gamma^{\nu}u(K',s') = \frac{1}{2}\{S^{\mu\nu}(K,K') + 8m^2 g^{\mu\nu}\} \quad \text{(A.2.3)}$$

Proof of A.2.1

$L^{\mu\nu}(k,k') = \mathrm{Tr}\,(\not{k}' + m)\gamma^{\mu}(\not{k} + m)\gamma^{\nu}$ by using the first of Eqs. (A.1.12)

Using (A.1.16), (A.1.17) and (A.1.18) the identity (A.2.1.) is derived.

Proof of A.2.2

$S^{\mu\nu}(k,k') = \mathrm{Tr}(\not{k}' + m)\gamma^{\mu}(1-\gamma^5)(\not{k} + m)\gamma^{\nu}(1-\gamma^5)$ by using the first of Eqs. (A.1.12) .

Using the fact that γ^5 anticommutes with γ^{μ} and also (A.1.16) and (A.1.21) we get

$$S^{\mu\nu}(k,k') = 2\mathrm{Tr}(\not{k}'\gamma^{\mu}\not{k}\gamma^{\nu} - \not{k}'\gamma^{\mu}\not{k}\gamma^{\nu}\gamma^5)$$

from which by applying (A.1.18) and (A.1.20) the identity (A.2.2) is derived.

Proof of A.2.3

It is a straightforward calculation if one uses (A.1.16), (A.1.18), (A.1.17) and (A.1.20).

In order to find the corresponding identities when either u(p,s) is replaced by υ(k,s) or u(k',s') by υ(k',s') or both we must observe that from Eqs. A.1.12 we have $\sum_{\pm s} u(k,s)\bar{u}(k,s) = (\not{k}+m)$ while $\sum_{\pm s}\upsilon(k,s)\bar{\upsilon}(k,s) = -(-\not{k} + m)$. Thus we are lead to the following rules.

Rule I

"If u(k,s) → υ(k,s) (u(k',s') → υ(k',s') then the identities (A.2.1), (A.2.2), (A.2.3) still hold provided that in the right hand side of each identity k → -k (k' → -k') and the overall result is multiplied by (-1)."

Rule II

"If u(k,s) → υ(k,s) and u(k',s') → υ(k',s') then the identities (A.2.1), (A.2.2), (A.2.3) still hold provided that in the right hand side of each identity k → -k, k' → -k'".

In calculating cross-sections we shall frequently use the following identities whose derivation is straightforward if one takes into account (A.2.1), (A.2.2) and (A.2.3).

$$L^{\mu\nu}(K_1,K_2)\,L_{\mu\nu}(K_1',K_2') = 32\{K_1\cdot K_1'\,K_2\cdot K_2' + K_1\cdot K_2'\,K_2\cdot K_1' + m^2 K_1'\cdot K_2' - m^2 K_1\cdot K_2 + 2m^2m'^2\} \quad \text{(A.2.4)}$$

$$S^{\mu\nu}(K_1,K_1)\,S_{\mu\nu}(K_1',K_2') = (16)^2\,K_1\cdot K_1'\,K_2\cdot K_2' \quad \text{(A.2.5)}$$

$$L^{\mu\nu}(K_1,K_2)\,S_{\mu\nu}(K_1',K_2') = 64\{K_1\cdot K_1'\,K_2\cdot K_2' + K_1\cdot K_2'\,K_2\cdot K_1' - m^2 K_1'\cdot K_2'\} \quad \text{(A.2.6)}$$

$$L^{\mu}{}_{\mu}(K_1,K_2) = 8\{2m^2 - K_1\cdot K_2\} \quad \text{(A.2.7)}$$

$$S^{\mu}{}_{\mu}(K_1,K_2) = -16\,K_1\cdot K_2 \quad \text{(A.2.8)}$$

APPENDIX 3

a) Unpolarized Differential Cross-section for the Inelastic Process $e^- + p \to e^- + X$.

We work in proton's laboratory system. By $(E,\vec{K})$ and $(E', \vec{K}')$ we denote the incoming and outgoing electron's four momenta. M is the mass of the proton. The differential cross-section for the process $e^- + p \to e^- + F$, where "F" is a definite state of "n" particles, is given by (see A.1.28).

$$d\sigma_F = (2\pi)^4 \frac{\delta^{(4)}(K+P-K'-P_F)}{|\vec{v}_1 - \vec{v}_2|} \frac{1}{4EM} \frac{d\vec{K}'}{(2\pi)^3(2E')} dQ_F \overline{\sum_{\lambda,s}} \sum_{\lambda'} |M_F|^2 . \quad (A.3.1)$$

$\overline{\sum_{\lambda,s}}$ denotes average over the initial spins and $\sum_{\lambda'}$ sum over the final electron spins. The phase space dQ_F is given by,

$$dQ_F = \prod_{i=1}^{n} \frac{d\vec{p}_i}{(2\pi)^3 (2E_i)} .$$

The matrix element M_F is given by

$$M_F = e^2 \bar{u}(K',\lambda') \gamma^\mu u(K,\lambda) \frac{-ig^{\mu\nu}}{q^2} \langle F | J_\nu^{(em)}(0) | P,s \rangle . \quad (A.3.2)$$

In (A.3.2) $J_\mu^{(em)}(x)$ is the electromagnetic current four vector and $q = (K-K')$.

Using the identity (A.2.1) we get

$$(2\pi)^4 \delta^{(4)}(K+P-K'-P_F) \overline{\sum_{\lambda,s}} \sum_{s'} |M_F|^2 = \frac{4m\alpha^2}{q^2} L^{\mu\nu}(K,K') W_{\mu\nu}(F) \quad (A.3.3)$$

$$W_{\mu\nu}(F) = \frac{1}{2} \overline{\sum_s} (2\pi)^3 \delta^{(4)}(q+P-P_F) \langle P,s | J_\mu^+(0) | F \rangle \langle F | J_\nu(0) | P,s \rangle . \quad (A.3.4)$$

The differential cross-section (unpolarized) for the reaction $e^- + p \to e^- + (\text{anything})$ is

$$d\sigma = \sum_F d\sigma_F \tag{A.3.5}$$

so that we get

$$d\sigma = \frac{1}{4EM}\frac{1}{|\vec{v}_1 - \vec{v}_2|}\frac{d^3\vec{k}'}{(2\pi)^3(2E')}\frac{4\pi e^4}{q^4} L^{\mu\nu}(k,k') W_{\mu\nu}(p,q) \tag{A.3.6}$$

with

$$W_{\mu\nu}(p,q) = \frac{(2\pi)^3}{2}\overline{\sum_s}\sum_n \delta^{(4)}(p+q-p_n)\langle p,s|J_\mu^\dagger(0)|n\rangle\langle n|J_\nu(0)|p,s\rangle . \tag{A.3.7}$$

The most general form of the tensor $W_{\mu\nu}^\dagger$ is

$$\left.\begin{aligned} W_{\mu\nu}(p,q) = &\left(-g_{\mu\nu} + \frac{q_\mu q_\nu}{q^2}\right)W_1 + \frac{1}{M^2}\left(p_\mu - \frac{p\cdot q}{q^2}q_\mu\right)\left(p_\nu - \frac{p\cdot q}{q^2}q_\nu\right)W_2 + \\ &+ i\frac{\varepsilon_{\mu\nu\alpha\beta}p^\alpha q^\beta}{2M^2}W_3 + \frac{q_\mu q_\nu}{M^2}W_4 + \frac{(p_\mu q_\nu + p_\nu q_\mu)}{2M^2}W_5 + i\frac{(p_\mu q_\nu - p_\nu q_\mu)}{2M^2}W_6 . \end{aligned}\right\} \tag{A.3.8}$$

The $W_{1,2\ldots6}$ are real and depend upon the variables $\nu = p\cdot q/M$ and $Q^2 = -q^2$.

Note that current conservation and parity gives

$W_3 = W_4 = W_5 = W_6 = 0$.

Setting the electron mass equal to zero we get

$$\frac{d^2\sigma}{dE'd\omega} = \frac{4\alpha^2}{Q^4}\frac{E'^2}{M}\left\{2W_1(\nu,Q^2)\sin^2\frac{\theta}{2} + W_2(\nu,Q^2)\cos^2\frac{\theta}{2}\right\} . \tag{A.3.9}$$

θ' is the scattering angle of the outgoing electron.

---

† $W_{\mu\nu}$ is dimensionless

b) The Tensor $W^{\mu\nu}(p,q)$

Using the property $e^{-iP.x} J_{\mu}^{+}(x) e^{iP.x} = J_{\mu}^{+}(o)$, where P is the momentum operator, we get

$$\left.\begin{aligned} W_{\mu\nu}(p,q) = \frac{1}{4\pi} \sum_{s} \int d^4x\, e^{iq\cdot x} \langle p,s|J_{\mu}^{+}(x) J_{\nu}(o)|p,s\rangle = \\ \frac{1}{4\pi} \sum_{s} \int d^4x\, e^{iq\cdot x} \langle p,s|[J_{\mu}^{+}(x), J_{\nu}(o)]|p,s\rangle . \end{aligned}\right\} \quad (A.3.10)$$

In (A.3.10) $J_{\mu}(x)$ denotes the electromagnetic current .

c) Differential Cross-section for $e^- + p \to e^- + X$ Scattering with Polarized Beam and Target.

We seek the expressions for the differential cross sections when the beam electron and the proton have parallel spins ($d\sigma(\uparrow\uparrow)$) and when their spins are antiparallel ($d\sigma(\uparrow\downarrow)$).

The tensor $L^{\mu\nu}(k,k')$ in (A.3.3) is now replaced by the tensor [see Ref. 51 for instance]

$$L^{\mu\nu}(+) \equiv L^{\mu\nu}(S) + L^{\mu\nu}(A) \quad (A.3.11)$$

with

$$L^{\mu\nu}(S) = 2(K^{\mu}K'^{\nu} + K'^{\mu}K^{\nu} - g^{\mu\nu} K\cdot K') \quad (A.3.12a)$$

$$L^{\mu\nu}(A) = -2i\,\varepsilon^{\mu\nu\lambda\sigma} K_{\lambda} K'_{\sigma} \quad . \quad (A.3.12b)$$

(S stands for symmetric and A for antisymmetric part)

Similarly the tenson $W_{\mu\nu}$ is now replaced by

$$W_{\mu\nu} = W_{\mu\nu}(S) + W_{\mu\nu}(A) \quad (A.3.13)$$

where $W_{\mu\nu}(S)$ is given by Eq. (A.3.8) (with $W_3=W_4=W_5=W_6=0$) and $W_{\mu\nu}(A)$ is given by the expression

$$W_{\mu\nu}(A) = i\varepsilon_{\mu\nu\lambda\sigma} q^{\lambda}\left\{ s^{\sigma} d(\nu,Q^2) + p^{\sigma}(q\cdot s)\, g(\nu,Q^2)\right\} . \qquad (A.3.14)$$

In (A.3.14) the functions $d(\nu,Q^2)$ and $g(\nu,Q^2)$ are scalars and s^{μ} is the spin four vector which in proton's rest frame is $s^{\mu} = (0,0,0,1)$.

The differential cross-sections $d\sigma(\uparrow\uparrow)$ and $d\sigma(\uparrow\downarrow)$ are given by the following expressions

$$d\sigma(\uparrow\uparrow) = \frac{\alpha^2}{2Q^4}\frac{E'}{EM}\left\{ L^{\mu\nu}(S) W_{\mu\nu}(S) + L^{\mu\nu}(A) W_{\mu\nu}(A)\right\} \qquad (A.3.15)$$

$$d\sigma(\uparrow\downarrow) = \frac{\alpha^2}{2Q^4}\frac{E'}{EM}\left\{ L^{\mu\nu}(S) W_{\mu\nu}(S) - L^{\mu\nu}(A) W_{\mu\nu}(A)\right\} . \qquad (A.3.16)$$

d) Differential Cross-sections for the Neutrino (Antineutrino) Processes $\nu(\bar{\nu}) + N \to \mu^-(\mu^+) + X$

In calculating $\frac{d\sigma}{dE'd\underline{o}'}$ $\nu N \to \mu^- X$ we must take into account the fact that the Lagrangian interaction is

$$\mathcal{L} = g_w\left\{ J_{\mu}^{(-)} W^{\mu+} + h.c.\right\} \qquad (A.3.17)$$

and that the leptonic part of $J_{\mu}^{(-)}$ has the form

$$J_{\mu}^{(-)} = \bar{\mu}\gamma_{\mu}(1-\gamma_5)\nu_{\mu} + \bar{e}\gamma_{\mu}(1-\gamma_5)\nu_e \qquad (A.3.18)$$

We must also use the fact that the neutrinos (antineutrinos) are always left-handed (right-handed) and thus a factor "1" instead of "$\frac{1}{2}$" must be put when averaging over the initial neutrino and antineutrino spins.

The expression for the differential cross section $\nu p \to \mu^- X$ or $\bar{\nu} p \to \mu^+ X$ is

$$\frac{d^2\sigma^{\nu p,\bar{\nu}p}}{dE'd\Omega'} = \frac{G^2}{2\pi}\frac{E'^2}{M}\left\{2W_1(\nu,Q^2)\sin^2\frac{\theta}{2} + W_2(\nu,Q^2)\cos^2\frac{\theta}{2} \mp \left(\frac{E+E'}{M}\right)W_3(\nu,Q^2)\sin^2\frac{\theta}{2}\right\} . \quad \text{(A.3.19)}$$

The current tensor $W_{\mu\nu}$, the analog of (A.3.10) in the electroproduction case, has the following form

$$W_{\mu\nu}(p,q) = \frac{1}{4\pi}\sum_s \int d^4x\, e^{iqx}\langle p,s|[J_\mu^{(-)}(x), J_\nu^{(+)}(0)]|p,s\rangle . \quad \text{(A.3.20)}$$

In (A.3.20) $J_\mu^{(+)} \overset{def}{\equiv} J_\mu^{(-)\,+}$.

$$W_{\mu\nu}^{(effective)}(p,q) = \left(-g_{\mu\nu} + \frac{q_\mu q_\nu}{q^2}\right)W_1 + \frac{1}{M^2}\left(p_\mu - \frac{p\cdot q}{q^2}q_\mu\right)\left(p_\nu - \frac{p\cdot q}{q^2}q_\nu\right)W_2 + i\frac{\varepsilon_{\mu\nu\alpha\beta}p^\alpha q^\beta}{2M^2}W_3 \quad \text{(A.3.21)}$$

with W_1, W_2, W_3 being real functions of ν and Q^2. The differential cross sections for $\nu n \to \mu^- X$ and $\bar{\nu} n \to \mu^+ X$ have the same form as (A.3.19) where $W_{1,2,3}$ are the corresponding functions for the neutron case and M is the neutron mass. The differential cross sections $\frac{d\sigma^{2\ \nu N,\bar{\nu}N}}{dE'd\Omega'}$ are defined as

$$\frac{d^2\sigma^{\nu N,\bar{\nu}N}}{dE'd\Omega'} = \frac{1}{2}\left\{\frac{d^2\sigma^{\nu p,\bar{\nu}p}}{dE'd\Omega'} + \frac{d^2\sigma^{\nu n,\bar{\nu}n}}{dE'd\Omega'}\right\} . \quad \text{(A.3.22)}$$

APPENDIX 4

In this appendix we first calculate the differential cross section for the process $LQ \to L'Q'$ where the Lagrangian interaction is given by the following form

$$\mathcal{L} = g\{\bar{L}'\gamma_\mu(g_V - g_A\gamma_5)L + \bar{Q}'\gamma_\mu(f_V - f_A\gamma_5)Q\}X^\mu + h.c. \quad . \quad (A.4.1)$$

The Feynman diagram (Born term) for the process $LQ \to L'Q'$ is shown in Fig. 1A .

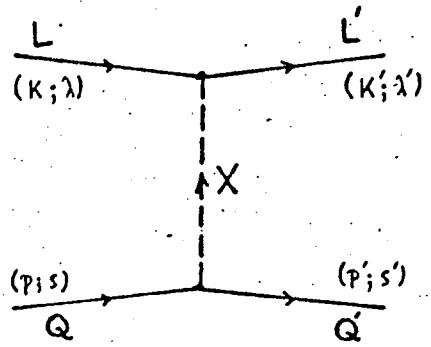

FIGURE 1A. Kinematics of the process $LQ \to L'Q'$ which is mediated by the exchange of the spin-1 object X.

We assume that L,L' are leptons and take their masses equal to zero. The matrix element $|M|^2$ of (A.1.28) is given by

$$\left.\begin{aligned} |M_{\lambda s;\lambda' s'}|^2 = \frac{g^4}{(q^2-M^2)^2}\,|\bar{u}_{L'}(K',\lambda')\gamma^\mu(g_V - g_A\gamma_5)u_L(K,\lambda)\times \\ \times\ \bar{u}_{Q'}(p',s')\gamma_\mu(f_V - f_A\gamma_5)u_Q(p,s)|^2 \quad . \end{aligned}\right\} (A.4.2)$$

Averaging over the initial spins and summing over the final yields

$$\left.\begin{aligned} \overline{\sum_{\lambda,s}}\sum_{\lambda',s'}|M_{\lambda s;\lambda' s'}|^2 = \{(2s_L+1)(2s_Q+1)\}^{-1}\frac{g^4}{(q^2-M^2)^2}\ \times \\ \times\ \sum_{s,s'}\bar{u}_{Q'}(p',s')\gamma^\mu(f_V - f_A\gamma_5)u_Q(p,s)\,\bar{u}_Q(p,s)\gamma^\nu(f_V^* - f_A^*\gamma_5)u_{Q'}(p',s')\times \\ \times\ \sum_{\lambda,\lambda'}\bar{u}_{L'}(K',\lambda')\gamma_\mu(g_V - g_A\gamma_5)u_L(K,\lambda)\,\bar{u}_L(K,\lambda)\gamma_\nu(g_V^* - g_A^*\gamma_5)u_L(K',\lambda') \quad . \end{aligned}\right\} (A.4.3)$$

Using (A.1.12) and (A.1.13) we get

$$\left.\begin{aligned}\overline{\sum_{\lambda,s}}\sum_{\lambda',s'}|M_{\lambda s;\lambda' s'}|^2 &= \{(2s_L+1)(2s_Q+1)\}^{-1}\frac{g^4}{(q^2-M^2)^2}\times\\ \times\ Tr\{(\not k'+m_{L'})\gamma^\mu(g_V-g_A\gamma_5)(\not k+m_L)\gamma^\nu(g_V^*-g_A^*\gamma_5)\}&\times\\ \times\ Tr\{(\not p'+m_{Q'})\gamma_\mu(f_V-f_A\gamma_5)(\not p+m_Q)\gamma_\nu(f_V^*-f_A^*\gamma_5)\}&\end{aligned}\right\}\quad(A.4.4)$$

and also from the trace properties (A.1.12-A.1.27) we get,

$$\begin{aligned}&Tr\{(\not k'+M)\gamma^\mu(V-A\gamma^5)(\not k+m)\gamma^\nu(V^*-A^*\gamma^5)\} =\\ &Tr\{(\not k'+M)\gamma^\mu(V-A\gamma^5)(V^*-A^*\gamma^5)\not k\gamma^\nu +\\ &\qquad +m(\not k'+M)\gamma^\mu(V-A\gamma^5)(V^*+A^*\gamma^5)\gamma^\nu\} =\\ &Tr\{(|V|^2+|A|^2)(\not k'+M)\gamma^\mu\not k\gamma^\nu-2Re(VA^*)(\not k'+M)\gamma^\mu\gamma^5\not k\gamma^\nu+\\ &+m(|V|^2-|A|^2)(\not k'+M)\gamma^\mu\gamma^\nu+i2m\,Im(VA^*)(\not k'+M)\gamma^\mu\gamma^5\gamma^\nu\} =\end{aligned}$$

= (using the identities A.1.16 to A.1.27) =

$$\begin{aligned}&(|V|^2+|A|^2)\,Tr(\not k'\gamma^\mu\not k\gamma^\nu)-2Re(VA^*)\,Tr(\gamma^5\not k'\gamma^\mu\not k\gamma^\nu)+\\ &\qquad +mM(|V|^2-|A|^2)\,Tr(\gamma^\mu\gamma^\nu) =\end{aligned}$$

$$\begin{aligned}&4(|V|^2+|A|^2)(k'^\mu k^\nu+k^\mu k'^\nu-g^{\mu\nu}k\cdot k')+4mM(|V|^2-|A|^2)g^{\mu\nu}-\\ &\qquad -8i\,Re(VA^*)\varepsilon_{\alpha\mu\beta\nu}\,k'^\alpha k^\beta\ .\end{aligned}$$

Thus we have

$$\left.\begin{aligned}&Tr\{(\not k'+M)\gamma^\mu(V-A\gamma^5)(\not k+m)\gamma^\nu(V^*-A^*\gamma^5)\}=\\ &4\{(|V|^2+|A|^2)(k'^\mu k^\nu+k^\mu k'^\nu-g^{\mu\nu}k\cdot k')+\\ &+mM(|V|^2-|A|^2)g^{\mu\nu}+2i\,Re(VA^*)\varepsilon_{\mu\nu\alpha\beta}k'^\alpha k^\beta\}.\end{aligned}\right\}\quad(A.4.4a)$$

The expression (A.4.4) in the approximation $m_L = m_L' = 0$ is

written as

$$\overline{\sum_{\lambda,s}}\sum_{\lambda',s'}|M_{\lambda s;\lambda' s'}|^2=\{(2s_L+1)(2s_Q+1)\}^{-1}\frac{16g^4}{(q^2-M^2)^2}\times$$

$$\times\{(|g_V|^2+|g_A|^2)(K'^\mu K^\nu+K^\mu K'^\nu-g^{\mu\nu}K\cdot K')+2i\,\mathrm{Re}(g_V g_A^*)\varepsilon^{\mu\nu}{}_{\alpha\beta}K'^\alpha K^\beta\}\times$$

$$\times\{(|f_V|^2+|f_A|^2)(P'_\mu P_\nu+P_\mu P'_\nu-g_{\mu\nu}P\cdot P')+m_Q m_{Q'}(|f_V|^2-|f_A|^2)g_{\mu\nu}+$$

$$+2i\,\mathrm{Re}(f_V f_A^*)\varepsilon_{\mu\nu\alpha\beta}P'^\alpha P^\beta\}=$$

$$\{(2s_L+1)(2s_Q+1)\}^{-1}\frac{16g^4}{(q^2-M^2)^2}\times$$

$$\times\{(|g_V|^2+|g_A|^2)(|f_V|^2+|f_A|^2)(K'^\mu K^\nu+K^\mu K'^\nu-g^{\mu\nu}K\cdot K')(P_\mu P'_\nu+P_\nu P'_\mu-g_{\mu\nu}P\cdot P')+$$

$$+m_Q m_{Q'}(|g_V|^2+|g_A|^2)(|f_V|^2-|f_A|^2)(-2K\cdot K')-4\mathrm{Re}(f_V f_A^*)\mathrm{Re}(g_V g_A^*)\varepsilon^{\mu\nu\alpha\beta}\varepsilon_{\mu\nu\lambda\beta}K'^\lambda K_\alpha P'^\lambda P^\beta\}=$$

$$\{(2s_L+1)(2s_Q+1)\}^{-1}\frac{16g^4}{(q^2-M^2)^2}\times$$

$$\times\{2(|g_V|^2+|g_A|^2)(|f_V|^2+|f_A|^2)(p'K\,p\cdot K'+p'\cdot K'\,p\cdot K)-2m_Q m_{Q'}(|g_V|^2+|g_A|^2)\times$$

$$\times(|f_V|^2-|f_A|^2)(K\cdot K')+8\,\mathrm{Re}(g_V g_A^*)\mathrm{Re}(f_V f_A^*)K'^\lambda{}_\beta P^{\prime\lambda B}(g_A^\alpha g_B^\beta-g_B^\alpha g_A^\beta)\} \qquad \text{(A.4.4b)}$$

where we have used the identity

$$\varepsilon^{\mu\nu\alpha\beta}\varepsilon_{\mu\nu\lambda B}=-2(g_\lambda^\alpha g_B^\beta-g_B^\alpha g_\lambda^\beta) \qquad \text{(A.4.4c)}$$

In the rest frame of the Q-particle the energies of the incoming and outgoing electron are denoted by E and E' respectively. If we denote by θ the scattering angle of the lepton L', then we have

$$\{p'\cdot K'\,p\cdot K+p'\cdot K\,p\cdot K'\}=2m_Q^2EE'\left\{1+\frac{E-E'}{m_Q}\sin^2\frac{\theta}{2}\right\} \qquad \text{(A.4.5)}$$

$$\{p'K'p\cdot K - p'Kp\cdot K'\} = 2m_a^2 EE'\left(\frac{E+E'}{m_a}\right)\sin^2\frac{\theta}{2} \quad . \qquad (A.4.6)$$

Using (A.4.5) and (A.4.6) we write

$$\overline{\sum_{\lambda,s}}\sum_{\lambda',s'}|M_{\lambda s;\lambda' s'}|^2 = \{(2s_L+1)(2s_Q+1)\}^{-1}\frac{32g^4}{(q^2-M^2)^2}(2m_a^2 EE')\times$$

$$\times\left\{(|g_v|^2+|g_A|^2)(|f_v|^2+|f_A|^2)\left(1+\frac{E-E'}{m_a}\sin^2\frac{\theta}{2}\right)-\frac{m_a'}{m_a}(|g_v|^2+|g_A|^2)\times\right. \qquad (A.4.7)$$

$$\left.\times\,(|f_v|^2-|f_A|^2)\sin^2\frac{\theta}{2}+4\,\mathrm{Re}\,(g_v g_A^*)\,\mathrm{Re}\,(f_v f_A^*)\left(\frac{E+E'}{m_a}\right)\sin^2\frac{\theta}{2}\right\} .$$

The differential cross-section for the process $LQ \to L'Q'$ has the form (see A.1.28)

$$d\sigma^{LQ\to L'a'} = (2\pi)^4\delta^{(4)}(p+q-p')\frac{1}{4EM|\vec{v}_{rel}|}\frac{d^3\vec{p}'}{(2\pi)^3(2E_p')}\frac{d^3\vec{K}'}{(2\pi)^3(2E_{K'})}\overline{\sum_{\lambda s}}\sum_{\lambda' s'}|M_{\lambda s;\lambda' s'}|^2 . \qquad (A.4.7a)$$

Integrating with respect p'' and putting $m_L = m_L' = 0$ we finally get

$$\frac{d^2\sigma^{LQ\to L'a'}}{dE'd\Omega'} = \delta(Q^2-2p\cdot q+m_{a'}^2-m_a^2)\frac{2g^4}{\pi^2(2s_L+1)(2s_Q+1)}\cdot\frac{m_a E'^2}{(Q^2+M^2)^2}\times$$

$$\times\left\{A\cos^2\frac{\theta}{2}+\left[A\left(1+\frac{E-E'}{m_{a'}}\right)-\frac{m_{a'}}{m_a}B+\frac{(E+E')}{m_a}C\right]\sin^2\frac{\theta}{2}\right\} \qquad (A.4.8)$$

with $Q^2 = -q^2$ and

$$A = (|g_v|^2+|g_A|^2)(|f_v|^2+|f_A|^2) \qquad (A.4.9)$$

$$B = (|g_v|^2+|g_A|^2)(|f_v|^2-|f_A|^2) \qquad (A.4.10)$$

$$C = 4\,\mathrm{Re}(g_v g_A^*)\,\mathrm{Re}(f_v f_A^*) \quad . \qquad (A.4.11)$$

In the case in which the interaction is of electromagnetic nature

and L = L' = electron, while Q = Q' = pointlike "proton" of mass M, we get from (A.4.8)

$$\frac{d^2\sigma^{ep\to ep}}{dE'd\Omega} = \delta(Q^2-2p\cdot q)\frac{e^4}{2\pi^2Q^4}\,ME'^2\left\{\cos^2\frac{\theta}{2}+\frac{E-E'}{M}\sin^2\frac{\theta}{2}\right\}$$

or using the variable $\nu = p\cdot q/M$

$$\frac{d^2\sigma^{ep\to ep}}{dE'd\Omega'} = \frac{4\alpha^2}{Q^4}E'^2\left\{\cos^2\frac{\theta}{2}+\left(\frac{Q^2}{4M^2}\right)2\sin^2\frac{\theta}{2}\right\}\delta\left(\frac{Q^2}{2M}-\nu\right). \qquad (A.4.12)$$

In order to find the differential cross-section $\frac{d^2\sigma}{dE'd\Omega'}$ for the process $L\bar{Q}' \to L'\bar{Q}$ we must notice that the spinor $\bar{u}_{Q'}(p',s')$ is replaced by $\bar{v}_{\bar{Q}}(p,s)$ and $u_Q(p,s)$ by $v_{\bar{Q}}(p',s')$. Thus in the course of the calculation the expression $(\not{p}' + m'_Q)$ must be replaced by $(\not{p}-m'_Q)$ and $(\not{p} + m_Q)$ by $(\not{p}' - m_Q)$. The necessary changes in the expression for the matrix element $\overline{\sum_{spin}}|M|^2$ (A.4.4b) are $p \rightleftharpoons p'$ $m_Q \to -m_Q$ and $m'_Q \to -m_Q'$; this has as an effect $A \to A$, $B \to B$ and $C \to -C$ and consequently we have

$$\left.\begin{aligned}\frac{d^2\sigma^{L\bar{Q}'\to L'\bar{Q}}}{dE'd\Omega'} &= \delta(Q^2-2p\cdot q+m_Q^2-m_{Q'}^2)\frac{2g^4}{\pi^2(2s_L+1)(2s_Q+1)}\cdot\frac{m_{Q'}E'^2}{(Q^2+M^2)^2}\times\\ &\times\left\{A\cos^2\frac{\theta}{2}+\left[A\left(1+\frac{E-E'}{m_{Q'}}\right)-\frac{m_Q}{m_{Q'}}B-\frac{(E+E')}{m_{Q'}}C\right]\sin^2\frac{\theta}{2}\right\}.\end{aligned}\right\}(A.4.13)$$

To find the differential cross-section for the process $\bar{L}'Q \to \bar{L}Q'$ we only need to interchange the role of k and k' in (A.4.8) having thus

$$\left.\begin{aligned}\frac{d^2\sigma^{\bar{L}'Q\to\bar{L}Q'}}{dE'd\Omega'} &= \delta(Q^2-2p\cdot q+m_{Q'}^2-m_Q^2)\frac{2g^4}{\pi^2(2s_{L'}+1)(2s_Q+1)}\cdot\frac{m_Q E'^2}{(Q^2+M^2)^2}\times\\ &\times\left\{A\cos^2\frac{\theta}{2}+\left[A\left(1+\frac{E-E'}{m_Q}\right)-\frac{m_{Q'}}{m_Q}B-\frac{(E+E')}{m_Q}C\right]\sin^2\frac{\theta}{2}\right\}.\end{aligned}\right\}(A.4.14)$$

Finally for the process $\bar{L}'\bar{Q}' \to \bar{L}\,\bar{Q}$ we have the interchanges $p \rightleftarrows p'$, $k \rightleftarrows k'$, $m_Q \to -m_Q$, $m_{Q'} \to -m_{Q'}$ and thus

$$\frac{d\sigma^{\bar{L}'\bar{Q}'\to\bar{L}\bar{Q}}}{dE'd\Omega'} = \delta(Q^2 - 2p\cdot q + m_q^2 - m_{q'}^2)\frac{2g^4}{\pi^2(2s_{l'}+1)(2s_{q'}+1)}\cdot\frac{m'_q E'^2}{(Q^2+M^2)^2}\times$$
$$\times\left\{A\cos^2\frac{\theta}{2} + \left[A\left(1+\frac{E-E'}{m_{q'}}\right) - \frac{m_q}{m_{q'}}B + \frac{(E+E')}{m_{q'}}C\right]\sin^2\frac{\theta}{2}\right\} \qquad \text{(A.4.15)}$$

APPENDIX 5

In this appendix we find the cross-sections for the processes $\nu(\bar{\nu}) + \phi_i \to \nu(\bar{\nu}) + \phi_i$ and $\nu(\bar{\nu}) + \bar{\phi}_i \to \nu(\bar{\nu}) + \bar{\phi}_i$ where the interaction Lagrangian is given by (see Chapter II, 2.58).

$$\mathcal{L} = \frac{g}{2\cos\theta_w} Z_\mu \sum_i \bar{\phi}_i \left\{ \left(\frac{n_i}{2} - 2zQ_i \right) - \frac{n_i}{2}\gamma^5 \right\} \gamma^\mu \phi_i \quad . \qquad (A.5.1)$$

$\cos\theta_w$ is the well known Weinberg angle.

The Lagrangian (A.5.1) is useful when calculating cross-sections for neutral current processes. When i = ν (neutrino field) then $n_\nu = 1$ and $Q_\nu = 0$; in order to find the cross sections mentioned above we use the results of the Appendix 4, with the replacements $g \to f = g/2\cos\theta$, $g_A = g_V = 1/2$, $f_V = \frac{n_i}{2} - 2\,z\,Q_i$ and $f_A = \frac{n_i}{2}$.

Thus from (A.4.9), (A.4.10), (A.4.11) we find

$$A_i = \frac{1}{2}\left(\frac{n_i^2}{2} - 2z n_i Q_i + 4z^2 Q_i^2 \right) \qquad (A.5.2)$$

$$B_i = \frac{1}{2}\left(-2z n_i Q_i + 4z^2 Q_i^2 \right) \qquad (A.5.3)$$

$$C_i = \frac{1}{2}\left(\frac{n_i^2}{2} - 2z n_i Q_i \right) \quad . \qquad (A.5.4)$$

If the ϕ_i is a parton carrying fraction x_i of the hadrons momentum then we find† (from A.4.8)

$$\frac{d^2\sigma^{\nu\phi_i \to \nu\phi_i}(x_i)}{dE'd\Omega'} = \delta(x - x_i)\frac{G^2}{2\pi^2}\frac{E'^2}{M}\left\{ 2A_i \frac{xM}{\nu}\cos^2\frac{\theta}{2} + 2\left[A_i + (A_i - B_i)\frac{xM}{\nu} \right]\sin^2\frac{\theta}{2} + \left(\frac{E+E'}{M} \right)\frac{2MC_i}{\nu}\sin^2\frac{\theta}{2} \right\} . \qquad (A.5.5)$$

---

† $x = Q^2/2M\nu$

To derive (A.5.5) use was made of the fact

$$\frac{f^4}{2\pi^2(Q^2+M_z^2)^2} \simeq \frac{G^2}{\pi^2} \tag{A.5.6}$$

which holds as long as $M_z^2 \gg Q^2$.

In the Bjorken limit we have

$$\left.\begin{aligned}\frac{d^2\sigma^{\nu\phi_i\to\nu\phi_i}(x_i)}{dE'd\Omega'} = \delta(x-x_i)\frac{G^2}{2\pi^2}\frac{E'^2}{M}\Big\{ & W_2^{(\nu\phi_i)}\cos^2\frac{\theta}{2} + \\ & + 2W_1^{(\nu\phi_i)}\sin^2\frac{\theta}{2} - W_3^{(\nu\phi_i)}\left(\frac{E+E'}{M}\right)\sin^2\frac{\theta}{2}\Big\}\end{aligned}\right\} \tag{A.5.7}$$

where the "structure functions" $W_{1,2,3}^{(\nu\phi i)}$ are given by the relations

$$W_1^{(\nu\phi_i)} = A_i\,\delta\left(\frac{Q^2}{2M\nu} - x_i\right) \tag{A.5.8}$$

$$\frac{\nu W_2^{(\nu\phi_i)}}{M} = 2A_i\,\delta\left(\frac{Q^2}{2M\nu} - x_i\right)x_i \tag{A.5.9}$$

$$\frac{\nu W_3^{(\nu\phi_i)}}{M} = -2C_i\,\delta\left(\frac{Q^2}{2M\nu} - x_i\right) \tag{A.5.10}$$

For the process $\nu\bar{\phi}_i \to \nu\bar{\phi}_i$ we use (A.4.13) and find

$$W_{1,2}^{(\nu\bar{\phi}_i)} = W_{1,2}^{(\nu\phi_i)}, \quad W_3^{(\nu\bar{\phi}_i)} = -W_3^{(\nu\phi_i)}. \tag{A.5.11}$$

For antineutrinos by virtue of (A.4.14) we have

$$\left.\begin{aligned}\frac{d^2\sigma^{\bar{\nu}\phi_i\to\bar{\nu}\phi_i}(x_i)}{dE'd\Omega'} = \delta(x-x_i)\frac{G^2}{2\pi^2}\frac{E'^2}{M}\Big\{ & W_2^{(\bar{\nu}\phi_i)}\cos^2\frac{\theta}{2} + \\ & + 2W_1^{(\bar{\nu}\phi_i)}\sin^2\frac{\theta}{2} + W_3^{(\bar{\nu}\phi_i)}\left(\frac{E+E'}{M}\right)\sin^2\frac{\theta}{2}\Big\}\end{aligned}\right\} \tag{A.5.12}$$

with

$$W_{1,2,3}^{(\bar{\nu}\phi_i)} = W_{1,2,3}^{(\nu\phi_i)} \tag{A.5.13}$$

For the case $\bar{\nu}\,\bar{\phi}_i \to \bar{\nu}\,\bar{\phi}_i$ (A.5.12) holds but with

$$W_{1,2}^{(\bar{\nu}\bar{\phi}_i)} = W_{1,2}^{(\bar{\nu}\phi_i)}, \quad W_3^{(\bar{\nu}\bar{\phi}_i)} = -W_3^{(\bar{\nu}\phi_i)} \quad . \tag{A.5.14}$$

It is obvious now that for the neutral current processes† $\nu h \to \nu X$ and $\bar{\nu} h \to \bar{\nu} X$ we have

$$\frac{d^2\sigma^{(\nu h,\bar{\nu}h)}}{dE'd\Omega'} = \frac{G^2}{2\pi^2}\frac{E'^2}{M}\left\{ W_2^{(\nu h,\bar{\nu}h)} \cos^2\frac{\theta}{2} + 2W_1^{(\nu h,\bar{\nu}h)} \sin^2\frac{\theta}{2} \mp W_3^{(\nu h,\bar{\nu}h)} \left(\frac{E+E'}{M}\right) \sin^2\frac{\theta}{2} \right\} \tag{A.5.15}$$

where the structure functions $W_{1,2,3}$ are given by

$$W_1^{(\nu h,\bar{\nu}h)} \equiv F_1^{(\nu h,\bar{\nu}h)}(x) = \sum_i f_i^{(h)}(x)\, A_i \tag{A.5.16}$$

$$\frac{\nu W_2^{(\nu h,\bar{\nu}h)}}{M} \equiv F_2^{(\nu h,\bar{\nu}h)}(x) = 2x \sum_i f_i^{(h)}(x)\, A_i \tag{A.5.17}$$

$$\frac{\nu W_3^{(\nu h,\bar{\nu}h)}}{M} \equiv F_3^{(\nu h,\bar{\nu}h)}(x) = -2 \sum_i \xi_i f_i^{(h)}(x)\, C_i \quad . \tag{A.5.18}$$

To derive (A.5.15 - A.5.18) parton model techniques were used. The - (+) sign in (A.5.15) stands for neutrinos (antineutrinos); The ξ_i in (A.5.18) is either +1 or -1 for parton and antiparton respectively. The constants A^i and C^i, when i = antiparton, are the same as those for the corresponding parton; that is $A^{\bar{i}} = A^i$, $C^{\bar{i}} = C^i$.

---

† "h" is either a proton or neutron.

APPENDIX 6

The differential cross-sections $\frac{d\sigma}{dy}^{CC,NC}(\nu,\bar{\nu})$ (see Ch. III, 3.30) are given by the following expression

$$\frac{d\sigma}{dy}^{CC,NC}(\nu,\bar{\nu}) = \frac{G^2 ME}{\pi}\left\{(1-y)^2\, a^{CC,NC}(\nu,\bar{\nu}) + b^{CC,NC}(\nu,\bar{\nu})\right\} \qquad (A.6.1)$$

with

$$a^{CC,NC}(\nu,\bar{\nu}) = \int_0^1 \left(F_1^{CC,NC} \pm \frac{F_3^{CC,NC}}{2}\right) dx \qquad (A.6.2)$$

$$b^{CC,NC}(\nu,\bar{\nu}) = \int_0^1 \left(F_1^{CC,NC} \mp \frac{F_3^{CC,NC}}{2}\right) dx \quad . \qquad (A.6.3)$$

In Eq. (A.6.2) the + is for neutrinos and - for antineutrinos. In Eq. (A.6.3) the role of $\pm$ sign is interchanged.

We assume that there are only four constituent quarks, namely p, n, λ and p'.

In this case the constants a^{CC}, b^{CC} are given, for the two cases of above and below charm production threshold, by the following expressions

Above charm threshold

$$\begin{cases} a^{cc}(\nu) = b^{cc}(\bar{\nu}) = 4c & (A.6.4) \\ b^{cc}(\nu) = a^{cc}(\bar{\nu}) = 3u + 4c & (A.6.5) \end{cases}$$

Below charm threshold

$$\begin{cases} a^{cc}(\nu) = b^{cc}(\bar{\nu}) = 2c & (A.6.6) \\ b^{cc}(\nu) = a^{cc}(\bar{\nu}) = 3u + 2c \quad . & (A.6.7) \end{cases}$$

The constants υ and c are defined by $\upsilon = \int_0^1 x\upsilon(x)dx$ and $c = \int_0^1 xc(x)dx$ where $\upsilon(x)$ and $c(x)$ are the valence and core distribution functions respectively. From Eq. (A.6.1) and (A.6.4 - A.6.7)we have

Above charm threshold

$$\sigma^{cc}(\nu) = \frac{G^2ME}{\pi}\left(3\upsilon+\frac{16}{3}c\right) \tag{A.6.8}$$

$$\sigma^{cc}(\bar{\nu}) = \frac{G^2ME}{\pi}\left(\upsilon+\frac{16}{3}c\right) \tag{A.6.9}$$

$$R \equiv \frac{\sigma^{cc}(\bar{\nu})}{\sigma^{cc}(\nu)} = \frac{\left(\upsilon+\frac{16}{3}c\right)}{\left(3\upsilon+\frac{16}{3}c\right)} \tag{A.6.10}$$

Below charm threshold

$$\sigma^{cc}(\nu) = \frac{G^2ME}{\pi}\left(3\upsilon+\frac{8}{3}c\right) \tag{A.6.11}$$

$$\sigma^{cc}(\bar{\nu}) = \frac{G^2ME}{\pi}\left(\upsilon+\frac{8}{3}c\right) \tag{A.6.12}$$

$$R \equiv \frac{\sigma^{cc}(\bar{\nu})}{\sigma^{cc}(\nu)} = \frac{\left(\upsilon+\frac{8}{3}c\right)}{\left(3\upsilon+\frac{8}{3}c\right)} . \tag{A.6.13}$$

For the quantities $\langle xy\rangle_{\nu,\bar{\nu}}$ we have:

$$\frac{d^2\sigma^{cc}(\nu,\bar{\nu})}{dx\,dy} = \frac{G^2ME}{\pi}x\left\{(1-y)^2\left(F_1 \pm \frac{F_3}{2}\right)^{cc} + \left(F_1 \mp \frac{F_3}{2}\right)^{cc}\right\} . \tag{A.6.14}$$

From (A.6.14) we have

$$\left.\int_0^1 dx\,dy\; xy\;\frac{d^2\sigma^{cc}(\nu,\bar{\nu})}{dx\,dy} = \frac{G^2ME}{\pi}\int_0^1 dx\; x^2\left\{\frac{1}{12}\left(F_1 \pm \frac{F_3}{2}\right)^{cc} + \frac{1}{2}\left(F_1 \mp \frac{F_3}{2}\right)\right\}.\right\} \tag{A.6.15}$$

Equation (A.6.15) yields

$$\int_0^1 dx\,dy\; xy\;\frac{d^2\sigma^{cc}(\nu)}{dx\,dy} = \frac{G^2ME}{\pi}\left(\frac{3}{2}\upsilon' + \frac{7}{3}c'\right) \tag{A.6.16a}$$

$$\int_0^1 dx\,dy\; xy\; \frac{d^2\sigma^{cc}(\bar{\nu})}{dx\,dy} = \frac{G^2ME}{\pi}\left(\frac{1}{4}v' + \frac{7}{3}c'\right). \qquad \text{(A.6.16b)}$$

The expressions (A.6.16a - A.6.16b) are valid when we are above the charm production threshold. For the below the charm production threshold $\frac{7}{3}c'$ should be replaced by $\frac{7}{6}c'$. The constants v' and c' are defined as $v' = \int_0^1 x^2 v(x)dx$, $c' = \int_0^1 x^2 c(x)dx$.

Thus for the quantities $\langle xy\rangle_{\nu,\bar{\nu}}$ we have

Above charm threshold

$$\begin{cases} \langle xy\rangle_\nu = (9v'+14c')/(18v+32c) & \text{(A.6.17)} \\ \langle xy\rangle_{\bar{\nu}} = (3v'+28c')/(12v+64c) & \text{(A.6.18)} \end{cases}$$

Below charm threshold

$$\begin{cases} \langle xy\rangle_\nu = (9v'+7c')/(18v+16c) & \text{(A.6.19)} \\ \langle xy\rangle_{\bar{\nu}} = (3v'+14c')/(12v+32c). & \text{(A.6.20)} \end{cases}$$

(a) Kuti-Weisskopf Quark Parton Model

In the Kuti-Weisskopf quark parton model

$$v(x) = \frac{\Gamma(9/2)}{\Gamma(1/2)\Gamma(4)}\, x^{-1/2}(1-x)^3, \quad c(x) = G_g\, x^{-1}(1-x)^{7/2}. \qquad \text{(A.6.21)}$$

The constant Gg has the value $G_g = 1/10$. Using the integral expression

$$\int_0^1 x^\nu (1-x)^\mu dx = \frac{\Gamma(\mu+1)\Gamma(\nu+1)}{\Gamma(\mu+\nu+2)}, \quad (\mathrm{Re}(\mu+1), \mathrm{Re}(\nu+1) > 0) \qquad \text{(A.6.22)}$$

(see 3.191(1) in "Table of Integrals Series and Products" by I.S. Gradshteyn, I.M. Ryzhik [Academic Press 1965]) we find for the

v, v', c, c'

$$v = \frac{1}{9} \quad , \quad v' = \frac{1}{33} \tag{A.6.23a}$$

$$c = G_g \frac{2}{9} = \frac{1}{45} \, , \quad c' = G_g \frac{4}{99} = \frac{2}{495} \, . \tag{A.6.23b}$$

Using Eqs. (A.6.8) to (A.6.13) and (A.6.17) to (A.6.20) we find

$$\left.\begin{aligned} &\sigma^{cc}(\nu) = \frac{G^2 ME}{\pi} .45 \, , \quad \sigma^{cc}(\bar{\nu}) = \frac{G^2 ME}{\pi} .23 \\ &R = .51 \, , \quad \langle xy \rangle_\nu = .120 \, , \quad \langle xy \rangle_{\bar{\nu}} = .074 \end{aligned}\right\} \tag{A.6.24}$$

$$\left.\begin{aligned} &\sigma^{cc}(\nu) = \frac{G^2 ME}{\pi} .39 \, , \quad \sigma^{cc}(\bar{\nu}) = \frac{G^2 ME}{\pi} .17 \\ &R = .43 \, , \quad \langle xy \rangle_\nu = .128 \, , \quad \langle xy \rangle_{\bar{\nu}} = .070 \, . \end{aligned}\right\} \tag{A.6.25}$$

Eqs. (A.6.24) and (A.6.25) correspond to the two cases of above and below charm production threshold respectively.

(b) Modified R.Mc.Elhaney-S.F.Tuan Model (Chapter III, section 2B)

In this part we give the expressions for the moments $V = \int_0^1 xV(x)dx$, $V' = \int_0^1 x^2 V(x)dx$, $C = \int_0^1 xc(x)\,dx$ and $C' = \int_0^1 x^2 c(x)dx$, which are used in calculating the physical quantities given in Table X and XI of the main text.

The function $V(x)$ is given by the expression

$$V(x) = \frac{1}{3}\left(2v(x) + d(x)\right) \tag{A.6.26}$$

where (see Chapter III, Eqs.(3.44))

$$v(x) = \lambda v_1(x) + (1-\lambda) v_2(x) \tag{A.6.27}$$

$$d(x) = \lambda d_1(x) + (1-\lambda) d_2(x) \tag{A.6.28}$$

$$c(x) = \lambda c_1(x) + (1-\lambda) c_2(x) \, . \tag{A.6.29}$$

The functions υ_1, d_1, c_1 are given by Eqs. (3.43) for $\alpha(o) = {}^1/_2$, $\gamma = 3$; υ_2, d_2, c_2 are given by the same expressions but with $\alpha(o) = 0$, $\gamma = 2$. Using (A.6.22) we find†

$$V = \frac{7}{6}\left\{\lambda \frac{t}{5+t} + (1-\lambda)\frac{t'}{5+t'}\right\} \tag{A.6.30}$$

$$C = G_g\left\{\lambda \frac{1}{4+t} + (1-\lambda)\frac{1}{4+t'}\right\} \tag{A.6.31}$$

$$V' = \frac{4}{3}\left\{\lambda \frac{t(1+t)}{(5+t)(6+t)} + (1-\lambda)\frac{t'(1+t')}{(5+t')(6+t')}\right\} \tag{A.6.32}$$

$$C' = G_g\left\{\lambda \frac{1}{(4+t)(5+t)} + (1-\lambda)\frac{1}{(4+t')(5+t')}\right\}. \tag{A.6.33}$$

For $t = {}^1/_2$ and $t' = 1$ we have

$$V = \frac{7}{6}\,\frac{11-5\lambda}{66}\,, \quad C = G_g\,\frac{9+\lambda}{45} \tag{A.6.34}$$

$$V' = \frac{4}{3}\,\frac{143-80\lambda}{3003}\,, \quad C' = G_g\,\frac{33+7\lambda}{990} \tag{A.6.35}$$

---

† $t = 1 - \alpha_1(0)$ and $t' = 1-\alpha_2(0)$ with $\alpha_1(0) = 1/2$, $\alpha_2(0) = 0$

APPENDIX 7

From the Eq. (3.53a) we find for the cross-section $\frac{d\sigma}{dQ^2}$ regarding the process $p + p \to \mu^- \mu^+ + X$

$$\frac{d\sigma}{dQ^2} = \frac{4\pi\alpha^2}{3}\frac{\tau}{Q^4}\int_0^1 dx\,dy\;\delta(xy-\tau)F(x)c(y) \qquad (A.7.1)$$

with,

$$F(x) \equiv \frac{8}{9}u(x) + \frac{1}{9}d(x) + \frac{10}{9}c(x)$$

and,

$$u(x) = \frac{9\lambda}{8}B^{-1}\left(\tfrac{1}{2},4\right)x^{-1/2}(1-x)^3\left\{1-\frac{1}{8}(1-x)\right\} + (1-\lambda)B^{-1}(1,5)\left\{1-\frac{1}{4}(1-x)\right\}(1-x)^3 \qquad (A.7.2)$$

$$d(x) = \frac{9\lambda}{8}B^{-1}\left(\tfrac{1}{2},4\right)x^{-1/2}(1-x)^4 + (1-\lambda)B^{-1}(1,5)(1-x)^4 \qquad (A.7.3)$$

$$c(x) = G_2\left\{\lambda x^{-1}(1-x)^{7/2} + (1-\lambda)x^{-1}(1-x)^4\right\} \qquad (A.7.4)$$

($u(x)$, $d(x)$, and $c(x)$ can be found in Chapter III, Eqs 3.44a-3.44c).

Using the fact that,

$$\int_0^1 dx \int_0^1 dy\; F(x)c(y)\delta(xy-\tau) = \int_\tau^1 \frac{dx}{x}F(x)c\left(\frac{\tau}{x}\right) \qquad (A.7.5)$$

we get†

$$\tau\int_0^1 dx\int_0^1 dy\; F(x)c(y)\delta(xy-\tau) =$$

---

† $G' = \frac{10}{9}G$

$$\frac{9}{10}\Bigg\{\frac{\lambda^2 G'}{B(\frac{1}{2},4)}\int_\tau^1 dx\, x^{-4}(1-x)^3(x-\tau)^{7/2}+\frac{8}{9}\frac{\lambda(1-\lambda)G'}{B(1,5)}\times$$

$$\times\int_\tau^1 dx\, x^{-7/2}(1-x)^3(x-\tau)^{7/2}-\frac{\lambda(1-\lambda)G'}{9B(1,5)}\int_\tau^1 dx\, x^{-7/2}(1-x)^4(x-\tau)^{7/2}+$$

$$+\lambda^2 G'^2\int_\tau^1 dx\, x^{-7/2}(1-x)^{7/2}(x-\tau)^{7/2}+\lambda(1-\lambda)G'^2\int_\tau^1 dx\, x^{-9/2}(1-x)^4(x-\tau)^{7/2}+$$

$$+\frac{\lambda(1-\lambda)G'}{B(\frac{1}{2},4)}\int_\tau^1 dx\, x^{-9/2}(1-x)^4(x-\tau)^4+\frac{8}{9}\frac{(1-\lambda)^2 G'}{B(1,5)}\times$$

$$\times\int_\tau^1 dx\, x^{-4}(1-x)^3(x-\tau)^4-\frac{(1-\lambda)^2 G'}{9B(1,5)}\int_\tau^1 dx\, x^{-4}(1-x)^4(x-\tau)^4+$$

$$+\lambda(1-\lambda)G'^2\int_\tau^1 dx\, x^{-5}(1-x)^{7/2}(x-\tau)^4+(1-\lambda)^2 G'^2\times$$

$$\times\int_\tau^1 dx\, x^{-5}(1-x)^4(x-\tau)^4\Bigg\}\ . \qquad \text{(A.7.6)}$$

It is obvious that we need to calculate the integral having the following general form

$$I(\nu;\mu;\sigma)\overset{def}{\equiv}\int_\tau^1 dx\, x^{-\nu}(1-x)^\mu(x-\tau)^\sigma \qquad \text{(A.7.7)}$$

By changing the variable of integration x as

$$x=(1-\tau)(1-z)+\tau \qquad \text{(A.7.8)}$$

we get,

$$I(\nu;\mu;\sigma)=(1-\tau)^{\sigma+\mu+1}\int_0^1 dz\, z^\mu(1-z)^\sigma(1-\alpha z)^{-\nu} \qquad \text{(A.7.9)}$$

with $\alpha = 1-\tau$. Because $|\alpha| = |1-\tau| = 1-\tau < 1$ we have for the integral above (see 3.197 (3) in "Table of Integrals,Series and Products" by I.S. Grandshteyn, I.M. Ryzhik [Academic Press 1965])

$$\left.\begin{aligned}\int_0^1 dz\, z^{\mu}(1-z)^{\sigma}(1-\alpha z)^{-\nu} &= B(\mu+1,\sigma+1)\times \\ \times F(\nu,\mu+1;\mu+\sigma+2;\alpha) &\quad \text{for } \mathrm{Re}(\mu+1),(\nu+1)>0,|\alpha|<1\end{aligned}\right\} \text{(A. 7.10)}.$$

So for the $I(\nu;\mu;\sigma)$ we have

$$I(\nu;\mu;\sigma) = (1-\tau)^{\sigma+\mu+1} B(\sigma+1,\mu+1) F(\nu,\mu+1;\mu+\sigma+2;1-\tau). \quad \text{(A. 7.11)}$$

The function F(...) appearing in Eqs. (A.7.10) and (A.7.11) is well-known Hypergeometric function. For the values $\lambda = .624$ and $G = .0407$ we get

$$Q^4 \frac{d\sigma}{dQ^2} = \frac{4\pi\alpha^2}{3} (9. \times 10^{-7}) \times$$

$$\times \Big\{ 95.748\, G(4;3;\tfrac{7}{2};\tau) + 234.442\, G(\tfrac{7}{2};3;\tfrac{7}{2};\tau) -$$

$$- 13.782\, G(\tfrac{7}{2};4;\tfrac{7}{2};\tau) + 2.670\, G(\tfrac{9}{2};\tfrac{7}{2};\tfrac{7}{2};\tau) +$$

$$+ 1.122\, G(\tfrac{9}{2};4;\tfrac{7}{2};\tau) + 41.434\, G(\tfrac{9}{2};3;4;\tau) +$$

$$+ 101.445\, G(4;3;4;\tau) - 5.636\, G(4;4;4;\tau) +$$

$$+ 1.122\, G(5;\tfrac{7}{2};4;\tau) + .4586\, G(5;4;4;\tau) \Big\}. \quad \text{(A. 7.12)}$$

The function $G(a;b;c;\tau)$ appearing in (A.7.12) is defined as

$$G(a;b;c;\tau) \overset{\text{def.}}{\equiv} (1-\tau)^{b+c+1} F(a;b+1;b+c+2;1-\tau). \quad \text{(A. 7.13)}$$

APPENDIX 8

In this appendix we calculate the basic formulae given in Chapter V.

8a)

In this part we calculate the cross-sections $\frac{d^2\sigma}{dp'd\cos\theta'}$ $\sigma(e^-e^+ \to \phi\bar{\phi})$, regarding the process $e^-e^+ \to \phi\bar{\phi}$, where p' is the magnitude of the ϕ's momentum and θ its scattering angle in the e^-e^+ center of mass system. The interaction Lagrangian is assumed to be $\mathcal{L} = f(\bar{e}\phi X + h.c)$ or $\mathcal{L} = f(\bar{e}\gamma^\mu\phi X_\mu + h.c)$.

The Born term for this process is shown below (Fig. 2A)

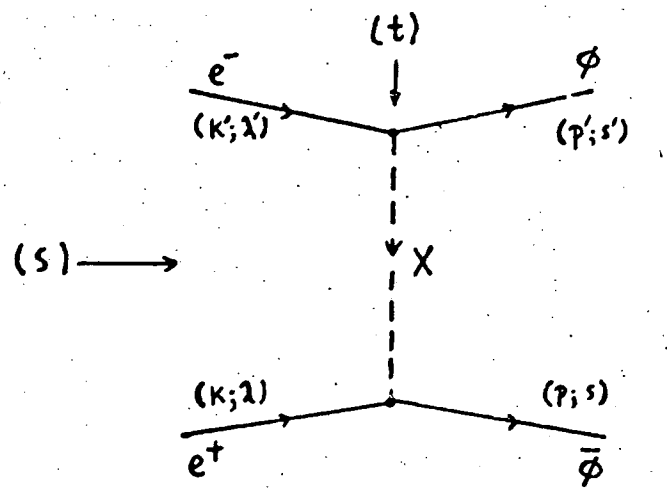

FIGURE 2A. Kinematics of the process $e^-e^+ \to$ gluon + antigluon.

When the interaction Lagrangian is $\mathcal{L} = f(\bar{e}\phi X + h.c.)$ then the scattering amplitude corresponding to this diagram is

$$T_{\lambda\lambda';ss'} = -i(2\pi)^4 \int \delta^{(4)}(k+k'-p-p') \frac{\bar{u}(p',s')u_e(k',\lambda')\bar{v}_e(k,\lambda)v(p,s)}{(q^2-M_X^2)} \quad (A.8.1)$$

The momenta and spins are labelled in Fig. 2A. Summing over the final and averaging over the initial spins yields†

$(t = q^2 = (p' - K')^2)$

$$\overline{\sum_{spins}} |T_{\lambda\lambda';ss'}|^2 = (2\pi)^8 \delta^{(4)}(0)\, \delta^{(4)}(K+K'-p-p') f^4 \left(\frac{t}{t-M_x^2}\right)^2 . \qquad (A.8.2)$$

Thus according to (A.1.28)

$$|M|^2 = f^4 \left(\frac{t}{t-M_x^2}\right)^2 . \qquad (A.8.3)$$

From the Eq. (A.1.28) we have

$$d\sigma = (2\pi)^{-2} \delta^{(4)}(p+p'-K-K') \frac{|M|^2}{4E_1E_2|\vec{v}_{rel}|} \delta^{(+)}(p^2-m^2)\delta^{(+)}(p'^2-m'^2) d^4p d^4p' \qquad (A.8.4)$$

where m is the mass of the ϕ-particle.

Performing the integration over p and taking into account the fact that $4E_1E_2|\vec{v}_{rel}| = 2s$, $(s \equiv (K + K')^2)$, we get

$$d\sigma = \frac{(2\pi)^{-1}}{16s} \delta\left(\frac{\sqrt{s}}{2} - p'\right) f^4 \left(\frac{t}{t-M_x^2}\right)^2 dp' d\cos\theta \qquad (A.8.5)$$

and from this

$$p' \frac{d^2\sigma}{dp' d\cos\theta} = f^4 \frac{(2\pi)^{-1}}{32\sqrt{s}} \delta\left(\frac{\sqrt{s}}{2} - p'\right) \left(\frac{t}{t-M_x^2}\right)^2 . \qquad (A.8.6)$$

---

† All masses have been put equal to zero since we are working in the high energy region.

The mass M_x is assumed to be very large. For large "s" such that $s \ll M_x^2$ we have from (A.8.6)

$$p' \frac{d^2\sigma}{dp'd\cos\theta} = g^2 \frac{(2\pi)^{-1}}{32\sqrt{s}} \delta\left(\frac{\sqrt{s}}{2} - p'\right) \frac{s^2}{4}(1-\cos\theta)^2 \qquad \text{(A.8.7)}$$

where $g = (f/M_x)^2$.

By integrating (A.8.7) with respect p' and $\cos\theta$ we get for the total cross section $\sigma(e^-e^+ \to \phi\bar{\phi})$

$$\sigma(e^-e^+ \to \phi\bar{\phi}) = \frac{g^2}{48\pi} s \qquad \text{(A.8.8)}$$

Eq. (A.8.8) is valid for large s but $s \ll M_x^2$. For energies such that $s \gg M_x^2$ Eq. (A.8.7) yields

$$\sigma(e^-e^+ \to \phi\bar{\phi}) = \frac{f^4}{16\pi s} \qquad \text{(A.8.9)}$$

We now examine the case in which the interaction Lagrangian has the form $\mathcal{L} = f(\bar{e}\gamma^\mu \phi X_\mu + h.c)$. In this case the scattering amplitude is

$$T_{\lambda\lambda';ss'} = +i(2\pi)^4 f^2 \delta^{(4)}(K+K'-p-p') \frac{\left(g^{\mu\nu} - \frac{q^\mu q^\nu}{M_x^2}\right)}{(q^2 - M_x^2)} \times$$
$$\times \bar{u}(p',s')\gamma_\mu u_e(K',\lambda')\, \bar{v}_e(K,\lambda)\gamma_\nu v(p,s) \,. \qquad \text{(A.8.10)}$$

Summing over the final and averaging over the initial spins† yields

$$\overline{\sum_{\text{spins}}} |T_{\lambda\lambda';ss'}|^2 = (2\pi)^8 \delta^{(4)}(0)\delta^{(4)}(K+K'-p-p') \frac{f^4 s^2}{2(t-M_x^2)^2} \times$$
$$\times \left[4 + (1+\cos\theta)^2\right]^2 \,. \qquad \text{(A.8.11)}$$

---

† See footnote of page 156 .

Thus according to (A.1.28)

$$|M|^2 = \frac{f^4 s^2}{2(t-M_x^2)^2}\left[4+(1+\cos\theta)^2\right] \qquad (A.8.12)$$

and consequently

$$p'\frac{d^2\sigma}{dp'd\cos\theta} = \frac{(2\pi)^{-1}}{32\sqrt{s}}\delta\left(\frac{\sqrt{s}}{2}-p'\right)\frac{f^4 s^2}{2}\frac{\left[4+(1+\cos\theta)^2\right]}{(t-M_x^2)^2}\,. \qquad (A.8.13)$$

For large s, but $s \ll M_x^2$, we have

$$p'\frac{d^2\sigma}{dp'd\cos\theta} = g^2\frac{(2\pi)^{-1}}{32\sqrt{s}}\delta\left(\frac{\sqrt{s}}{2}-p'\right)\frac{s^2}{2}\left(5+2\cos\theta+\cos^2\theta\right) \qquad (A.8.14)$$

where g is given by $g = (f/M_x)^2$.

For the cross-section $\sigma(e^-e^+ \to \phi\bar{\phi})$ we find

$$\sigma(e^-e^+\to\phi\bar{\phi}) = \frac{g^2}{6\pi}s \qquad (A.8.15)$$

for large s.

The contribution of this cross-section to the quantity $R = \sigma(e^-e^+ \to \text{Hadrons})/\sigma(e^-e^+ \to \mu^-\mu^+)$ is such that it gives

$$R = \frac{1}{2}\sum_i Q_i^2 + 2\left(\frac{g}{e^2}\right)^2 s^2\,. \qquad (A.8.16)$$

For large s, such that $s \gg M^2$, we have

$$\sigma(e^-e^+\to\phi\bar{\phi}) = \frac{f^4}{4\pi M_x^2} \qquad (A.8.17)$$

from which

$$R = \frac{1}{2}\sum_i Q_i^2 + 3\left(\frac{f^4}{e^4}\right)\frac{s}{M_X^2} \quad . \qquad \text{(A.8.18)}$$

8b)

Formulae for the differential cross-section $\frac{d\sigma}{dE'\,d\underline{o}'}$ associated with the process $e^-\bar{\phi} \to e^-\bar{\phi}$ are calculated in this part; E' and $\underline{o}'$ is the energy and the scattering angle of the outgoing electron. The Lagrangian interactions assumed are those of the previous section of this Appendix.

The Feynman graphs for the two processes $e^-\phi \to e^-\phi$ and $e^-\bar{\phi} \to e^-\bar{\phi}$ are shown in Fig. 3A .

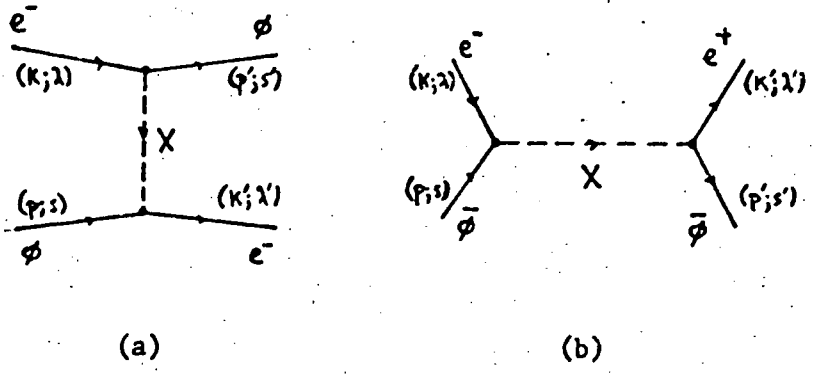

(a) (b)

FIGURE 3A. a) Kinematics of the process e^-+gluon $\to$ e^-+gluon.

b) Kinematics of the process e^-+antigluon $\to$ e^-+antigluon.

When the interaction Lagrangian has the form $\mathcal{L} = f(\bar{e}\,\phi\,X + h.c.)$ then the matrix element for the process $e^-\phi \to e^-\phi$ is given by

$$T^{\phi}_{\lambda s;\lambda' s'} = -i(2\pi)^4 f^2 \delta^{(4)}(K+p-K'-p')\,\frac{\bar{u}(p';s')u_e(K,\lambda)\,\bar{v}(p;s)v_e(K';\lambda')}{(\underset{\sim}{q}^2 - M_X^2)} \quad . \qquad \text{(A.8.19)}$$

From this we have in the usual way

$$\overline{\sum_{\text{spins}}} \left| T^{\phi}_{\lambda_j \lambda_{s'}} \right|^2 = (2\pi)^8 \delta^{(4)}(0) \delta^{(4)}(K - p' + \underset{\sim}{q}) \int^4 \frac{4(p'K)(pK')}{(\underset{\sim}{q}^2 - M_x^2)^2} \quad . \quad (A.8.20)$$

In Eqs. (A.8.19), (A.8.20), $\underset{\sim}{q}$ denotes the momentum transfer $\underset{\sim}{q} = p - K' = p' - K$.

In order to apply parton model techniques we need the differential cross section $\frac{d^2\sigma(xi)}{dE'\,d\underline{o}'}$ when ϕ (or $\bar{\phi}$) carries fraction x_i of proton's momentum. In the course of the derivation we omit all lepton masses ($m_e = 0$). Putting $p_i = x_i p$ we have for the amplitude† $|M^{\phi}|^2$ (see A.1.28)

$$|M^{\phi}(x_i)|^2 = 4g^2 x_i \, MEE' \left\{ M x_i + \left(\frac{Q^2}{Mx} - 2E \right) \sin^2 \frac{\theta}{2} \right\} \quad . \quad (A.8.21)$$

In (A.8.21) "x" denotes the variable $x = \frac{Q^2}{2Mv}$.

The differential cross-section $d\sigma(x_i)$ is written as follows (A.1.28)

$$d\sigma(x_i) = \frac{(2\pi)^2 \delta^{(4)}(K + p - K' - p')}{4EMx_i} \frac{d^3\vec{K}'}{(2\pi)^3 (2E')} |M^{\phi}(x_i)|^2 d^4p' \delta^{(+)}(p'^2 - m^2) \quad . \quad (A.8.22)$$

Integrating upon d^4p' we get

$$\frac{d^2\sigma(x_i)}{dE'd\Omega'} = \frac{4\alpha^2}{Q^4} \frac{E'^2}{M} \left\{ \frac{Q^2}{8EE'} \frac{|M^{\phi}(x)|^2}{e^4} \right\} \delta(x - x_i) \quad . \quad (A.8.23)$$

---

† We assume $Q^2 \ll M_x^2$

In the expression (A.8.23) "α" denotes the hyperfine structure constant $\alpha = \frac{e^2}{4\pi}$.

Replacing $|M^{\phi}(x)|^2$ (from A.8.21) in the expression (A.8.23) we have

$$\frac{d^2\sigma(x_i)}{dE'd\Omega'} = \frac{4\alpha^2}{Q^4}\frac{E'}{M}\delta(x-x_i)\left(\frac{g}{e^2}\right)^2\left\{\frac{M}{\nu}\left(\frac{Q^4x}{4}\right)\cos^2\frac{\theta}{2} + \right.$$
$$\left. + \frac{Q^2}{2}\left(\frac{x^2M^2}{2} - xME + \frac{Q^2}{2}\right)2\sin^2\frac{\theta}{2}\right\} . \quad \text{(A.8.24)}$$

The amplitude $|M^{\bar{\phi}}(x)|^2$ for the process $e^- \bar{\phi} \to e^- \bar{\phi}$ is given by

$$|M^{\bar{\phi}}(x_i)|^2 = 4g^2 x_i MEE'\left\{Mx_i + 2E\sin^2\frac{\theta}{2}\right\} . \quad \text{(A.8.25)}$$

In the case in which the interaction Lagrangian is $\mathcal{L} = f[\bar{e}\gamma^{\mu}\phi X_{\mu} + h.c]$ we get for the amplitudes $|M^{\phi}(xi)|^2$ and $|M^{\bar{\phi}}(xi)|^2$

$$|M^{\phi}(x_i)|^2 = 8g^2 x_i MEE'\left\{Mx_i + \left(E + \frac{Q^2}{2Mx} + Mx_i\right)2\sin^2\frac{\theta}{2}\right\} \quad \text{(A.8.26)}$$

$$|M^{\bar{\phi}}(x_i)|^2 = 8g^2 x_i MEE'\left\{Mx_i + \left(-2E + \frac{3Q^2}{2Mx} + Mx_i\right)2\sin^2\frac{\theta}{2}\right\} . \quad \text{(A.8.27)}$$

It is a straightforward calculation to show that

$$\frac{d\sigma^{\bar{e}\psi\to\bar{e}\psi}(x_i)}{dE'd\Omega'} = \frac{4\pi\alpha^2}{Q^4}\frac{E'}{M}\left\{2A^{\psi}\sin^2\frac{\theta}{2} + B^{\psi}\cos^2\frac{\theta}{2}\right\}\delta(x-x_i) . \quad \text{(A.8.28)}$$

In (A.8.28) the symbol "ψ" denotes either a ϕ or a $\bar{\phi}$ particle and the functions A^{ψ}, B^{ψ} are given by the following expressions

$$(S): \quad A^{\phi} = \frac{Q^2}{2}\left(\frac{g^2}{e^4}\right)\left(\frac{x^2M^2}{2} - xME + \frac{Q^2}{2}\right) \tag{A.8.29}$$

$$(V): \quad A^{\phi} = Q^2\left(\frac{g^2}{e^4}\right)\left(\frac{3x^2M^2}{2} + xME + \frac{Q^2}{2}\right) \tag{A.8.30}$$

$$(S): \quad A^{\bar{\phi}} = \frac{Q^2}{2}\left(\frac{g^2}{e^4}\right)\left(\frac{x^2M^2}{2} + xME\right) \tag{A.8.31}$$

$$(V): \quad A^{\bar{\phi}} = Q^2\left(\frac{g^2}{e^4}\right)\left(\frac{3x^2M^2}{2} - xME + Q^2\right) \tag{A.8.32}$$

$$(S): \quad B^{\phi} = B^{\bar{\phi}} = \left(\frac{g^2}{e^4}\right)\frac{Q^4x}{4}\frac{M}{\nu} \tag{A.8.33}$$

$$(V): \quad B^{\phi} = B^{\bar{\phi}} = \left(\frac{g^2}{e^4}\right)\frac{Q^4x}{2}\frac{M}{\nu} \quad . \tag{A.8.34}$$

In the expressions (A.8.29) - (A.8.34) the (S) and (V) denote the two cases in which the interaction Lagrangian is $\mathcal{L} = f(\bar{e}\phi X + h.c)$ and $\mathcal{L} = f(\bar{e}\gamma^{\mu}\phi X_{\mu} + h.c)$ respectively.

8c)

The differential cross-section $\frac{d\sigma}{dQ^2}(\phi\bar{\phi} \to \mu^-\mu^+)$ is calculated in this section where Q^2 is the mass of the $\mu^-\mu^+$ pair. This cross-section is of interest because it is applied when considering the process $p + p \to \mu^-\mu^+ + X$ in the context of the parton model. Omitting masses, the general form of the $\frac{d\sigma}{dQ^2}$ is

$$\frac{d\sigma}{dQ^2}(\phi\bar{\phi} \to \mu^-\mu^+) = \frac{\pi}{2}\frac{(2\pi)^{-2}}{4s}\delta(s - Q^2)\int_{\underline{\Omega}} |M|^2 d\underline{\Omega} \quad . \tag{A.8.35}$$

In this expression "s" is the usual s-variable and $|M|^2$ is the scattering amplitude squared in the notation of (A.1.28). $\underline{\Omega}$ denotes

the solid angle in which the outgoing μ^- is scattered into, and the integration is over all the directions $\underline{O}$.

The amplitudes $|M|^2$ for the cases (S) and (V), defined in the previous section, are given by (see A.8.3 and A.8.12)

$$(S): \qquad |M|^2 = f^4 \left(\frac{t}{t-M_x^2} \right)^2 \qquad \text{(A.8.36)}$$

$$(V): \qquad |M|^2 = f^4 \frac{[4+(1+\cos\theta)^2]}{(t-M_x^2)^2} \frac{s^2}{2} \quad . \qquad \text{(A.8.37)}$$

The mass M_x is assumed to be large and thus we consider the case in which $Q^2 \ll M_x^2$; the Q^2 is equal to s because of the $\delta(s-Q^2)$ appearing in (A.8.35) so that we are really considering the case $s \ll M_x^2$.

Thus the amplitudes $|M|^2$ in Eqs. (A.8.36) and (A.8.37) are written as

$$(S): \qquad |M|^2 = g^2 \frac{s^2}{4} (1-\cos\theta)^2 \qquad \text{(A.8.38)}$$

$$(V): \qquad |M|^2 = g^2 \frac{s^2}{2} (5+2\cos\theta+\cos^2\theta) \qquad \text{(A.8.39)}$$

where $g = (f/M_x)^2$.

Putting the expressions above into (A.8.35) and integrating with respect $\underline{O}$ we get

$$(S): \qquad \frac{d\sigma}{dQ^2} = \frac{\pi}{2} \left(\frac{g}{4\pi} \right)^2 \left(\frac{2Q^2}{3} \right) \delta(s-Q^2) \qquad \text{(A.8.40)}$$

$$(V): \qquad \frac{d\sigma}{dQ^2} = \frac{\pi}{2} \left(\frac{g}{4\pi} \right)^2 \left(\frac{16Q^2}{3} \right) \delta(s-Q^2) \quad . \qquad \text{(A.8.41)}$$

The corresponding cross-sections when the $\phi, \bar{\phi}$ particles carry fractions x_1 and x_2 of the proton's momentum are given by

$$(S): \quad \frac{d\sigma}{dQ^2}(x_1,x_2) = \frac{4\pi \underset{\sim}{g}^2}{3Q^4}\left(\frac{Q^4\tau}{4}\right)\delta(x_1x_2-\tau) \qquad (A.8.42)$$

$$(V): \quad \frac{d\sigma}{dQ^2}(x_1,x_2) = \frac{4\pi \underset{\sim}{g}^2}{3Q^4}(2Q^4\tau)\delta(x_1x_2-\tau) \; . \qquad (A.8.43)$$

In the expressions above τ is the variable $\tau = Q^2/s$ where s is the center of mass energy squared of the p-p system, and g is defined as $\underset{\sim}{g} = g/4\pi$.

8d)

In this section we assume an interaction Lagrangian term given by $\mathcal{L} = -\sum_q f_q(\bar{e}q)X_q + h.c.$ Our aim is to calculate the ratio $R = \dfrac{\sigma(e^-e^+ \to \text{Hadrons})}{\sigma(e^-e^+ \to \mu^-\mu^+)}$.

The amplitude for the process $e^-e^+ \to q\bar{q}$ is given pictorially in Fig. 4A where the first diagram represents the electromagnetic term.

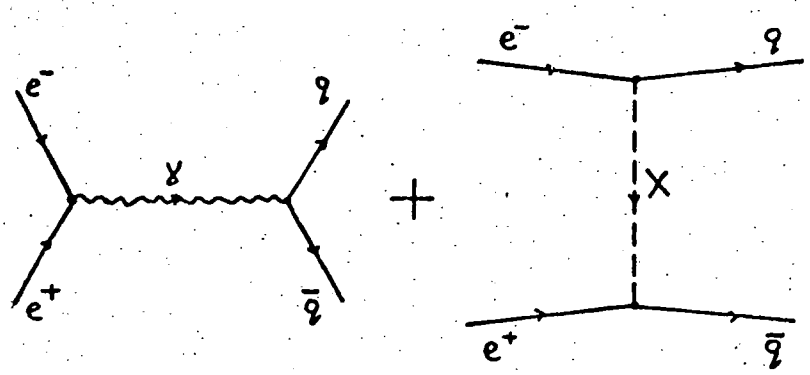

FIGURE 4A. The electromagnetic and the "anomalous" interaction contribution to the process $e^-e^+ \to q\,\bar{q}$.

Omitting mass terms the amplitude $\sum_{spin} |M|^2$ is found to be

$$\sum_{spin} |M|^2 = \frac{1}{4}\left\{\left(g_q^2 s^2 + 2g_q e^2 Q_q s + 2e^4 Q_q^2\right)(1-\cos\theta)^2 + 2e^4 Q_q^2 (1+\cos\theta)^2\right\} \; . \qquad (A.8.44)$$

In Eq. (A.8.44) Q_q is the charge (in electron units) of the q-quark; thus $Q_p = -\frac{2}{3}$, $Q_n = Q_\lambda = \frac{1}{3}$. g_q is the constant† $g_q \equiv (f_q/M_q)^2$ where M_q is the mass of the X_q field.

From (A.8.44) and (A.1.28) we get

$$\sigma(e^-e^+ \to q\bar{q}) = \frac{4\pi\alpha^2}{3s}\left\{\bar{f}_q^2 \frac{s^2}{4} + \bar{f}_q Q_q \frac{s}{2} + Q_q^2\right\} \qquad \text{(A.8.45)}$$

with $\bar{f}_q \equiv g_q/e^2 = (f_q/eM_q)^2$.

Thus the ratio R is given by

$$R = \sum_q \left\{Q_q^2 + \bar{f}_q Q_q \frac{s}{2} + \bar{f}_q^2 \frac{s^2}{4}\right\} \qquad \text{(A.8.46)}$$

---

† We assume that $s \ll M_q^2$

APPENDIX 9

In this appendix we calculate the decay rates $\Gamma_{(em.)}\ (\pi \to e^- e^+)$ and $\Gamma_{(em.)}\ (\eta \to \mu^- \mu^+)$ due to the Lagrangian interaction terms $\mathcal{L} = -f \sum_q (\bar{e}q)X_q + h.c.$ and $\mathcal{L} = -f \sum_q (\bar{\mu}q)X_q + h.c.$

The decay rate of a particle m having mass M and which disintegrates into a $\ell\bar{\ell}$ pair (ℓ = lepton) is given by (see for example Appendix of Ref. 1).

$$\Gamma(m \to \ell\bar{\ell}) = \frac{(2\pi)^{-2}}{2M(2s_m+1)} \int \frac{d^3\vec{k}}{(2E)} \frac{d^3\vec{k}'}{(2E')} \delta^{(4)}(P_i - P_f) \sum_{spins} |\langle f|M|m\rangle|^2 . \quad (A.9.1)$$

In this expression $|f>$ is the $\ell\bar{\ell}$ state normalized covariantly (see A.1.29); k^μ and $k^{\mu'}$ are the momenta of the leptons ℓ and $\bar{\ell}$. The symbol $\sum_{spin}$ denotes summation over the spin indices λ and λ' of the ℓ and $\bar{\ell}$.

The state $|m>$ of the decaying particle is also normalized covariantly.

To find the amplitude $|<f|M|m>|^2$ we apply techniques found in section 10.3 of Ref.[93]. Because the states $|f>$ and $|m>$ are covariantly normalized we find (see the above Reference)

$$|\langle f|M|m\rangle|^2 = (2M)\,|f(M,0)|^2 \left| \sum_{q,r,r'} C_q(r,r') \langle f|M|q(r)\bar{q}(r')\rangle \right|^2 . \quad (A.9.2)$$

The state $|q(r)\bar{q}(r')>$ is the q-type quark-antiquark state where the quarks carry no momentum and their spin indices are r and r'.

The constant $C_q(r,r')$ is spin-unitary spin Glebsch-Gordan coefficient; r,r' take the values 1 or 2 for spin up and down respectively.

The matrix element $\langle f|M|q(r)\bar{q}(s)\rangle$ is given by

$$\langle f|M|q(r)\bar{q}(r')\rangle = g_q\ \bar{u}(\lambda)u(r)\,\bar{v}(r')\,u(\lambda') \quad . \qquad (A.9.3)$$

In (A.9.3) g_q is the constant $g_q = (f_q/M_x)^2$, and the spinors u, v for simplicity are labelled only by their spin indices.

By virtue of (A.9.2) we have

$$\left.\begin{aligned}\sum_{spins}|\langle f|M|m\rangle|^2 &= (2M)\,|f(M,0)|^2\ \times \\ &\times \sum_{q,r,r'}\sum_{q',s,s'} C_q(r,r')C_{q'}^*(s,s')\,g_q g_{q'}^*\,R^{qq'}(r,s;r',s')\end{aligned}\right\} (A.9.4)$$

where $R^{qq'}(r,s;r',s')$ is given by

$$\left.\begin{aligned}R^{qq'}(r,s;r',s') &= Tr\left((\not{k}+m_q)u(r)\bar{u}(s)\right)Tr\left((\not{k}'-m_q)v(s')\bar{v}(r')\right) = \\ &(\not{k}+m_q)_{\alpha\beta}\,(u(r)\bar{u}(s))_{\beta\alpha}\,(\not{k}'-m_q)_{\mu\nu}\,(v(s')\bar{v}(r'))_{\nu\mu} \quad .\end{aligned}\right\} (A.9.5)$$

It is easy to verify that

$$(u(r)\bar{u}(s))_{\alpha\beta} = \delta_{\beta r}\delta_{\alpha s} \quad , \quad (v(s')\bar{v}(r'))_{\nu\mu} = -\delta_{\nu,s'+2}\delta_{\mu,r'+2} \qquad (A.9.6)$$

having thus

$$R^{qq'}(r,s;r',s') = -(\not{k}+m_q)_{rs}\,(\not{k}'-m_q)_{s+2,r'+2} \quad . \qquad (A.9.7)$$

The shash vector k is given by the expression (see A.1.2)

$$\not{k} = k_0\begin{pmatrix}1 & 0\\ 0 & -1\end{pmatrix} - \vec{k}\cdot\begin{pmatrix}0 & \vec{\sigma}\\ -\vec{\sigma} & 0\end{pmatrix} \quad . \qquad (A.9.8)$$

So from (A.9.8) we have $(k)_{rs} = \delta_{rs} k_o$ and similarly $(k')_{s'+2,r'+2} = \delta_{s'r'} k_o'$.

It is evident now that

$$R^{22'}(r,s;r',s') = \left(\frac{M}{2} + m_\ell\right)^2 \delta_{rs}\,\delta_{r's'} \qquad \text{(A.9.9)}$$

because $k_o = k_o' = M/2$.

The amplitude $|\langle f|M|m\rangle|^2$ of Eq. (A.9.4) is written now

$$\left.\begin{aligned}\sum_{spins} |\langle f|M|m\rangle|^2 = (2M)\,|f(M,0)|^2\left(\frac{M}{2}+m_\ell\right)^2 \times \\ \times \sum_{q,r}\sum_{q',r'} g_q\, g_{q'}\, C_q(r,r')\,C_{q'}(r,r') \quad .\end{aligned}\right\} \qquad \text{(A.9.10)}$$

When we deal with $J^P = 0^-$ mesons $C_q(r,r') = -C_q(r',r)$ and thus

$$\left.\begin{aligned}\sum_{spins} |\langle f|M|m\rangle|^2 = (2M)\,|f(M,0)|^2\left(\frac{M}{2}+m_\ell\right)^2 \times \\ \times\, 2\,\Big|\sum_q g_q\, C_q(1,2)\Big|^2 \quad .\end{aligned}\right\} \qquad \text{(A.9.11)}$$

This is because $C_q(1,2) = -C_q(2,1)$ and $C_q(1,1) = C_q(2,2) = 0$.

The expression (A.9.11) can be also written as

$$\left.\begin{aligned}\sum_{spins} |\langle f|M|m\rangle|^2 = |f(M,0)|^2\,\frac{M^3}{3}\left(1+\frac{2m_\ell}{M}\right)^2 \times \\ \times \left(\sum_q g_q\,\alpha_q\right)^2 \quad .\end{aligned}\right\} \qquad \text{(A.9.12)}$$

In (A.9.12) $\alpha_q = \sqrt{2}\, C_q(1,2)$ being thus an SU(3) Clebsh-Gordan coefficient; the coupling constants g_q have been taken real.

The integral $(2\pi)^{-2}\int \frac{d^3\vec{k}}{(2E)}\frac{d^3\vec{k}'}{(2E')}\ldots$ in Eq. (A.9.1) has the value

$$(2\pi)^{-2}\int \frac{d^3\vec{k}}{(2E)}\frac{d^3\vec{k}'}{(2E')}\ldots = \frac{(2\pi)^{-1}}{4}\left(1-\frac{4m_\ell^2}{M^2}\right)^{1/2} \qquad \text{(A.9.13)}$$

so that the final expression for $\Gamma_{(an.)}(m \to \ell\bar{\ell})$ is

$$\Gamma_{(an.)}(m \to \ell\bar{\ell}) = \frac{\pi\alpha^2}{2} |f(M,0)|^2 M^2 \left(1 - \frac{4m_\ell^2}{M^2}\right)^{1/2} \times \left(1 + \frac{2m_\ell}{M}\right)^2 \left(\sum_q \alpha_q \bar{f}_q\right)^2 . \qquad \text{(A.9.14)}$$

$\bar{f}_q$ is defined as $\bar{f}_q \equiv {}^{g_q}/_{e^2}$; the constant α is the hyperfine structure constant.

For completeness we give the SU(3) wave functions for the π^0 and η mesons.

$$|\pi^0\rangle = \frac{1}{\sqrt{2}} |\bar{p}p\rangle - \frac{1}{\sqrt{2}} |\bar{n}n\rangle \qquad \text{(A.9.15)}$$

$$|\eta\rangle = \left(\frac{\cos\theta}{\sqrt{6}} + \frac{\sin\theta}{\sqrt{3}}\right)\left(|\bar{p}p\rangle + |\bar{n}n\rangle\right) + \left(\frac{-2\cos\theta}{\sqrt{6}} + \frac{\sin\theta}{\sqrt{3}}\right)|\bar{\lambda}\lambda\rangle . \qquad \text{(A.9.16)}$$

The value of the mixing angle θ is 11°.

From (A.9.15) and (A.9.16) we have

$$(\pi^0): \quad \alpha_p = \alpha_n = 1/\sqrt{2} \;, \; \alpha_\lambda = 0 \qquad \text{(A.9.17)}$$

$$(\eta): \quad \alpha_p = \alpha_n = .511 \;, \; \alpha_\lambda = -.691 \qquad \text{(A.9.18)}$$

REFERENCES

1. J.D. Bjorken, S.D. Drell, "Relativistic Quantum Mechanics", McGraw Hill, New York, 1964.
2. J. Bernstein, "Elementary Particles and Their Currents", W.H. Freeman and Company, San Francisco, 1968.
3. B.H. Bransden and R.G. Moorhouse, "The Pion-Nucleon System", Princeton University Press, New Jersey, 1973.
4. F.J. Ernst, R.G. Sachs and K.C. Wali, Phys. Rev. 119, 1105 (1960).
5. J.R. Dunning et al., Phys. Rev. 141, 1286 (1966).
6. S.D. Drell, A.C. Finn and M.H. Goldhaber, Phys. Rev. 157, 1402 (1967).
7. R.J. Budnitz et al., Phys. Rev., 173, 1357 (1968).
8. C.H. Llewellyn Smith, Physics Reports 3C, No. 5 (1972).
9. F.E. Close, Daresbury Nuclear Physics Laboratory report No. DNPL/P154.
10. J.J. Aubert et al., Phys. Rev. Lett. 33, 1404 (1974).
11. S.D. Drell and T.M. Yan., Phys. Rev. Lett. 25, 316 (1970).
12. R. Jaffe, Phys. Rev. D5, 2622 (1970).
13. N. Cabbibo, G. Parisi and M. Testa., Lettere al Nuovo Cimento 4, 35 (1970).
14. G. Tarnopolosky et al., Phys. Rev. Lett. 32, 432 (1974)
    _____ A. Litke et al., Phys. Rev. Lett. 30, 189 (1973).
15. J.D. Bjorken, SLAC report No. SLAC-PUB-1318 also in "Proceedings of the Sixth International Symposium on Electron and Photon Interactions at High Energies", Bonn, Germany, 1973, edited by H. Rollnik and W. Pfeil (North Holland, Amsterdam 1974).
16. R.H. Cahn and J. Ellis., SLAC report No. SLAC-PUB-1384.
17. C.H. Llewellyn Smith, CERN report No. CERN TH. 1849.
18. P. Carruthers, Physics Reports 1C, No. 1 (1971).

19. E. Pittet., Rutherford Laboratory report No. RPP/T/49 (1973).

20. J.D. Bjorken, Phys. Rev. 179, 1547 (1969).

21. G. Miller et al., Phys. Rev. D5, 528 (1972).

22. K. Wilson, in "Proceedings of the 1971 International Symposium on Electron and Photon Interactions", edited by N.B. Mistry (Laboratory of Nuclear Studies, Cornell University, Ithaca, New York 1972).

23. G. Preparata, in "Proceedings of the Sixth International Symposium on Electron and Photon Interactions at High Energies", Bonn, Germany, 1973, edited by H. Rollnik and W. Pfeil (North Holland, Amsterdam, 1974).

24. J. Ellis, SLAC report No. SLAC-PUB 1353 (T/E).

25. S. Coleman, in "Properties of the Fundamental Interactions", edited by A. Zichichi (Editrice Compositori, Bologna, 1973).

26. D. Politzer, Physics Reports 14C, No. 4(1974).

27. F.E. Close, Daresbury Nuclear Physics Laboratory report No. DNPL/R31.

28. F.J. Gilman, Physics Reports 4C, No 3 (1972).

29. F.J. Gilman, Physics Review 167, 1365 (1968).

30. L.N. Hand, Phys. Rev. 129, 1834 (1963).

31. H.R. Rubinstein, in "Springer Tracts in Modern Physics", 62, page 72 (Springer-Verlag, Berlin, Heidelberg, New York, 1972).

32. F.J. Gilman, in "International Symposium on Electron and photon Interactions at High Energies, Liverpool, England", 1969, edited by D.W. Braben and R.E. Rand (Daresbury Nuclear Physics Laboratory, Daresbury, Lancashire, England 1970).

33. C.G. Callan and J.D. Gross, Phys. Rev. Lett. 22, 156 (1969).

34. T. Eichten et al., Phys. Lett. 46B, 274 (1973).

35. A. Benvenuti et al., Phys. Rev. Lett. 30, 1084 (1973).

36. S. Weinberg, Phys. Rev. Lett. 19, 1264 (1967); ibid., 27, 1688 (1971); Phys. Rev. D5, 1412 (1972).

37. A. Salam, in "Elementary Particle Physics" page 367, edited by N. Suartholm (Almquist and Wiksells, Stockholm, 1968).

38. G. 'tHooft, Nuclear Physics B33, 173 (1971).

39. P.W. Higgs, Phys. Lett. 12, 132 (1964); Phys. Rev. Lett. 13, 508 (1964); Phys. Rev. 145, 1156 (1965).

40. H. Georgi and S.L. Glashow, Phys. Rev. Lett. 28, 1494 (1972).

41. E.S. Abers and B.W. Lee, Physics Reports 9C, No. 1 (1973).

42. B. Zumino, CERN report No. CERN TH-1550.

43. S.L. Glashow, J. Iliopoulos and L. Maiani, Phys. Rev. D2, 1285 (1970).

44. D. Amati, H. Bacry, J. Nuyts and J. Prentki, Nuous Cimento 35, 1732 (1964).

45. C. Bacci et al, Phys. Rev. Lett. 33, 1408 (1974).

46. J.-E. Augustin et al., Phys. Rev. Lett. 33, 1406 (1974).

47. G.S. Abrams et al., Phys. Rev. Lett. 33, 1453 (1974).

48. F.J. Hasert et al., Phys. Lett. 46B, 138 (1973).

49. B. Aubert et al., Phys. Rev. Lett. 32, 1457 (1974).

50. R.P. Feynman, in "High Energy Collisions", Third International Conference held at State University of New York, Stony Brook, 1969, edited by C.N. Yang, J.A. Cole, M.Good, R. Hwa, and J.Lee-Franzini (Gordon and Breach, New York 1969).

51. J.K. Kuti and V.F. Weisskopf., Phys. Rev. D4, 3418 (1971).

52. S.D. Drell and T.M. Yan., Annals of Physics 66, 578 (1971).

53. J.D. Bjorken and E.A. Paschos, Phys. Rev. 185, 1975 (1969).

54. P.V. Landshoff and J.C. Polkinghorne, Physics Reports 5C, No. 1 (1972).

55. J. Kogut and L. Susskind, Physics Reports 8C, No. 2 (1973).

56. G. Altarelli, Rivista del Nuovo Cimento 4, 335 (1974).

57. M. Gronau, F. Raundal and Y. Zarmi, Nuclear Physics B51, 611 (1973).

58. S.M. Berman, J.D. Bjorken and J.B. Kogut., Phys. Rev. D4, 3388 (1971).

59. C.H. Llewellyn Smith, in "Springer Tracts in Modern Physics" 62, page 51 (Springer Verlag,Berlin, Heidelberg, New York 1972).

60. E. Bloom and F.J. Gilman, Phys. Rev. D4, 2901 (1971).

61. S.L. Adler, Phys. Rev. 143, 1144 (1966).

62. D.J. Gross and C.H. Llewellyn Smith, Nuclear Physics B14, 337 (1969).

63. O. Nachtmann, Nuclear Physics B38, 397 (1972).

64. E.D. Bloom and F.J. Gilman, Phys. Rev. Lett. 25, 1140 (1970).

65. A. Love, G.G. Ross and D.V. Nanopoulos, Nuclear Physics B49, 513 (1972).

66. L.M. Sehgal, Nuclear Physics, B65, 141 (1973).

67. D.H. Perkins, Oxford University Report No. 67-73.

68. P. Musset, reported at the Aix-en-Provence International Conference on Elementary Particles (1973).

69. T. Eichten et al., Phys. Lett. 46B, 281 (1973).

70. Gargamelle-CERN group, papers No. 511, 512, 513 submitted to the 17th International Conference on High Energy Physics, London 1974.

71. B. Aubert et al., papers No. 692, 694 submitted to the 17th International Conference on High Energy Physics, London 1974.

___ B.C. Barish et al, papers No. 586, 588 submitted to the same Conference.

72. D.C. Cundy, reported at the 17th International Conference on High Energy Physics, London 1974.

73. "Proceedings of the 17th International Conference on High Energy Physics, London 1974, edited by J.R. Smith.

74. A. Lahanas, Lettere al Nuovo Cimento 11, 363 (1974).

75. J. Bell and R. Jackiw, Nuovo Cimento 60, 47 (1967).

___ S.L. Adler, Phys. Rev. 177, 2424 (1969).

76. P. Zumino, Lectures given at the Gargesse Summer School in July 1972, also CERN report No. CERN TH-1550.

77. A. Bodek et al., Phys. Rev. Lett. 30, 1087 (1973).

78. R. Mc.Elhaney and S.F. Tuan, Phys. Rev. D8, 2267 (1972).

79. F.J. Gilman, reported at the 17th International Conference on High Energy Physics, London 1974.

80. A. Bodek, MIT Thesis, COO-3069-116 (1972).

81. E.D. Bloom et al., Phys. Rev. Lett. 23, 930 (1969).

82. E.D. Bloom, in "Proceedings of the Sixth International Symposium on Electron and Photon Interactions at High Energies", Bonn, Germany 1973, edited by H. Rollnik and W. Pfeil (North Holland, Amsterdam, 1974).

83. J.J. Sakurai, H.B. Thacker and S.F. Tuan, Nuclear Physics B48, 353 (1972).

84. R.P. Bajpai and S. Mukherjee, Phys. Rev. D10, 290 (1974).

85. J.H. Christenson et al., Phys. Rev. D8, 2016 (1973).

86. J.C. Pati and A. Salam, Phys. Rev. Lett. 31, 661.(1973), Phys. Rev. D8, 1240 (1973), Phys. Rev. D10, 275 (1974).

87. O.W. Greenberg and G.B. Yodh., Phys. Rev. Lett. 32, 1473 (1974).

88. D.V. Nanopoulos and S.D.P. Vlassopoulos, Lettere al Nuovo Cimento 10, 751 (1974).

89. B. Richter, reported at the 17th International Conference on High Energy Physics, London 1974.

90. Ikaros I.Y. Bigi and J.D. Bjorken, SLAC report No. SLAC-PUB 1422.

91. A. Soni, Phys. Lett. 52B, 332 (1974).

92. J.J.J. Kokkedee, "The Quark Model" (W.A. Benjamin, New York, Amsterdam, 1969).

93. B.D. Hyams et al., Phys. Lett. 29B, 128 (1969).

_____ Particle Data Group, Reviews of Modern Physics 45, S61 (1973).

94. A.S. Carroll et al., in "Proceedings of the 17th International Conference on High Energy Physics, London 1974, edited by J.R. Smith.

95. A.B. Lahanas and G.D. Spathis, Sussex University report (unpublished).

96. M. Froissart, Phys. Rev. 123, 1053 (1961).

97. E. Leader and V. Maor, Phys. Lett. 43B, 505 (1973)

_____ P.D.B. Collins, F.D. Gault and A. Martin, Nuclear Physics B80, 135 (1974).